VALORISATION OF CARBOHYDRATE-RICH FOOD WASTE FOR SYNTHESIS OF HYDROXYMETHYLFURFURAL (HMF)

KA MING YU

PhD

The Hong Kong Polytechnic University

2018

The Hong Kong Polytechnic University

Department of Civil and Environmental Engineering

Valorisation of Carbohydrate-Rich Food Waste for Synthesis of Hydroxymethylfurfural (HMF)

Ka Ming YU

A thesis submitted in partial fulfilment of the

requirements for the degree of Doctor of Philosophy

April 2018

CERTIFICATE OF ORIGINALITY

I hereby declare that this thesis is my own work and that, to the best of my knowledge and belief, it reproduces no material previously published or written, nor material that has been accepted for the award of any other degree or diploma, except where due acknowledgement has been made in the text.

Ka Ming YU

Abstract

Food waste that amounts to over one billion tonnes per year globally is a potential renewable feedstock for biorefinery. This thesis focuses on the development of high-throughput catalytic systems to produce value-added chemicals, such as hydroxymethylfurfural (HMF), from various selected food waste that is rich in starch, cellulose, or sugars. Different homogeneous catalysts and solvents are scrutinised to pursue an efficient conversion system. The findings highlight that the derived Brønsted acidity and intrinsic Lewis acidity of metals (e.g., Sn(IV) and Al(III)) are critical for HMF selectivity, by maneuvering the kinetics of desirable tandem reactions and undesirable side reactions. These acidities depend on the electrochemical properties of metal ions, e.g., electronegativity and charge density. Adding a co-catalyst (e.g., maleic acid) to the metal-based catalytic systems is demonstrated to be a feasible means to control conversion rate and selectivity. In addition, solvents are evidenced to play an important role beyond serving as a reaction medium. Production of HMF in a binary mixture of water and acetone or acetonitrile (i.e., acetone/H_2O and acetonitrile/H_2O, respectively) is substantially faster than that in dimethyl sulfoxide/H_2O and tetrahydrofuran/H_2O. Replacing the industrial co-solvents by greener alternatives, e.g., propylene carbonate and γ-valerolactone, can further accelerate the conversion, in which HMF of 20-25 mol% can be produced from bread waste within 20 min under microwave heating at 120^{o}C. The solvent medium interacts with the substrates and catalysts, altering their reactivity during catalysis. These research efforts elucidate the roles of different parameters, advise the design of high-performance solid catalyst for recycling purpose, and demonstrate a good potential of food waste valorisation for synthesis of value-added chemicals in real-life applications.

Publications Arising from PhD Study

<u>First Author Journal Papers of Food Waste Recycling:</u>

1. **Yu, I.K.M.**; Xiong, X.; Tsang, D.C.W.*; Wang, L.; Hunt, A.J.; Song, H.; Shang, J.; Ok, Y.S.; Poon, C.S. Aluminium-biochar composites as sustainable heterogeneous catalysts for glucose isomerisation in a biorefinery. Green Chem., 2018, 10.1039/c8gc02466a *[Impact Factor: 9.125]*
2. **Yu, I.K.M.**; Tsang, D.C.W.*; Yip, A.C.K.; Hunt, A.J.; Sherwood, J.; Shang, J.; Song H.C.; Ok, Y.S.; Poon, C.S. Propylene carbonate and γ-valerolactone as green solvents enhance Sn(IV)-catalysed hydroxymethylfurfural (HMF) production from bread waste. Green Chem., 2018, 20, 2064-2074. *[Impact Factor: 9.125]*
3. **Yu, I.K.M.**; Tsang, D.C.W.*; Su, Z.; Yip, A.C.K.; Shang, J.; Ok, Y.S.; Kim, K.H.*; Poon, C.S. Contrasting roles of maleic acid in controlling kinetics and selectivity of Sn(IV)- and Cr(III)-catalyzed hydroxymethylfurfural synthesis. ACS Sustain. Chem. Eng., 2018, 10.1021/acssuschemeng.8b02931 *[Impact Factor: 6.14]*
4. **Yu, I.K.M.**; Ong, K.L.; Tsang, D.C.W.*; Haque, M.A.; Kwan, T.H.; Chen, S.S.; Uisan, K.; Kulkami, S.; Lin, C.S.K.* Chemical transformation of food and beverage waste derived fructose to hydroxymethylfurfural as a value-added product. Catal. Today, 2018, 314, 70-77.
5. **Yu, I.K.M.**; Tsang, D.C.W.*; Chen, S.S.; Wang, L.; Hunt, A.J.; Sherwood, J.; De Oliveira Vigier, K.; Jerome, F.; Ok, Y.S.; Poon, C.S. Polar aprotic solvent-water mixture as the medium for catalytic production of hydroxymethylfurfural (HMF) from bread waste. Bioresource Technol., 2017, 245, 456-462. *[Impact Factor: 5.600; Grade A (#1 in Agricultural Engineering), Credit: 0.7]*

6. **Yu, I.K.M.**; Tsang, D.C.W.*; Yip, A.C.K.; Chen, S.S.; Ok, Y.S.; Poon, C.S. Valorization of starchy, cellulosic, and sugary food waste into hydroxymethylfurfural by one-pot catalysis. Chemosphere, 2017, 184, 1099-1107.
7. **Yu, I.K.M.**; Tsang, D.C.W.* Conversion of biomass to hydroxymethylfurfural: A review of catalytic systems and underlying mechanisms. Bioresource Technol., 2017, 238, 716-732.
8. **Yu, I.K.M.**; Tsang, D.C.W.*; Yip, A.C.K.; Chen, S.S.; Wang, L.; Ok, Y.S.; Poon, C.S. Catalytic valorization of food waste into hydroxymethylfurfural (HMF): Controlling relative kinetics for high productivity. Bioresource Technol., 2017, 237, 222-230.
9. **Yu, I.K.M.**; Tsang, D.C.W.*; Yip, A.C.K.; Chen, S.S.; Ok, Y.S.; Poon, C.S. Valorization of food waste into hydroxymethylfurfural: Dual role of metal ions in successive conversion steps. Bioresource Technol., 2016, 219, 338-347.
10. **Yu, I.K.M.**; Tsang, D.C.W.*; Yip, A.C.K.; Su, Z.; De Oliveira Vigier, K.; Jerome, F.; Poon, C.S.; Ok, Y.S. Organic acid-regulated Lewis acidity for selective catalytic hydroxymethylfurfural production from rice waste: An experimental-computational study. ACS Sustain. Chem. Eng., 2018, under review.

Other Journal Papers of Food/Organic Waste Recycling

1. Cao, L.; **Yu, I.K.M.**; Chen, S.S.; Tsang, D.C.W.*; Wang, L.; Xiong, X.; Zhang, S.; Kwon, E.; Song, H.; Ok, Y.S.; Poon, C.S. Production of 5-hydroxymethylfurfural from starch-rich food waste catalyzed by sulfonated biochar. Bioresource Technol., 2018, 252, 76-82.
2. Chen, S.S.; Wang, L.; **Yu, I.K.M.**; Tsang, D.C.W.*; Hunt, A.J.; Jerome, F.; Zhang S.; Ok, Y.S.; Poon, C.S. Valorization of lignocellulosic fibres of paper waste into

levulinic acid using solid and aqueous Brønsted acid. Bioresource Technol., 2018, 247, 387-394.

3. Lam, C.M.; **Yu, I.K.M.**; Hsu, S.C.*; Tsang, D.C.W.*. Life-cycle assessment on food waste valorisation to value-added products. J. Clean. Prod., 2018, in press.
4. Lam, C.M.; **Yu, I.K.M.;** Medel-Jimenez, F.J.; Tsang, D.C.W.*; Hsu, S.C.*; Poon, C.S. Life-cycle cost-benefit analysis on sustainable food waste management: the case of Hong Kong International Airport. J. Clean. Prod., 2018, 187, 751-762.
5. Mohanty, S.K.*; Valenca, R.; Berger, A.; **Yu, I.K.M.**; Xiong, X.; Saunders, T.; Tsang, D.C.W.* Plenty of room for carbon on the ground: Potential applications of biochar for stormwater treatment. Sci. Total Environ., 2018, 625, 1644-1658.
6. Xiong, X.; **Yu, I.K.M.**; Chen, S.S.; Tsang, D.C.W.*; Cao, L.; Zhang, S.; Kwon, E.; Song, H.; Ok, Y.S.; Poon, C.S. Sulfonated biochar as acid catalyst for sugar hydrolysis and dehydration. Catal. Today, 2018, in press.
7. Chen, S.S.; **Yu, I.K.M.**; Tsang, D.C.W.*; Yip, A.C.K.; Khan, E.; Wang, L.; Ok, Y.S.*; Poon, C.S. Valorization of cellulosic food waste into levulinic acid catalyzed by heterogeneous Brønsted acids: Temperature and solvent effects. Chem. Eng. J., 2017, 327, 328-335.
8. Xiong, X.; **Yu, I.K.M.**; Cao, L.; Tsang, D.C.W.*; Zhang, S.; Ok, Y.S. A review of biochar-based catalysts for chemical synthesis, biofuel production, and pollution control. Bioresource Technol., 2017, 254-270.
9. Cao, L.; **Yu, I.K.M.**; Tsang, D.C.W.*; Zhang, S.; Ok, Y.S.; Kwon, E.E.; Song, H.; Poon, C.S. Phosphoric acid-activated wood biochar for catalytic conversion of carbohydrates into glucose and 5-hydroxymethylfurfural. Bioresource Technol., under review.
10. Yang, X.; **Yu, I.K.M.**; Tsang, D.C.W.*; Chen, S.S.; Tessonier, J.P.; Yip,

A.C.K.; Wang, L.; Ok, Y.S.*; Poon, C.S. Tin-impregnated wood biochar as a sustainable Lewis acid catalyst for glucose isomerization. Chem. Eng. J., 2018, under review. *[Impact Factor: 4.181; Grade A (Chemical Engineering), Credit: 0.7]*

11. Mak, T.M.W.; **Yu, I.K.M.;** Tsang, D.C.W.*; Hsu, S.C.*; Poon, C.S. Promoting food waste recycling in commercial and industrial sector by extending the theory of planned behaviour: A Hong Kong case study. J. Clean. Prod., 2018, under review.

Other Journal Papers of Other Waste Recycling

1. Hossain, M.U.; Wang, L.; **Yu, I.K.M.**; Tsang, D.C.W.*; Poon, C.S.* Environmental and technical feasibility study of upcycling wood waste into cement-bonded particleboard. Constr. Build. Mater., 2018, 173, 474-480.
2. Wang, L.; **Yu, I.K.M.**; Tsang, D.C.W.*; Yu, K.; Li, S.; Poon, C.S.* Dai, J.G. Upcycling wood waste into fibre-reinforced magnesium phosphate cement particleboards. Constr. Build. Mater., 2018, 159, 54-63.
3. Wang, L.; **Yu, I.K.M.**; Tsang, D.C.W.*; Li, S.; Li, J.S.; Poon, C.S.; Wang, Y.S.; Dai, J.G. Transforming wood waste into water-resistant magnesia-phosphate cement particleboard modified by alumina and red mud. J. Clean. Prod., 2017, 168, 452-462.
4. Wang, L.; **Yu, I.K.M.**; Tsang, D.C.W.*; Li, S.; Poon, C.S. Mixture design and reaction sequence for recycling contaminated wood into rapid-shaping magnesia-phosphate cement particleboard. Ind. Eng. Chem. Res., 2017, 56, 6645-6654.
5. Mak, T.M.W.; **Yu, I.K.M.**; Wang, L.; Yeung, T.L.Y.; Li, C.N.; Hsu, S.C.; Zhang, R.; Tsang, D.C.W.*; Poon, C.S.* Extended theory of planned behaviour for

promoting construction waste recycling in Hong Kong. Waste Manage., 2017, under review.

Conference Proceedings/Abstracts of Food Waste Recycling

1. **Yu, I.K.M.**; Xiong, X.; Tsang, D.C.W. Sulfonated biochar as a new catalyst for upcycling carbohydrate-rich food waste into hydroxymethylfurfural (HMF). International Conference on Geochemistry in the Tropics & Sub-Tropics: Ecotoxicology of Persistent Toxic Substances in Food Production, 9-12 December, Shenzhen, China, 2017.
2. **Yu, I.K.M.**; Tsang, D.C.W. Catalytic conversion of food waste to hydroxymethylfurfural in polar aprotic solvent-water medium. 17th Congress, Asian Pacific Confederation of Chemical Engineering, 23-27 August, Hong Kong, China, 2017.
3. **Yu, I.K.M.**; Chen, S.S.; Tsang, D.C.W. Solvent effect on catalytic conversion of starch-rich food waste to hydroxymethylfurfural. The 2nd International Conference on Biological Waste as Resource 2017 (BWR2017), 25-28 May, Hong Kong, China, 2017.
4. **Yu, I.K.M.**; Tsang, D.C.W. Metal-catalyzed conversion kinetics of food waste to hydroxymethylfurfural. 4th International Symposium on Green Chemistry, 16-19 May, La Rochelle, France, 2017.
5. **Yu, I.K.M.**; Tsang, D.C.W. Kinetic and thermodynamic insights into catalytic conversion of food waste to hydroxymethylfurfural. 253rd American Chemical Society National Meeting, 2-6 April, San Francisco, USA, 2017.
6. **Yu, I.K.M.**; Tsang, D.C.W. Valorization of starchy, cellulosic, and sugary food

waste into value-added chemicals. 253rd American Chemical Society National Meeting, 2-6 April, San Francisco, USA, 2017.

7. **Yu, I.K.M.**; Tsang, D.C.W.; Yip, A.C.K.; Poon, C.S. Roles of Lewis and Brønsted acidity in carbohydrates valorization into hydroxymethylfurfural. Asia-Pacific Symposium on Biotechnology for Waste Conversion, 6-8 December, Hong Kong, China, 2016.
8. **Yu, I.K.M.**; Tsang, D.C.W. Valorization of pre-consumer food waste into hydroxymethylfurfural. 1st International Conference on Bioresource Technology for Bioenergy, Bioproducts and Environmental Sustainability, 23-26 October, Sitges, Spain, 2016.
9. **Yu, I.K.M.**; Tsang, D.C.W. Valorization of food waste into hydroxymethylfurfural. G2C2 4th Annual Symposium, 18-19 July, Chengdu, China, 2016.
10. **Yu, I.K.M.**; Chen, S.S.; Tsang, D.C.W. Food waste management in Hong Kong: Centralized or decentralized? Anaerobic digestion, composting, or landfill disposal? 3rd International Conference on Solid Waste, 20-23 May, Hong Kong, China, 2015.
11. Tsang, D.C.W.; **Yu, I.K.M.** Green solvents for valorisation of starch-rich food waste into value-added chemicals. The International Conference on Sustainable Energy and Environmental Challenges (SEEC-2018), 1-3 January, India, 2018.
12. Cao, L.; **Yu, I.K.M.**; Tsang, D.C.W. Using biochar-supported acid for catalytic production of hydroxymethylfurfural (HMF) from bread waste. International Conference on Geochemistry in the Tropics & Sub-Tropics: Ecotoxicology of Persistent Toxic Substances in Food Production, 9-12 December, Shenzhen, China, 2017.

13. Mak, T.M.W.; **Yu, I.K.M.**; Tsang, D.C.W. Extended theory of planned behaviour for promoting construction waste recycling in Hong Kong. 20th Conference on Process Integration, Modelling and Optimisation for Energy Saving and Pollution Reduction, 21-24 August, Tianjin, China, 2017.
14. Chen, S.S.; **Yu, I.K.M**.; Tsang, D.C.W. Catalytic conversion of towel paper to levulinic acid. The 2nd International Conference on Biological Waste as Resource 2017 (BWR2017), 25-28 May, Hong Kong, China, 2017.
15. Chen, S.S.; **Yu, I.K.M.**; Tsang, D.C.W.; Yip, A.C.K. Valorisation of cellulosic food waste to value-added chemicals by heterogeneous Brønsted catalysts: A kinetic study. 4th International Symposium on Green Chemistry, 16-19 May, La Rochelle, France, 2017.
16. Mak, T.M.W.; **Yu, I.K.M.**; Tsang, D.C.W. A system dynamic approach to enhance resources recycling in urban cities. Asia-Pacific Symposium on Biotechnology for Waste Conversion, 6-8 December, Hong Kong, China, 2016.
17. Yoo, J.C.; Wang, L.; Beiyuan, J.; **Yu, I.K.M.**; Tsang, D.C.W. Recycling sewage sludge and waste wood into biochar for soil remediation. 3rd International Conference on Contaminated Land, Ecological Assessment and Remediation, 20-27 November, Taipei, Taiwan, 2016.
18. Lam, C.M.; Medel-Jimenez, F.J.; Hsu, S.C.; **Yu, I.K.M.**; Chen, S.S.; Tsang, D.C.W. Integrated life-cycle assessment and cost-benefit analysis of food waste treatment scenarios at airport: A Hong Kong case study. 9th Asia-Pacific Landfill Symposium, 9-11 November, Hong Kong, China, 2016.

Awards

Best Award for Student Oral Presentation **(GeoTrop 2017, 9-12 December, China)**	**2017**
Best Award for Student Poster Presentation **(GeoTrop 2017, 9-12 December, China)**	**2017**
PolyU Micro Fund **(Hong Kong Polytechnic University)**	**2015**

Acknowledgements

I would like to thank my supervisor, Dr. Dan Tsang, for all the opportunities, from which I progressively learn skills and gain confidence with his guidance and encourangement. He is passionate to share his vast knowledge and thoughtful insight, which always inspire and improve my research as well as stimulate my personal growth. I also need to express my gratitude and respect to Prof. Chi Sun Poon for his continual support and indispensable help when I am in need.

Thanks must also go to the lab technicians, Mr. W.S. Lam, Ms Celine Che, Ms Darby Lam, and Mr. Ka On Tse, who always provide swift technical support upon request and maintain a clean and safe environment for me and colleagues. I have to thank Mr. Lam in particular, who also offers practical advices on experimental setup and analytical protocals, and takes care of maintanence and modification of equipment. What he does for us is often beyond the scope of his work.

I am also grateful to have my strong group members – Season Chen, Lei Wang, Jingzi Beiyuan, Yuqing Sun, Xinni Xiong, Tiffany Mak, Jiamin Li, Leichang Cao, Liang Chen et al., who are so generous to back me up with their time, skill sets, and knowledge. Without their help, some of my work cannot be accomplished at all. They are fun and cheerful, making my adventure here happier than I ever expected.

I must not miss my family. It is my greatest luck and honour to have my brilliant Mom and Dad, who I can never surpass. Mom is forever way more diligent and tougher than me as she devotes herself in raising me and my little sister up out of difficult situations. Her love and care are countless. She is also a wise woman who manages to handle multiple tasks at a time. Dad was talented, loved reading and storytelling, and used to show me creative ways to solve daily problems, from which I learn that I can create lots of things with my bare hands. He was also a gentleman and was keen to help people in need. All credit goes to my parents with no doubt. I also feel thankful to have my adorable sister who always takes care of me, cheers me up, and puts up with me. She is my best friend and little assistant – sometimes she provides feedback on my illustration work.

Lastly, it is my old friends who keep me company since young age. I am thankful for their understanding, care, and support throughout the years. They bring me happy moments to revitalise me so that I can move on. Their inspiring sharings often boost my self-reflection and personal development, making me in a better shape to face any future challenges.

Table of Contents

Chapter 1 – Introduction

1.1 Background

Global food wastage that amounts to around 1.3 billion tonnes annually embeds a massive dissipation of resources and incurs a high carbon footprint of 3.3 billion tonnes of CO_2 equivalent, among which one fifth was attributed to the end-of-life processing such as landfill disposal (FAO, 2013). Recycling of food waste can mitigate the greenhouse gas emissions and, more importantly, realise the bioeconomy concept by turning unwanted materials to valuable marketable resources (Lin et al., 2013; Pleissner et al., 2016). Anaerobic digestion and composting are the conventional recycling options that produce biogas and fertilisers from food waste (Li et al., 2013; Gou et al., 2014; Wei et al., 2014). Despite their high reliability, these biological processes require a duration of at least a few weeks to several months (Arsova, 2010; Li et al., 2013). Recent research interests extend to new organic waste treatments such as hydrothermal carbonisation (Poerschmann et al., 2015), pyrolysis (Yu et al., 2016a), biomaterial extraction (Scaglia et al., 2016), and fermentation (Zhang et al., 2016). They are applicable for recycling the post-consumer food waste (e.g., unsortable leftovers), which are unlikely to give high-value products owing to the heterogeneous nature. New and high-throughput valorisation options may be developed to target at the homogeneous pre-consumer waste streams (e.g., sorted kitchen waste) for achieving recycling with high economic incentives.

The composition of food wastes depends on the status of urban development as well as food culture. For instance, food waste in Asian places generally contain a higher water content than the Western food. Typical food waste that contains 33−74%

of carbohydrate on a dry basis (Pleissner et al., 2013; Pleissner et al., 2014) appears as a potential feedstock for synthesis of value-added chemicals, such as hydroxymethylfurfural (HMF). As a versatile platform chemical, HMF can be transformed into a diversity of chemicals, including ethoxymethylfurfural, 2,5-furandicarboxylic acid, furfuryl alcohol, dimethylfuran, and 2,5-diformylfuran, which can substitute their petroleum-derived counterparts for the synthesis of common consumer products, e.g., pharmaceuticals, polymers, solvents, and biofuels. A previous study has achieved a maximum HMF yield of 4.3% from catering waste and articulated the associated economic benefit (Parshetti et al., 2015), illustrating the significance and need for technology development. Therefore, this research scrutinises the fundamental roles of system components (i.e., feedstock, catalysts, and solvents) in order to master the underlying principles for engineering high-performance catalytic systems.

1.2 Scope and objectives

Different types of food waste (e.g., bread waste, rice waste, and vegetable waste) are recycled for synthesis of HMF, using metal chlorides (e.g., $SnCl_4$ and $AlCl_3$) or mineral acids (e.g., H_2SO_4) as catalysts under microwave heating. A diversity of organic solvent-water mixtures are studied for serving as the reaction medium. Batch experiments are carried out and data are presented in forms of product distributions and kinetic profiles. Analyses of solids are also performed to further characterise specific catalytic systems.

The objectives of the thesis are listed below.

- To prove the concept of valorisation of food waste for HMF synthesis;

- To identify the critical properties of effective catalytsts;
- To reveal the kinetics of catalytic conversions;
- To improve the selectivity of HMF production;
- To identify roles of solvents beyond serving as a reaction medium;
- To validate the use of novel and green solvents to replace common industrial solvents.

1.3 Thesis overview

This thesis contains ten chapters in total (**Fig. 1.1**). Following **Chapter 1** as the introduction, **Chapter 2** is the literature review that summerises the advances in conversion of food waste and other biomass waste (e.g., forestry residues) to HMF. It discusses the performance of different feedstocks, catalysts, and solvents reported in the recent literature, in consideration of their conversion efficiency, product yield, recyclability, and environmental compatibility. As such, research gaps are highlighted, which lay the cornerstone of this thesis.

Chapter 3 describes the methodology, including the collection and characterisation of food waste as well as catalytic conversion experiments with various selected feedstocks, catalysts, and solvents, which were designed on basis of the corresponding research questions.

Chapter 4 – 9 investigate the roles and inteplay between the three important system components, i.e., feedstock, catalyst, and solvent, in determining the efficiency and selectivity of conversion of food waste to HMF. The first step is to verify the conversion feasibility of different food waste (rich in starch, cellulose, or sugars) in selected catalytic systems (**Chapter 4**). To improve system design, it is necessary to identify the important physicochemical properties of catalysts in controlling each individual reaction (i.e., starch hydrolysis, glucose isomerisation, and fructose dehydration) (**Chapter 5**) and examine the kinetics of these desirable reactions relative to the side reactions (i.e., polymerisation and rehydration of HMF) that governs the HMF selectivity (**Chapter 6**). An addition of a co-catalyst is proposed to modify the kinetics and selectivity of the metal-based catalytic systems (**Chapter 7**). Solvents also play an important role in determining the conversion efficiency. The critical properties of solvents are highlighted by assessing a range of common polar aprotic solvents (**Chapter 8**) as well as green solvents (**Chapter 9**).

Chapter 10 concludes the key findings in this thesis and suggests the next-stage research to achieve sustainable valorisation of food waste/biomass waste in the future.

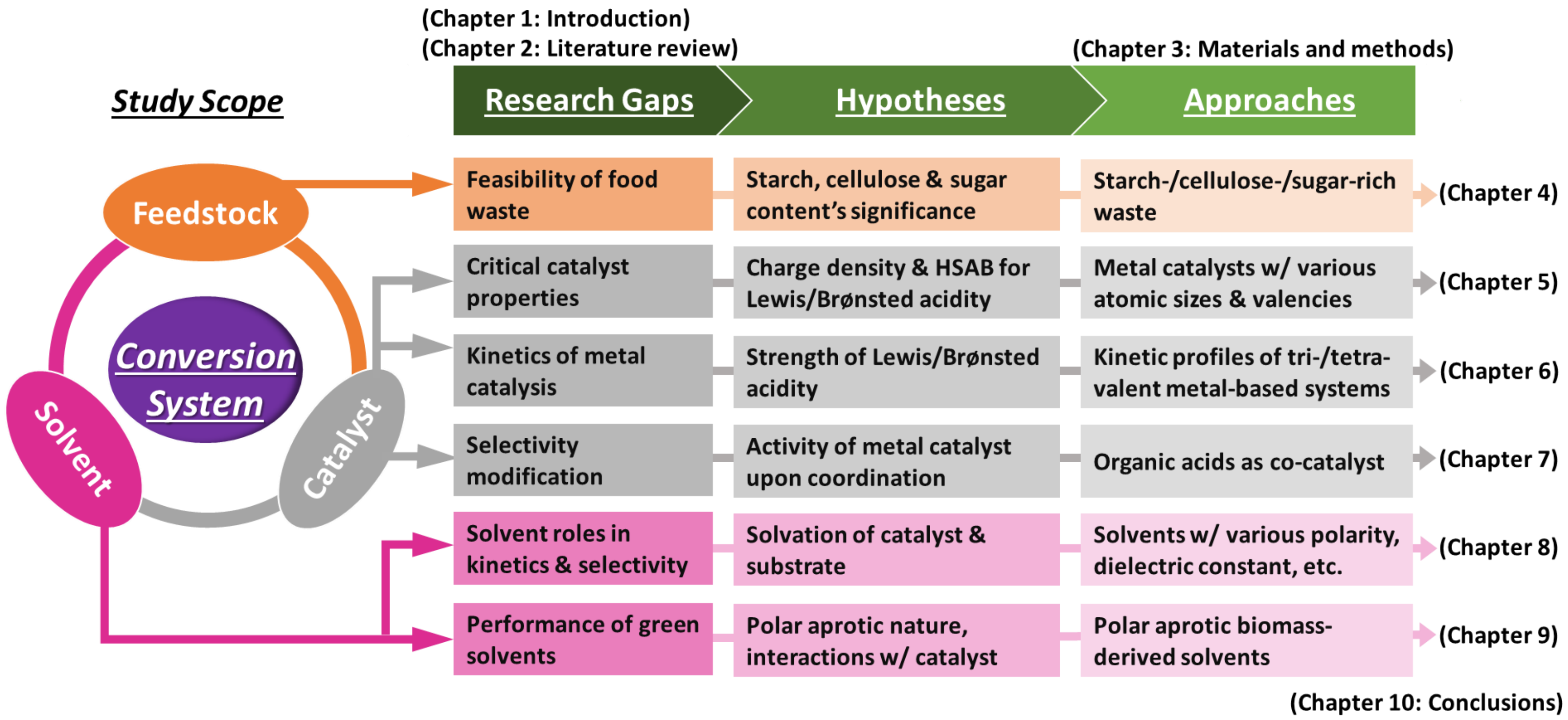

Figure 1.1. Overview of thesis

Chapter 2 – Literature Review

Abstract

Conversion of biomass waste to hydroxymethylfurfural (HMF), a value-added platform chemical, has captured great research interests driven by the economic and environmental incentives. This chapter evaluates the recent development of biomass conversion systems for high HMF yield and selectivity, with a focus on the performance of emerging catalysts and solvents from a mechanistic view. It is highlighted that the ratio and strength of Brønsted and Lewis acid in bifunctional catalyst are critical for maximizing HMF production by selective improvement in the kinetics of desirable reactions (hydrolysis, isomerization, and dehydration) over undesirable reactions (rehydration, polymerization). The characteristics of solvent mixture such as functional groups and speciation govern the reactivity of substrate towards desirable reactions and stability of HMF and intermediates against side reactions. Research efforts to unravel the interactions among co-catalysts/co-solvents and between catalysts and solvents are needed, thereby engineering a synergistic conversion system for biomass valorization.

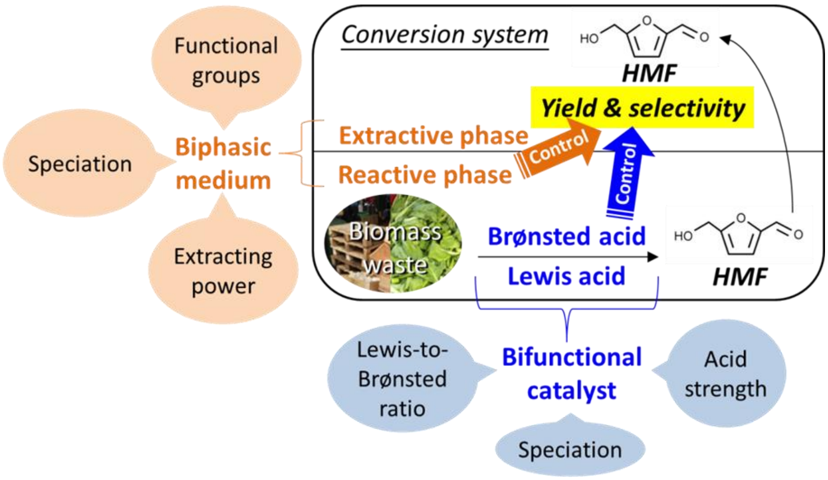

Figure 2.1. Graphical abstract of **Chapter 2.**

2.1 Introduction

Biomass waste has exerted significant burdens on the global waste management. For example, lignocellulosic residues of over 340 million tonnes (on a dry mass basis) was produced in United States in 2012 (Ge et al., 2016), whereas in Hong Kong, the daily disposal of biodegradable waste (i.e., food, yard, and paper waste) amounts to 6174 tonnes, contributing to approximately 60% of the municipal solid waste (HK EPD, 2016). Apart from the traditional treatments such as combustion and anaerobic digestion, valorization of the waste to tradable bulk chemicals has attracted immense research interests in recent years driven by the high market incentive (Tuck et at., 2012), thriving bio-based economy, and urge for the petrochemical substitutes (Mohan et al., 2016).

Hydroxymethylfurfural (HMF), a top value-added biomass-derived chemical, appears as a rewarding target product as it can be transformed to various derivatives, for example, ethoxymethylfurfural, 2,5-furandicarboxylic acid, furfuryl alcohol, dimethylfuran, and 2,5-diformylfuran (Dashtban et al., 2014; Mukherjee et al., 2015; Rout et al., 2016). These chemicals serve as the building blocks of diverse commodities including pharmaceuticals, polymers, resins, solvents, fungicides, and biofuels. Such broad versatility has earned HMF a high market value that ranges from USD 2.0 to 300 per kilogram depending on the chemical quality (Yu et al., 2017). In addition, the gobal market of HMF was USD 56 million in 2017, which is expected to rise to USD 63 million by 2025 (Market Research Hub, 2018). Representative reaction schemes can be found in previous studies (Román-Leshkov et al., 2010; Yu et al., 2016). However, current commercial production of HMF predominantly relies on the syrups extracted from energy crops (Kläusli, 2014). Potential use of renewable biomass resources as an alternative feedstock enables more sustainable manufacturing practice.

Cellulose and starch in biomass can be transformed to HMF through a series of chemical reactions: (a) hydrolysis of glucan to glucoses, (b) isomerisation of glucose to fructose, and (c) dehydration of fructose into HMF (**Fig. 2.2**). To facilitate the tandem conversion, a wide spectrum of homogeneous and heterogeneous catalysts have been studied, including Brønsted acids (e.g., HCl, H_2SO_4, and Amberlyst) that favour hydrolysis and dehydration, as well as Lewis acids (e.g., $AlCl_3$, $CrCl_3$, and Sn-beta) that promote isomerization (Mukherjee et al., 2015; Rout et al., 2016). Research efforts have also been made on the use of solvents, including water, polar aprotic solvents (e.g., dimethyl sulfoxide, tetrahydrofuran, and methyl isobutyl ketone) and ionic liquids (i.e., liquid salts), which serve multiple purposes such as dissolution of reactants and extraction of products (Dashtban et al., 2014).

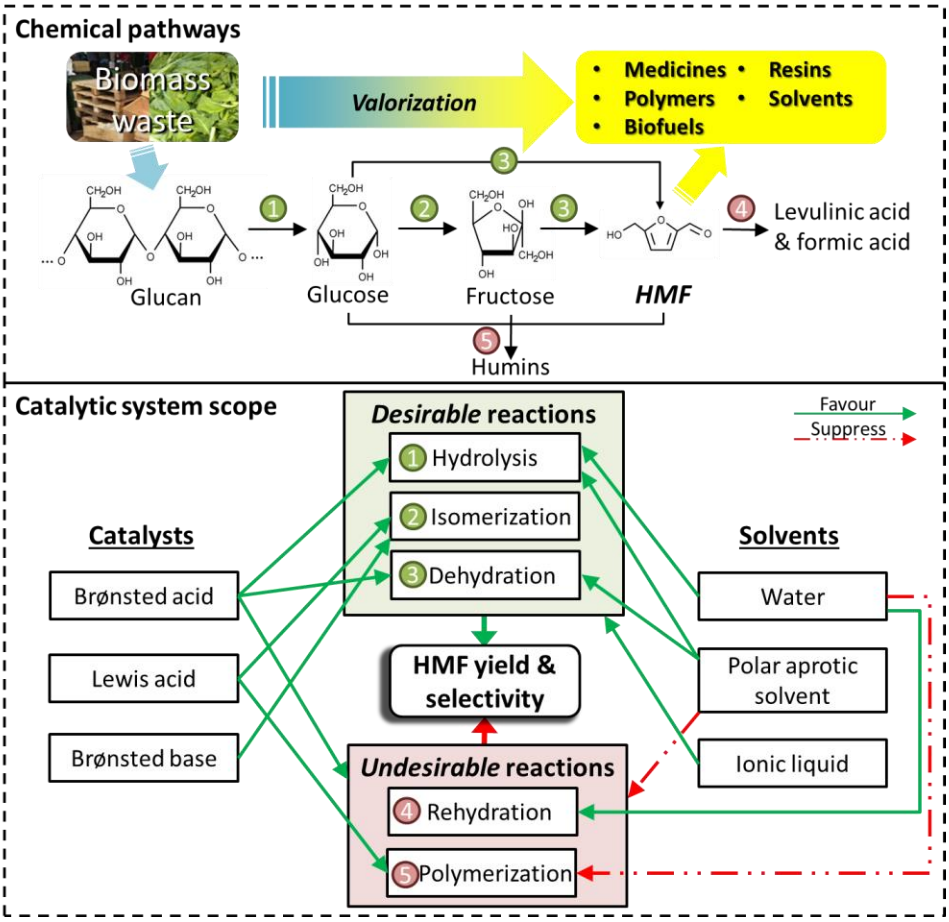

Figure 2.2. Chemical pathways and roles of catalysts and solvents in the catalytic conversion of biomass.

Active investigations into these system components are still underway to address the persisting challenges that hamper the mass production of HMF. For instance, the biomass recalcitrance restricts the one-step conversion, where HMF yield was less than 50% of the cellulose content (Mirzaei and Karimi, 2016; Zhang et al., 2017). In addition, the pronounced off-path reactions that reduce the product selectivity, i.e., rehydration of HMF and polymerization between the sugars and HMF (**Fig. 2.2**), still remained as a major hurdle in the latest studies (Kreissl et al., 2016; Moreno-Recio et al., 2016; Yu et al., 2017).

A high-performance conversion system demands critical selection of the catalysts and solvents, which requires a comprehensive understanding on the success factors upfront. It has been remarked that the catalyst characteristics, e.g., active species, active sites, pore size, and surface area, determine the catalytic activity and selectivity towards the desirable intermediates and product (De et al., 2016; Delidovich and Palkovits, 2016). For solvents, properties such as partition coefficient, boiling point, and thermal stability are considered as the indication of performance and recyclability (Saha and Abu-Omar, 2014; Yi et al., 2015). While the recent reviews focus on the technological feasibility from an engineering perspective, there is a missing link between our mechanistic understanding and the performance and physiochemical properties of catalysts and solvents in different catalytic systems. Filling in this knowledge gap can inspire inventions of more productive and selective catalyst-solvent design for biomass valorization.

This review summarizes and scrutinizes the latest experimental and computational studies on the conversion of biomass and carbohydrates employing different catalysts, solvents, and operational parameters (e.g., heating methods, temperature, recycling practices, etc.). Performance of the system components as a function of their properties is interpreted at the molecular level together with advanced mechanistic findings. Emerging issues such as bifunctional catalysts and green solvents are discussed, where the Lewis-to-Brønsted acid ratio, acid strength, as well as synergies between the catalytic sites and biphasic solvent systems play a significant role in determining the HMF yield and selectivity. The interactions among the biomass substrates, catalysts, solvents, and operating conditions will present important knowledge for constructing a synergistic system. Chemical recycling, product separation, environmental compatibility, and economic viability will also be reviewed.

2.2 Biomass substrates

A wide range of biomass substrates have been investigated (**Table 2.1**), including agricultural/forestry residues (e.g., sugarcane bagasse, maple wood, corncob, corn stover, pinewood, eucalyptus, wheat straw, barley husk) as well as food waste (e.g., waste cooked rice, bread waste, vegetable waste, and fruit waste). The conversion of biomass is much more challenging than model carbohydrates as the decomposition behaviour of the feedstock depends on the interactions between the cellulose, hemicellulose, and lignin (Asghari and Yoshida, 2010). In view of the comparable composition of these substrates (27-49 wt% cellulose, 14-36.9 wt% hemicellulose, and 16-32.9 wt% lignin in lignocellulosic biomass; **Table 2.2**), the diverse results of HMF yield ranging from 2 to 60% were probably attributed to the variations in the conversion systems (**Table 2.1**).

Subcritical water tended to give a lower yield of HMF (< 10%) even in the presence of catalyst such as HCl and H_2SO_4 (Yemiş and Mazza, 2012; Cai et al., 2013; Iryani et al., 2013), while the effect of substrate particle size was found negligible in a similar study reporting HMF yields of ~18-25 wt% from pinewood (Asghari and Yoshida, 2010) (**Table 2.1**). The latter study demonstrated that the milled wood chips with the size 180-1400 µm and outside the boundaries gave nearly the same HMF yield and total organic carbon, suggesting that the use of subcritical water may eliminate the need for heavy pulverizing of substrates. Adding a solvent such as tetrahydrofuran (THF) to 1 wt% H_2SO_4 solution could significantly enhance the conversion of maple wood as the HMF yield increased from 2.4% to 21% (Cai et al., 2013). In a mixture of dimethyl sulfoxide (DMSO)/water, ~22 wt% HMF could be yielded from waste cooked rice and bread waste (Yu et al., 2016a, 2017), although some starch remained unreacted and the interference of impurities (e.g., proteins and fats) needed further examinations. The use of γ-valerolactone (GVL) as medium and an acidic polymer as catalyst also produced a higher HMF yield of 27.1 mol% from corncob (Zhang et al., 2017). Yet, there was a three-fold decline in the HMF production when substrate loading increased from 40 to 70 mg (equivalent to 2 and 3.5 wt%, respectively), possibly because higher concentrations of reactants and intermediates in the medium facilitated the HMF-consuming side reactions. Biphasic systems, e.g., immiscible methyl isobutyl ketone (MIBK) coupled with water, produced a promising HMF yield of 47.5 wt% of cellulose content at a slightly higher loading of ~2.6 wt% maple wood over HCl as the catalyst (Zhang et al., 2013). Comparable biphasic systems were also applied to convert different biomass substrates such as straw, barley husk (Mirzaei and Karimi, 2016), grass, and poplar (Yang et al., 2012).

Table 2.1. Biomass waste as feedstock for HMF production under different catalytic systems.

Substrate	Catalyst	Solvent	Phase system	Conditions	HMF yield	FF yield	Heating	Reference
Bagasse of sugarcane	-	Subcritical water	Mono; unary	270ºC, 10 min	3.1 wt%	-	Salt bath	Iryani et al., 2013
4 wt% bagasse	20 mol% $Zr(O)Cl_2/CrCl_3$ (w.r.t. cellulose)	DMA-10 wt% LiCl/[BMIM]Cl (1:1 wt/wt)	Mono; binary	120ºC, 5 min	42%	-	Microwave	Dutta et al., 2012
4 wt% bagasse		DMA-10 wt% LiCl	Mono; unary	120ºC, 5 min	29%	-	Microwave	
25 mg barley husk	48 mol% sulphanilic acid	3 ml water-DMSO/2-butanol-MIBK (0.3, 0.7/0.6, 1.4 ml)	Biphasic	150ºC, 60 min	41 mol%	41 mol%	Oil bath	Mirzaei and Karimi, 2016[a]
1 g bread crust	55.5 mM $SnCl_4$	20 ml DMSO/water (1:1 v/v)	Mono; binary	140ºC, 20 min	9.5 wt%	-	Microwave	Yu et al., 2016b
1 g bread waste	55.5 mM $SnCl_4$	20 ml DMSO/water (1:1 v/v)	Mono; binary	160ºC, 20 min	21.4 wt%	-	Microwave	Yu et al., 2017
40 mg corncob	12 mg SPTPA	2 ml GVL	Mono; unary	175ºC, 45 min	27.1 mol%	62.4 mol%	Oil bath	Zhang et al., 2017[a]
50 mg corncob			Mono; unary	175ºC, 45 min	14.8 mol%	57.6 mol%	Oil bath	
60 mg corncob			Mono; unary	175ºC, 45 min	11.4 mol%	50.8 mol%	Oil bath	
70 mg corncob			Mono; unary	175ºC, 45 min	8.5 mol%	29 mol%	Oil bath	
70 mg corncob			Mono; unary	175ºC, 60 min	6.8 mol%	22.7 mol%	Oil bath	
1 wt% corn stover (Step 1)	-	GVL/water	Mono; binary	157-217ºC ramp in 2 h	80% C_6 sugar	89% C_5 sugar	Al block	Luterbacher et al., 2014
(Step 2)	$AlCl_3$	SBP/water$_{\text{step 1}}$	Biphasic	170ºC, <20 min	60%	70%	Oil bath	
5 wt% corn stover	1 wt% $FeCl_3$	4:1 THF/water (1:1 v/v)	Mono; binary	170ºC, 80 min	45 mol%	95 mol%	Steam boiler	Cai et al., 2014[a]
0.05 g corn stover	0.1 mmol $AlCl_3{\cdot}6H_2O$	4 ml water-(0.35 g)NaCl/THF (1:3 v/v)	Biphasic	180ºC, 30 min	19 mol%	~55 mol%	Microwave	Yang et al., 2012[a]
0.4 g eucalyptus	0.1 g levulinic acid	20 g MTHF/water (1:1 wt/wt)	Biphasic	180ºC, 15 min	93 mg L^{-1}	565 mg L^{-1}	-	Seemala et al., 2016
0.05 g grass	0.1 mmol $AlCl_3.6H_2O$	4 ml water-(0.35 g)NaCl/THF (1:3 v/v)	Biphasic	180ºC, 30 min	23 mol%	66 mol%	Microwave	Yang et al., 2012[a]
1 g kiwifruit waste	55.5 mM $SnCl_4$	20 ml DMSO/water (1:1 v/v)	Mono; binary	140ºC, 20 min	13.7 wt%	-	Microwave	Yu et al., 2016a
20 g maple wood	0.1 M HCl	780 g MIBK/water (~1:1 wt/wt)	Biphasic	170ºC, 30 min	47.5 wt%	50.8 wt%	Sand bath	Zhang et al., 2013[a]
5 wt% maple wood	1 wt% H_2SO_4	Water	Mono; unary	170ºC, 40 min	2.4%	62%	Fluidized sand bath	Cai et al., 2013[a]
5 wt% maple wood	1 wt% H_2SO_4	THF/water (3:1 v/v)	Mono; binary	170ºC, 40 min	21%	87%		
5 wt% maple wood	1 wt% $FeCl_3$	4:1 THF/water (1:1 v/v)	Mono; binary	170ºC, 60 min	51 mol%	95 mol%	Steam boiler	Cai et al., 2014[a]
0.05 g pinewood	0.1 mmol $AlCl_3{\cdot}6H_2O$	4 ml water-(0.35 g)NaCl/THF (1:3 v/v)	Biphasic	180ºC, 30 min	35 mol%	~62 mol%	Microwave	Yang et al., 2012[a]
0.2 g pinewood	-	4.5-6.0 g water	Mono; unary	270ºC, 10 min	~18 wt%	~10 wt%	Salt bath	Asghari and Yoshida, 2010
0.2 g pinewood	0.1 M H_3PO_4 (pH 2)	4.5-6.0 g water	Mono; unary	270ºC, 3 min	~25 wt%	~15 wt%	Salt bath	
0.4 g pinewood	0.1 g levulinic acid	20 g MTHF/water (1:1 wt/wt)	Biphasic	180ºC, 15 min,	307 mg L^{-1}	288 mg L^{-1}	-	Seemala et al., 2016
0.4 g pinewood			Biphasic	200ºC, 15 min	803 mg L^{-1}	535 mg L^{-1}	-	
0.05 g poplar	0.1 mmol $AlCl_3.6H_2O$	4 ml water-(0.35 g)NaCl/THF (1:3 v/v)	Biphasic	180ºC, 30 min	26 mol%	51 mol%	Microwave	Yang et al., 2012[a]
25 mg straw	48 mol% sulphanilic acid	3 ml water-DMSO/2-butanol-MIBK (0.3, 0.7/0.6, 1.4 ml)	Biphasic	150ºC, 60 min	41 mol%	50 mol%	Oil bath	Mirzaei and Karimi, 2016[a]
0.76 wt% wheat straw	HCl (pH 0.21)	Water	Mono; unary	146ºC, 30 min	3.4%	66%	Microwave	Yemiş and Mazza, 2012[a]
1 g vegetable waste	55.5 mM $SnCl_4$	20 ml DMSO/water (1:1 v/v)	Mono; binary	140ºC, 20 min	4.9 wt%	-	Microwave	Yu et al., 2016a
1 g waste cooked rice	55.5 mM $SnCl_4$		Mono; binary	140ºC, 40 min	22.6 wt%	-	Microwave	
1 g waste cooked rice	55.5 mM $FeCl_3$		Mono; binary	160ºC, 20 min	18.1 wt%	-	Microwave	
1 g watermelon waste	55.5 mM $SnCl_4$		Mono; binary	140ºC, 20 min	13.1 wt%	-	Microwave	

[a] Product yield with respect to the corresponding sugar content in biomass was reported in the reference. Abbreviations: furfural (FF); dimethylacetamide (DMA); dimethyl sulfoxide (DMSO); methyl isobutyl ketone (MIBK); tetrahydrofuran (THF); methyltetrahydrofuran (MTHF); polytriphenylamine–SO_3H (SPTPA); γ--valerolactone (GVL); 2-s-butyl-phenol (SBP).

Table 2.2. Compositions of biomass feedstock for HMF production.

Biomass	Cellulose (wt%)	Hemicellulose (wt%)	Lignin (wt%)	Other (wt%)	Reference
Bagasse	43.4	21.7	20.3	7.9 (ash & wax)	Iryani et al., 2013
Barley husk	27	14	25	-	Mirzaei and Karimi, 2016
Corncob	30.2	36.9	32.9	-	Zhang et al., 2017
Corn stover	32.7 (glucan)	20.7 (xylan)	16	30.6	Cai et al., 2014
Eucalyptus	38-49	15-17	28-31	-	Seemala et al., 2016
Grass	35 (hexose)	23 (pentose)	-	-	Yang et al., 2012
Maple wood	40.9 (glucan)	15.5 (xylan)	24.4	19.2	Cai et al., 2014
Pinewood	41.7	20.6	25.9	-	Seemala et al., 2016
Poplar	45 (hexose)	29 (pentose)	-	-	Yang et al., 2012
Straw	32	27	28	-	Mirzaei and Karimi, 2016

These results highlight the significance of catalyst and solvent on the efficiency of biomass conversion to HMF, but there is insufficient information about their corresponding contribution. Such knowledge is needed to facilitate the manoeuvring of catalyst and solvent to maximize the HMF production and increase the system capacity. Thus far, relatively low feedstock loadings (≤ 5 wt%) have been adopted in most of the lab-scale studies (**Table 2.1**), which presents a hurdle to upscaling and commercialization of the conversion technology. Therefore, **Sections 2.3 and 2.4** review both experimental and computational studies to differentiate and elucidate the effects of catalyst and solvent on the consecutive as well as parallel pathways during the conversion process.

2.3 Catalysts

2.3.1 Brønsted acid

Brønsted acid can facilitate the glucan hydrolysis as well as fructose and glucose dehydration depending on the strength of acidity (**Fig. 2.2**). Their reported performances in the literature are summarized in **Table 2.3A&B**.

Table 2.3. Catalysts for conversion of model carbohydrates to HMF.

Substrate	Catalyst	HMF yield	HMF selectivity	Solvent	Conditions	Heating	Reference
A. Brønsted acid (inorganic)							
Liquid							
30 wt% fructose	0.25 M HCl	25.5 wt%	51 wt%	Water	180°C, 2.5-3 min	-	Roman-Leshkov et al., 2006[a]
27 wt% fructose	0.01 M HCl	53%	56%	Water	200°C, 1 min	Microwave	Hansen et al., 2009[b]
1 wt% fructose	HCl (pH 1.5-2.15)	38-43 mol%	-	Water	150°C, 2 h	Autoclave	de Souza et al., 2012
0.15 g fructose	0.05 M HCl	91%	92%	4.5 ml sat. KBr/MeCN (1:2 v/v)	160°C, 1 min	Microwave	Wrigstedt et al., 2016[b]
0.15 g fructose	0.05 M HCl	79%	84%		160°C, 40 min	Oil bath	
0.15 g fructose	0.05 M H_2SO_4	85%	86%		160°C, 1 min	Microwave	
0.15 g fructose	0.05 M HNO_3	87%	88%		160°C, 1 min	Microwave	
0.15 g fructose	0.05 M H_3PO_4	60%	88%		160°C, 1 min	Microwave	
0.15 g fructose	0.05 M TFA	86%	89%		160°C, 1 min	Microwave	
0.15 g fructose	Sat. NH_4Br	81%	84%	4.5 ml sat. salt/MeCN (1:2 v/v)	160°C, 2 min	Microwave	
0.15 g fructose	Sat. NH_4Cl	70%	80%		160°C, 2 min	Microwave	
0.15 g fructose	Sat. NH_4I	65%	66%		160°C, 2 min	Microwave	
250 mM glucose	100 mM HCl	9.5% HMF; 34.4% fructose	13.1% HMF; 47.5% fructose	100 mM $AlCl_3$, water	140°C, 24 min	-	Zhang et al., 2016a[b]
1 g cellulose	HCl (pH 3)	20.7 mol%	-	30 ml water	300°C, 0 min	Muffle furnace	Yin et al., 2011
Solid							
0.15 g fructose	21 mg Amberlyst-38(wet)	88%	89%	4.5 ml sat. KBr/MeCN (1:2 v/v)	160°C, 1 min	Microwave	Wrigstedt et al., 2016[b]
0.15 g fructose	26 mg Dowex-50	83%	84%		160°C, 1 min	Microwave	
100 mg glucose	40 mg Amberlite IRN-77	30.7 mol%	60 mol%	1 g [BMIM]Cl	140°C, 30 min	Oil bath	Hu et al., 2013[b]
100 mg glucose	40 mg Amberlyst-15	25.6 mol%	52 mol%		140°C, 30 min	Oil bath	
100 mg starch	40 mg CCC	42.8	-		160°C, 15 min	Oil bath	
0.1 g cellulose	30 mg PDVB	34.6-37.1 mol%	-	2 g [EMIM]-Cl	120°C, 30 min	-	Zhang et al., 2015a
B. Brønsted acid (organic)							
Liquid							
1 wt% fructose	10 wt% acetic acid	~29 mol%	~76 mol%	Water	150°C, 2 h	Autoclave	de Souza et al., 2012[b]
1 wt% fructose	20 wt% acetic acid	43 mol%	~69 mol%		150°C, 2 h	Autoclave	
1 wt% fructose	50 wt% acetic acid	~48 mol%	~57 mol%		150°C, 2 h	Autoclave	
1 wt% fructose	10 wt% formic acid	~51 mol%	~67 mol%		150°C, 2 h	Autoclave	
1 wt% fructose	20 wt% formic acid	53 mol%	~54 mol%		150°C, 2 h	Autoclave	
1 wt% fructose	20 wt% lactic acid	50 mol%	~66 mol%		150°C, 2 h	Autoclave	
1 wt% fructose	50 wt% lactic acid	64 mol%	~67 mol%		150°C, 2 h	Autoclave	
0.2 mmol glucose	2.5 mmol glycolic acid	42%	-	2.0 mmol $B(OH)_3$, 2.5 mmol choline dihydrogencitrate salt	140°C, 2 h	Dry bath	Matsumiya and Hara, 2015
0.2 mmol glucose	2.5 mmol malic acid	35%	-		140°C, 2 h	Dry bath	
0.2 mmol glucose	2.5 mmol mandelic acid	28%	-		140°C, 2 h	Dry bath	
0.2 mmol glucose	2.5 mmol oxalic acid	7%	-		140°C, 2 h	Dry bath	
0.2 mmol glucose	2.5 mmol salicylic acid	26%	-		140°C, 2 h	Dry bath	
0.2 mmol glucose	2.5 mmol succinic acid	9%	-		140°C, 2 h	Dry bath	
250 mM glucose	100 mM maleic acid	2.1% HMF; 14.9% fructose	12.2% HMF; 86.6% fructose	100 mM $AlCl_3$, water	140°C, 24 min	-	Zhang et al., 2016a[b]
0.4 g glucose	0.1 g levulinic acid	1570 mg L^{-1}	-	20 g MTHF/water (1:1 wt/wt)	180°C, 15 min	-	Seemala et al., 2016
0.4 g cellulose	0.1 g levulinic acid	555 mg L^{-1}	-		180°C, 1 h		
C. Lewis acid							

Liquid							
0.25 mmol glucose	0.1 mmol $AlCl_3•6H_2O$	22 mol%	22 mol%	1 ml water	160ºC, 10 min	Microwave	Yang et al., 2012[b]
1 g glucose	55.5 mM $AlCl_3$	25 mol%	33 mol%	20 ml DMSO/water (1:1 v/v)	140ºC, 20 min	Microwave	Yu et al., 2016b
1 M glucose	50 mM $AlCl_3$	~52 mol%	~53 mol%	1.75 ml DMSO	140ºC, 15 min	Microwave	Rasrendra et al., 2012[b]
1 M glucose	50 mM $CrCl_2$	~54 mol%	~55 mol%		140ºC, 15 min	Microwave	
1 M glucose	50 mM $CrCl_3$	~54 mol%	~55 mol%		140ºC, 15 min	Microwave	
50 mg glucose	5 mol% $CrCl_3.6H_2O$ (w.r.t. glucose)	16.6, 21.5%, 20.1%, 17.6%	-	1 ml DMSO/H_2O (X_w = 0, 0.17, 0.3, 0.50)	120ºC, 3 h	Autoclave	Jia et al., 2014
1 g glucose	55.5 mM $CrCl_3$	21 mol%	28 mol%	20 ml DMSO/water (1:1 v/v)	140ºC, 20 min	Microwave	Yu et al., 2016b
1 M glucose	50 mM $SnCl_4$	~30 mol%	~40 mol%	1.75 ml DMSO	140ºC, 15 min	Microwave	Rasrendra et al., 2012[b]
1 g glucose	55.5 mM $SnCl_4$	21 mol%	54 mol%	20 ml DMSO/water (1:1 v/v)	140ºC, 20 min	Microwave	Yu et al., 2016b
1 g glucose	55.5 mM $Zr(O)Cl_2$	12 mol%	21 mol%		140ºC, 20 min	Microwave	
5 wt% glucose	10 mol% $Zr(O)Cl_2$	39%	-	Water	120ºC, 5 min	Microwave	Saha et al., 2013
5 wt% glucose	10 mol% $RuCl_3$	32%	-		120ºC, 5 min	Microwave	
Solid							
10 wt% glucose	Sn-beta (1:50 Sn:glucose mol)	34% fructose	52% fructose	Water	90ºC, 3.5 h	Oil bath	Lew et al., 2012[b]
10 wt% glucose	Sn-beta (1:50 Sn:glucose mol)	32 wt% fructose	58 wt% fructose	1.5 g water	110ºC, 30 min	Oil bath	Moliner et al., 2010[b]
10 wt% glucose	Ti-beta (1:50 Ti:glucose mol)	14 wt% fructose	54 wt% fructose		110ºC, 1.5 h	Oil bath	
0.25 mmol glucose	10 mg LPSnP-1	34 mol%	46 mol%	3 ml water/MIBK (1:2 v/v)	140ºC, 20 min	Microwave	Dutta et al., 2014[b]
0.25 mmol glucose	10 mg LPSnP-1	50 mol%	62.5 mol%		150ºC, 20 min	Microwave	
0.25 mmol sucrose	10 mg LPSnP-1	51 mol%	53 mol%		150ºC, 20 min	Microwave	
0.25 mmol cellulose	10 mg LPSnP-1	32 mol%	-		150ºC, 20 min	Microwave	
0.25 mmol cellulose	10 mg LPSnP-1	7 mol%	-		150ºC, 20 min	Oil bath	
1 wt% sucrose	1 wt% hy-Nb-TEOA	27%	-	15 ml water	180ºC	Autoclave	Kreissl et al., 2016
1 wt% sucrose	1 wt% hy-Nb	32%	-		180ºC	Autoclave	
1 wt% sucrose	1 wt% Mesoporous Nb_2O_5	36%	-		180ºC	Autoclave	

D. Bifunctional catalyst

Substrate	**Bonsted acid**	**Lewis acid or Bronsted base**	**HMF yield**	**HMF selectivity**	**Solvent**	**Conditions**	**Heating**	**Reference**
5 wt% glucose	HCl (pH 2.5)	5 mM $AlCl_3$	62 mol%	68 mol%	Sat. NaCl:SBP (1:2 wt/wt)	170ºC, 40 min	Oil bath	Pagán-Torres et al., 2012[a]
5 wt% glucose	HCl (pH 2.5)	5 mM VCl_3	49 mol%	53 mol%		170ºC, 1.5 h	Oil bath	
5 wt% glucose	HCl (pH 2.5)	25 mM $DyCl_3$	38 mol%	41 mol%		170ºC, 2.7 h	Oil bath	
5 wt% glucose	HCl (pH 2.5)	25 mM $GaCl_3$	45 mol%	50 mol%		170ºC, 2 h	Oil bath	
5 wt% glucose	HCl (pH 2.5)	25 mM $InCl_3$	45 mol%	52 mol%		170ºC, 2.5 h	Oil bath	
5 wt% glucose	HCl (pH 2.5)	25 mM $LaCl_3$	38 mol%	44 mol%		170ºC, 4 h	Oil bath	
5 wt% glucose	HCl (pH 2.5)	25 mM $YbCl_3$	43 mol%	46 mol%		170ºC, 2 h	Oil bath	
0.15 g cellobiose	21 mg Amberlyst-38(wet)	10 mol% $CrCl_3$.6H2O	71%	-	4.5 ml sat. KBr/GVL (1:2 v/v)	175ºC, 3 min	Microwave	Wrigstedt et al., 2016
0.15 g MC cellulose	21 mg Amberlyst-38(wet)	10 mol% $CrCl_3$.6H2O	40%	-		175ºC, 3 min	Microwave	
0.15 g glucose	50 mg H-ZSM5 zeolite		42 mol%	53 mol%	5 ml water-(20 wt%)NaCl/MIBK	195ºC, 30 min	-	Moreno-Recio et al., 2016
0.1 g glucose	40 mg HZSM-5(Si/Al = 30)		16.2 mol%	46 mol%	1g [BMIM]Cl	140ºC, 30 min	Oil bath	Hu et al., 2013[b]
0.28 mmol glucose	24 mol% sulphanilic acid		16 mol%	20 mol%	3 ml water/MIBK (1:2 v/v)	150ºC, 1 h	-	Mirzaei and Karimi, 2016[b]
0.28 mmol glucose	24 mol% sulphanilic acid		78 mol%	80 mol%	3 ml water-DMSO/2-butanol-MIBK (0.3,0.7/0.6,1.4 ml)	150ºC, 1 h	-	
0.15 mmol cellulose	48 mol% sulphanilic acid		52 mol%	63 mol%		150ºC, 1 h	-	

[a] HMF yield was calculated based on the glucose conversion and HMF selectivity given by the reference (HMF yield = glucose conversion x HMF selectivity).

[b] HMF selectivity was calculated based on the glucose conversion and HMF yield given by the reference (HMF selectivity = HMF yield/glucose conversion).

Abbreviations: trifluoroacetic acid (TFA); acetonitrile (MeCN); cellulose-derived carbonaceous catalyst (CCC); polydivinylbenzene (PDVB); methyltetrahydrofuran (MTHF); dimethyl sulfoxide (DMSO); large-pore mesoporous tin phosphate (LPSnP-1); methyl isobutyl ketone (MIBK); 2-sec-butylphenol (SBP); γ--valerolactone (GVL).

2.3.1.1 Catalytic mechanisms

During the acid-catalyzed hydrolysis of polysaccharide, protons weaken the C-O-C glycosidic bond by attacking the oxygen atom of the linkage (Zhou et al., 2013). Fructose dehydration illustrates a similar catalytic mechanism as depicted by Antal et al. (1990): proton attaches to the C2 hydroxyl group of fructose to initiate the elimination of the first water molecule, resulting in a carbonium ion. Such intermediate transforms into an enol, which is subsequently condensed to give HMF by releasing two more water molecules.

Recent research suggests that Brønsted acid can simultaneously promote direct dehydration of glucose to form HMF, bypassing the glucose-fructose isomerization (Yang et al., 2015a). A cyclic mechanism for such alternative route has been proposed using Car-Parrinello based *ab initio* molecular dynamics and metadynamics simulation (Qian, 2012), and microkinetic modelling based on density function theory (DFT) (Yang et al., 2015a). According to these computational studies, the conversion process starts with protonation at the hydroxyl group of glucose C2, leading to the formation of a five-membered ring intermediate that is ready for dehydration. However, as the activation energy for the direct glucose dehydration is relatively high, e.g., 36.4 kcal mol^{-1} compared to 29.4 kcal mol^{-1} for fructose dehydration (Enslow et al., 2015), we can expect that this pathway becomes dominant only under strong Brønsted acidity. A recent study demonstrated that an acidity of pH 2.0 could produce 15% HMF from glucose in an organic solvent-water mixture with no fructose detected, whereas a slightly less acidic environment (pH 2.3) resulted in only 4% HMF (Yu et al., 2017), pointing to the insignificance of direct glucose dehydration under weak Brønsted acidity.

2.3.1.2 Inorganic acids

Mineral acids are widely used as Brønsted acid catalysts because of their low cost and easy accessibility, as well as robust handling practices in the industry. The commonly used HCl usually give a satisfactory HMF yield of 26-53% from fructose in water (**Table 2.3A**). A recent study reported a narrow range of HMF yield, i.e., 85-91%, produced from fructose using HCl, H_2SO_4, HNO_3, and trifluoroacetic acid (TFA) in a water-organic solvent medium (Wrigstedt et al., 2016; **Table 2.3A**), implying that these mineral acids shared a similar catalytic activity in fructose dehydration. However, H_3PO_4 yielded noticeably less HMF (60%), possibly due to its lower acid dissociation constants ($pK_{a1} = 2.12$) compared to other strong mineral acids (e.g., pK_a of $HNO_3 = -1.3$), leading to lower Brønsted acidity in the medium. Similarly, saturated ammonium salt as the weak acid produced a lower HMF yield of 65-81% albeit given a longer reaction time in the same study. Strong mineral acids are also applicable for cellulose conversion, for example, HCl could produce HMF of around 21% in water (Yin et al., 2011; **Table 2.3A**).

Solid Brønsted acid catalysts, which present sulfonate groups as the active sites in particular, have been successfully applied for the conversion of standard compounds. Commercial sulfonated resins, e.g., Dowex-50 and Amberlyst-38 (wet), could efficiently catalyze fructose conversion to 83% and 88% HMF, respectively, in a biphasic system (Wrigstedt et al., 2016; **Table 2.3A**). Other comparable options would be sulfonated carbon (42.8% HMF from starch in ionic liquid) (Hu et al., 2013) and sulfonated polymer, e.g., polydivinylbenzene–SO_3H (PDVB) (34.6-37.1% HMF from cellulose in ionic liquid) (Zhang et al., 2015a) (**Table 2.3A**). In addition to the strength and quantity of acid sites, the hydrophobicity of catalyst also plays a significant role in achieving high HMF productivity, through preventing the HMF-consuming side reactions induced by water (Zhang et al., 2015a). These solid catalysts could be recycled and reused 4-6 times with a trivial loss of $–SO_3H$ groups for operation ≤ 160^{o}C, e.g., < 2% drop in S content (Zhang et al., 2015a), displaying a good potential for scale-up.

2.3.1.3 Organic acids

Organic acids that present lower toxicity and higher safety than mineral acids are also evaluated for HMF production. For fructose dehydration to HMF, de Souza et al. (2012) investigated the use of lactic acid, formic acid, and acetic acid, which produced a maximum yield of 48-64% at different optimal concentrations (**Table 2.3B**). We further calculated the HMF selectivity (produced HMF/reacted fructose) based on the reported data. In case of formic acid and acetic acid, HMF selectivity dropped as the acid concentration increased despite the rise in HMF yield, implying that the higher acid loading enhanced the kinetics of the side reactions more than that of the fructose dehydration. The optimal concentration of both formic acid and acetic acid for the highest HMF selectivity was 10 wt% in this study (de Souza et al., 2012). In contrast, HMF selectivity remained constant over the increasing dosage of lactic acid. It is noted that at a constant HMF yield ~50%, formic acid and lactic acid showed a similar HMF selectivity (~67%), which was higher than that of acetic acid (57%). These comparisons suggest that the catalysts promote fructose dehydration over side reactions to different degrees and thus lead to distinctive HMF selectivity under different conditions, probably depending on the pK_a and electrochemical characteristics of the parent chain. Nevertheless, negligible HMF was produced from glucose conversion (de Souza et al., 2012), implying that these mild organic acids were unable to facilitate the isomerization or direct dehydration of glucose in the studied system.

To convert glucose to HMF, Matsumiya and Hara (2015) evaluated a range of carboxylic acids in the presence of an isomerization promoter (boric acid) and choline salt (**Table 2.3B**). Glycolic acid generated the highest HMF yield (42%), followed by malic acid (35%), mandelic acid (28%), salicylic acid (26%), succinic acid (9%) and oxalic acid (7%). Interestingly, although these organic acids are considered weak (pK_a = 1.27-4.21; Matsumiya and Hara, 2015), they incurred significant off-path reactions that an inverse relationship between HMF yield and acid strength was observed (Matsumiya and Hara, 2015). These results contrasted the ineffective glucose conversion observed by de Souza et al. (2012), despite comparable acid strength of the tested candidates. This implies the significance of co-catalysts.

Synergistic effect between maleic acid and $AlCl_3$ (an isomerization catalyst) has been reported recently (Zhang et al., 2016a), which enhanced the total selectivity of fructose and HMF to 98.8% in comparison to 60.6% in the $HCl/AlCl_3$ system (**Table 2.3A&B**). Maleic acid could facilitate a higher rate of HMF formation than humin production by forming a favourable complex with $AlCl_3$ (Zhang et al., 2016a), which reduced the activation energy for glucose isomerization to 94.5 kJ mol^{-1} (**Table 2.4**). Yet, the low product yields (2.1% HMF; 14.9% fructose; **Table 2.3B**) and the high activation energy for fructose dehydration (158 kJ mol^{-1}; **Table 2.4**) over maleic acid/$AlCl_3$ may indicate the slow kinetics of glucose conversion in this studied co-catalyst system.

Seemala et al. (2016) recently applied levulinic acid (pKa = 4.17) to achieve 1570 and 555 mg L^{-1} HMF from glucose and cellulose, respectively, at a higher temperature of 180^{o}C (**Table 2.3B**). While the authors proposed that levulinic acid acted as a Lewis acid (**Section 2.3.2**) to facilitate the isomerization pathway, there was another possibility that the weak acid may promote the direct glucose dehydration to HMF under sufficiently high energy supply (Yu et al., 2016a, 2017).

Table 2.4. Activation energies based on kinetics of different catalytic reaction steps in different solvents.

Medium	**Catalytic Conditions**	E_a **(kJ mol^{-1})**	**Remarks**	**Reference**
Cellulose→glucose				
GVL/H_2O (1:1)	H_2SO_4	118	Cellobiose→glucose; apparent E_a	Mellmer et al., 2014
GVL/H_2O (4:1)	H_2SO_4	81		
Water	H_2SO_4	131		
Glucose→fructose				
[BMIM]Cl	CCC; 120-160ºC	97.9	Glucose conversion	Hu et al., 2013
DMSO	$Al(OTf)_3$ (50 mM); 100-140ºC	138	Glucose conversion	Rasrendra et al., 2012
Water	$AlCl_3$; 100-130ºC	110±2	Apparent E_a	Tang et al., 2015
Water	$CrCl_3$	100±5		Swift et al., 2015
Water	$CrCl_3$	104 (simulated value); 112 (experimental value)	Hydride shift; free energy of activation	Mushrif et al., 2014
Water	$CrCl_3$ (3 mol% w.r.t. glucose)	64	Glucose conversion; apparent E_a	Choudhary et al., 2013
Water	$Nb^{5+}/WO_3 \cdot H_2O$	106	Hydride shift	Li et al., 2016a
Water	$WO_3 \cdot H_2O$	98		
Water	$WO_3 \cdot H_2O$	159		
Water	$Ta^{5+}/WO_3 \cdot H_2O$	96		
Water	$Ti^{4+}/WO_3 \cdot H_2O$	52		
Water	$V^{5+}/WO_3 \cdot H_2O$	138		
Water	$Zr^{4+}/WO_3 \cdot H_2O$	46		
Water	HCl and $AlCl_3$	149		Zhang et al., 2016a
Water	Maleic acid and $AlCl_3$	94.5		
SBP/sat. NaCl (2:1 wt/wt)	$AlCl_3$	125±3	Glucose conversion; apparent E_a	Wang et al., 2015
	$DyCl_3$	121±2		
	$GaCl_3$	93±3		
	$InCl_3$	128±18		
	$LaCl_3$	169±10		
	$YbCl_3$	87±3		
Fructose→HMF				
Water	HCl and $AlCl_3$	128		Zhang et al., 2016a
Water	Maleic acid and $AlCl_3$	158		
HMF→levulinic acid + formic acid				
Water	HCl and $AlCl_3$	72.1		Zhang et al., 2016a
Water	Maleic acid and $AlCl_3$	51.1		
Humin formation				
Water	$CrCl_3$	114±6	Fructose→humins	Swift et al., 2015
Water	$CrCl_3$	71±19	Glucose→humins	
Water	$CrCl_3$	56±9	HMF→humins	
Water	Maleic acid and $AlCl_3$	112	Fructose→humins	Zhang et al., 2016a
Water	Maleic acid and $AlCl_3$	69.9	HMF→humins	
Water	HCl and $AlCl_3$	106	Fructose→humins	
Water	HCl and $AlCl_3$	89.1	HMF→humins	

Abbreviations: γ--valerolactone (GVL); 2-s-butyl-phenol (SBP); dimethyl sulfoxide (DMSO); cellulose-derived carbonaceous catalyst (CCC).

2.3.2 Lewis acid

Lewis acid is able to catalyze isomerization of glucose into fructose (**Fig. 2.2**), of which the performances are summarized in **Table 2.3C**. It is a critical step for conversion of polymeric carbohydrates/biomass, because glucose released from glucan hydrolysis has a stable six-membered pyranose structure against the dehydration reaction (Hu et al., 2013; Carraher et al., 2015) while fructose is more reactive.

2.3.2.1 Catalytic mechanisms

The catalytic mechanism of glucose isomerization in an aqueous system has been elucidated by means of isotope labelling and nuclear magnetic resonance (NMR) spectroscopy (Binder et al., 2010; Román-Leshkov et al., 2010), molecular dynamics (Mushrif et al., 2014), and DFT (Li et al., 2016a). During the catalysis, Lewis acid facilitates the ring opening of the glucose, which then forms a complex with the acyclic glucose at its hydroxyl oxygen at C1 and C2. Such coordination allows the electron-deficient Lewis acid to polarize the carbonyl group (C1 of glucose), hence promoting the transfer of hydride from C2 to C1 to form fructose. This mechanism is applicable for different types of Lewis acid catalysts, including $CrCl_3$ (Mushrif et al., 2014), $AlCl_3$ (Tang et al., 2015), other trivalent metal chlorides (e.g., $GaCl_3$ and $InCl_3$) (Nguyen et al., 2016), Sn-containing zeolite (Li et al., 2014), as well as Ti^{4+}- and Zr^{4+}-doped tungstite (Li et al., 2016a).

In the medium of dimethyl sulfoxide (DMSO), a similar mechanism featuring the critical hydride transfer is postulated for the ionic liquid-catalyzed isomerization using NMR spectroscopy (Amarasekara and Razzaq, 2014). Yet, in the medium of ionic liquid, the hydride shift from O2 instead of C2 to C1 is driven by the Lewis acid metal chlorides, and the ring opening of glucose is suggested to be the rate-limiting step (Guan et al., 2011), contrary to the hydride shift as the rate-limiting step in the aqueous system (Mushrif et al., 2014; Tang et al., 2015).

2.3.2.2 Metal salts and minerals

Rasrendra et al. (2012) demonstrated that chlorides of chromium ($CrCl_3$ and $CrCl_2$) and aluminium ($AlCl_3$) gave the best performance in glucose conversion in DMSO, achieving a HMF yield of ~54% and ~52%, respectively, followed by $SnCl_4$ that produced ~30% HMF (**Table 2.3C**). These metals have also proved promising in other experimental studies using water-containing medium (Jia et al., 2014; Yu et al., 2016b; **Table 2.3C**). Some metals were less effective. For example, $CuCl_2$ produced no HMF from glucose and $ZnCl_2$ reached only ~6% HMF in an organic solvent (Rasrendra et al., 2012), as well as < 5% HMF from glucose in water-organic solvent mixture (Yu et al., 2016b). However, factors that contribute to the variation in their performance require further elucidation.

By means of DFT calculation and X-ray absorption spectroscopy (XAS), the formation of complex between the metal centre and glucose via ligand exchange was confirmed as a prerequisite for the isomerization step in ionic liquid (Pidko et al., 2010). The exchange between the Cl^- ligand of Cr^{2+} and the hydroxyl group of glucose was thermodynamically feasible, while such coordination was not favourable between Cu^{2+} and glucose. This corroborated the abovementioned experimental results that Cr^{2+} was promising in glucose isomerization but Cu^{2+} was inactive. The coordination feasibility may depend on the electrochemical properties of the metals. Recent experimental studies suggested that metal with a higher charge density catalyzed glucose conversion more effectively, due to its stronger electrostatic interaction with the sugar (Wang et al., 2015; Yu et al., 2016b). The metals exhibiting higher hardness also tended to interact with the hard hydroxyl group of glucose for favourable complex formation. The water exchange rate that represented the tendency of water ligand to be substituted from the metal centre also governed the formation of metal-glucose complex in an aqueous system (Wang et al., 2015). Furthermore, the speciation of metals in the system played an important role as only particular species was active for catalysis such as $[Cr(H_2O)_5OH]^{2+}$ (Choudhary et al., 2013; Swift et al., 2015; Mushrif et al., 2014) and $[Al(OH)_{2(aq)}]^+$ (Tang et al., 2015). These postulations should be verified by more mechanistic studies to establish a sound understanding on the critical catalytic properties for tailoring the biomass conversion systems.

Some solid Lewis acid catalysts are also effective for conversion of standard carbohydrates. Moliner et al. (2010) demonstrated the efficacy of metal-containing zeolites in water, i.e., Sn-beta and Ti-beta, which achieved a fructose yield of 32% and 14% from glucose, respectively (**Table 2.3C**). A similar yield of fructose (34%) was obtained from glucose over Sn-beta in another study (Lew et al., 2012). The framework tetrahedral Sn sites on Sn-beta acted as a Lewis acid to facilitate isomerization via 1,2-hydride shift (**Section 2.3.2.1**). Apart from the metal species, the hydroxyl groups neighbouring the metal centre also played a critical role in facilitating the rate-determining hydride shift by exerting stabilization effect, as revealed by a DFT study on Sn-containing zeolites (Li et al., 2014). Such hydroxyl group was derived from water molecule coordinated to the metal centre or from the proximate silanol group (Si-O-H) on the zeolite.

Other solid catalysts such as mesoporous Sn phosphate also gave a high HMF yield of 50% from glucose in the biphasic system (Dutta et al., 2014) (**Table 2.3C**). Sucrose and cellulose could be converted to 51% and 32% HMF, respectively. Similarly, sucrose was transformed to 27-36% HMF over Nb oxides with varying Lewis acidity (108-269 $\mu mol\ g^{-1}$) (Kreissl et al., 2016). Despite the coexisting

Brønsted acid sites on both Sn phosphate and Nb oxides, the contribution of Lewis acid sites to the hydrolysis reaction should not be overlooked.

The catalytic activity of metals on the hydrolysis of glycosidic bond (**Fig. 2.2**) was assessed apart from glucose isomerization. A previous study found that the paired $CuCl_2$/$PdCl_2$ was more effective for cellulose hydrolysis than the strong mineral acid H_2SO_4 and HCl at the same molar loading under similar conditions (Su et al., 2011), suggesting the synergistic effect arising from proton release upon the hydrolysis of metal-coordinated water as well as the enhancement of solvent structure. Yu et al. (2016b) further depicted a positive relationship between the medium pH and HMF yield resulting from disaccharide conversion over a range of metal chlorides ($AlCl_3$, $FeCl_3$, $InCl_3$, $SnCl_4$, $ZrCl_4$, etc). In addition, it was possible that the metal attacked the C-O-C linkage in similar fashion to the proton-mediated hydrolysis mechanism (Yu et al., 2016b).

Lewis acid site indirectly promotes fructose dehydration (**Fig. 2.2**) with the Brønsted acid derived from metal hydrolysis in water as mentioned above (Jia et al., 2014; Yu et al, 2016b). The protons released from metal hydrolysis in the aqueous medium can attack the hydroxyl group of fructose to initiate the elimination of water molecules as described in **Section 2.3.1.1**. However, such indirect catalytic function may vary with the selection of reaction solvents. For example, metal hydrolysis of $Zr(O)Cl_2$/$CrCl_3$ was not possible in both dimethylacetamide (DMA)-LiCl and DMA-LiCl-water mixture (Dutta et al., 2012). Besides, the metal centre with a higher electronegativity tended to promote fructose dehydration to HMF, indicating the involvement of the metal centre in the catalysis (Yu et al., 2016b). The metal may coordinate and polarize a carbonium intermediate to facilitate the rate-limiting step, i.e., an internal hydride transfer. Higher electronegativity of the metal catalysts may result in more polar bonds with the intermediate that favour the internal transfer of hydride.

2.3.3 Bifunctional catalysts

As hydrolysis and dehydration are catalyzed by Brønsted acid whereas isomerization is facilitated by Lewis acid, a catalyst with the two types of catalytic sites is desirable to facilitate the one-pot conversion of glucose and polymeric carbohydrate, e.g., starch and cellulose. For example, $SnCl_4$ that possessed strong Brønsted acidity and moderate Lewis acidity could convert bread waste and glucose to ~21% HMF under heating for 20 min at 160 and 140^oC, respectively (Yu et al., 2016b, 2017; **Table 2.1 & 2.3C**). The latest studies have proposed the combined uses of metal chloride and mineral acid (or solid acid) to catalyze the production of HMF from glucose and cellulose (**Table 2.3D**). For example, a promising HMF yield of 40% was produced from cellulose over Amberlyst 38 and $CrCl_3$ (Wrigstedt et al., 2016). Sulphanilic acid as an organocatalyst with an appropriate balance of acidity and basicity also accomplished a high HMF yield of 52% from cellulose (Mirzaei and Karimi, 2016), demonstrating the effectiveness of bifunctional catalyst. It could be reused for at least five runs without significant compromise in the performance. Another Lewis-Brønsted acid catalyst was exemplified by the H-ZSM-5 zeolite, which yielded HMF of 42% from glucose in a biphasic system (Moreno-Recio et al., 2016).

It is highly important that the Lewis-to-Brønsted acid (L:B) ratios (as summarized in **Table 2.5**) should be manoeuvred to promote a faster kinetics of the desirable reactions (i.e., hydrolysis, isomerization, and dehydration) relative to those of the undesirable pathways (i.e., rehydration and polymerization) for high HMF productivity (Yu et al., 2017). Lewis acid could induce more pronounced polymerization compared to Brønsted acid, despite its enhancement on glucose isomerization. For instance, the rate coefficients of the polymerization reactions mediated by $AlCl_3$ (0.08-0.23 min^{-1}) were higher than HCl (0.05-0.13 min^{-1}) in an aqueous medium (Zhang et al., 2015b). This kinetic information substantiated the experimental findings of previous study (Ordomsky et al., 2013), where the HMF selectivity increased from ~27 to ~55% as the L:B ratio of phosphate catalyst decreased from 5.3 to 1 in water (**Table 2.5**).

Table 2.5. Lewis:Brønsted (L:B) ratios of catalysts for conversion of standard glucose to HMF.

L:B (mol/mol)	HMF selectivity (mol)	HMF yield (mol%)	Glucose conversion (mol%)	Catalyst	Conditions	Reference
1.0	**~55**	**~11**	**20**	NbPO-f	Water, 135°C	Ordomsky et al., 2013[a,b]
1.6	~50	~10	20	TiPO		
2.3	~46	~9.2	20	ZrPO/Si		
3.7	~34	~6.8	20	NbPO		
5.3	~27	~5.4	20	ZrPO		
0.5	57.7	14.1	24.4	NbPO-pH2	Water, 140°C, 1 h	Zhang et al., 2015c[b]
1.4	**49.3**	**33.6**	**68.1**	NbPO-pH7		
1.9	35.1	32.6	93.1	Na-NbPO-pH7		
4.5	60.3	7.3	12.1	NbPO-pH10		
14.3	35.6	18.2	50.9	Nb_2O_5		
1.1	58.6	51.4	87.7	$Nb_{0.40}Al_{0.60}Si_{25}O$	Sat. NaCl/THF (biphasic), 160°C, 1.5 h	Li et al., 2016b[b]
1.4	68	55.9	82.2	$Nb_{0.30}Al_{0.70}Si_{25}O$		
1.5	**71.5**	**57.8**	**80.8**	$Nb_{0.15}Al_{0.85}Si_{25}O$		
0.8	67.1	46	68.6	AlSiO-20/B		
2.1	48.5	47.9	98.8	AlSiO-10		
3.3	30	28.9	96.3	AlSiO-20/L		
3.8	**68.8**	**63.1**	**91.7**	AlSiO-20		
7.7	68.7	48.5	70.6	Na-AlSiO-20		
0.5	44.6	21.5	88.2	NbPO-pH2		
1.0	**39.8**	**38.2**	**95.9**	Al-NbPO-pH2		
0.25	8.5	~5.1	~60	H-ZSM-5	Water/MIBK (biphasic), 195°C, 2.5 h	Moreno-Recio et al., 2016[a]
0.7	**30**	**~29**	**~97**	Fe-ZSM-5		
2.5	26	~26	~100	Cu-ZSM-5		
Not Detected	-	13	-	Nb_2O_5	Water, 180°C	Kreissl et al., 2016[c]
Brønsted	-	18	-	HNb_3O_8		
0.6	-	28	-	hy-Nb-TEOA		
0.7	-	**36**	-	Mesoporous Nb_2O_5		
1.0	-	32	-	hy-Nb		

[a] HMF yield was calculated based on the glucose conversion and HMF selectivity given by the reference (HMF yield = glucose conversion x HMF selectivity).

[b] L:B ratio was converted from the B:L ratio given in the reference.

[c] Maximum yields were reported; L:B ratios were calculated based on the acid site numbers given by the reference.

Abbreviations: Lewis-to-Brønsted acid (L:B) ratio; tetrahydrofuran (THF); methyl isobutyl ketone (MIBK).

Remarks: optimum L:B ratio (in bold) was selected considering both the selectivity and yield of HMF.

The enhanced selectivity implied that the HMF-forming reactions became more competitive over the HMF-consuming reactions, due to the reduction in Lewis acid sites from an excess. It is worth noting that a balance between the acids instead of a decreasing L:B ratio is favourable, because the curve of HMF selectivity against L:B ratio exhibited a volcano shape (Li et al., 2016b). However, the optimal L:B ratio may vary from 0.7 to 3.8 in conversion systems with different solid catalysts and solvent mixtures (**Table 2.5**). This suggests that the solvent characteristics as well as other catalyst properties, e.g., porosity and hydrophobicity, may also contribute to the HMF selectivity.

In addition to the L:B ratios, the strength of acids should be carefully selected. In cases of silica-alumina composite (AlSiO) and Nb oxides as catalysts, weak Lewis acid sites (Li et al., 2016b) and weak Brønsted acid sites (Kreissl et al., 2016) selectively promoted the desirable glucose isomerization and fructose dehydration, respectively. Yet the strong ones tended to reduce the product selectivity by inducing prominent side reactions. Based on these findings, we may speculate that the desirable pathways are less sensitive to the strength of catalyst in comparison to the side reactions.

Moreover, the interplay between the Lewis and Brønsted acidity should be taken into account. Maleic acid (Brønsted organic acid) could form a complex with $AlCl_3$ (Lewis acid) to lower the activation energy for glucose isomerization and thus enhance the HMF selectivity (as discussed in **Section 2.3.1.3**) and the proposed reaction mechanisms can be referred to Zhang et al. (2016a). Previous studies reported that excessive Brønsted acidity supressed the effectiveness of Lewis acid for glucose isomerization by reducing the equilibrium concentration of the required metal species

(Choudhary et al., 2013) or restraining the coordination between glucose and Lewis acid site (Matsumiya and Hara, 2015; Wrigstedt et al., 2015). Future studies are needed to investigate the kinetic change of HMF selectivity (**Table 2.5**) at the same glucose conversion in different solvent systems for optimizing the parameter of L:B ratio and acid strength.

2.4 Solvents

Solvent may serve multiple roles during the biomass conversion: (i) dissolving the substrates and catalyst for desirable reactions; (ii) stabilizing the substrates, intermediates, and products to enhance the thermodynamic equilibrium for higher product yield; and (iii) acting as catalyst to improve the reaction kinetics. The performances of commonly studied solvents are summarized in **Table 2.6**.

2.4.1 Polar protic solvent – subcritical water

Water is an example of polar protic solvents, which provide protons and high polarity. Subcritical water is defined as liquid water under pressure at a temperature between 100 °C and the critical temperature, i.e., 374°C. A previous study reported maximum HMF yield of 46% from fructose at 220°C and 30% from glucose at 240°C in catalyst-free subcritical water for 10 min (Möller et al., 2012; **Table 2.6A**). Apart from serving as the reaction medium, subcritical water also catalyzed different reaction steps by offering protons and hydroxyl ions, as the result of decreased dielectric constant and increased ionic products upon temperature increase (Möller et al., 2012; 2013). Organic acids as the decomposition products also turned the medium acidic (~pH 3.5) for autocatalysis (Asghari and Yoshida, 2010).

Table 2.6. Solvents for conversion of model carbohydrates to HMF.

Substrate	Solvent	Phase system	HMF yield	HMF selectivity	Catalyst	Conditions	Heating	Reference
A. Subcritical water								
55.5 mM fructose	15 ml water	Mono; unary	46 mol%	49.1 mol%	-	220 ºC, 10 min	Microwave	Möller et al., 2012
55.5 mM glucose	15 ml water	Mono; unary	29.5 mol%	36.3 mol%	-	240 ºC, 10 min	Microwave	
0.2 g cellulose	4.5-6.0 g water	Mono; unary	~12 wt%	-	-	270ºC, 7 min	Salt bath	Asghari and Yoshida, 2010
0.2 g cellulose	4.5-6.0 g water	Mono; unary	~25 wt%	-	PO^{4-} buffer (pH 2)	270ºC, 2 min	Salt bath	
MCC (equiv. 62 mM glucose)	15 ml water	Mono; unary	4.4 mol%	-	-	185ºC, 1 h	Microwave	Möller et al., 2013
MCC (equiv. 62 mM glucose)	15 ml water	Mono; unary	12.1 mol%	-	-	185ºC, 1.8 h	Microwave	
MCC (equiv. 308 mM glucose)	15 ml water	Mono; unary	5.7 mol%	-	-	185ºC, 1.8 h	Microwave	
B. Dimethyl sulfoxide (DMSO)								
50 mg fructose	1 ml DMSO	Mono; unary	67.2%	~70%	-	130ºC, 1 h	Autoclave	Jia et al., 2014[b]
0.38 g fructose	5 g DMSO	Mono; unary	93 mol%	93 mol%	Amberlyst-70	140ºC, 1 h	Oil bath	Morales et al., 2014[b]
0.5 g fructose	6 ml DMSO	Mono; unary	91.2%	91.2%	0.4 g Glu-TsOH	130ºC, 1.5 h	-	Wang et al., 2011
1 M glucose	1.75 ml DMSO	Mono; unary	~52 mol%	~53 mol%	50 mM $Al(OTf)_3$	140ºC, 15 min	Microwave	Rasrendra et al., 2012[b]
0.38 g glucose	5 g DMSO	Mono; unary	33.7 mol%	33.7 mol%	Amberlyst-70	147ºC, 24 h	Oil bath	Morales et al., 2014[b]
50 mg glucose	1 ml $DMSO/H_2O$ ($X_w = 0.17$)	Mono; binary	35%	-	5 mol% $CrCl_3.6H_2O$	130ºC, 3 h	Autoclave	Jia et al., 2014
0.1 g cellulose	5 g DMSO	Mono; unary	31.2%	-	$AlCl_3/H_2SO_4$ (8.2 mg, 23 mg)	150ºC, 9 h	Oil bath	Xiao et al., 2014
0.1 g cellulose	5 g DMSO/[BMIM]Cl (9:1 wt/wt)	Mono; binary	54.9%	-	8.2 mg $AlCl_3$	150ºC, 9 h	Oil bath	
C. Tetrahydrofuran (THF)								
0.15 g fructose	4.5 ml sat. KBr/THF (1:2 v/v)	Biphasic	76%	80%	1 M HCl	160ºC, 1 min	Microwave	Wrigstedt et al., 2016[b]
0.2 g glucose	8 ml THF/sat. NaCl (3:1 v/v)	Biphasic	65.7 mol%	71 mol%	0.2 g $Nb_{0.15}Al_{0.85}Si_{25}O$	160ºC, 1.5 h	Autoclave	Li et al., 2016b
0.2 g glucose	8 ml THF/sat. NaCl (3:1 v/v)	Biphasic	65.3 mol%	68.5 mol%	0.2 g $Nb_{0.30}Al_{0.70}Si_{25}O$	160ºC, 1.5 h	Autoclave	
0.2 g glucose	8 ml THF/sat. NaCl (3:1 v/v)	Biphasic	56.0 mol%	57.3 mol%	0.2 g $Nb_{0.40}Al_{0.60}Si_{25}O$	160ºC, 1.5 h	Autoclave	
0.25 mmol glucose	4 ml THF/water (3:1 v/v)	Biphasic	52%	53%	0.1 mmol $AlCl_3 \cdot 6H_2O$	160ºC, 10 min	Microwave	Yang et al., 2012[b]
0.25 mmol glucose	4 ml THF/water-(0.35 g)NaCl (3:1 v/v)	Biphasic	61%	62%		160ºC, 10 min	Microwave	
1 g cellulose	44 ml THF/water (10:1 v/v)	Biphasic	53.2 mol%	-	$NaHSO_4/ZnSO_4$ (1.8, 2.8 mmol)	160ºC, 1 h	-	Shi et al., 2013
5 g cellulose	44 ml THF/water (10:1 v/v)	Biphasic	42.5 mol%	-		160ºC, 1 h		
D. Methyl isobutyl ketone (MIBK)								
30 wt% fructose	3 g MIBK/water (1:1 wt/wt)	Biphasic	54.6 wt%	60 wt%	0.25M HCl	180ºC, 2.5-3 min	-	Roman-Leshkov et al., 2006[a]
30 wt% fructose	4.5 g MIBK/water (2:1 wt/wt)	Biphasic	54.8 wt%	73 wt%	0.25M HCl	180ºC, 2.5-3 min	-	
30 wt% fructose	3 g MIBK/water-DMSO(8:2) (1:1 wt/wt)	Biphasic	63 wt%	67 wt%	0.25M HCl	180ºC, 2.5-3 min	-	

50 wt% fructose	3 g MIBK/water (1:1 wt/wt)	Biphasic	30.6 wt%	47 wt%	0.25M HCl	180ºC, 2.5-3 min	-	
50 wt% fructose	3 g MIBK-2-butanol(7:3)/water (1:1 wt/wt)	Biphasic	41.9 wt%	59 wt%	0.25M HCl	180ºC, 2.5-3 min	-	
0.9 g fructose	10 ml MIBK/water (4:1 v/v)	Biphasic	74 mol%	76%	-	160ºC, 2 h	Autoclave	Ma et al., 2015[b]
5 wt% glucose	MIBK/Water (1:1 v/v)	Biphasic	42%	-	10 mol% Zr(O)Cl$_2$	120ºC, 5 min	Microwave	Saha et al., 2013
5 wt% glucose	MIBK/Water (1:1 v/v)	Biphasic	35%	-		120ºC, 1 h	Oil bath	
5 wt% sucrose	MIBK/Water (1:1 v/v)	Biphasic	39%	-		120ºC, 5 min	Microwave	
5 wt% starch	MIBK/Water (1:1 v/v)	Biphasic	19%	-		120ºC, 5 min	Microwave	
0.25 mmol cellobiose	3 ml MIBK/water (2:1 v/v)	Biphasic	39 mol%	41 mol%	10 mg LPSnP-1	150ºC, 20 min	Microwave	Dutta et al., 2014[b]
E. Dimethylacetamide (DMA)								
0.5 g fructose	6 ml DMA	Mono; unary	60.4%	62.3%	0.4 g Glu-TsOH	130ºC, 1.5 h	-	Wang et al., 2011
1 mmol glucose	5 ml DMA	Mono; unary	59.6%	64%	7 mol% CrCl$_3$	120ºC, 1 h	Oil bath	Yang et al., 2015b[b]
4 wt% cellulose fibre	DMA-(10 wt%)LiCl	Mono; unary	24%	-	20 mol% CrCl$_3$	120ºC, 5 min	Microwave	Dutta et al., 2012
4 wt% cellulose fibre	DMA-(10 wt%)LiCl	Mono; unary	30%	-	20 mol% Zr(O)Cl$_2$	120ºC, 5 min	Microwave	
4 wt% cellulose fibre	DMA-(10 wt%)LiCl	Mono; unary	21%	-	20 mol% AlCl$_3$	120ºC, 5 min	Microwave	
4 wt% cellulose fibre	DMA-(10 wt%)LiCl/ [BMIM]Cl (1.3:1 wt/wt)	Mono; binary	57%	-	20 mol% Zr(O)Cl$_2$/CrCl$_3$ (3:1 mol/mol)	120ºC, 5 min	Microwave	
F. Ionic liquid (IL)								
5 wt% glucose	[BMIM]Cl/MIBK (1:1 v/v)	Biphasic	66%	-	10 mol% Zr(O)Cl$_2$	120ºC, 5 min	Microwave	Saha et al., 2013
5 wt% glucose		Biphasic	53%	-		120ºC, 1 h	Oil bath	
100 mg glucose	1 g [BMIM]Cl	Mono; unary	28.4 mol%	57 mol%	40 mg Cs$_{2.5}$H$_{0.5}$PW$_{12}$O$_{40}$	140ºC, 30 min	Oil bath	Hu et al., 2013[b]
100 mg glucose	1 g [BMIM]Cl	Mono; unary	25 mol%	51 mol%	40 mg (SO$_4$)$^{2-}$/TiO$_2$-ZrO$_2$	140ºC, 30 min	Oil bath	
100 mg glucose	1 g [BMIM]Cl	Mono; unary	46.4 mol%	-	40 mg CCC	160ºC, 15 min	Oil bath	
50 mg glucose	0.5 g [C$_2$OHmim]Cl-IL4	Mono; binary	~90%	-	2.3 mg CrCl$_2$	100ºC, 2 h	-	Siankevich et al., 2016
50 mg starch	1 g [C$_2$OHmim]Cl-IL4	Mono; binary	51%	-	16 mg CrCl$_2$	140ºC, 4 h	-	
100 mg cellulose	1 g [C$_2$OHmim]Cl-IL4	Mono; binary	38%	-	10 mg CrCl$_2$	140ºC, 4 h	-	
100 mg cellulose	1 g [C$_2$OHmim]Cl-IL4/DME[c]	Biphasic	62%	-	10 mg CrCl$_2$, 11 mg acidic IL	140ºC, 4 h	-	
100 mg cellulose	1 g [C$_2$OHmim]Cl-IL4/MIBK[c]	Biphasic	51%	-		140ºC, 4 h	-	
100 mg cellulose	1 g [BMIM]Cl	Mono; unary	40.5 mol%	-	40 mg CCC	160ºC, 15 min	Oil bath	Hu et al., 2013
G. Others								
0.5 g fructose	6 ml DMF	Mono; unary	59.7%	60.7%	0.4 g Glu-TsOH	130ºC, 1.5 h	-	Wang et al., 2011
0.5 g fructose	6 ml NMP	Mono; unary	85.8%	87.6%	0.4 g Glu-TsOH	130ºC, 1.5 h	-	

[a] HMF yield was calculated based on the glucose conversion and HMF selectivity given by the reference (HMF yield = glucose conversion x HMF selectivity).

[b] HMF selectivity was calculated based on the glucose conversion and HMF yield given by the reference (HMF selectivity = HMF yield/glucose conversion).

[c] Replacement of organic solvent for every 80 min.

Abbreviations: microcrystalline cellulose (MCC); dimethyl sulfoxide (DMSO); carbon based acid catalyst (Glu-TsOH); methyl isobutyl ketone (MIBK); large-pore mesoporous tin phosphate (LPSnP-1); tetrahydrofuran (THF); dimethylacetamide (DMA); ionic liquid (IL); cellulose-derived carbonaceous catalyst (CCC); 1,2-dimethoxyethane (DME); dimethylformamide (DMF); N-methylpyrrolidone (NMP).

Nonetheless, a lower yield of HMF (4-12%) resulted from cellulose even at a higher temperature (270°C) or longer retention time (1-1.8 h) in similar studies, unless Brønsted acid was added (Asghari and Yoshida, 2010; Möller et al., 2013; **Table 2.6A**). The conversion of cellulose is usually challenging owing to its stable crystalline structure constructed by extensive intra- and inter-molecular hydrogen bonds, as well as stacking forces including van der Waals interactions, π-π interactions, and hydrophobic attraction (Parthasarathi et al., 2011). In aqueous systems, as the off-path rehydration of HMF is favourable in the presence of water, the formation of levulinic acid and formic acid as rehydration products was widely reported (Yin et al., 2011; Möller et al., 2012).

2.4.2 Polar aprotic solvents

This category of solvents has moderate polarity but no acidic hydrogen. They have attracted great attention in view of their promising performance for HMF production.

2.4.2.1 Dimethyl sulfoxide

In dimethyl sulfoxide (DMSO), Jia et al. (2014) obtained an HMF yield of 67% from fructose at 130°C without the addition of catalyst, while the others reported a higher yield >90% in the presence of Brønsted acid, e.g., Amberlyst-70 and sulfonated carbon, under similar conditions (Wang et al., 2011; Morales et al., 2014; **Table 2.6B**). The HMF production in DMSO was significantly more effective than the aqueous catalytic system (38-53% HMF; **Table 2.3A**). Solvation modelling revealed that the fructose dehydration was thermodynamically more favourable in DMSO than in water, for which the Gibbs free energy at room temperature was -36 and -26 kcal mol^{-1} (-151 and -109 kJ mol^{-1}), respectively (Choudhary et al., 2012). The free energy further dropped to -42 kcal mol^{-1} (-176 kJ mol^{-1}) at 120°C in DMSO, while it remained almost unchanged in water.

The enhanced thermodynamics of fructose dehydration in DMSO may pertain to the favourable solvation of substrate and product that result in high reactivity and stability. Fructose maintained in the furanose form (five-membered ring) in DMSO that can be readily dehydrated (Binder et al., 2010; Mirzaei and Karimi, 2016). According to a computational study, fructose interacts more strongly with the sulfonyloxygen of DMSO than water oxygen via hydrogen bonding (Mushrif et al., 2012). The DMSO molecules preferentially arrange themselves in the immediate vicinity of hydrogen atoms of the hydroxyl groups, enabling proton attack on fructose to initiate dehydration. In addition, the strong dehydration ability of DMSO due to its anhydrous nature (Jia et al., 2014) may also shift the equilibrium to the product side and facilitate the water elimination from fructose.

The suppression of side reactions in DMSO is important to secure the product yield and selectivity (Wang et al., 2011). Such advantage of DMSO was ascribed to the appropriate coordination with the carbonyl group of HMF (Mushrif et al., 2012), which alleviated HMF rehydration and humin formation. A computational simulation study indicated a reduced susceptibility of HMF to nucleophlic attack and side reactions upon solvation in DMSO (Tsilomelekis et al., 2014), because the lowest unoccupied molecular orbital energy of HMF was higher in DMSO than in water. The reduction in HMF rehydration was also attributed to the low water content in the solvent (Rasrendra et al., 2012; Morales et al., 2014). However, such hygroscopic property facilitated undesirable condensation reactions such as formation of anhydroglucose (Morales et al., 2014).

In addition, DMSO may play a catalytic role to enhance the conversion kinetics considering the promising HMF yield obtained in the catalyst-free DMSO (Jia et al., 2014; **Table 2.6B**). Amarasekara et al. (2008) identified a key intermediate during fructose conversion in DMSO and proposed a dehydration mechanism using NMR analysis, i.e., (4R,5R)-4-hydroxy-5-hydroxymethyl-4,5-dihydrofuran-2-carbaldehyde, with which the DMSO may interact to promote the HMF formation. The same intermediate was recently evidenced by a combined experimental and computational study (Zhang et al., 2016b), suggesting a similar DMSO-mediated mechanism of fructose dehydration. Besides, DMSO exerted an indirect catalytic effect by releasing acidic species when it decomposed at temperature $\geq 80^{o}$C in the presence of oxygen (Zhang et al., 2016b), which therefore accelerated the hydrolysis and dehydration process (as described in **Section 3.1.1**). Morales et al. (2014) suggested that DMSO potentially catalyzed the isomerization step, but there was a lack of mechanistic information in the literature. The use of DMSO is compatible with a wide range of catalysts (**Table 2.3 & 2.6B**). Its high hygroscopicity enables the application of water-sensitive catalysts such as Amberlyst-70, of which the sulfonic acid sites are prone to deactivation after water adsorption (Morales et al., 2014).

2.4.2.2 Tetrahydrofuran

Tetrahydrofuran (THF) is water-miscible and forms a single layer upon mixing with water. Yang et al. (2012) reported that the THF/water mixture attained a high HMF yield of 52% from glucose in the presence of $AlCl_3$ (**Table 2.6C**), while the aqueous system only resulted in 22% (**Table 2.3C**). The THF/water mixture achieved a higher rate of glucan (e.g., cellulose) hydrolysis and sugar dehydration relative to the water medium under the same conditions (Cai et al., 2013), accounting for the enhanced reaction kinetics in THF.

By adding salts to decrease the miscibility between solvents, the THF/water mixture can be transformed to a biphasic system, where the production and extraction of HMF occur in the aqueous and organic phase, respectively. Such biphasic system generated a high HMF yield from fructose (61%; NaCl as salt) (Yang et al., 2012) and cellulose (43-53%; $NaHSO_4$/$ZnSO_4$ as salt and catalyst) (Shi et al., 2013) (**Table 2.6C**). This was because the catalysts were concentrated in the thin aqueous layer, while the organic phase acted as a dispersing agent that increased the substrate exposure to the catalysts. An efficient diffusion of produced HMF to the THF layer also played an important role in impeding the side reactions (Shi et al., 2013). It was noteworthy that THF possessed a high extracting power up to 7.3, which was at least two-fold higher than other cyclic ethers, ketones and alcohols (Román-Leshkov and Dumesic, 2009). However, the degradation of THF at temperature higher than 180^{o}C arises as the major limitation of its application for intensive thermal process.

2.4.2.3 Methyl isobutyl ketone

Methyl isobutyl ketone (MIBK) has low water solubility and serves as the extractive phase in a biphasic system. Román-Leshkov et al. (2006) reported a HMF yield of 55% from fructose in the water/MIBK medium using HCl as the catalyst (**Table 2.6D**), which was higher than that of the pure water systems (**Table 2.3A**). A satisfactory HMF yield of 31% can be obtained even at a high fructose loading of 50 wt% (**Table 2.6D**), demonstrating the potential for scale-up biomass conversion. An outstanding HMF production could be achieved by increasing the proportion of MIBK (74 mol% HMF; Ma et al., 2015), replacing the water partly by DMSO, or supplying

2-butanol as an additive (42-63% HMF; Román-Leshkov et al., 2006) (**Table 2.6D**). More details on the use of additives will be illustrated in **Section 2.4.4**. The water/MIBK system is also applicable for the conversion of glucose, sucrose, cellobiose, and starch (Saha et al., 2013; Dutta et al., 2014) (**Table 2.6D**). The promising performance results from efficient extraction of HMF to the MIBK phase, which protects the product from the side reactions and shifts the equilibrium in the reactive phase. However, it is noted that MIBK may react with HMF to give aldolic side products through acid-catalyzed condensation reaction (Karimi and Mirzaei, 2013).

2.4.2.4 N,N-dimethylacetamide

N,N-dimethylacetamide (DMA) is a water-soluble solvent. A high HMF yield of 60% could be obtained from fructose and glucose in DMA using carbon-based solid acid (Glu-TsOH, prepared from glucose and *p*-toluenesulfonic acid) or $CrCl_3$ as the catalyst (Wang et al., 2011; Yang et al., 2015b) (**Table 2.6E**). With the addition of LiCl to the DMA medium, Dutta et al. (2012) obtained 21-30% HMF from cellulose in the presence of different metal chloride catalysts (**Table 2.6E**). Similar to the function of ionic liquid, the matrix provided a high concentration of chlorides to disrupt the extensive network of intra- and inter-molecular interactions within the cellulose (Dutta et al., 2012). The DMA-Li^+ macrocations resulted in a high concentration of weakly ion-paired chlorides that could form hydrogen bonds with the hydroxyl groups of cellulose, facilitating the dissolution of cellulose for hydrolysis.

2.4.2.5 Biomass-derived solvents

The biomass-derived methyltetrahydrofuran (MTHF) is an emerging green solvent. Although its chemical structure resembles THF to some extent, MTHF has distinctive physical properties that are similar to toluene, such as low solubility in water, high stability, and high boiling point (Seemala et al., 2016). The biphasic MTHF/water system with levulinic acid as the catalyst could facilitate the conversion of pinewood and eucalyptus to yield 93-307 mg L^{-1} of HMF (**Table 2.1**) and conversion of cellulose and glucose to yield 555-1570 mg L^{-1} of HMF (**Table 2.3B**), respectively (Seemala et al., 2016). In contrast, pure MTHF as a solvent was not effective for the biomass conversion although levulinic acid was completely soluble in MTHF (Seemala et al., 2016), because pure MTHF solvent altered the ability of proton transfer. Hence, the MTHF-to-water ratio plays a significant role in controlling the distribution of acid catalysts between the layers and determining the catalytic activity of the aqueous phase for biomass conversion.

As shown in **Table 2.1**, γ-Valerolactone (GVL) is another promising biomass-derived candidate. A satisfactory HMF yield of 27.1% was produced from corncob in GVL over the acidic polymer catalyst in one pot (Zhang et al., 2017). A two-step conversion protocol could reach a higher yield of 60% HMF from corn stover (Luterbacher et al., 2014). In the first step, a GVL/water mixture was used to release 80% C_6 sugars from biomass, followed by separation of the aqueous layer upon salt addition. The sugars retained in the aqueous phase were then transformed to HMF in the presence of $AlCl_3$ and extractive organic solvent.

The impressive performance of GVL was ascribed to the disruption of cellulose crystallinity associated with an increased amorphous fraction, and the inhibited re-precipitation of lignin by-products on the cellulose surface, which otherwise limits the accessibility to cellulose in water (Luterbacher et al., 2014).

Another study revealed that the solvation of proton (from strong Brønsted acids in particular, e.g., pKa < 0) in GVL rendered it more reactive than in water, thus facilitating faster hydrolysis of cellobiose to glucose (Mellmer et al., 2014). This is also reflected by the lower apparent activation energy of cellobiose hydrolysis in the GVL/water mixture (81-118 kJ mol^{-1}) relative to that in water (131 kJ mol^{-1}) (**Table 2.4**). Such benefit is applicable to other polar aprotic solvents such as THF (Mellmer et al., 2014).

2.4.3 Ionic liquids

Ionic liquids are salts in liquid state that enable efficient HMF production. An outstanding HMF yield of about 90% was produced from glucose in a mixture of ionic liquids coupled with metal chloride catalyst at the moderate temperature of 100^{o}C (Siankevich et al., 2016) (**Table 2.6F**), demonstrating the reduction in energy barriers. Therefore, ionic liquid is popular for cellulose conversion. For example, in the presence of ionic liquids, 38% HMF was yielded from cellulose over $CrCl_2$ catalyst (Siankevich et al., 2016), whereas a comparable yield of 40.5% HMF was generated over a sulfonated carbonaceous catalyst (Hu et al., 2013) (**Table 2.6F**). Higher HMF production (51-62%) could be attained by adding a co-solvent, e.g., MIBK and dimethoxyethane (DME) (Siankevich et al., 2016), which will be further discussed in **Section 2.4.4**. The key role of ionic liquid is to disrupt and dissolve the polysaccharide macrostructure for subsequent hydrolysis via extensive hydrogen bonding (Siankevich et al., 2016). Therefore, any solvents possessing high hydrogen bonding ability may be capable to facilitate the cellulose conversion. An analogous candidate is the eutectic solvent comprising the choline salt and carboxylic acids (Matsumiya and Hara, 2015).

2.4.4 Biphasic and binary systems

Two solvents or more are often used as medium in the literature. We hereby categorize different combinations for a clearer picture of the existing literature (**Table 2.6**): (i) monophasic system that can be further classified as unary (one solvent) and binary (two miscible solvents); (ii) biphasic system containing two immiscible layers, which serve as the reactive and extractive phases enabling concurrent production and extraction of product, respectively. Each layer may consist of two solvents or more, meaning that the biphasic system could be a complicated mix of multiple solvents. It is important to differentiate the binary and biphasic systems. The binary systems induce a greater impact on the conversion chemistry in view of direct solvation in the two miscible solvents in a single phase. The biphasic systems often give a better performance for biomass conversion (**Table 2.1**), although the monophasic systems can produce comparable HMF yield from model sugars (**Table 2.6**).

In view of the above literature, three strategies are hereby summarised to modify the biphasic systems as below.

(1) Reduce the miscibility between layers by selecting solvent with a lower solubility in water (e.g., MIBK: 19.1 mg mL^{-1} at 20 °C). Alternatively, a biphasic system can evolve from a binary system upon the addition of inorganic salt, which disrupts the inter-solvent bonding and increases the upper critical solubility temperature of the solvent mixture (Román-Leshkov and Dumesic, 2009).

(2) Increase the partitioning coefficient of HMF into the extractive phase by supplying a secondary solvent (e.g., 2-butanol as polar protic solvent) as an additive (Román-Leshkov et al., 2006; Mirzaei and Karimi, 2016).

(3) Accelerate the diffusion rate of HMF by increasing the volume of the

extractive phase (i.e., maintaining a low concentration). However, this may affect the catalyst concentration in the reactive phase depending on the solubility of catalyst (Seemala et al., 2016).

There are a few considerations for formulating a high-performance biphasic system. Although water facilitates the undesirable off-path HMF rehydration, an appropriate amount of water is beneficial for biomass conversion (**Table 2.1**) as it enhances substrate hydrolysis, suppresses humin formation, and maintains a low viscosity (Matsumiya and Hara, 2015; Yu et al., 2017). In general, the addition of DMSO offers a satisfactory HMF yield from model carbohydrates (**Table 2.6B**). Besides, DMSO is compatible with the use of MIBK as the extractive solvent (**Table 2.6D**) in view of negligible carryover of DMSO into MIBK (< 0.8 wt% DMSO in MIBK) (Román-Leshkov et al., 2006).

2.5 Heating systems

2.5.1 Conventional heating

Oil bath, salt bath, autoclave, and aluminium heating block as conventional heating equipment are often adopted for HMF production (**Table 2.1, 2.3 & 2.6**), among which oil bath is the most popular. A conventional 1-L oil bath could reach the desired temperature within 2 min and maintain the temperature with a small fluctuation by 5°C only (Carraher et al., 2015). It is preferred for heating over the aluminium block, because the latter possesses a lower heat capacity and undergoes temperature drop of 10°C in case of high loading of reaction vials despite its good thermal conductivity (Carraher et al., 2015). Stirring can enhance the mass transfer between the reactive and extractive phases (Seemala et al., 2016). However, conventional heating often involves a long reaction time due to low heat transfer efficiency.

2.5.2 *Microwave heating*

There has been a growing use of microwave heating for conversion of biomass (**Table 2.1**) and model carbohydrates (**Table 2.3 & 2.6**), as it effectively shortens the reaction time, improves the product yields, and diminishes the side reactions (Saha et al., 2013). Wrigstedt et al. (2016) obtained 91% HMF from fructose within 1 min under microwave heating, but a lower yield of 79% in a 40-min oil-bath heating (**Table 2.3A**). Similar findings could be observed with different catalysts (Dutta et al., 2014) (**Table 2.3C)** and different solvents (Saha et al., 2013) **(Table 2.6D&F**). Fan et al. (2013) revealed the interactions between the microwave photons and CH_2OH group of cellulose. Further mechanistic studies are required to elucidate such characteristic performance.

Microwave heating offers an energy saving up to 85-fold compared to traditional heating via convection and conduction (Yemiş and Mazza, 2012). Yet, its application is limited by the ability of the reaction medium to absorb irradiation. For instance, the dielectric constant of water considerably decreases at temperature above 200^{o}C, leading to a lowered heating rate due to reduced microwave absorbance (Möller et al., 2012). Water becomes microwave-transparent near its critical temperature (374^{o}C) so microwave heating cannot generate a near-critical water system (**Table 2.6A**). Therefore, the microwave absorptivity of the solvent mixtures should be considered upfront, which can be improved by adding ionic or polar additives, e.g., salts (Möller et al., 2012). It is noted that the use of probe sonication technique also reduced the reaction time from hours to minutes compared to conventional heating methods

(Sarwono et al., 2017). Hence, emerging heating techniques for biomass valorization warrant further investigation.

2.6 Reaction temperature and time

The reaction temperature for HMF production varies by a wide range (80-300^{o}C) depending on the system components (**Table 2.1, 2.3 & 2.6**). Recent kinetic studies on monophasic aqueous systems revealed that an increase in temperature only reduced the time to reach the maximum HMF yield, but did not boost the magnitude of the HMF maximum (Swift et al., 2015; Yu et al., 2017). This was because energy input improved the kinetics of desirable pathways (i.e., hydrolysis, isomerization, and dehydration) and competitive side reactions (i.e., polymerization and rehydration) to a similar degree, because of their comparable activation energies. Thus, to maximize the yield of HMF, it is necessary to identify and manoeuvre the system components that are conducive to a faster relative kinetics of the desirable pathways, such as the L:B ratio of the catalysts (**Section 2.3.3**).

It is typical that HMF yield declines from the peak under prolonged reaction time, due to the occurrence of HMF-consuming side reactions (Mirzaei and Karimi, 2016; Yu et al., 2016b). The degree of HMF loss depends on the solvent mixtures of conversion system (**Section 2.4.4**). Matsumiya and Hara (2015) reported a significant drop of standard HMF by 22% and 44% after 2 and 6 h, respectively, at 140^{o}C in the monophasic molten mixture of choline salt and carboxylic acid. In comparison, Seemala et al. (2016) showed that the optimum HMF yield from biomass conversion remained stable for an hour in the biphasic MTHF/water system at 200^{o}C. Similar results were reported in other biphasic systems (Yang et al., 2012; Shi et al., 2013).

This suggests an improved HMF stability in the biphasic system because of isolation from the reactants, which is important for a high selectivity by dampening the rate of side reactions. Interestingly, the HMF selectivity rose from 46 to 62.5% upon an increase in temperature form 140 to 150^{o}C in the immiscible MIBK/water mixture (Dutta et al., 2014) (**Table 2.3C**), implying that the kinetics of desirable reactions was enhanced to greater extent than the undesirable ones in the biphasic systems. Hence, the effect of energy input in HMF productivity may vary among different solvent systems, which require further investigation.

2.7 Catalyst/solvent recycling and HMF separation

The solid catalysts can be easily recycled by filtration and washing with water and organic solvent (e.g., ethanol), followed by drying for reuse (Morales et al., 2014; Zhang et al., 2015b). In contrast, the soluble catalysts can be directly reused in conjunction with the solvent after HMF separation from the system. Saha et al. (2013) reused the homogenous monophasic system for glucose conversion ($Zr(O)Cl_2$-containing water) after removing HMF by diethyl ether as a non-polar solvent, which maintained a good HMF production (> 35%) for five runs. Ethyl acetate as a polar aprotic solvent was an alternative candidate for HMF extraction (Xiao et al., 2014). Similarly, the reuse of a monophasic system for cellulose conversion ($Zr(O)Cl_2/CrCl_3$ as catalyst; DMA-Li/[BMIM]Cl as solvent) showed only 4% loss in HMF yield after four cycles (Dutta et al., 2012). For a homogenous biphasic system (water/MIBK-2-butanol), Mirzaei and Karimi (2016) separated the phases by decantation and reused the sulphanilic acid-containing aqueous phase with the addition of fresh glucose and organic phase. Five cycles were performed without significant drop in the HMF yield.

Further isolation and purification of HMF from the solvents depends on its boiling point and affinity to HMF. Low boiling point solvents such as diethyl ether (35^{o}C) and THF (66^{o}C) allow room temperature vacuum distillation and flash separation (Cai et al., 2013; 2014). However, moderate to high boiling point solvents including MIBK (118^{o}C) and DMSO (189^{o}C) require more energy-intensive processes (Mushrif et al., 2012; Saha and Abu-Omar, 2014). For instance, vacuum evaporation at 13 mbar and 70^{o}C can recover > 99% MIBK at the expense of 2.5% loss of HMF (Saha and Abu-Omar, 2014). More cost-effective methods are still in need. For example, Rajabbeigi et al. (2012) performed the selective adsorption of HMF on porous carbons (0.104-0.16 g HMF per g adsorbent) from fructose/DMSO mixtures at room temperature. The stream that contained HMF and fructose in equal amounts (0.11 g ml^{-1}) was fed into a fixed bed column (30-cm length, 5-mm inner diameter) packed with the commercial porous carbons (e.g., BP2000 from CABOT and Norit1240 from Norit), and subsequent HMF extraction from the carbons was performed using ethanol.

2.8 Environmental compatibility and economic feasibility

The use of complicated mix of chemicals in the conversion system often arouses environmental considerations. For instance, metal chlorides such as $AlCl_3$ may cause neurological damage, while possible oxidation of Cr^{2+} and Cr^{3+} to carcinogenic Cr^{6+} needs careful handling. It is favourable to employ bifunctional catalyst (**Section 2.3.3**) or organic compounds that are naturally present in the environment and/or associated with low toxicity.

The biomass-derived chemicals also present environmental merit, such as

MTHF and GVL as green solvents (**Section 2.2 & 2.4.2.5**). While water is a well-known green option, there is room for improvement of its performance (**Section 2.4.1**). Environmentally benign candidates can be selected with reference to the available solvent guides (Byrne et al., 2016). For example, the latest CHEM21 selection guide ranks the commonly used solvents by “recommended”, “problematic”, “hazardous”, and “highly hazardous”, based on the safety, health, and environment criteria (Prat et al., 2016). New protocols are also available for identifying green alternatives with comparable properties to substitute the commonly used solvents (Alves Costa Pacheco et al., 2016).

The environmental compatibility of the conversion system as a whole varies with specific operational parameters, including the dosage, toxicity, and recyclability of catalysts and solvents, as well the product yield and purification. Therefore, comprehensive evaluation in a life-cycle approach, which is an information gap in the existing literature, is necessary to advise the greenness of different emerging systems. The inventory analysis may appear as a challenge due to the lack of existing database on the impacts associated with the new or tailored materials (e.g., MTHF, functionalized zeolite/polymer/carbon).

Regarding the economic feasibility, Kazi et al. (2011) assessed a biphasic system ($NaCl_{aq}$/butanol as medium, HCl as catalyst) for conversion of pure fructose to HMF using the techno-economic analysis. The simulated plant with a capacity of 300 tonnes fructose per day consisted of a continuous stirring tank reactor for simultaneous HMF production and extraction; a decantation unit for phase separation; an evaporator, a flash separator, and distillation columns for HMF purification and extraction of recyclable materials. Assuming 13% HMF loss during the manufacturing processes and 20-year operation, this study indicated a minimum selling price of HMF at USD 1.33 per litre, which was the most sensitive to the product yield and the feedstock (fructose) cost. Therefore, the use of the biomass waste as renewable feedstock presents an enormous advantage over the use of energy crop-derived sugars. Similar economic assessments should be conducted to justify and maximize the commercial viability of high-performance systems.

2.9 Reseach gaps and hypotheses

Conversion of biomass to HMF needs enhancement in product yield and selectivity by devising high-performance cooperative catalyst-solvent system. Bifunctional catalyst containing Brønsted and Lewis acidity in appropriate ratio and strength selectively facilitates kinetics of desirable reactions (hydrolysis, isomerization, and dehydration) over off-path reactions (rehydration, polymerization). Solvents in biphasic system protect HMF from side reactions for high selectivity, depending on functional groups, speciation, and extraction power. This review suggests concerted efforts to manoeuvre the interactions among co-catalysts/co-solvents, and between catalysts and solvents, with the goal to develop synergistic function and avoid antagonistic effect by tuning the system components.

Therefore, this thesis aims to elucidate the significant factors in determining the efficiency of a biomass conversion system, in consideration of the interactions among different system components which were seldom discussed in the literature.

The following chapters address three main system components: feedstock, catalyst, and solvent (**Fig. 1.1**), using methods introduced in **Chapter 2**. In summary, **Chapter 3** verifies the feasibility of biomass feedstocks, which are rich in different types of carbohydrates including starch, cellulose, and sugars, for catalytic conversion to HMF. **Chapter 4** illustrates the roles of catalysts, in relation to their physicochemical properties, in the tandem reactions (i.e., hydrolysis of starch/cellulose, isomerisation of glucose, and dehydration of fructose) during conversion of biomass. With selected catalysts and feedstock, **Chapter 5** reveals the kinetics of conversion to scrutinise the characteristics of representative catalytic systems. In view of the importance of product selectivity, **Chapter 6** proposes modifying the catalytic activities (i.e., Lewis and Brønsted acidity) to change the system preference for desirable tandem reactions over side reactions, via addition of a co-catalyst. As for reaction media, **Chapter 7** examines the critical properties of solvents in governing the kinetics and selectivity of biomass conversion, highlighting the multifunctions that solvents can offer beyond serving as media. **Chapter 8** underlines the benefits of selected green solvents for boosting the conversion efficiency, advocating the use of green solvents to substitute common industrial solvents in catalytic systems to achieve sustianbale valorisation. The findings of this thesis can be applied in development technologies for the valorisation of food waste.

Chapter 3 – Materials and Methods

3.1 Food waste

Pre-consumer kitchen waste generated from the Hong Kong International Airport and local wet markets were used as the food waste substrates in this study (**Figure 3.1**). They were categorized on the basis of their primary components with reference to the literature as follows (**Table A.1, Appendix A**): (1) cooked rice and cooked penne were considered as surrogates of starchy waste; (2) raw mixed vegetables were cellulosic waste; (3) watermelon flesh and unskinned kiwifruit represented sugary waste. All the samples were freeze-dried as received (**Figure 3.2**), except that watermelon flesh was blended and dewatered by centrifugation before freeze-drying due to its excessive water content. The dried samples were ground, sieved through a 0.2-mm-mesh, and stored in air-tight storage containers at 4 ^{o}C in the dark for the subsequent characterisation as well as conversion experiments.

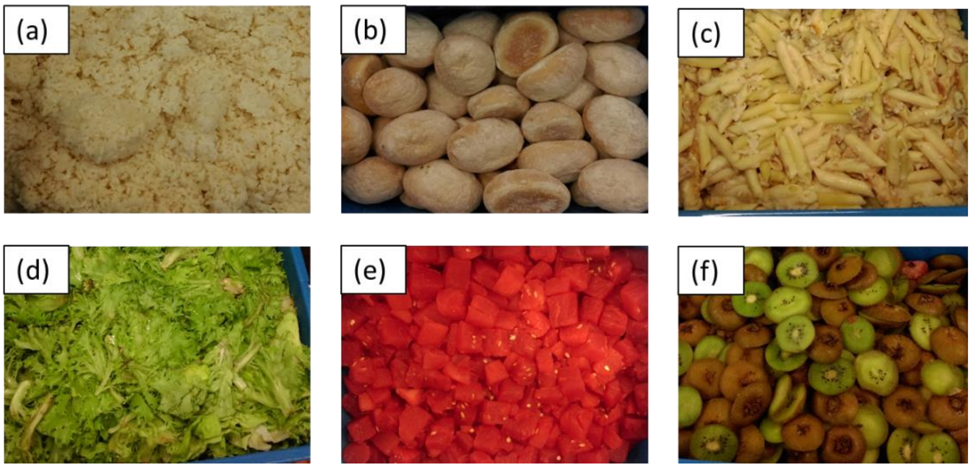

Figure 3.1. (a) Cooked rice waste, (b) bread waste, (c) penne waste, (d) mixed vegetabls, (e) watermelon flesh, and (f) kiwifruit waste.

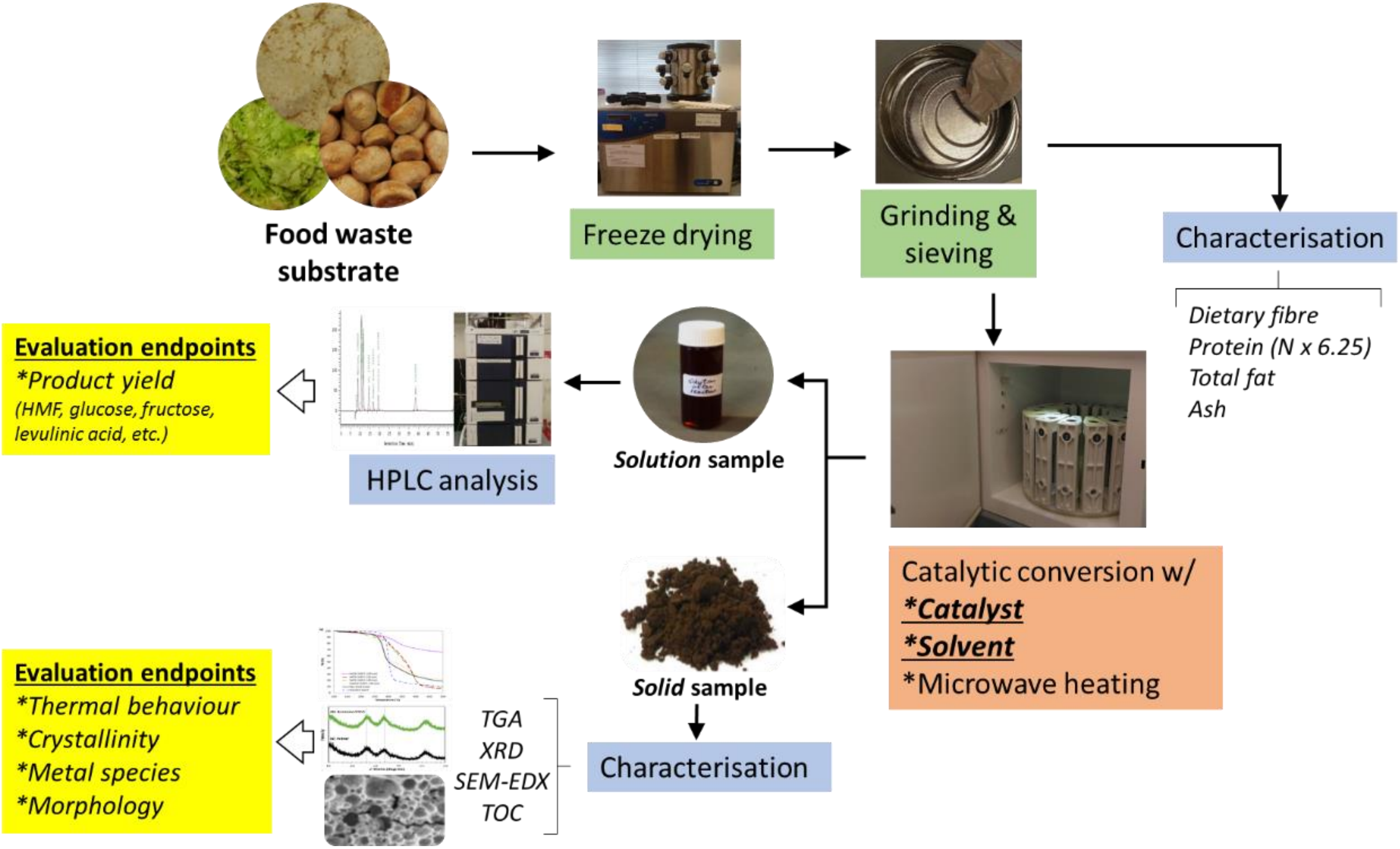

Figure 3.2. Experimental procedure at a glance.

Characterisation was conducted in terms of dietary fibre (including cellulose, hemicellulose, lignin, and pectin; AOAC 985.29), protein (N x 6.25, Kjeldahl Nitrogen Method, AOAC 928.08), total fat (acid hydrolysis and gravimetric method, AOAC 922.06), and ash (AOAC 923.03). Available carbohydrate was estimated on the basis of a mass balance (HK FEHD, 2008):

$$\text{Available carbohydrate} = 100 - \frac{(\text{Dietary fibre} + \text{Protein} + \text{Fat} + \text{Ash} + \text{Alcohol})\ \text{g}}{100\ \text{g Dried substrate}}, \qquad (1)$$

where alcohol was omitted in view of its negligible concentration shown in the USDA National Nutrient Database. Free sugars were quantified as the sum of disaccharides, glucose, and fructose dissolved in water using high-performance liquid chromatography (HPLC). Starch content was estimated by subtracting the content of available carbohydrates by free sugars (HK FEHD, 2008). Water content was calculated based on the change in sample mass before and after freeze-drying. The total organic carbon (TOC) content was measured using the TOC analyser (Shimadzu SSM-5000A). The composition of samples is shown in **Table 3.1**.

Table 3.1. Characterization of food waste samples used in this study.

	TC[a] (wt% dry basis)	Composition (wt% dry basis)							Water (wt%)
		Total dietary fibre[b]	Available carbohydrates[c]	Starch[d]	Free sugars	Protein	Total fat	Ash	
Cooked rice (Batch 1)[e]	51.5	1.6	88.6	88.5	0.1	7.8	1.5	0.5	63.8
Cooked rice (Batch 2)[e]	-	B.D.[f]	90.3	90.1	0.2	8.4	1	0.3	59.7
Cooked penne	60.9	5.2	58.4	58	0.4	20.3	13.3	2.8	68.9
Bread waste	41.5	4.2	72.6	67.6	5	14.8	6.1	2.3	28.1
Mixed vegetables[g]	53.1	46.3	1.2	-	-	26	5.5	21	96.5
Kiwifruit	60	23.3	61.2	-	51.9	6.6	3.3	5.6	84.1
Watermelon	31.5	30	48.7	-	35.4	13.5	4.5	3.3	-

[a] Total carbon (TC);

[b] including cellulose, hemicellulose, lignin, and pectin;

[c] available carbohydrates were calculated according to HK FEHD (2008): 100 – [dietary fibre + protein + fat + water + ash + alcohol(ethanol)] g / 100 g substrate; alcohol was omitted in view of negligible concentration shown in the USDA National Nutrient Database;

[d] starch content was estimated by subtracting the content of available carbohydrates by free sugars (HK FEHD, 2008);

[e] batch 1 and 2 of rice waste were collected separately on different days. Batch 1 was used in Chapter 5, while Batch 2 was used in Chapter 7.

[f] below detection limit (i.e., 1 wt%);

[g] the other batch of mixed vegetable waste was used for characterization because the batches for conversion experiment were out of stock. The low carbohydrate content pertained to a different sample preparation protocol: before freeze-drying, the vegetables were blended with water, followed by centrifugation and decantation, during which the soluble carbohydrates (e.g., free sugars) were lost.

Specific type of waste was selected in **Chapter 6-9**, with respect to the initial results illustrated in **Chapter 4 and 5** as well as the environmental significance of the waste:

Chapter 6, 8&9: Bread waste was selected as the substrate because it is rich in starch as a highly feasible precursor of HMF (**Table 3.1**). In addition, bread waste is one of the significant type of waste wordwide. For example, 680,000 tonnes of avoidable bakery waste is discarded annually in UK (Taylor, 2012), while 5.95 million loaves of bread were wasted per day in 2012 in Turkey (OECD-FAO, 2014).

Chapter 7: Rice waste was used as the substrate due to its starch-rich content (**Table 3.1**). In addition, it should be noted that rice waste has significant environmental relevance in view of its worldwide abundance. For instance, in the Philippines, over 300,000 tonnes of rice were wasted annually (Manila Times, 2017); in the United Kingdom, there were 40,000 tonnes of rice waste from household (WRAP, 2013a) and carbohydrates (including rice) accounted for 40% of the commercial food waste (WRAP, 2013b).

3.2 Chemicals

3.2.1 Model carbohydrates

Model compounds were used as substrates in supplementary tests to improve our understanding about the observed results of food waste conversion. They also served as standards in the calibration for sample analysis. Glucose (99%), cellobiose (≥98%), levulinic acid (98%), and formic acid (98%) were purchased from Alfa Aesar; maltose monohydrate (≥98%) from Wako; HMF (≥99%) from Sigma Aldrich; and levoglucosan from Fluorochem, respectively. Their molecular structures were provided in **Fig. 3.3**. All the chemicals were used as received.

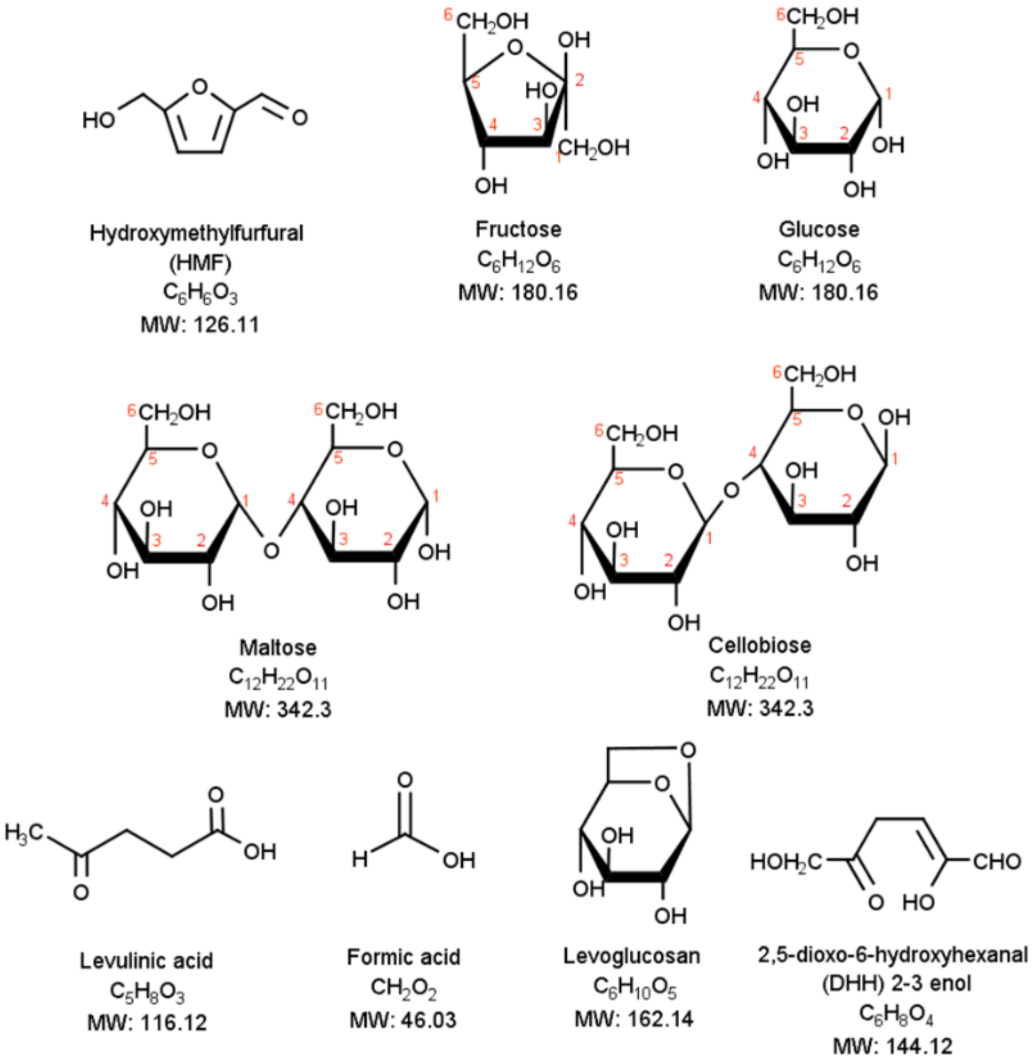

Figure 3.3. Molecular structure, molecular formula, and molar mass of different carbohydrates and their derivatives.

3.2.2 *Catalysts*

A range of metal chloride catalysts were selected in view of their good performance reported in the literature (**Chapter 2**). The catalysts were purchased from Sigma Aldrich, including $CrCl_3{\cdot}6H_2O$ (≥98%), $FeCl_3$ (97%), $CuCl_2$ (99%), $ZnCl_2$ (≥98%), $InCl_3$ (98%), $SnCl_4{\cdot}5H_2O$ (98%), $YbCl_3{\cdot}6H_2O$ (99.9%) as well as H_3PO_4 (≥85% in water), whereas $Zr(O)Cl_2{\cdot}8H_2O$ (99.0+%) and $AlCl_3{\cdot}6H_2O$ (ACS grade) were from

Wako and Anaqua, respectively. Concentrated H_2SO_4 (95%) from BDH Prolabo was used to adjust the pH of the reaction medium in supplementary tests. An organic acid as a co-catalyst in **Chapter 7**, maleic acid (98+%), was obtained from Alfa Aesar. All the chemicals were used as received.

3.2.3 Solvents

The common polar aprotic solvents including DMSO (≥99.9%) and THF (≥99.8%) from RCI Labscan, and acetonitrile (ACN) (99.9%) and acetone (99.5%) from Duksan Pure Chemicals, respectively, were used to prepare the solvent-water mixture as the reaction medium. These solvents were commonly reported in the literature (**Chapter 2.4**). In particular, DMSO is the major solvent used in **Chapter 4-8** due to its promising performance for model compounds or pure carbohydrates (Jia et al., 2014; Morales et al., 2014; Yu et al., 2016b). The DMSO solvent meets the criteria of safety and occupational health for field-scale operations according to the CHEM21 selection guide of solvents (Prat et al., 2016), while the overall environmental impact of solvent use via a holistic life cycle analysis is under investigation in our ongoing studies. Green solvents, including propylene carbonate (PC) (99%) and γ-valerolactone (GVL) (98%) were purchased from Alfa Aesar and Acros Organics, respectively. All the chemicals were used as received.

3.3 Catalytic valorisation

3.3.1 Major experiments

For the catalytic valorization, substrate (freeze-dried food waste substrate or model carbohydrate) of 5 wt/v% was added to a medium, except that vegetable waste adopted a loading of 2.5 wt/v% because of substrate swelling. The model compounds were used to probe the effects of the solvents on the individual conversion steps, *i.e.,* hydrolysis, isomerisation, and dehydration. The medium was a mixture of water and organic solvent (e.g., DMSO, acetone, acetronirile (ACN), THF, PC, and GVL), or water only. In real-life application, the indigenous moisture in food waste should serve as a part of the reaction medium. The solvent-water ratio of 1:1 (v/v) was selected as it is the average water content of starch-rich food waste, *i.e.,* with a range of 28−69% (**Chapter 3.1**). The solvent-water mixture as the medium was denoted as DMSO/H_2O, acetone/H_2O and so on. The metal catalyst was added to the medium to give a concentration of 55.5 mM. The metal chlorides of 20 mol% with respect to monosaccharide (Dutta et al., 2012), i.e., 55.5 mM, were used, instead of 5 mol% (i.e., 13.9 mM) as reported by Jia et al. (2014) that produced less HMF in our preliminary experiments (**Fig. A.1**).

The reaction mixture with a total volume of 20 ml (except **Chapter 9** that adopted 10 ml) was subjected to heating in the Ethos UP Microwave Reactor (Milestone, maximum power 1900 W). The temperature was controlled using a temperature sensor which was inserted into one reference vessel. The microwave power was varied with the aid of the sensor in order to follow the programmed temperature profile. After a ramping time of 5 min (Möller et al., 2012), the reaction mixture was subject to heating at 120-160^{o}C for up to 150 min under continuous stirring in the Ethos UP Microwave Reactor. The adopted temperatures and durations were comparable to previous studies on microwave-assisted conversion (Möller et al., 2012; Yemiş and Mazza, 2012; Qu et al., 2014; Wrigstedt et al., 2016), and they were considered on the low side relative to conventional heating (Wang et al., 2014; Ma et al., 2015). All the parameters were determined for the purpose of validating the feasibility and performance of food waste substrates and metal catalysts for HMF production in this study. A time period of 40 min was allowed for the cooling of the vessels by continuous mechanical/forced ventilation in the reactor.

After the reaction, the samples were extracted, diluted with deionized water in a volume ratio of 1:1, and filtered through 0.22-µm mixed cellulose esters filter for product analysis. For selected sampels, the reacted mixture was centrifuged to separate the liquid and solid phase for different product analysis. The solution sample was prepared following the above protocol. The solid residue was washed three times by vortexing with DI water, centrifugation, and decantation to remove the solvent and soluble compounds. The washed solid was then freeze-dried for subsequent characterization. All trials were duplicated. Student's t-test with a significant level $p \leq 0.05$ was conducted to compare the different conversion systems.

3.3.2 Control experiments

The control experiments were conducted under selected conditions without the addition of catalysts and without the addition of substrates.

Chapter 7: To assess the catalytic activity of MA, control tests were conducted by following the above procedure (at 140 ^{o}C for 10 min in DMSO/H_2O) after replacing metal chlorides with 167 mM NaCl (equivalent to the chloride concentration in 55.5 mM $CrCl_3$). Control runs were also performed by heating the mixture of MA and $SnCl_4$ or $CrCl_3$ in DMSO/H_2O (i.e., no substrate) at 140 ^{o}C for 10 min.

Chapter 8: Mixtures without the addition of $SnCl_4$ were prepared as the control runs under heating at 140 ^{o}C for 20 min.

Chapter 9: The controls comprising mixtures containing no $SnCl_4$ or substrate were carried out at 120 ^{o}C, 10 min.

3.3.3 Supplementary experiments

To verify the result-based speculations in this study, supplementary tests were conducted by modifying the above protocol.

Chapter 4: Test on co-existing fructose and glucose, where 1.5 wt/v% fructose and 0.9 wt/v% glucose (equivalent to the initial sugar contents in the control experiment of kiwifruit conversion) in DMSO/H_2O were subjected to heating at 140 ^{o}C for 20 min.

Chapter 5: (1) Diluted H_3PO_4 of pH 1.2 was used to replace metal chloride to represent the benchmark trial with Brønsted acid only, in DMSO/H_2O under heating at 140 ^{o}C for 20 min. (2) Two types of metal chlorides were selected on the basis of the initial results and added as a binary catalyst in a sequential or simultaneous manner to the reaction medium. For sequential addition, batches of glucose were first heated for 20 min in the presence of 20 mol% $InCl_3$ or $AlCl_3$ in DMSO/H_2O at 140 ^{o}C. The same dose of $FeCl_3$ was then added to the vessels and subject to the second round of 20-min heating at 140 ^{o}C. In simultaneous addition, $FeCl_3$ was dosed along with $InCl_3$ or $AlCl_3$ and the mixture was continuously heated for 40 min. Glucose batches with no catalyst and single catalyst were used for comparison. (3) As for evaluation of acidity from *Lewis acids* in the studied system, a concentration of 55.5 mM of each metal chloride (the same as those in carbohydrate conversion) was prepared in DMSO/water (1:1 v/v). The pH of the mixture was measured under room temperature. To evaluate acidity from *levulinic acid and formic acid*, the acidic by-products of different concentrations were prepared in DMSO/water (1:1 v/v) according to the quantity range produced in our samples (0.234 to 1.468 mg/ml for formic acid and 0.184 to 1.954 mg/ml for levulinic acid). Each of the standard acids of 1 gram was dissolved in 250 ml DI water and further diluted with a factor of 0.8, 0.6, 0.4, 0.2 and 0.08, respectively. Each dilution was added to DMSO in a ratio of 1:1 v/v for pH measurement. As for evaluation of acidity from *decomposition of DMSO,* a mixture of DMSO/water (1:1 v/v) was heated under 140°C for 20 min. The pH of the medium was measured after cooling down.

Chapter 6: Glucose was used as the substrate and added to DMSO/H_2O (1:1 v/v) without metal chloride catalyst. The reaction mixture was adjusted using concentrated H_2SO_4 to reach a pH value ranging from 1.3 to 3.1, before heating at 160°C for 30 min.

Chapter 9: The solid and liquid phases obtained from the control runs without the substrate were separated by centrifugation. The model compounds were then added to the respective phases for conversion in order to evaluate the catalytic activity. For conversion over the solid phase, fresh solvent medium was also added (same composition as the medium from which the solids were produced). To examine the effect of pressure, dried bread waste in $SnCl_4$-containing medium was heated to 120 °C for 2.5 min. After cooling down to room temperature, the vessels were opened to release the autogenous in-vessel pressure, followed by another 2.5-min heating step. The total reaction time of 5 min was shorter than the optimal time for HMF production identified initially, and was used in order to avoid the masking effect of the HMF-consuming side reactions. Control tests were also performed as above, but without pressure release after the first heating step. The effect of pressure was examined by comparing the HMF yield between the trials with and without pressure release.

3.4 Sample analysis

3.4.1 Product analysis

High-performance liquid chromatography (HPLC) was performed using Chromaster (Hitachi) with a 5110 pump, 5210 autosampler, 5310 column oven, and 5450 refractive index (RI) detector. The HPLC system was equipped with an Aminex HPX-87H column (Bio-rad), using 0.01 M H_2SO_4 at a flow rate of 0.5 ml min^{-1} as the mobile phase under the column temperature of 50^{o}C (Ohara et al., 2010). Blank (i.e., DMSO/water in 1:1 v/v) and spiked samples (i.e., model compounds) were injected before every series of sample analysis for quality assurance.

When using standard sugars as the substrate, the yield, carbon recovery, and selectivity of products were calculated as follows.

$$Product\ yield\ (mol\%) = \frac{P_f (mg\ ml^{-1})/MW_P}{S_i\ (mg\ ml^{-1})/MW_S} \times 100, \tag{2}$$

$$Product\ carbon\ (mol\%) = \frac{P_f (mg\ ml^{-1}) \times Cn_p/MW_P}{S_i\ (mg\ ml^{-1}) \times Cn_S/MW_S} \times 100, \tag{3}$$

$$Product\ selectivity (mol\%) = \frac{P_f (mg\ ml^{-1})/MW_P}{(S_i - S_f)(mg\ ml^{-1})/MW_S} \times 100, \tag{4}$$

where P_f was referred to the concentration of final product, i.e., fructose, glucose, HMF, levoglucosan, levulinic acid, and formic acid; S_i and S_f represented initial and final concentration of sugars, respectively; Cn_p and Cn_s were the numbers of carbons in the corresponding product and substrate, respectively; and MW was referred to molecular mass of the corresponding compound.

As for food waste and starch as the substrate, the yield of products was calculated on the basis of carbon content and/or mass as below.

$$Product\ yield\ (mol\%) = \frac{P_f(mg\ ml^{-1}) \times Vol(ml)/MW_P \times Cn_p}{C_S(mol)} \times 100, \tag{5}$$

$$Product\ yield\ (wt\%) = \frac{P_f(mg\ ml^{-1}) \times Vol\ (ml)}{S_i\ (mg)} \times 100, \tag{6}$$

where P_f was referred to the concentration of product as above; MW_p and Cn_p was the molecular mass and number of carbons in the corresponding product, respectively; C_s represented the organic carbon content in the food waste substrate; S_i represented the initial mass of substrate.

3.4.2 Characterisation

The pH of the resultant solution was measured using a pH meter (Shanghai Leici, Model E-201F). It described the Brønsted acidity qualitatively for comparing samples generated using the same solvent mixture only, as calibration protocols were not available for the organic solvent-water media selected in this study to our best knowledge.

Selected solid samples were subject to the thermogravimetric analysis (TGA; Rigaku Thermo plus EVO2) to study the thermal behaviour as the temperature increased from 100 to 500^{o}C at a rate of 10^{o}C min^{-1}. The morphology was observed using the scanning electron microscopy coupled with energy dispersive X-ray spectroscopy (SEM-EDX; TESCAN VEGA3) after gold coating. The organic carbon content was measured using total organic carbon analyzer (TOC; Shimadzu SSM-5000A). X-ray diffraction analysis (XRD; Rigaku SmartLab) was performed in a scanning range of 10−60° 2θ at a rate of 5° min^{-1} at 45 kV and 200 mA.

Chapter 4 – Valorisation of Starchy, Cellulosic, and Sugary Food Waste

Abstract

This chapter aims to produce a high-value platform chemical, hydroxymethylfurfural (HMF), from food waste and evaluate the catalytic performance of trivalent and tetravalent metals such as $AlCl_3$, $CrCl_3$, $FeCl_3$, $Zr(O)Cl_2$, and $SnCl_4$ for one-pot conversion. Starchy food waste, e.g., cooked rice and penne produced 4.0−8.1 wt% HMF and 46.0−64.8 wt% glucose over $SnCl_4$ after microwave heating at 140°C for 20 min. This indicates that starch hydrolysis was effectively catalyzed but the subsequent glucose isomerization was rate-limited during the food waste valorization, which could be enhanced by 40-min reaction to achieve 22.7 wt% HMF from cooked rice. Sugary food waste, e.g., kiwifruit and watermelon, yielded up to 13 wt% HMF over Sn catalyst, which mainly resulted from naturally present fructose. Yet, organic acids in fruits may hinder Fe-catalyzed dehydration by competing for the Lewis acid sites. In contrast, conversion of raw mixed vegetables as cellulosic food waste was limited by marginal hydrolysis at the studied conditions (120-160°C and 20-40 min). It is noted that tetravalent metals enabled HMF production at a lower temperature and shorter time compared to trivalent metals.

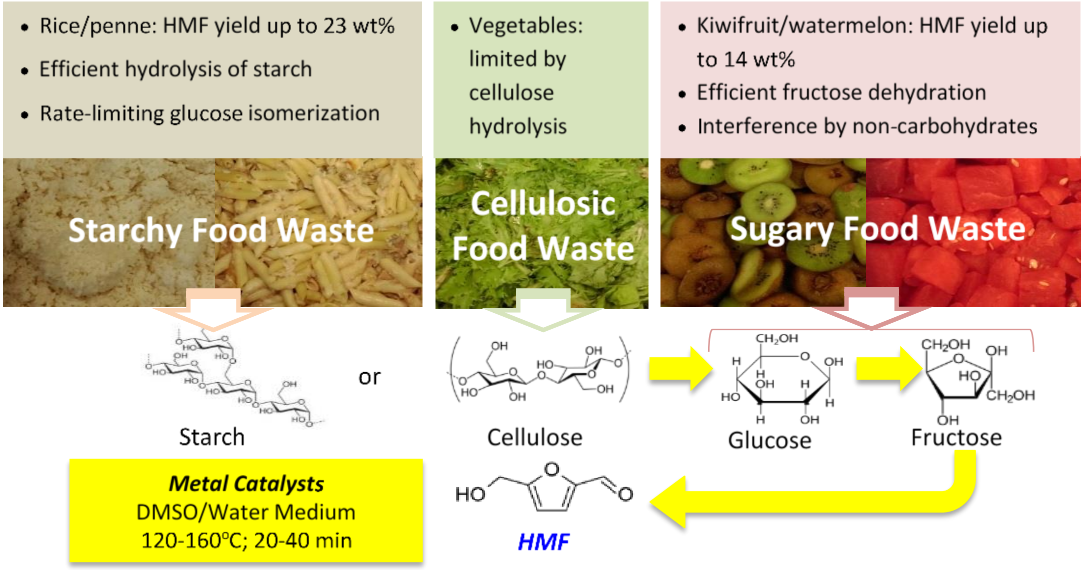

Figure 4.1. Graphical abstract of **Chapter 3**.

4.1 Reseach questions

As introduced in **Chapter 1**, there are three chemical steps to produce HMF from biomass, including hydrolysis of glucan to glucose, isomerisation of glucose to fructose, and dehydration fructose to HMF (**Fig**. **4.2**). It is noted that the conversion of biomass that contains polysaccharide as a dominant carbohydrate species remains challenging due to its high complexity. For example, wheat straw containing 34.2% glucan only produced a maximum HMF yield of 3.4% in acidic aqueous medium (Yemiş and Mazza, 2012). Birch, cornstalk, bagasse, poplar and pine gave about 10−20% HMF in a mixture of water and organic solvent (Wang et al., 2014), while standard fructose achieved 74−91% HMF in similar systems (Ma et al., 2015; Wrigstedt et al., 2016). A recent study using assorted catering remains as the substrate accomplished HMF yield of only 4.3% at most (Parshetti et al., 2015).

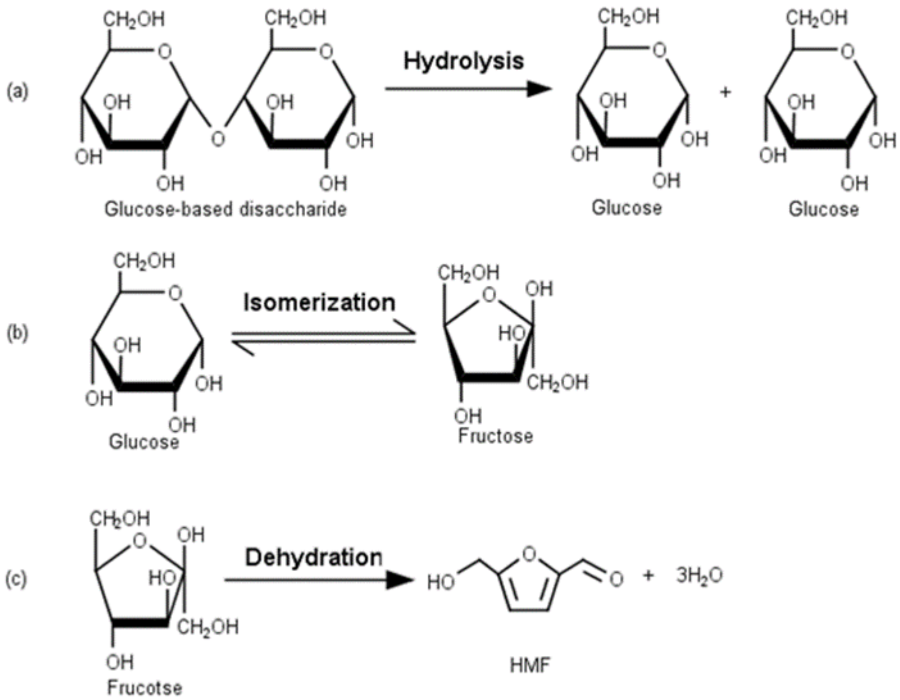

Figure 4.2. The reaction series involved in HMF production from glucose-based carbohydrates: (a) hydrolysis, (b) isomerization, and (c) dehydration.

To enhance the product yield, it is important to ascertain the feasibility of converting different carbohydrate-rich food wastes for catalyst design and feedstock selection. Such feasibility counts on both convertible fractions (i.e., starch, cellulose, and sugars) and unusable non-carbohydrate components, which potentially interfere with the food waste catalytic system. For instance, organic acids that display a strong affinity for metal ions (Martell and Smith, 1977) are possibly one of the problematic co-existing components imposing an inhibitory effect on the catalysis.

Transition metal and semi-metal ions have been widely employed as Lewis acid catalysts for isomerization of glucose to fructose (Enslow and Bell, 2015; Wang et al., 2015; Nguyen et al., 2016). The metals were suggested to develope Brønsted acidity through partial hydrolysis in an aqueous medium (Jia et al., 2014). The developed Brønsted acidity may serve as the catalyst for hydrolysis of glucans and dehydration of fructose, while the intrinsic Lewis acidity catalyses isomerisation. As such, the tandem reactions (**Fig. 4.2**) can be facilitated in one pot by the metal catalysts.

This chapter evaluates the viability of starchy, cellulosic, and sugary food waste as the selected substrates for catalytic production of HMF. The metal chlorides that possess Lewis sites and produce Brønsted acidity were scrutinized as bi-functional catalysts for the food waste valorization. The difference in the relative significance of the successive elementary steps (hydrolysis, isomerization, and dehydration) and side reactions (polymerization and rehydration) was illustrated with regard to the trivalent/tetravalent metals and the three types of food waste.

4.2 Results and discussion

4.2.1 Starchy food waste undergoes facile hydrolysis yet rate-limiting isomerization

The non-catalytic conversions of cooked rice and penne generated negligible products under all tested conditions. In the presence of metal catalysts, significant yield of the disaccharide, glucose, and HMF were achieved from the two substrates under heating at 140^{o}C for 20 min, both of which shared similar product distribution profile (**Fig. 4.3a&b**). The tetravalent catalysts $Zr(O)Cl_2$ and $SnCl_4$ that produced the strongest acidity of pH 1.9 and 1.5, respectively (**Fig. B.1, Appendix B**) resulted in the highest quantity of products, whereas $AlCl_3$ (pH 3.2-3.4), $CrCl_3$ (pH 2.6), and $FeCl_3$ (pH 2.1-2.2) yielded much lesser products. Protons released upon partial hydrolysis of the metal aqua complexes (i.e., Brønsted acidity) participated in the acid-mediated reactions including glucan hydrolysis and fructose dehydration (Caratzoulas et al., 2014; Enslow and Bell, 2015; Yu et al., 2016b). The present results further remarked the correlation between the strength of derived Brønsted acidity and the hydrolysis constant (pKa), which sharply differ for Sn^{4+} (-0.6) and Zr^{4+} (-0.3) than Al^{3+} (5.0), Cr^{3+} (4.0) and Fe^{3+} (2.2) (Wulfsberg, 1987). This explains the outstanding performance of tetravalent metals to catalyze hydrolysis of starch in food waste by means of strong Brønsted acidity derived from hydrolysis. Besides, the Lewis site of metals may also promote hydrolysis by attacking the oxygen atom of the glycosidic bond (Tao et al. 2011; Zhou et al., 2013).

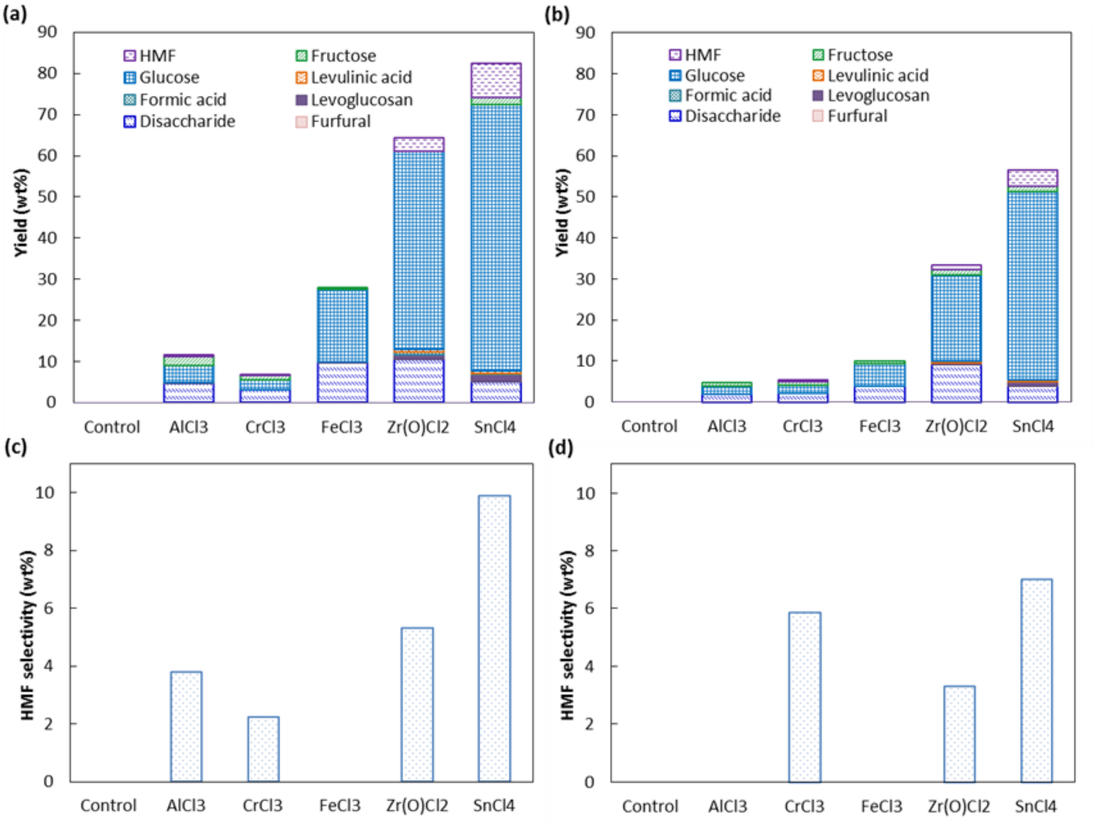

Figure 4.3. Yield of different products in conversion of (a) cooked rice and (b) cooked penne, and HMF selectivity of (c) cooked rice and (d) cooked penne in the presence of different metal chloride catalysts (conditions: 5 wt/v% substrate and 55.5 mM metal chloride in DMSO/water (1:1 v/v) at 140°C for 20 min; yield = $product_{wt}/substrate_{wt} \times 100\%$; selectivity = $HMF_{wt}/total\ products_{wt} \times 100\%$).

Interestingly, the rate of hydrolysis of starchy food waste was found higher than isomerization because glucose represented a larger proportion of the product profile than fructose and HMF (**Fig. 4.3a&b**). The starch in cooked rice and penne was hydrolysed effectively to release glucose but the following glucose-fructose transformation was rate-limited, which was corroborated by a recent study (Wang et al., 2015), leading to the accumulation of glucose in the medium over $Zr(O)Cl_2$ and $SnCl_4$. The deficiency of fructose produced by isomerization restrained its subsequent dehydration to HMF, resulting in low HMF selectivity in the product profiles (**Fig. 4.3c&d**). It should be noted that the isomerization was driven by Lewis acid rather than Brønsted acid, according to the finding that significantly more HMF was yielded from standard glucose over $CrCl_2$ than H_3PO_4 despite their comparable Brønsted acidity (pH 2.1) (**Chapter 5**). To capitalize the large quantity of resultant glucose, we further increased the reaction time and temperature, respectively, aiming to enhance the Lewis acid-mediated isomerization.

The conversion of cooked rice over $Zr(O)Cl_2$ and $SnCl_4$ after 40-min microwave heating notably increased the HMF yield at the expense of glucose released from hydrolysis ($p \leq 0.05$) (**Fig. 4.4a**). The maximum HMF production was 22.7±0.5 wt% (25 Cmol%) achieved over $SnCl_4$ (40 min), which outcompeted the yield obtained from lignocellulosic biomass such as rice straw (2.6−6 wt%) (Amiri et al., 2010) and bagasse (9.8 wt%) (Wang et al., 2014) in systems that employed similar catalysts and solvents. As the yield of HMF increased with reaction time, the isomerization step was mainly restricted by kinetics at 140°C rather than thermodynamic equilibrium or deactivation of metal catalysts. The rate-limiting character of isomerization was confirmed by the lower HMF yield obtained from standard glucose than from standard fructose (**Fig. B.2a&b**). Prolonged duration allowed the metal-catalyzed isomerization to increase the availability of fructose that was rapidly dehydrated into HMF, as reflected by higher HMF selectivity (**Fig. 4.4b**).

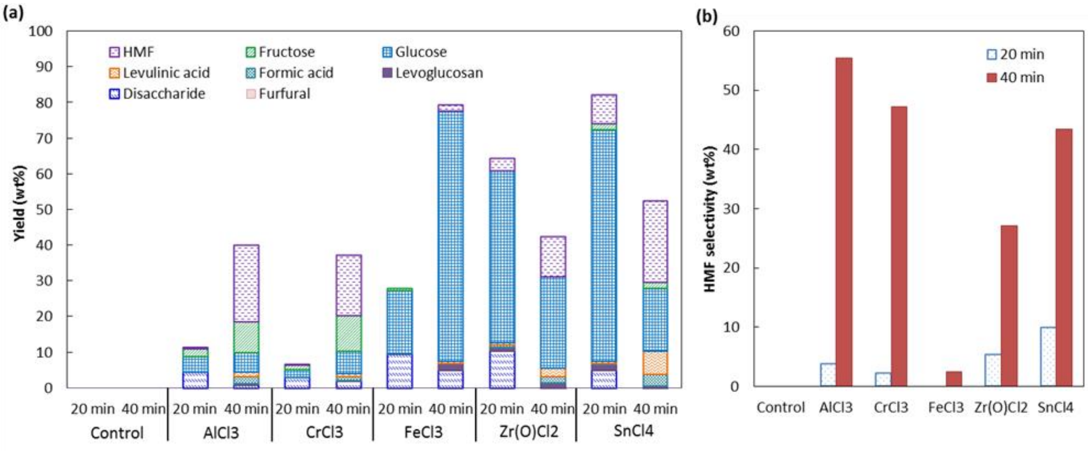

Figure 4.4. (a) Yield of different products and (b) HMF selectivity in conversion of cooked rice for 20 and 40 min in the presence of different metal chloride catalysts (conditions: 5 wt/v% substrate and 55.5 mM metal chloride in DMSO/water (1:1 v/v) at 140^{o}C; yield = product$_{wt}$/substrate$_{wt}$ × 100%; selectivity = HMF$_{wt}$/total products$_{wt}$ × 100%).

However, a long reaction time also led to the polymerization of sugars and HMF, which was an undesirable side reaction in parallel to the valorization pathway. The tetravalent catalysts Zr(O)Cl$_2$ and SnCl$_4$ resulted in a decreased sum of products from cooked rice after 40 min ($p \leq 0.05$) (**Fig. 4.4a**), possibly due to the formation of humins as reported in previous studies on carbohydrate conversion (Hu et al., 2015; Swift et al., 2015). It is suggested that the metal catalysts could initiate polymerization reactions, possibly by activating the carbonyl group of sugars (**Chapter 5**). In contrast, the trivalent metal catalysts, AlCl$_3$ and CrCl$_3$, produced a higher total product yield after 40 min ($p \leq 0.05$). It was interesting to note that they even generated a comparable amount of HMF relative to the most promising SnCl$_4$.

The results of this work highlighted that the tetravalent metals were more active than the trivalent ones in triggering the side reactions, resulting in a relatively lower HMF selectivity under lengthened reaction time (**Fig. 4.4b**). The performance of $FeCl_3$ was distinct from other catalysts because it significantly increased the glucose yield but marginally improved the HMF yield ($p \leq 0.05$) (**Fig. 4.4a**). Supplementary experiment using standard glucose as substrate evidenced that Fe catalyst was not effective in promoting isomerization at 140^{o}C (**Fig. B.2a**). Therefore, the pathway of $FeCl_3$-mediated conversion of cooked rice ceased at the hydrolysis step without subsequent isomerization at this temperature.

Hence, the heating temperature was varied on cooked rice valorization. At 120^{o}C, all the catalysts gave negligible HMF (**Fig. 4.5a**). Even the most promising tetravalent catalysts, $Zr(O)Cl_2$ and $SnCl_4$, yielded a moderate amount of disaccharide and glucose only, which could not be further transformed to HMF. A lower temperature supplied insufficient energy for the hydrolysis of rice starch and isomerization of glucose, thus inhibiting the necessary reaction steps that follow along the pathway.

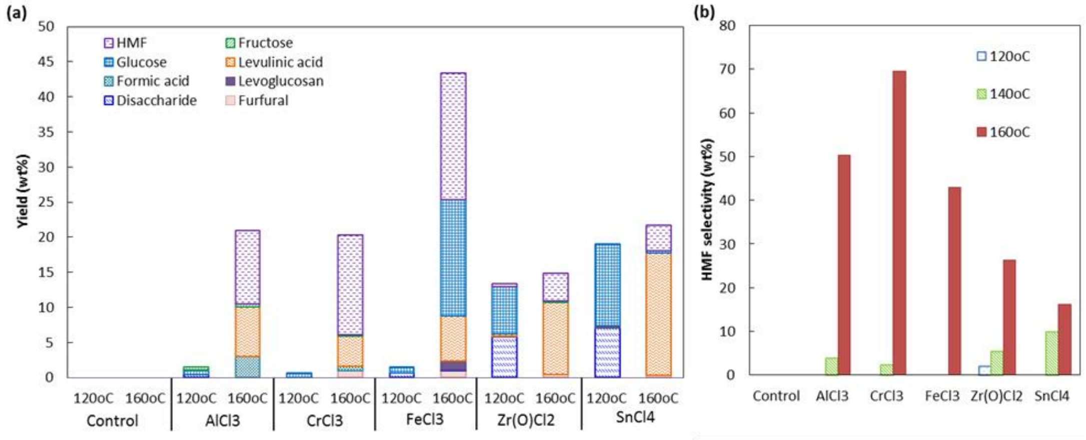

Figure 4.5. (a) Yield of different products and (b) HMF selectivity in conversion of cooked rice at 120 and 160^{o}C in the presence of different metal chloride catalysts (conditions: 5 wt/v% substrate and 55.5 mM metal chloride in DMSO/water (1:1 v/v) for 20 min; yield = product$_{wt}$/substrate$_{wt}$ × 100%; selectivity = HMF$_{wt}$/total products$_{wt}$ × 100%).

In contrast, heating at 160°C led to different product profiles over trivalent and tetravalent metal catalysts. The trivalent catalysts generated more HMF at 160°C than 140°C ($p \leq 0.05$) (by comparing **Fig. 4.3a and 3a**). Elevated temperature enhanced the reaction kinetics and accelerated endothermic steps (i.e., hydrolysis, isomerization, and dehydration), which significantly increased the selectivity of HMF production over $AlCl_3$, $CrCl_3$, and $FeCl_3$ in particular (**Fig. 4.5b**). The surprisingly good HMF production by $FeCl_3$ at 160°C was probably indicative of an alternative chemical pathway, i.e., direct dehydration of glucose into HMF without isomerization, in the presence of sufficient Brønsted acidity and high temperature (Yang et al., 2015). Yet, the newly formed levulinic acid (4.2±1.2 to 17.5±1.1 wt%) indicated the occurrence of HMF rehydration in all conversions, which was another side reaction reported in the literature (Bevilaqua et al., 2013; Wang et al., 2015).

The tetravalent metals, however, led to a reduction in the sum of products ($p \leq 0.05$) (by comparing **Fig. 4.3a and 3a**), in which only trace amounts of fructose and glucose were detected (< 1 wt%). This hinted that a large extent of polymerization took place over the tetravalent metals at 160°C. Similarly, HMF rehydration into levulinic acid was enhanced. Due to acceleration by increasing temperature, these side reactions appeared to compete against the preferred valorization pathway and limit the corresponding increase in HMF selectivity (**Fig. 4.5b**). Nonetheless, the effects of polymerization and rehydration were relatively minor over the trivalent metals even at 160°C, possibly because of their lower catalytic activity (as observed under prolonged reaction time), thereby producing an unexpectedly high product yield (**Fig. 4.5a**) and HMF selectivity (**Fig. 4.5b**).

Thus, the highly active tetravalent metals enabled a more selective production of HMF at a lower temperature (i.e., 140°C) and shorter reaction duration (i.e., 20 min), whereas the less active trivalent metals could achieve a high substrate conversion and HMF selectivity at a sufficiently high temperature, i.e., 160°C. The conversion efficiency of tetravalent metals was more prone to the limitation by irreversible detrimental side reactions (i.e., polymerization and rehydration), which were also time- and temperature-dependent. Therefore, understanding the kinetics and thermodynamics of all the necessary steps and side reactions over the trivalent and tetravalent metals is extremely important to optimize the reaction time and energy input for accomplishing the maximum food waste valorization in terms of HMF production.

4.2.2 Cellulosic food waste confronts thermodynamic hurdle of hydrolysis

Raw mixed vegetables as the surrogate of cellulosic food waste contained a small amount of naturally present fructose and glucose as observed from the control (**Fig. 4.6a**), unlike starchy food waste that released no soluble substances. However, the catalytic conversion of vegetable waste was not as promising as the other tested feedstocks in this study. Only 6.1±0.04 to 12.6±0.4 wt% of total products were converted from vegetable waste after heating at 140°C for 20 min. The resultant HMF amounted to at most 4.9±0.5 wt% (5.2 Cmol%) over $SnCl_4$, mainly originating from the free sugars, i.e., 5.7 wt% fructose and 3.9 wt% glucose naturally present in vegetable waste. The hydrolysis of vegetable cellulose was considered minor as advised by the supplementary test, where standard cellulose yielded relatively small quantity of products (**Fig. B.3**). This suggests ineffective dissolution of the polysaccharide in the reaction medium.

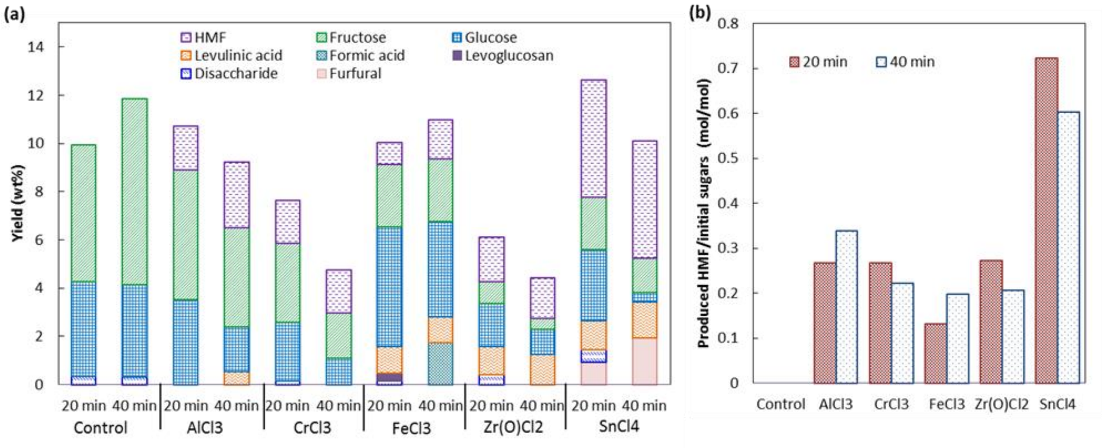

Figure 4.6. (a) Yield of different products and (b) ratio of produced HMF to naturally present sugars (in the control experiments) in conversion of raw mixed vegetables for 20 and 40 min in the presence of different metal chloride catalysts (conditions: 2.5 wt/v% substrate and 55.5 mM metal chloride in DMSO/water (1:1 v/v) at 140^{o}C; yield = product$_{wt}$/substrate$_{wt}$ × 100%).

The mole fraction of DMSO (X_{DMSO}) was approximately 0.2 in the medium used in this study. Water molecules were supposed to surround the cellulose with an estimated adsorption capacity at about 0.23 g water/g cellulose under room temperature based on a previous study (maximum adsorption = 0.32 g water/g cellulose at $X_{DMSO} \sim 0.1$) (Voronova et al., 2006). This revealed a limited access of water to the interior of polysaccharide. Cellulose has a highly crystalline structure (**Fig. B.4a**) comprising extensive intra- and inter-molecular hydrogen bonds, as well as stacking forces derived from van der Waals interactions, π-π interactions, and hydrophobic attraction (Parthasarathi et al., 2011). Such condensed structure hampers the dissolution of cellulose in water and organic solvents, and consequently limits the diffusion of catalysts to the glycosidic bonds that is a prerequisite step for hydrolysis (Su et al., 2011; Siankevich et al., 2016; Yu and Tsang, 2017).

The hurdle for cellulose hydrolysis persisted even though the reaction time increased from 20 to 40 min. The total product yield and distribution at 40 min were similar to those obtained at 20 min (**Fig. 4.6a**), and the molar ratios of produced HMF to free sugars in vegetable waste remained far below 1 (**Fig. 4.6b**). This implied that naturally present sugars were still the major precursor of HMF because of marginal cellulose hydrolysis. An elevated temperature at 160°C also failed to hydrolyze the cellulose into sugars, although there was an increase of HMF productivity from free sugars (**Fig. B.5**).

These results indicated that cellulosic structure of vegetables was resistant to hydrolysis under all the tested conditions, emerging as the kinetic hurdle (i.e., high energy barrier for bond cleavage) in this study. This contrasted the conversion of starchy food waste (an analog polysaccharide of cellulose) that yielded a larger quantity of HMF under lengthened reaction time and increased temperature (**Fig. 4.4 and 4.5**). The semi-crystalline structure of starch (**Fig. B.4b**) was found to absorb water upon the crystalline-to-amorphous transformation at a moderate temperature of 60−70°C (Deguchi et al., 2006). We thereby expected feasible occurrence of such water absorption in our conditions (i.e., 120-160°C), which may favour the catalytic hydrolysis. On the contrary, cellulose required much higher energy input (up to 320°C) to undergo a similar process (Deguchi et al., 2006), which was not possible at the low-temperature range (120−160°C) in the current study. Thermal/chemical pretreatment for the cellulosic food waste may be investigated in future studies.

4.2.3 Sugary food waste enables efficient dehydration of naturally present fructose

Unskinned kiwifruit containing 46.4 wt% sugars produced HMF of 4.7±0.6 to 13.7±1.3 wt% (13 Cmol%) over the tested metal catalysts; whereas watermelon flesh containing 32.0 wt% sugars generated HMF of 2.6±0.3 to 13.2±0.1 wt% after heating at 140°C for 20 min (**Fig. 4.7**). The tetravalent catalyst $SnCl_4$ gave the highest HMF yield from the two sugary substrates, similar to the results of starchy and cellulosic food waste. It seemed that HMF was primarily derived from free fructose in fruits since the fructose content decreased while the glucose content remained close to that of control experiments. The product profiles of fruits (excluding glucose) also resembled those of standard fructose with respect to different catalysts (**Fig. B.2b**).

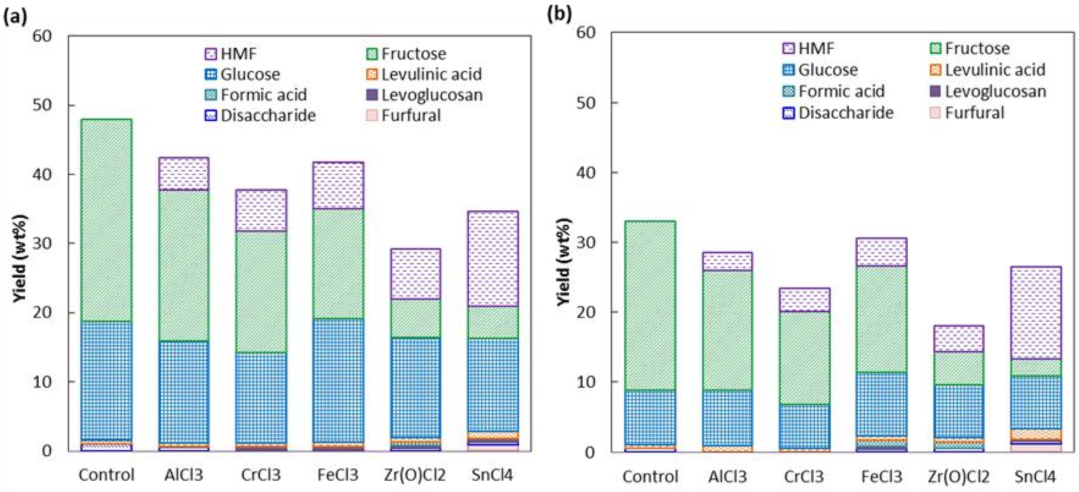

Figure 4.7. Yield of different products in conversion of (a) unskinned kiwifruit and (b) watermelon flesh in the presence of different metal chloride catalysts (conditions: 5 wt/v% substrate and 55.5 mM metal chloride in DMSO/water (1:1 v/v) at 140°C for 20 min; yield = $product_{wt}/substrate_{wt} \times 100\%$).

However, supplementary test on co-existing standard fructose and glucose (at loading levels corresponding to the control experiments of kiwifruit) showed that the contents of fructose and glucose decreased by 81−97 wt% and 72−94 wt%, respectively (**Fig. B.6**). This demonstrated the feasibility of glucose isomerization along with fructose dehydration in pure substrates over an adequate availability of Lewis sites. It was possible that the reacted glucose of small quantity was replenished by hydrolysis of cellulose (3.4−6.1% in kiwifruit) (**Table A.1**), while glucose isomerization might also be interfered by non-carbohydrate components in sugary food waste, such as lipid (3.3%), protein (6.6%), recalcitrant fibre (total fibre was 23.3%), and ash (5.6%) in kiwifruit (**Table 3.1**). The roles and influences of food waste impurities in respective reactions of HMF production require further investigations.

In spite of the higher pH values in the reaction medium, due to the presence of alkalizing agents such as potassium (Minich and Bland, 2007), unskinned kiwifruit and watermelon flesh yielded comparable ratios of HMF to naturally present fructose relative to standard fructose over most of the catalysts (**Fig. 4.8**). This implied that, in addition to Brønsted acidity, Lewis acid sites of metal catalysts also played an important role in dehydration of fructose, concurring on our findings (**Chapter 5**). However, $FeCl_3$ that was a promising catalyst in dehydration of pure fructose (**Fig. B.2b**) only gave a moderate performance over unskinned kiwifruit and watermelon flesh. The metal speciation calculation using Visual MINTEQ (**Table B.1**) revealed that nearly half of the dosed Fe^{3+} was bound to malic acid (32.4%) and citric acid (12.7%), which were the predominant organic acids in the unskinned kiwifruit (**Table A.1**). In comparison, the other tested metals principally remained in free and hydrated forms that were applicable for catalysis (**Table B.1**). This clearly illustrated the significance of understanding potential interference of non-carbohydrate impurities in food waste, which may reduce the catalyst availability and compromise the HMF yield.

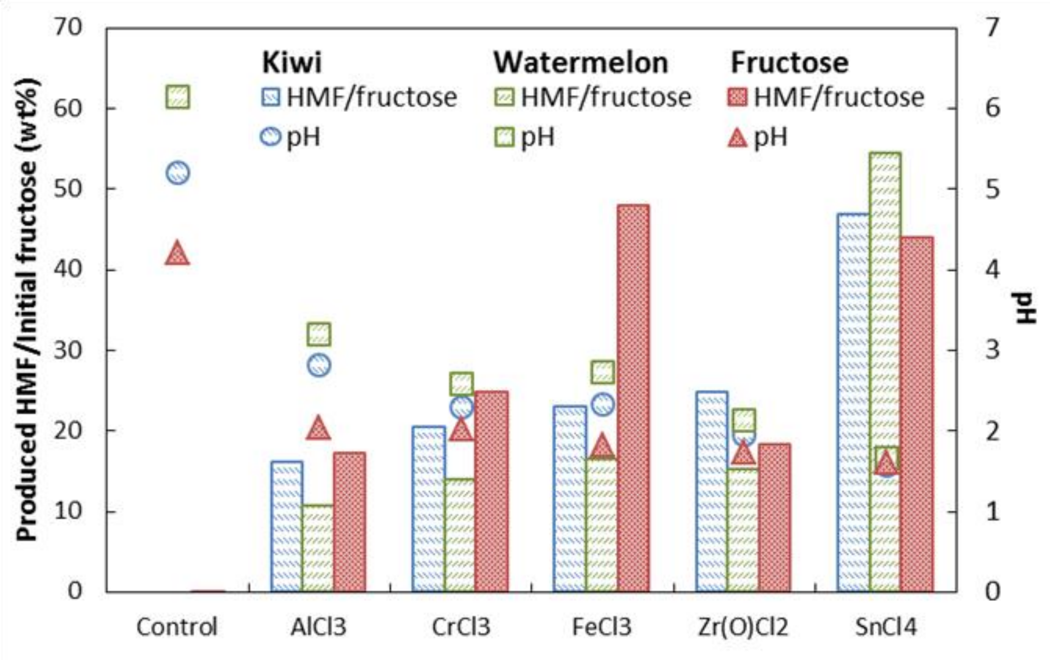

Figure 4.8. Correlation between the produced HMF (with respect to naturally present fructose in the controls) and pH in the conversion of unskinned kiwifruit, watermelon flesh, and standard fructose in the presence of different metal chloride catalysts (conditions: 5 wt/v% substrate and 55.5 mM metal chloride in DMSO/water (1:1 v/v) at 140^{o}C for 20 min).

We also attempted to facilitate the conversion of unskinned kiwifruit by increasing the process duration and operating temperature. The HMF yield and product profile of the 40-min reaction (**Fig. B.7a**) showed a high resemblance to that of 20-min reaction (**Fig. 4.7a**), suggesting the trivial improvement by increasing the reaction time. In contrast, the vast majority of naturally present glucose reacted when the temperature was raised to 160^{o}C (**Fig. B.7b**), which indicated nearly complete isomerization over the metal catalysts (except $FeCl_3$ despite its notable increase in HMF yield). These results demonstrated that the energy barrier to the glucose-fructose isomerization could be overcome by a moderate increment in operating temperature. Nonetheless, heating at 160^{o}C also produced levulinic acid and reduced the sum of products compared to 140^{o}C ($p \leq 0.05$) (by comparing **Fig. 4.7a and B7b**). This suggested the accelerated rates of side reactions including rehydration and polymerization under elevated temperature, which was similar to the cooked rice conversion.

4.3 Summary

This chapter examines three major types of food waste (i.e., starch-rich, sugar-rich, and cellulose-rich) as substrates for HMF production using trivalent and tetravalent metal catalysts under varying reaction time and temperature. The metal-catalyzed hydrolysis of starchy waste was efficient, whereas the subsequent isomerization might be kinetically limited and required a longer reaction time (i.e., 40 min in the current study). Sugary waste that was rich in fructose could yield an increased amount of HMF, although non-carbohydrate components may hinder the isomerization and dehydration. However, the valorization of cellulosic waste was less satisfying due to the limited hydrolysis of crystalline cellulose. Kinetics of catalytic hydrolysis, isomerization, and dehydration, as well as the interference of impurity (e.g., organic acids, proteins, and fats) on food waste valorization should be further studied.

Chapter 5 – Dual Role of Metal Ions in Successive Conversion Steps

Abstract

This chapter aims to transform food waste into a value-added chemical, hydroxymethylfurfural (HMF), and unravel the tangled effects induced by the metal catalysts on each single step of the successive conversion pathway. The results show that using cooked rice and bread crust as surrogates of starch-rich food waste, yields of 8.1-9.5% HMF and 44.2-64.8% glucose were achieved over $SnCl_4$ catalyst. Protons released from metal hydrolysis and acidic by-products rendered Brønsted acidity to catalyze fructose dehydration and hydrolysis of glycosidic bond. Lewis acid site of metals could facilitate both fructose dehydration and glucose isomerization via promoting the rate-limiting internal hydride shift, with the catalytic activity determined by its electronegativity, electron configuration, and charge density. Lewis acid site of a higher valence also enhanced hydrolysis of polysaccharide. However, the metals also catalyzed undesirable polymerization possibly by polarizing the carbonyl groups of sugars and derivatives, which should be minimized by process optimization.

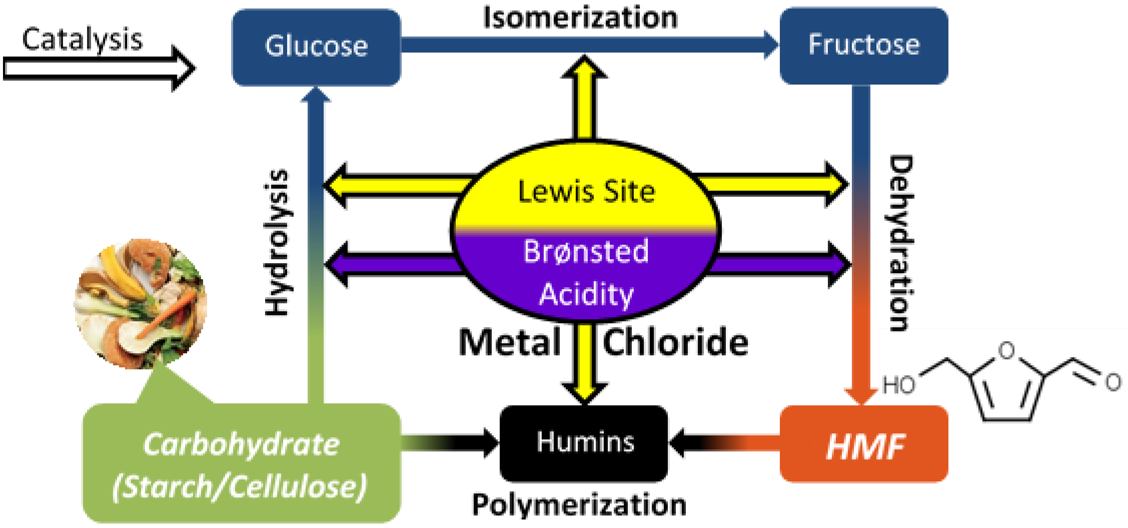

Figure 5.1. Graphical abstract of **Chapter 5**.

5.1 Research questions

While the conversion of glucan-rich food waste to HMF is feasible (**Chapter 4**), it is imperative to tailor the catalytic properties of the system to achieve high-efficieny conversion. Despite a broad spectrum of metal ions investigated in individual studies (**Chapter 2.3.2**), it is difficult to compare their performance in different publications due to varying conditions such as temperature, time, and loading, etc. Only a few studies examined a series of metal ions under the same conditions (Zhao et al., 2007; Dutta et al., 2012; Pagán-Torres et al., 2012; Rasrendra et al., 2012), but the factors leading to the discrepancy in their catalytic activity remained uncertain. It is necessary to fill this critical knowledge gap in order to develop robust and sustainable options for the catalytic systems. In addition, although recent investigations have evaluated the catalytic roles of Lewis acid property of metal ion on the isomerization step, Brønsted acidity derived from metal ions that potentially extends its functionality are seldom considered. It is postulated that protons (Brønsted acid) released from partial hydrolysis of metal ions in the aqueous medium could facilitate hydrolysis and dehydration, as well as off-path reactions such as polymerization and rehydration.

This chapter intends to assess the significance of the electrochemical characteristics of the inorganic metal chloride catalysts, which determine their ability to coordinate with the reactant to facilitate hydride shift, for the catalytic conversions of carbohydrates and food waste to HMF. A range of Lewis acids were scrutinized of the effects of their indirectly derived Brønsted acidity and electrochemical properties on each reaction step during the HMF production from carbohydrates.

5.2 Results and discussion

5.2.1 Fructose dehydration enhanced by Brønsted acidity and Lewis centres

The production of HMF from fructose was significant in the presence of Lewis acids as shown in **Fig. 5.2a**, where $FeCl_3$, $SnCl_4$, and $CuCl_2$ gave a high HMF yield of 69.2±4.8%, 62.8±1.9% and 60.4±9.3%, respectively, along with high fructose consumption (**Fig. 5.2b**). The chloride ions from Lewis acids did not show a noticeable effect on HMF production in our system ($p > 0.05$) (**Fig. C.1, Appendix C**), due to the relatively low concentration (0.17 mol L^{-1}) compared to those in the previous report (2.2 mol L^{-1}) (Binder and Raines, 2009).

An inverse correlation, in which Fe^{3+} and Sn^{4+} fairly fitted, was observed between the HMF yield and pH of the medium (**Fig. 5.2c**). These results also suggested pH lower than 3 as the minimum requirement to initiate the reaction, confirming the need of Brønsted acidity for dehydration (de Souza et al., 2012; Wrigstedt et al., 2015). There were three possible sources of protons in the studied system: 1) partial hydrolysis of metal ions in aqueous environment; 2) acidic species (e.g., sulphuric acid) resulted from DMSO decomposition by oxygen under high temperature (Zhang et al., 2016); and 3) levulinic acid and formic acid resulted from undesired HMF rehydration (Jin et al., 2005; de Souza et al., 2012). Our supplementary tests showed that pH was decreased by a range of 0.5 to 4 upon addition of various Lewis acids depending on their charge-to-radius ratio and electronegativity (**Fig. C.2a**), while levulinic acid and formic acid at the lowest concentration (i.e., 0.16 mg ml^{-1}) led to a slight decrease in pH by 0.7 and 1.6, respectively (**Fig. C.2b**). In contrast, the pH of catalyst-free DMSO/water (1:1 v/v) remained constant after heating at 140^{o}C for 20 min ($p > 0.05$) (**Fig. C.2c**). These results indicated that partial hydrolysis of Lewis metals and formation of by-products rendered significant Brønsted acidity to the reaction medium, facilitating the fructose dehydration in the tested system.

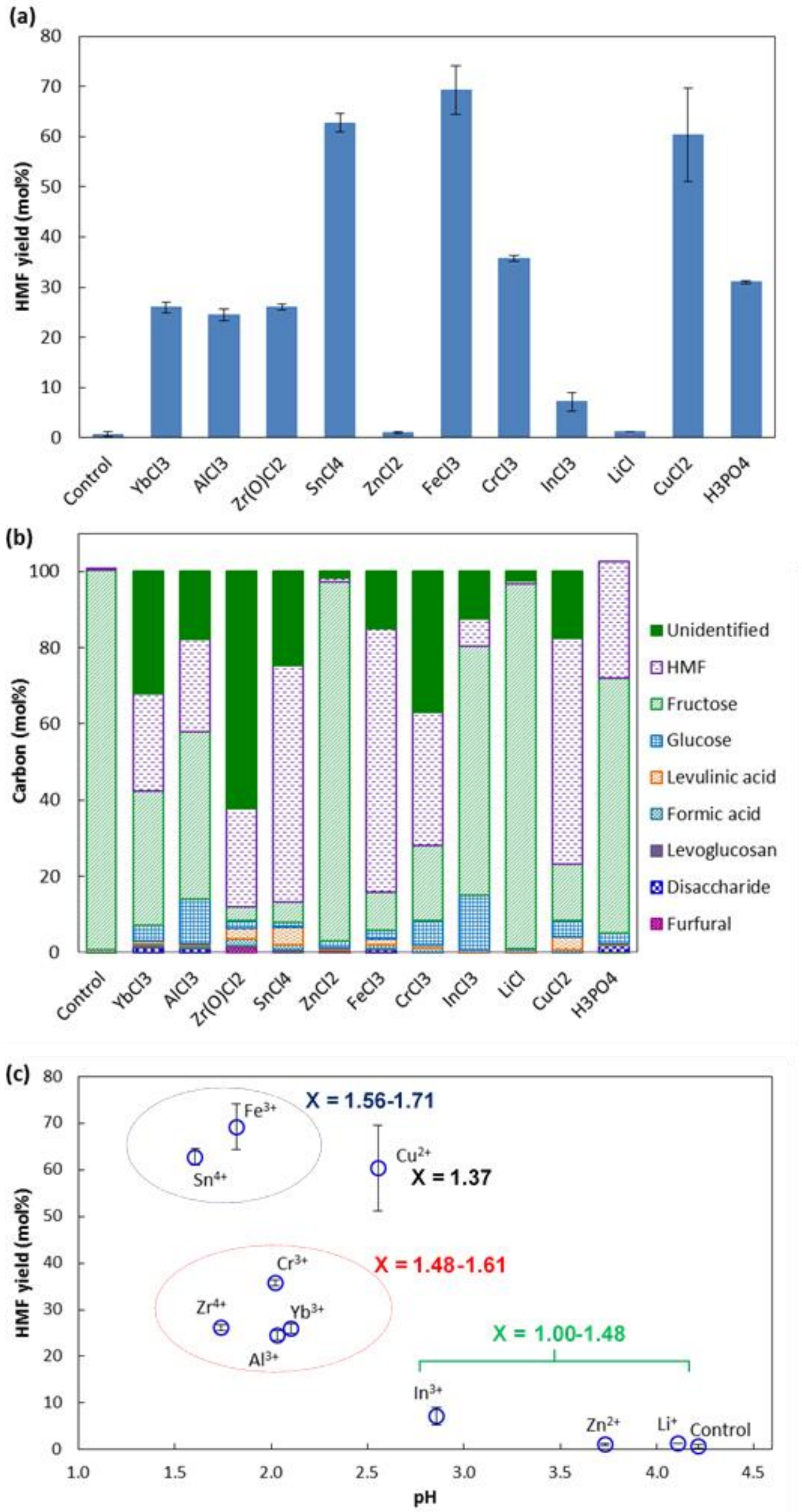

Figure 5.2. (a) HMF yield, (b) product carbon distribution, and (c) correlation between HMF yield and medium pH in fructose conversion in the presence of different Lewis acid catalysts (conditions: 5 wt/v% fructose and 55.5 mM Lewis acid catalyst in DMSO/water (1:1 v/v) at 140°C for 20 min; yield = product$_{mol}$/substrate$_{mol}$ × 100%; X was electronegativity based on crystal radii with a coordination number of 6 (Li and Xue, 2006)).

The correlation in **Fig. 5.2c** revealed that the metals with higher electronegativity (i.e., higher tendency to draw electron density to itself) in general resulted in higher HMF yield, indicating the important role of Lewis centre in fructose dehydration. A rate-limiting internal hydride transfer was observed in a previous microkinetic study (Nikbin et al., 2012), which was possibly catalyzed by the metal ion (**Fig. 5.3**). The metal centre may form a bidentate complex with a carbonium intermediate in a similar fashion as in the Lewis acid-mediated isomerization (Román-Leshkov et al., 2010). This configuration would enable the metal to polarize the carbonyl group of the intermediate to accelerate the hydride shift to the electron-deficient carbon. The higher electronegativity of the metal centre, the more polar the bond can be formed (Sposito, 1994). Besides, exceptionally effective HMF yield by Cu^{2+} may suggest its distinctive catalytic properties in facilitating the rate-determining internal hydride transfer. As the ligand field stabilization energy depends on the electron configuration in d-orbital of metal centre, the four strong equatorial bonds of Cu^{2+} complex is more stable than other divalent metals due to Jahn-Teller distortion (Martell and Hancock, 1996), which may thus be more capable of polarizing the carbonyl group for the subsequent hydride shift. The feasibility of the sugar-metal coordination may be examined via thermodynamics study using density function theory calculations in the future.

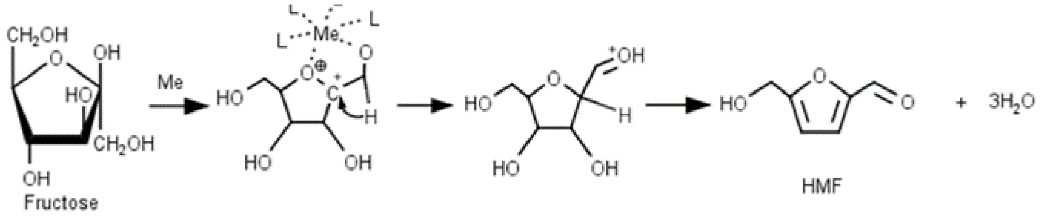

Figure 5.3. The Lewis acid-induced mechanisms proposed for dehydration of fructose (based on Román-Leshkov et al., (2010) and Nikbin et al., (2012)) (Me = metal ion; L = ligand).

5.2.2 Isomerization controlled by electrochemical properties of Lewis acids

The most effective catalyst in glucose conversion was $AlCl_3$, which gave an HMF yield of 24.8±1.8%, followed by $SnCl_4$ and $CrCl_3$ with a yield of approximately 21% (**Fig. 5.4a**). However, the HMF yield reflected the combined effects of individual catalyst on isomerization and dehydration. The sole effect on the midway glucose-fructose transformation should be examined by taking into account the total amounts of fructose and its derivatives i.e., HMF, levulinic acid, and formic acid. Fructose occupied a considerable portion in the carbon balance of reactions over $AlCl_3$ and $CrCl_3$ (**Fig. 5.4b**), which confirmed their good catalytic activity towards isomerization (Pagán-Torres et al., 2012; Rasrendra et al., 2012). The difference in performance given by the tested catalysts was correlated with the ionic radius and ionic charge (**Fig. 5.4c**), which were indicative of the binding abilities of metal catalysts during the course of cation-hexose coordination.

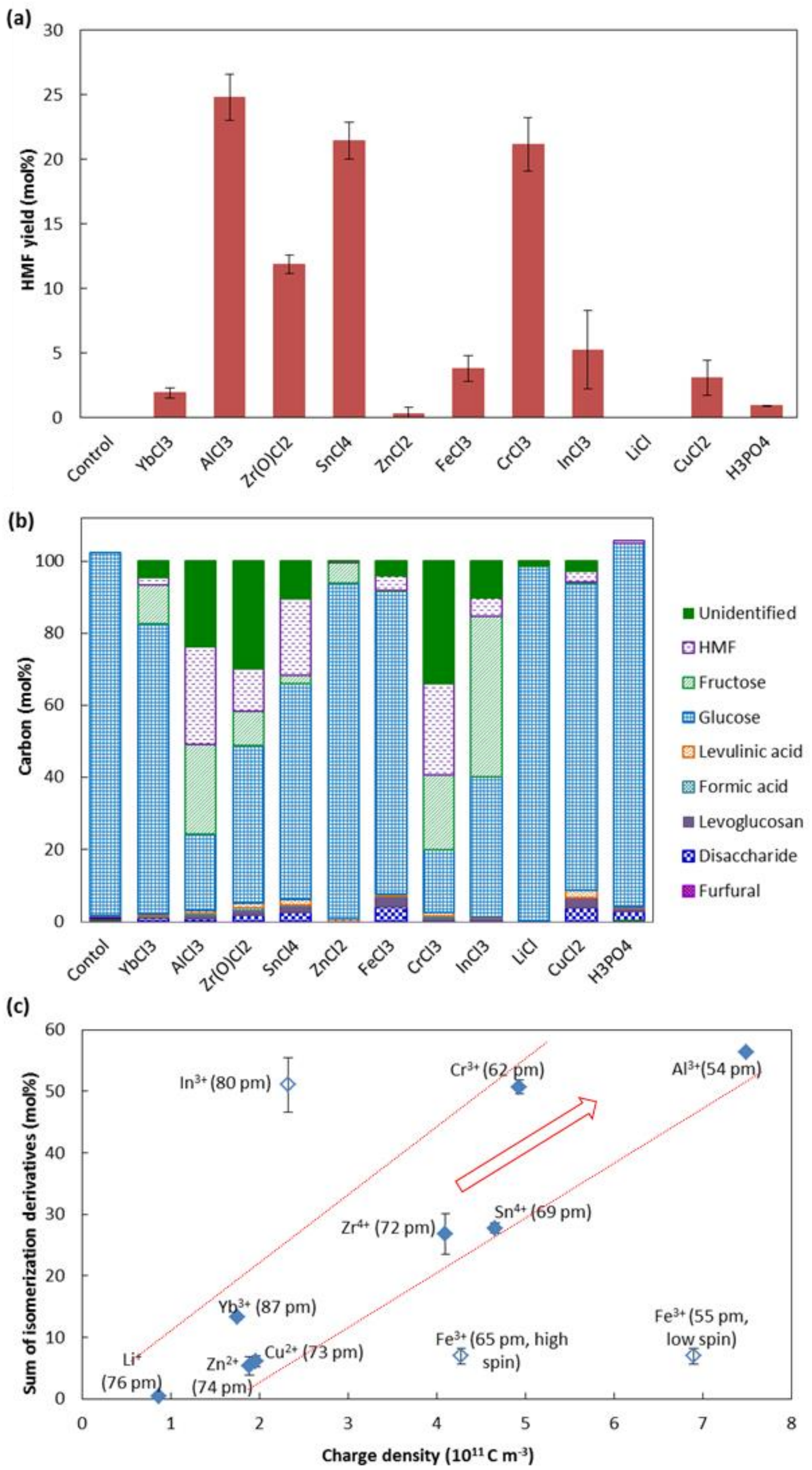

Figure 5.4. (a) HMF yield and (b) product carbon distribution of glucose conversion in the presence of different Lewis acid catalysts; and (c) correlation between sum of isomerization derivatives and charge density of Lewis metals (conditions: 5 wt/v% glucose and 55.5 mM Lewis acid catalyst in DMSO/water (1:1 v/v) at 140°C for 20 min; yield = product$_{mol}$/substrate$_{mol}$ × 100%; charge density were calculated using effective ionic radii in bracket, which were assumed in coordination with six anion O^{2-} with radius 140 pm (Shannon, 1976)).

The promising catalysts of Al^{3+} and Cr^{3+} are trivalent metals with relatively small effective ionic radius (54 and 62 pm, respectively), resulting in high charge density and strong electrostatic force that favours the coordination of ionic character, which was in consistence with the previous findings (Pagán-Torres et al., 2012; Wang et al., 2015). Yet, the moderately charged In^{3+} (2.3×10^{11} C m^{-3}) also resulted in an efficient isomerization probably because as a hard Lewis acid it would preferentially form stable complexes with hard ligands such as the hydroxyl groups of glucose (Pearson, 1968; Wang et al., 2015). Nevertheless, Fe^{3+} (hard Lewis acid) might be reduced by glucose into Fe^{2+} (borderline Lewis acid), with reference to the metal reduction shown in a spectroscopic study (Pidko et al., 2010), possibly accounting for its lower yield of isomerization product than expected.

The limited glucose isomerization by $FeCl_3$ resulted in about 5% yield of HMF with negligible fructose intermediate, while glucose isomerization by $InCl_3$ gave a fructose yield of 45% but a low HMF yield of 5% (**Fig. 5.4b**). This indicated that In^{3+}-catalyzed glucose isomerization was faster than fructose dehydration, whereas Fe^{3+}-catalyzed fructose dehydration was faster than glucose isomerization (by comparing **Fig. 5.2b and 5.4b**). Thus, a binary catalytic system was attempted to capitalize the rapid rates of the two consecutive reactions catalyzed by respective metals in order to improve the overall conversion efficiency.

Sequential catalyst addition of the dehydration-promoting $FeCl_3$ into isomerization-promoting $InCl_3$ or $AlCl_3$, where the stock of fructose was prominent, yielded more HMF than the control ($p \leq 0.05$) (**Fig. 5.5a**). Fructose formed during the first round of heating over $InCl_3$ or $AlCl_3$ was readily converted to HMF by $FeCl_3$ in the second round of heating. The binary catalysts accelerated the rate-limiting reactions, respectively (i.e., isomerization catalyzed by $InCl_3$ or $AlCl_3$ followed by dehydration catalyzed by $FeCl_3$), thus manoeuvring them into comparable rates. However, simultaneous addition of binary catalysts failed to improve the HMF production ($p > 0.05$) (**Fig. 5.5b**). A lower fructose yield with a larger amount of remaining glucose was measured in both binary catalytic systems with respect to those of single catalysts ($p \leq 0.05$) (**Fig. C.3**), remarking the significance of rate-limiting isomerization in the presence of $FeCl_3$. It was plausible that $FeCl_3$ further increased the acidity and hindered the formation of favourable In^{3+}-glucose or Al^{3+}-glucose complexes during isomerization (Wrigstedt et al., 2015). The subsequent dehydration process was then limited by fructose deficiency in case of simultaneous addition of $InCl_3$ and $FeCl_3$, or $AlCl_3$ and $FeCl_3$, leading to a significant decrease in HMF yield. Such negative effect of Brønsted acidity on Lewis acid-catalyzed isomerization needs to be addressed in detail in future studies.

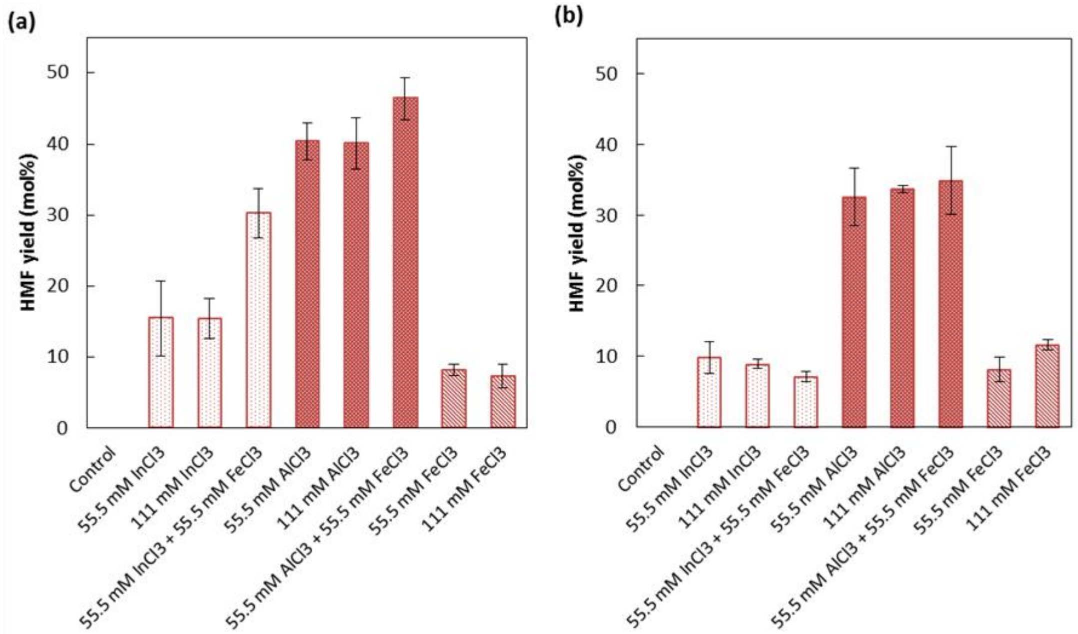

Figure 5.5. The HMF yield from glucose in the presence of single and binary catalyst in (a) sequential addition at 0 and 20 min, and (b) simultaneous addition at 0 min (conditions: 5 wt/v% glucose and 55.5 mM for single catalyst or 111 mM for binary catalyst in DMSO/water (1:1 v/v) at $140^{o}C$ for 40 min; yield = $product_{mol}/substrate_{mol} \times 100\%$).

5.2.3 Hydrolysis of glycosidic bonds by Brønsted acidity and Lewis centres

Cellobiose and maltose, which are glucose-based disaccharide anomers, showed comparable conversion rates over the tested metal chlorides (**Fig. C.4**). Both resulted in a lower HMF yield possibly due to the increased complexity of substrate and the additional hydrolysis step in the conversion pathway (**Fig. 5.6a&b**). Nonetheless, hydrolysis of glycosidic bond was notably enhanced by Lewis acids that the total amounts of hydrolysis derivatives (i.e., glucose, fructose, levoglucosan, HMF, formic acid, and levulinic acid) reached 84.8±0.8% from cellobiose and 81.4±2.7% from maltose in $SnCl_4$, respectively (**Fig. 5.6a&b**). A linear and inverse correlation between the sum of derivatives and pH was shown in **Fig. 5.6c**, corroborating that acidity was an important factor as reported in the literature (Tao et al., 2011; Zhou et al., 2013). Protons derived from partial hydrolysis of metal ions and the acidic by-products (as shown above) attacked the intramolecular C-O-C bond between sugar units to accelerate the cleavage of glucose. Based on the results of this study, a minimum acidity of pH 3 was required to initiate hydrolysis similar to fructose dehydration (**Fig. 5.6c**).

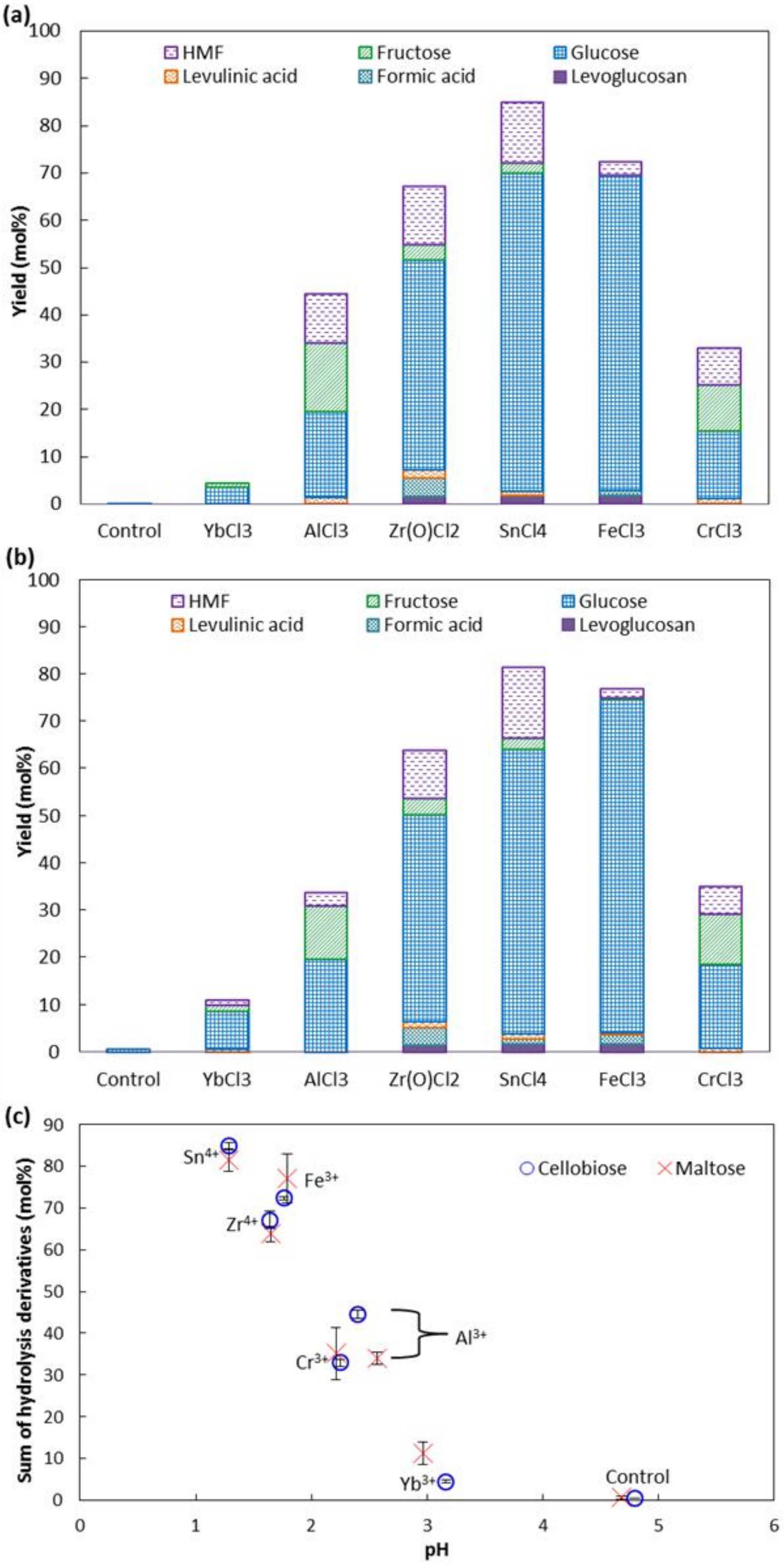

Figure 5.6. The yield of hydrolysis derivatives of (a) cellobiose and (b) maltose conversion under different Lewis acid catalysts; and (c) the correlation between the sum of derivatives and medium pH (conditions: 5 wt/v% glucose and 55.5 mM Lewis acid catalyst in DMSO/water (1:1 v/v) at 140°C for 20 min; yield = product$_{mol}$/substrate$_{mol}$ × 100%).

Interestingly, the use of cooked rice and bread crust (i.e., representative examples of sorted starch-rich food waste in this study) as substrate resulted in product distribution similar to standard maltose (**Fig. 5.7a&b**). The catalyst $SnCl_4$ also showed a good catalytic performance in food waste valorization, yielding 8.1±3.7% of HMF and 64.8±2.7% of glucose from rice, as well as 9.5±4.4% of HMF and 44.2±8.8% of glucose from bread crust, respectively. Both $SnCl_4$ and $Zr(O)Cl_2$ demonstrated comparable performance in the conversions of cooked rice and maltose ($p > 0.05$), while $AlCl_3$, $FeCl_3$, and $CrCl_3$ generated fewer products from rice than maltose ($p \leq 0.05$) (**Fig. 5.7c**). The solution pH was consistently higher in the conversion of cooked rice than those in maltose ($p \leq 0.05$). These results suggested that both Lewis acid site and Brønsted acidity played an important role for the hydrolysis of polymeric starch.

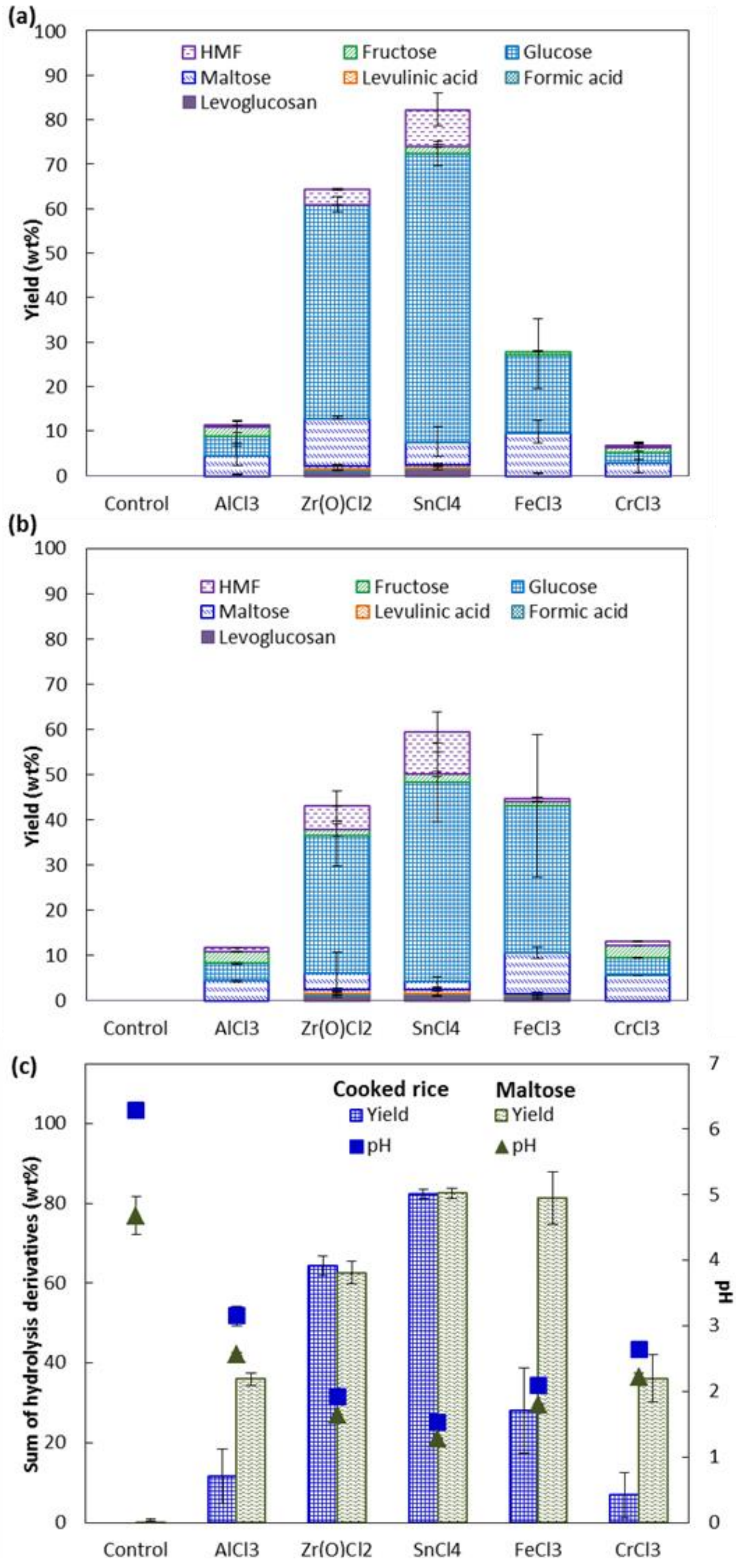

Figure 5.7. Yield of hydrolysis derivatives from (a) waste cooked rice and (b) bread crust; and (c) sum of derivatives and medium pH in conversion of rice and maltose (conditions: 5 wt/v% substrate and 55.5 mM Lewis acid catalyst in DMSO/water (1:1 v/v) at 140°C for 20 min; yield = product$_{wt}$/substrate$_{wt}$ × 100%).

The metal centre may attach to the glycosidic oxygen and weaken the (1-4)-α-linkage and (1-6)-α-linkage (Tao et al., 2011; Liu et al., 2013). Given that trivalent ions possess a less negative hydration enthalpy than tetravalent ions do (Marcus, 1987), Al^{3+}, Fe^{3+} and Cr^{3+} are less hydrated compared to Zr^{4+} and Sn^{4+}. The lower catalytic abilities of these trivalent metals could be ascribed to two possible reasons that reduced the amounts of available catalysts: 1) less hydrated metals were more easily attached to the oxygen atoms of carbohydrate chains; or 2) the hydrated species of Al^{3+}, Fe^{3+} and Cr^{3+} were physically entrapped in granule amorphous regions possibly due to metal hydrolysis and precipitation (Ciesielski et al., 2003; Szymońska et al., 2015). The product profile of cooked rice in this study was found to resemble that of standard starch (**Fig. C.5**), but the influence of impurities, e.g., proteins and fats, in other sorted food waste should be further studied.

5.2.4 *Undesirable polymerization induced by Lewis acids*

Polymerization, hexose internal condensation, and HMF rehydration are the side reactions that are often found responsible for the reduced selectivity of HMF (Ohara et al., 2010; Dutta et al., 2012). In the current study, the Brønsted acid H_3PO_4 gave the highest HMF selectivity in fructose conversion (95.7±6.5%, **Fig. C.6**), indicating that most of the reacted sugar was transformed into HMF in spite of the modest product yield (**Fig. 5.2**). In contrast, there was a lower HMF selectivity of some Lewis acids (**Fig. C.6**) such as $Zr(O)Cl_2$ (27.0±0.6%) and $CrCl_3$ (44.7±0.7%) despite their high product yield (**Fig. 5.2**). Similar results were also observed in glucose conversion (**Fig. 5.4&C.9**).

In these systems, only trace amount of off-path products, namely levulinic acid, formic acid and levoglucosan, were identified (**Fig. 5.2b&5.4b**), suggesting that undesired reactions such as rehydration of HMF and intramolecular condensation of glucose were negligible. The carbon balance was compromised by unidentified products resulted from unknown side reactions. Gas formation was unlikely as the total carbon recovery reached 95 to 99% in similar conversion studies (Asghari and Yoshida, 2007; Souza et al., 2012). Polymerization, on the other hand, was considered possible given the darkness of the product solution after the catalytic reaction. It has been reported that sugars, intermediates, and carbohydrates formed from the reaction may polymerize via aldol addition and condensation to form soluble polymers and insoluble humins (Patil et al., 2012; Hu et al., 2015). However, the determination of these by-products remains a challenge, because they could not be measured by gas chromatography–mass spectrometry (Zhang et al., 2015) or nuclear magnetic resonance (Kimura et al., 2013) in previous studies.

The effects of metal Lewis site were further evaluated and compared at a constant pH because Brønsted acidity was recognized as a controlling factor on polymerization (Hu et al., 2015). After fructose conversion, H_3PO_4 did not yield a noticeable amount of unidentified products while $YbCl_3$ generated approximately 30% at a pH around 2.1 ($p > 0.05$) (**Fig. 5.2b**). At a similar pH of 2.0 ($p > 0.05$), $AlCl_3$ and $CrCl_3$ resulted in 18% and 36% of unidentified products, respectively ($p \leq 0.05$). This implied that the Lewis acid sites had a higher tendency to result in polymerization than Brønsted acidity under comparable acidity (pH 2). The polymerization may result from binding of metal centre to the carbonyl oxygen of the carbohydrate species such as glucose (**Fig. 5.8**), polarizing the attached carbonyl group and rendering it more susceptible to the attack of a 2,5-dioxo-6-hydroxy-hexanal (DHH) enol. The latter was considered as the starting material for humins propagation derived from HMF (Patil et al., 2012). Such mechanism was similar to other carbonyl-involving addition reactions, for example, Mukaiyama aldol reaction and Roskamp reaction (Li et al., 2010; Román-Leshkov and Davis, 2011).

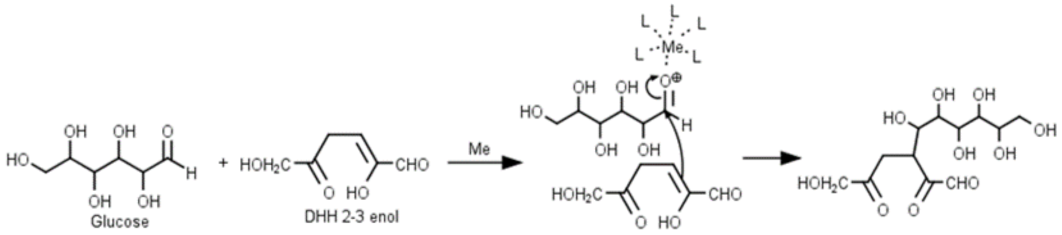

Figure 5.8. The Lewis acid-induced mechanisms proposed for (e) polymerization (based on Patil et al., (2012), and Román-Leshkov and Davis (2011)) (Me = metal ion; L = ligand).

5.3 Summary

This study articulated the dual roles of Lewis acid sites of the metal chlorides and their derived Brønsted characteristics for the valorization of food waste to HMF. Both fructose dehydration and disaccharide hydrolysis were improved by protons released from hydrolysis of metal catalysts, and formation of levulinic acid and formic acid. The Lewis acid sites could catalyze the rate-determining intramolecular hydride movement during fructose dehydration and glucose isomerization, which was governed by the electronegativity, electronic configuration, and charge density of metal ions. However, the Lewis acid sites led to unfavourable polymerization and lower carbon selectivity that required process optimization.

Chapter 6 – Relative Kinetics of Metal-Catalysed Tandem Reactions

Abstract

This chapter aims to maximize the valorization of bread waste, a typical food waste stream, into hydroxymethylfurfural (HMF) by improving our kinetic understanding. The highest HMF yield (30 mol%) was achieved using $SnCl_4$ as catalyst, which offered strong derived Brønsted acidity and moderate Lewis acidity. We evaluated the kinetic balance between these acidities to facilitate faster desirable reactions (i.e., hydrolysis, isomerization, and dehydration) relative to undesirable reactions (i.e., rehydration and polymerization). Such catalyst selectivity of $SnCl_4$, $AlCl_3$, and $FeCl_3$ was critical in maximizing HMF yield. Higher temperature made marginal advancement by accelerating the undesirable reactions to a similar extent as the desirable pathways. The polymerization-induced metal-impregnated high-porosity carbon was a possible precursor of biochar-based catalyst, further driving up the economic potential. Preliminary economic analysis indicated a net gain of USD 43-236 per kilogram bread waste considering the thermochemical-conversion cost and chemical-trading revenue.

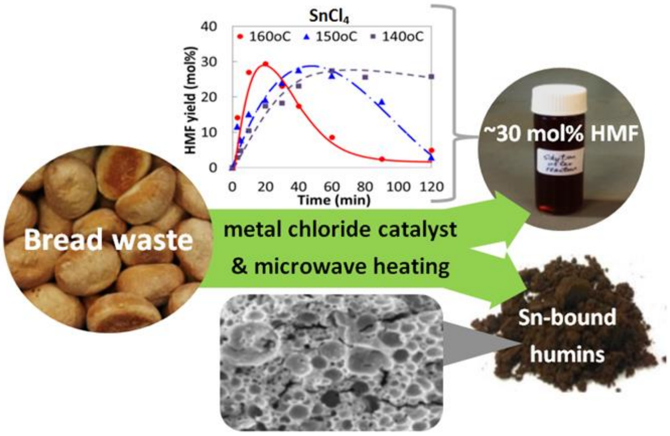

Figure 6.1. Graphical abstract of **Chapter 6**.

6.1 Research questions

Metal chlorides catalyze the consecutive steps of food waste conversion in a one pot efficiently with the synergistic function of the inherent Lewis acidity and developed Brønsted acidity, and a high HMF yield of 23% can be derived from waste cooked rice (**Chapter 5**). Meanwhile, other research explored various materials carrying Brønsted/Lewis acidity of different types and strengths, for example, ionic liquid (Qu et al., 2014), polymer nanotube (Zhang et al., 2015b), zeolite (Moreno-Recio et al., 2016), organic salt (Mirzaei and Karimi, 2016), and carboxylic acid (Seemala et al., 2016). Although these catalytic systems displayed a good productivity, undesirable off-path reactions, which may reduce yield and selectivity of HMF were often reported concomitantly (Qu et al., 2014; Kreissl et al., 2016; Moreno-Recio et al., 2016). These side reactions mainly refer to the rehydration of HMF to levulinic acid and formic acid as well as the polymerization of sugars and HMF to insoluble humins. Such challenge persists when the biomass-to-HMF process is scaled up. For example, Zhang et al. (2017) reported a threefold decline in the HMF yield from corncob due to the formation of humins when the substrate loading was increased from 40 to 70 mg in 2 mL reactive solvent. To enhance the system productivity, it is necessary to control the rates of both desirable reactions and undesirable reactions, which depends on multiple parameters such as catalyst use, temperature, and reaction time. However, the existing literature rarely address the simultaneous conversion reactions as an interactive complex system from a comprehensive perspective. As a result, the information regarding the effect, interplay, and relative importance of these parameters remain scattered and inconclusive, impeding the engineering applications of a selective catalytic system.

This chapter scrutinizes the crucial parameters, including the catalyst use, temperature, and reaction time to expedite the desirable reactions (i.e., hydrolysis, isomerization, and dehydration), and minimize the undesirable reactions (i.e., rehydration and polymerization) during thermochemical conversion of the starch-rich food waste to HMF. Bread waste was selected as the representative feedstock in view of its high feasibility towards conversion as well as high environmental relevance (**Chapter 3.1&4**). $SnCl_4$ served as the catalyst as it showed the best performance in **Chapter 4 and 5**.

6.2 Results and discussion

6.2.1 Efficient HMF production facilitated by $SnCl_4$

The excellent Brønsted acidity developed by $SnCl_4$ (pH 1.2–1.5) facilitated rapid hydrolysis of starch in bread waste, in which glucose surged to the peak of 48.2±1.3 mol% within 5 min at 140°C (**Fig. 6.2a**). Such acidity was largely derived from the protons released via partial hydrolysis of the Sn metal ion in the water-containing medium (Yu et al., 2016). After the 5-min reaction, the HMF concentration increased while the glucose content dropped because the rate of glucose utilization exceeded that of starch hydrolysis. The maximum HMF yield of 27.4±1.7 mol% (equivalent to about 20 wt% of bread waste) was reached at 60 min. It was higher than the reported yields from rice straw (2.6−6 wt%) (Amiri et al., 2010), bagasse (9.8 wt%) (Wang et al., 2014), maple wood (13–18 wt%), and corn stover (12–16 wt%) (Cai et al., 2014) under the thermochemical conversion systems consisting of comparable catalysts and solvents. Our results demonstrated that starch-rich food waste has a higher potential compared to some commonly studied lignocellulosic biomass as an appealing alternative feedstock for the production of HMF. The initial turnover frequency (TOF) for the conversion at 140 °C was ~3 mol HMF mol^{-1} Sn h^{-1}.

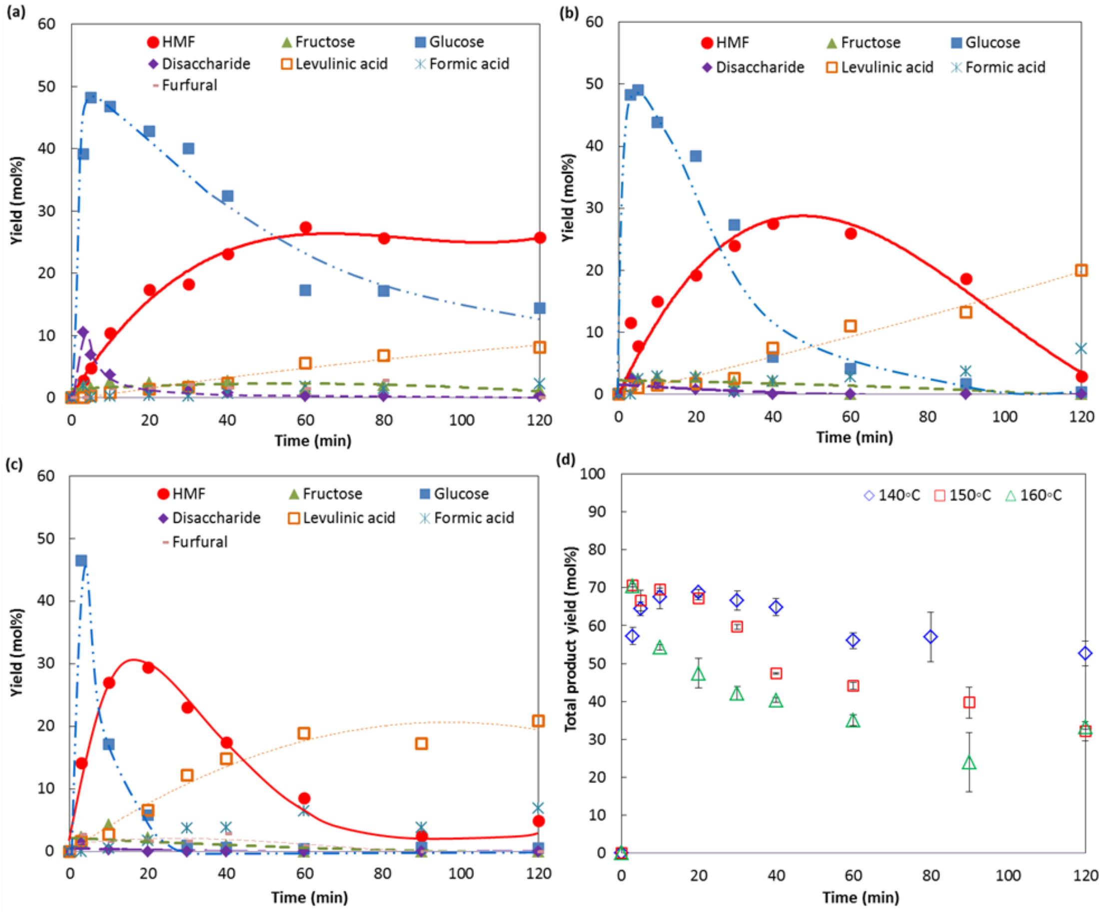

Figure 6.2. Product yields during the $SnCl_4$-mediated conversion of bread waste under heating at (a) 140°C, (b) 150°C, and (c) 160°C; and (d) total product yield at the three temperatures (conditions: 5 wt/v% substrate and 55.5 mM metal chloride in DMSO/water (1:1 v/v); yield = $product_{Cmol}/substrate_{Cmol} \times 100\%$).

Interestingly, limited amount of fructose (< 3 mol%) was detected during the process catalyzed by $SnCl_4$ at 140°C (**Fig. 6.2a**). The fructose might be dehydrated to HMF immediately by the strong derived Brønsted acidity after the glucose-fructose transformation (Enslow and Bell, 2015). Another plausible reason was that the glucose released from starch underwent direct dehydration to HMF without forming fructose as the intermediate under the highly acidic medium (Yang et al., 2015). This alternative route was initiated by the protonation at the C2 hydroxyl group of glucose and proceeded through the formation of a five-membered ring intermediate as revealed by a recent microkinetic analysis (Yang et al., 2015). Such pathway mediated by Brønsted acidity may be particularly important for the $SnCl_4$-facilitated production of HMF, in view of the moderate isomerization activity of $SnCl_4$ compared to other Lewis acids. For instance, the rate constant of the $SnCl_4$-catalyzd isomerization was 2.5×10^{-5} s^{-1} in an aqueous medium at 120°C, which was lower than that mediated by $AlCl_3$ i.e., 4.5×10^{-5} s^{-1} (Tang et al., 2015). Although the direct and indirect pathway may contribute in different proportions to produce HMF from glucose, their concomitant existence accounted for the outstanding catalytic performance of $SnCl_4$.

The kinetics of HMF formation was enhanced notably by the increase in temperature (**Fig. 6.2b&c**). The time to reach the peak of HMF yield shortened from 60 min to 40 and 20 min when the temperature rose from 140°C to 150 and 160°C, respectively, with the initial TOF increased to ~4.9 and ~18 mol HMF mol^{-1} Sn h^{-1}, respectively. Nevertheless, the maximum yield of HMF did not vary markedly with the increase of temperature (i.e., 27.4±1.7 mol% at 140°C; 27.6±0.3 mol% at 150°C; 29.5±1 mol% at 160°C). Such result implied that the rates of the desirable reactions (i.e., hydrolysis, isomerization, and dehydration) were comparable to the undesirable reactions (i.e., rehydration and polymerization) at the tested temperatures. These key reactions of bread waste valorization probably shared similar energy barriers under the catalysis and thus their kinetics were enhanced to a similar extent upon the temperature increase. This was corroborated by the estimated activation energies using model compounds in a recent study (Swift et al., 2015), e.g., 100 kJ mol^{-1} for glucose isomerization to fructose and 127 kJ mol^{-1} for fructose dehydration to HMF, in comparison to 97 kJ mol^{-1} for HMF redehydration to levulinic acid and 133 kJ mol^{-1}

for fructose polymerization to humins. A further study on computational kinetic modelling of our results would be carried out to quantify the activation energies for the simultaneous reactions of starch-rich food waste in our catalytic systems. The current results gave a strong indication that variation in energy input exerted a trivial effect in promoting the HMF maximum, which required faster desirable reactions relative to side reactions. In comparison, the selectivity of catalyst played a more important role, which was further addressed in **Section 3.2**.

While the considerable quantity of levulinic acid was indicative of the HMF rehydration (**Fig. 6.2a-c**), the decline in total product yield pointed to the formation of insoluble humins with increasing reaction time (**Fig. 6.2d**). It was a carbon-rich heterogeneous material resulting from the polymerization between sugars and HMF via aldol condensation and/or etherification (Zhang et al., 2015a; Tsilomelekis et al., 2016). The significant polymerization over $SnCl_4$ may be partly ascribed to the high concentration of HMF, which favoured the generation of 2,5-dioxo-6-hydroxyhexanal (DHH). The latter was identified as the initiator for humin growth, which originated from HMF upon water addition at C4 and C5 (Patil et al., 2012). Another study observed a direct engagement of Lewis acid in promoting sugars polymerization (Swift et al., 2015). In that case, the metal centre may bind to the intermediates in the conversion system, making them susceptible to the DHH attack as proposed in **Chapter 5.2.4**.

6.2.2 Conversion promoted by earth abundant metal chlorides

Production of HMF was effective over $AlCl_3$ but it generated product profiles different from $SnCl_4$. Disaccharide existed during the early stage of the $AlCl_3$-

catalyzed process (**Fig. 6.3a-c**), which was not significant over $SnCl_4$ (**Fig. 6.2a-c**), possibly due to the rapid hydrolysis at the lower pH (1.2–1.5 in $SnCl_4$ vs 2.3–3 in $AlCl_3$). The noticeable fructose content over $AlCl_3$ upheld the HMF production mechanism through the hydrolysis-isomerization-dehydration route, corroborating with the literature (Tang et al., 2015). Although the conversion over $AlCl_3$ resembled $SnCl_4$ in terms of the almost steady HMF maximum under the tested temperatures, $SnCl_4$ reached a higher peak of HMF yield than $AlCl_3$ (29.5±1 mol% vs 25.6±1 mol% at 160°C), indicating a faster HMF formation with respect to HMF consumption over the former catalyst. The initial TOF for the $AlCl_3$-catalysed conversion at 140 °C was ~0.37 mol HMF mol^{-1} Al h^{-1}.

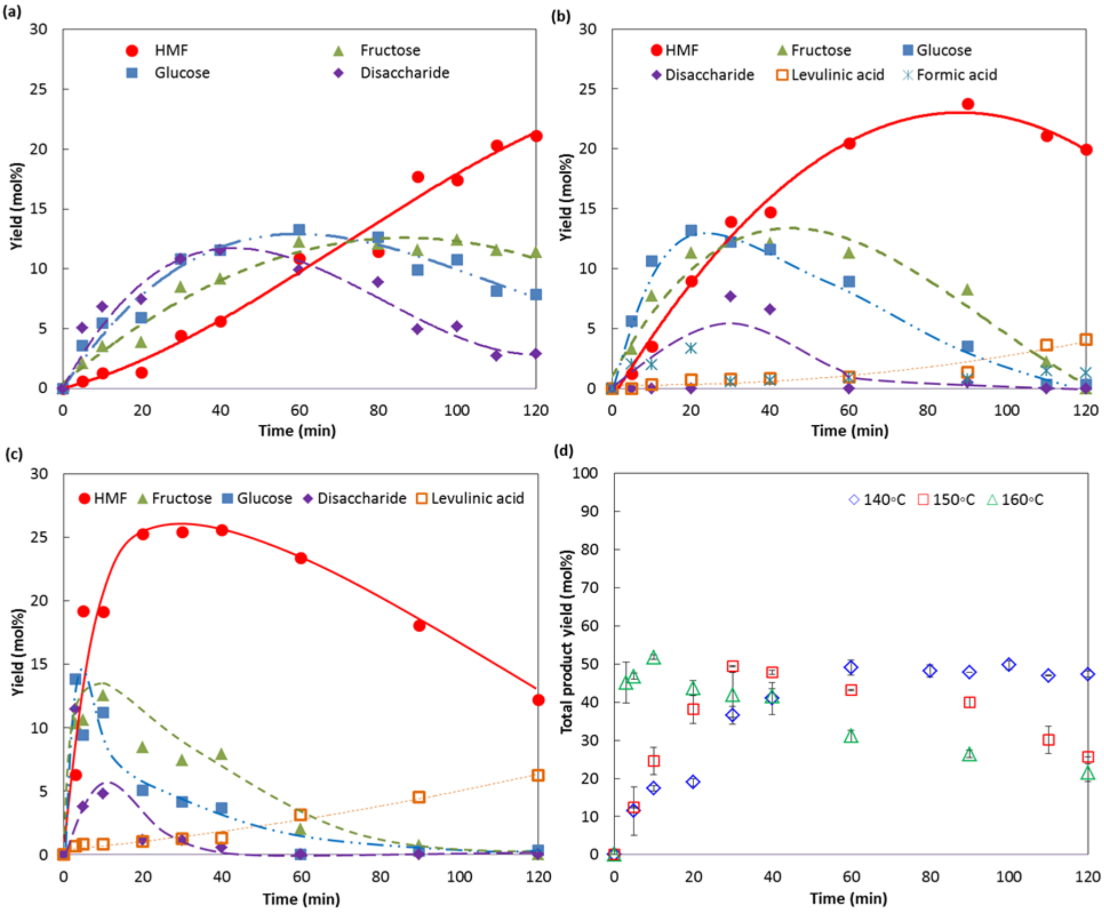

Figure 6.3. Product yields during the $AlCl_3$-mediated conversion of bread waste under heating at (a) 140°C, (b) 150°C, and (c) 160°C; and (d) total product yield at the three

temperatures (conditions: 5 wt/v% substrate and 55.5 mM metal chloride in DMSO/water (1:1 v/v); yield = $\text{product}_{\text{Cmol}}/\text{substrate}_{\text{Cmol}}$ × 100%).

The strong Brønsted acidity developed by $SnCl_4$ (pH 1.2–1.5) enabled fast hydrolysis to yield a high concentration of glucose and favoured the pH-dependent dehydration to produce HMF. The facile formation of HMF compensated for its loss to humins, resulting in a high total product yield (up to ~70 mol%) (**Fig. 6.2d**). In contrast, the mild Brønsted acidity given by $AlCl_3$ (pH 2.3–3) restrained the starch hydrolysis and fructose dehydration. These two rate-limiting reaction steps hindered the HMF production despite the efficient isomerization promoted by the Lewis acidity of $AlCl_3$. Taking into account the competitive humin formation that consumed HMF (**Fig. 6.3d**), the total product yield was lower over $AlCl_3$ (up to ~50 mol%) than $SnCl_4$. The significant polymerization was possibly induced by the strong Lewis acidity and binding ability of Al metal centre that assisted the DHH attack (discussed in **Section 6.2.1**). These results highlighted the importance of the ratio of Brønsted acidity to Lewis acidity in governing the kinetic profile of bread waste valorization, which was supported by the latest studies on conversion of model sugars (Kreissl et al., 2016; Li et al., 2016; Swift et al., 2016). Hence, an optimal balance between the two acidities can render the catalyst higher selectivity towards the desirable reactions over the undesirable reactions, which is essential to maximize HMF yield from food waste in our future studies.

In contrast, the $FeCl_3$-mediated conversion was distinctive from both $SnCl_4$ and $AlCl_3$. The former gave glucose as the major product because the hydrolysis reaction dominated under the sufficient Brønsted acidity (pH 1.7–2.3) derived from Fe hydrolysis (**Fig. 6.4a-c**). In comparison, HMF production was minor because the weak isomerization activity of $FeCl_3$ impeded the fructose-involved pathway

(**Chapter 5.2.2**), while its developed Brønsted acidity may not be strong enough to forward the direct glucose dehydration to HMF, for which the activation energy was suggested to be higher than glucose isomerization (Enslow and Bell, 2015; Swift et al., 2015). However, it is interesting to note that the HMF yield was improved at 160^{o}C and reached 9.8±1.9 mol% after 20 min (**Fig. 6.4c**), suggesting that even the moderate Brønsted acidity of $FeCl_3$ could produce HMF by direct glucose dehydration when the energy input was elevated. This was supported by the supplementary tests, where standard glucose at pH 2.0 (within the pH range given by $FeCl_3$) was converted to 15.1±2.2 mol% HMF in the absence of metal chloride at 160^{o}C (**Fig. D.1, Appendix D**). The glucose conversion also displayed a great dependence on the strength of Brønsted acidity as the HMF yield plummeted to 4 mol% or less at pH ≥ 2.3 (**Fig. D.1**). In addition, no fructose was detected, corroborating that the glucose-fructose transformation was negligible in a proton-mediated system (Yang et al., 2015).

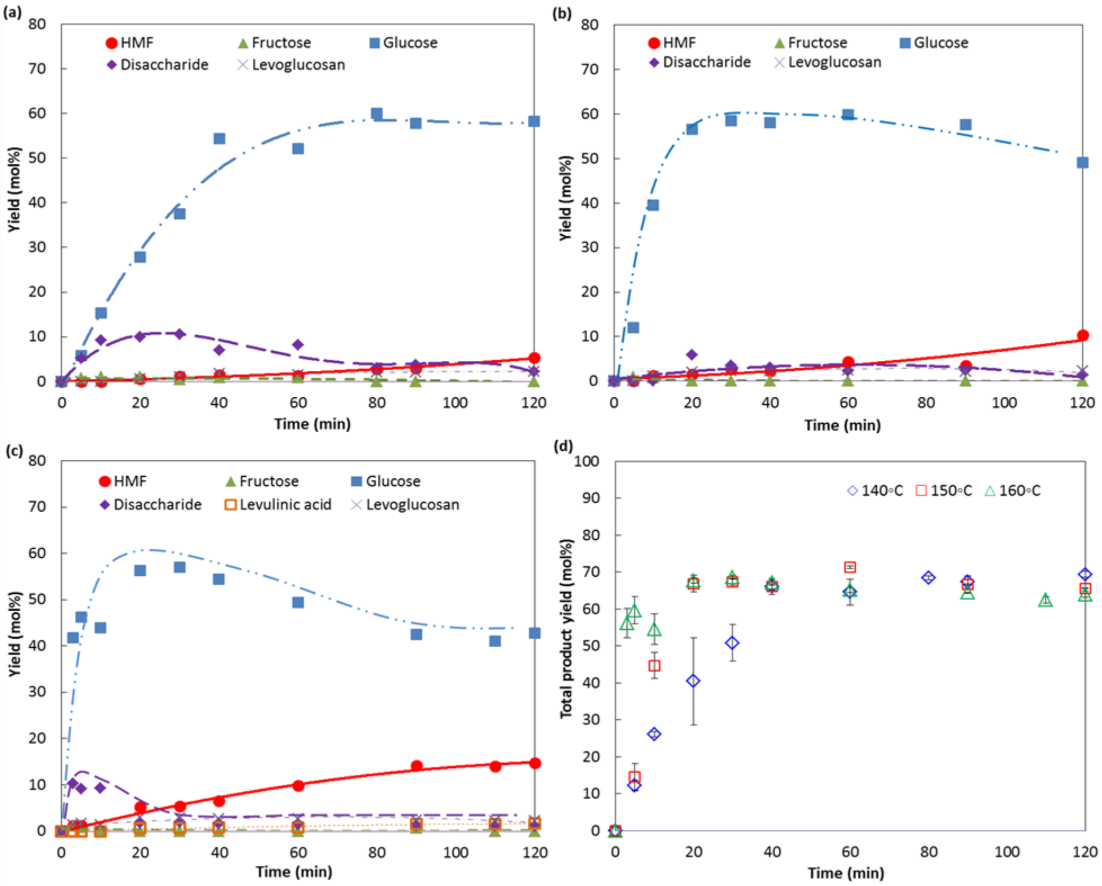

Figure 6.4. Product yields during the $FeCl_3$-mediated conversion of bread waste under heating at (a) 140°C, (b) 150°C, and (c) 160°C; and (d) total product yield at the three temperatures (conditions: 5 wt/v% substrate and 55.5 mM metal chloride in DMSO/water (1:1 v/v); yield = $\text{product}_{\text{Cmol}}/\text{substrate}_{\text{Cmol}} \times 100\%$).

Although $FeCl_3$ offered a higher Brønsted acidity than $AlCl_3$ (pH: 1.7–2.3 vs 2.3–3), the former induced negligible product loss to humins even at 160°C (i.e., total product yield reached as high as ~70 mol%) (**Fig. 6.4d**), contrasting with the results in $AlCl_3$ (**Fig. 6.3d**). This suggested that Brønsted acid played a relatively minor role in catalyzing the polymerization reactions during bread waste valorization, whereas Lewis acid may impose a more pronounced effect. Such supposition concurred with the recent findings on glucose conversion that the rate constants of HCl-mediated humin formation reactions were lower than those catalyzed by $AlCl_3$ (Zhang et al., 2015a) and that the medium to strong Lewis acid sites enhanced the formation of the undesired by-products (Li et al., 2016). The lower sensitivity of polymerization to Brønsted acidity further rationalized the higher maximum HMF yield obtained over $SnCl_4$ (**Fig. 6.2**) compared to $AlCl_3$ (**Fig. 6.3**) as discussed above. The desirable reactions (hydrolysis and dehydration in particular) that greatly depended on Brønsted acidity were much more favoured over $SnCl_4$ than $AlCl_3$, while the undesirable polymerization was less promoted, thus resulting in a faster kinetics of formation relative to consumption of HMF. This underscored again the importance of the dual acidic properties of metal catalyst in regulating its selectivity towards the desirable reactions to achieve a high HMF productivity.

6.2.3 HMF yield as a function of intermediate and by-products

The interesting kinetic correlations between the concentrations of HMF and its intermediate precursor, i.e., glucose over $SnCl_4$ and $AlCl_3$, could be characterized into three zones (**Fig. 6.5a&b**). The HMF content rose gradually with glucose in **Zone I** that described the beginning stage of the process, where the facile hydrolysis of starch in bread waste released glucose massively to simulate HMF formation. The HMF generation was the most productive at the expense of glucose in **Zone II**, which demonstrated the mid-stage of the conversion. Entering the final stage represented by **Zone III**, HMF yield decreased upon rehydration and polymerization, and only trace amount of glucose remained under prolonged reaction time. The HMF vs glucose pattern in $FeCl_3$ was distinctive that the HMF decline zone (**Zone III**) was absent (**Fig. 6.5c**) due to the high product stability maintained over $FeCl_3$ against polymerization as mentioned in **Section 6.2.2**. On the other hand, the yield of HMF also exhibited a positive relationship with its rehydration product, i.e., levulinic acid, in the first phase of the process (**Zone I**) over $SnCl_4$ and $AlCl_3$ (**Fig. D.2a&b**). It then decreased to yield more levulinic acid in the second phase (**Zone II**), where the HMF rehydration became more competitive than its formation.

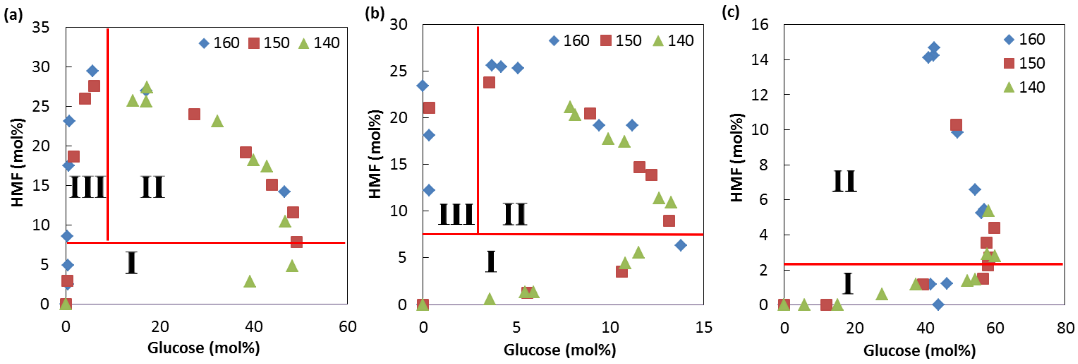

Figure 6.5. Concentration of HMF as a function of glucose during the conversion of bread waste over (a) $SnCl_4$, (b) $AlCl_3$, and (c) $FeCl_3$ at different temperatures (conditions: 5 wt/v% substrate and 55.5 mM metal chloride in DMSO/water (1:1 v/v); yield = $product_{Cmol}/substrate_{Cmol}$ × 100%; remarks: the product profiles were divided into Zone I, II, and III, which represented the beginning, middle, and final stage of the conversion, respectively).

These patterns demonstrated the strong dependence of HMF yield on the formation of intermediate precursor (i.e., glucose) and its by-product (i.e., levulinic acid), reiterating the relative significance of both desirable and undesirable reactions. More importantly, it was noted that the temperature increased from 140 to 160°C did not alter the product profiles (**Fig. 6.2-3**), but only reduced the reaction time to reach a particular status of the profile. This was clearly evidenced in **Fig. 6.5 and S3,** although the starting point of the curves progressively shifted from **Zone I** to **II** as the temperature increased, the shape of the curves as well as the HMF maxima remained unaffected. This aligned well with the observations addressed in **Section 6.2.1 and**

6.2.2 that the energy input enhanced the kinetics of all the reactions in the system, including both the desirable and undesirable ones, to a similar extent over the tested catalysts.

6.2.4 Formation of char-like humins

The solid residues collected from different catalytic conversions at 140°C for 120 min displayed distinctive appearances (**Fig. 6.6**). The TGA analysis showed that residue from control experiment and as-received bread waste contained 50–60% starch that produced a peak at about 240–340°C in DTG curves (**Fig. 6.7**). Within the same temperature window, the residues from $AlCl_3$- and $FeCl_3$-catalyzed reactions exhibited a mass loss of approximately 20% (**Fig. 6.7b**), which was possibly attributed to the unexploited crystalline starch under the tested catalytic conditions.

Figure 6.6. Solid residues from (a) $SnCl_4$-, (b) $AlCl_3$-, and (c) $FeCl_3$-catalyzed conversion of bread waste, and (d) control experiment (i.e., without metal chloride catalyst) (conditions: 5 wt/v% substrate and 55.5 mM metal chloride (except control) in DMSO/water (1:1 v/v) at 140°C for 120 min).

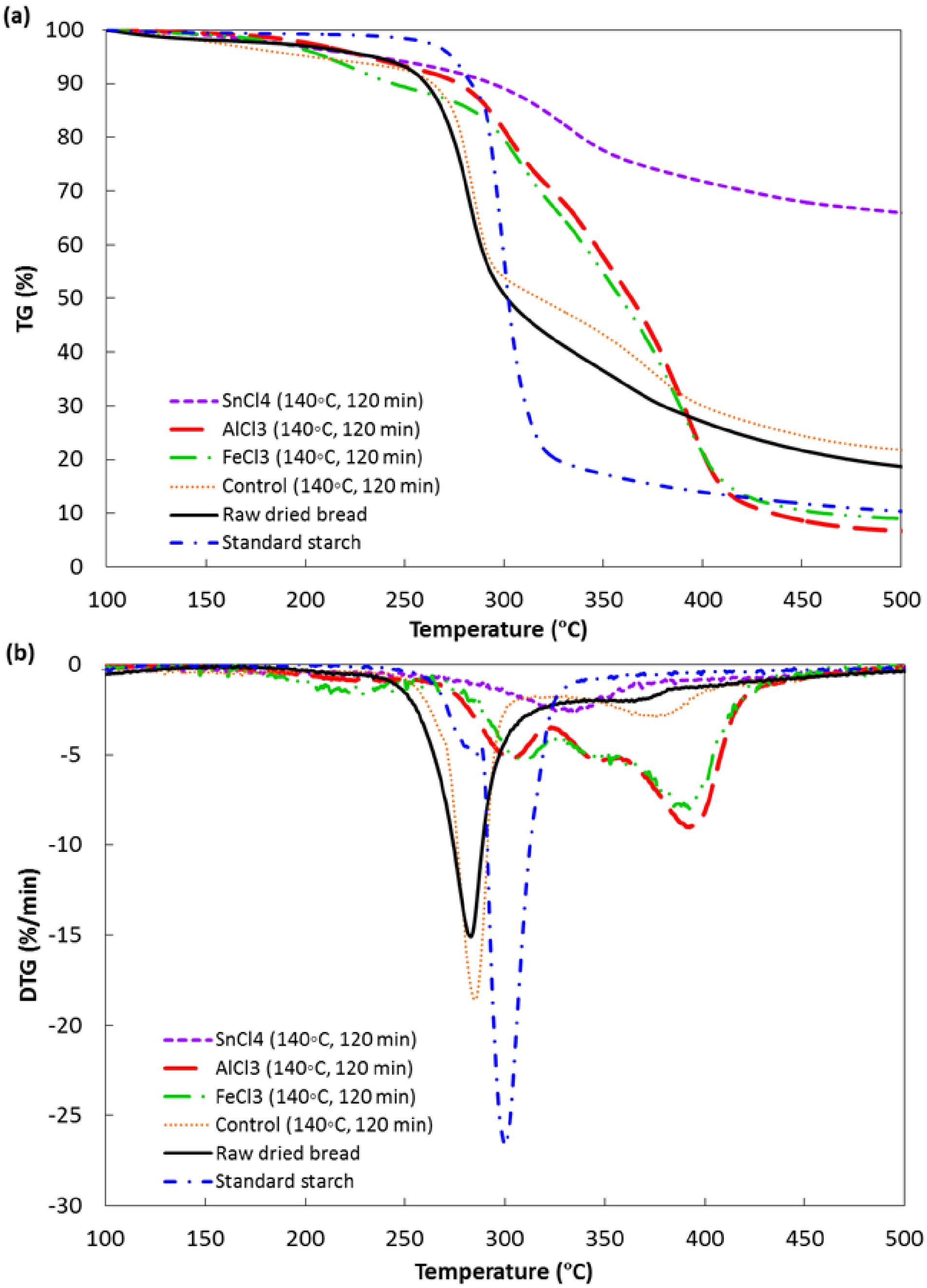

Figure 6.7. (a) Thermogravimetry (TG) and (b) derivative thermogravimetry (DTG) spectra of solid residues from catalytic conversions of bread waste and control (i.e., without metal chloride catalyst), raw dried bread waste, and standard starch.

The $SnCl_4$-mediated conversion gave dark-coloured powder residues (**Fig. 6.6a**), which contained no remaining starch (**Fig. 6.7b**) and displayed outstanding thermal stability as 70% of the initial mass was constant at 370°C and above (**Fig. 6.7a**). Increasing the conversion temperature from 140 to 150°C also generated solid residue with a similar thermogram over $AlCl_3$ (**Fig. D.3**), in which the carbon content was intensified to 59±2 wt% as indicated by TOC analysis (compared to 41.5±0.3 wt% in as-received bread waste). These findings confirmed the earlier speculation on product loss to the carbonaceous humins over $SnCl_4$ and $AlCl_3$ (in **Section 6.2.1 & 6.2.2**). It is noteworthy that the SEM images of the humins from $SnCl_4$-mediated conversion depicted a highly porous structure with the pore size of 1–10 µm (**Fig. 6.8a**), which far differed from the starch-containing residues of other systems under the same conditions (i.e., 140°C, 120 min) (**Fig. 6.8b-d**). In comparison, humins from the 150°C-process over $AlCl_3$ instead presented scattered clusters of tiny spherical particles (< 1 µm) (**Fig. D.4a**) that resembled the previously reported morphology (van Zandvoort et al., 2013; Tsilomelekis et al., 2016).

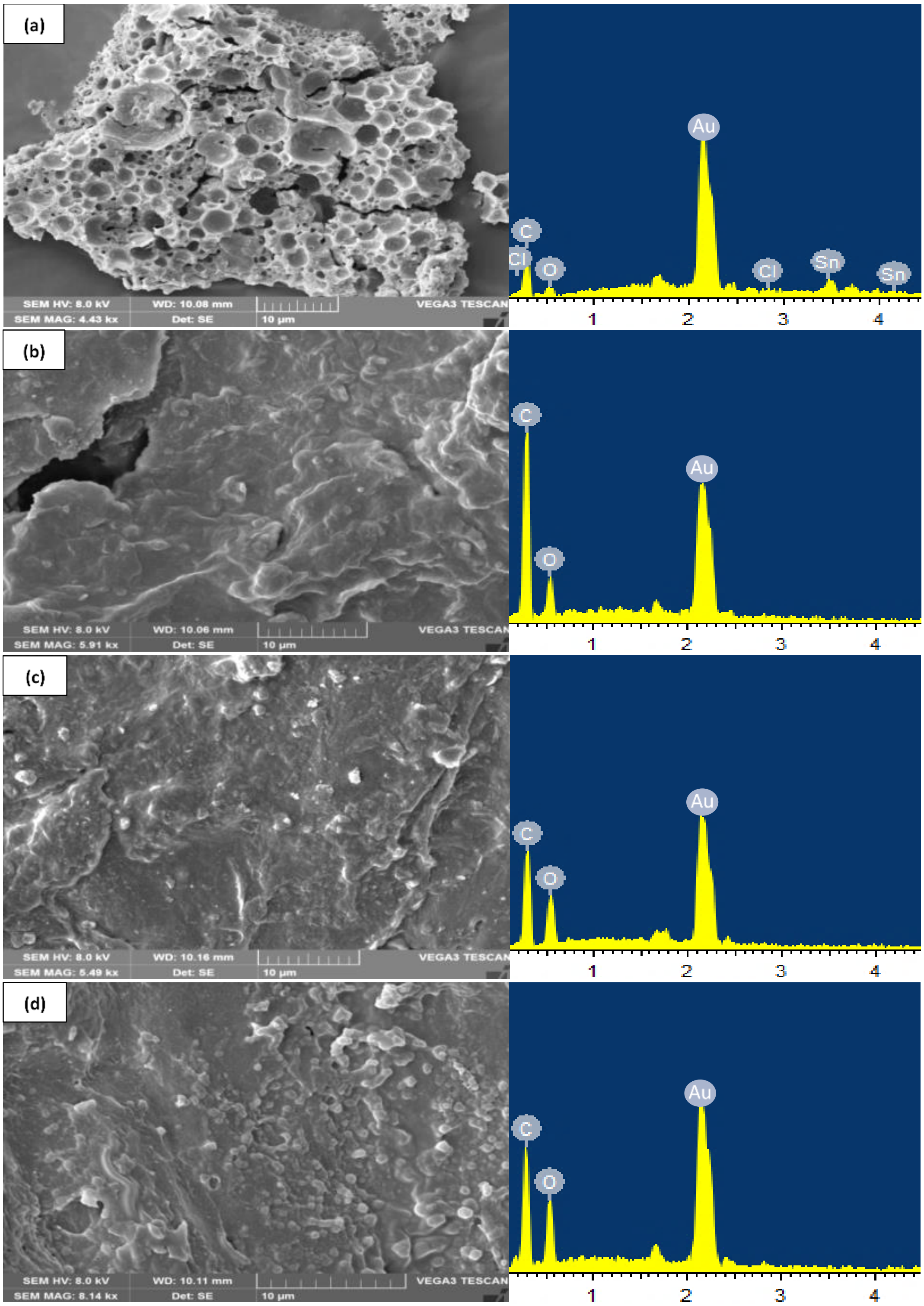

Figure 6.8. Scanning electron microscope (SEM) image and energy dispersive X-ray (EDX) spectra of solid residues from (a) $SnCl_4$-, (b) $AlCl_3$-, and (c) $FeCl_3$-catalyzed conversion of bread waste, and (d) control (i.e., without metal chloride catalyst) (conditions: 5 wt/v% substrate and 55.5 mM metal chloride (except control) in DMSO/water (1:1 v/v) at 140°C for 120 min; remarks: samples were coated by gold to enhance conductivity for analysis).

We thereby proposed the clusters of humins as the transition state of the porous material formation. Similar to the chemical activation of biochar (Liu et al., 2015; Rajapaksha et al., 2016), the clusters may undergo multiple steps such as dehydration, condensation, and volatile release to create a high porosity in the presence of catalysts. The strong derived Brønsted acidity and moderate Lewis acidity of $SnCl_4$ may deliver a rapid activation process, reducing the energy requirement (≤ 140^oC) for the porous structure synthesis. On the contrary, a higher temperature (≥ 150^oC) may be needed to generate an analogous structure over the less active $AlCl_3$. Previous studies also demonstrated the dependence of humin formation on the amount and strength of Lewis acid sites (Ordomsky et al., 2013; Li et al., 2016) as well as the Brønsted acidity (Tsilomelekis et al., 2016). Further investigations would be conducted to unravel the transformation mechanism of humins and the change of its physiochemical properties over the catalysts with different Brønsted/Lewis acid ratios and properties. Nonetheless, the consumption of metal catalyst would be less considerable within 20-60 min, at which the highest HMF was achieved over $SnCl_4$ (**Fig. 6.2a-c**).

The resulted porous materials could be subject to further pyrolysis into biochar for remediation of contaminated water and soil (Rajapaksha et al., 2016). It may also serve as a biochar-based solid catalyst (Liu et al., 2015; Qian et al., 2015), since the Sn metal deposition was observed on the porous carbon structure (**Fig. 6.8a**), amounting to approximately 67 wt% of the solid according to the EDX analysis. It was also interesting that metals was not detected in solid samples from the $AlCl_3$- and $FeCl_3$-mediated conversion, possibly due to their lower catalytic activity in comparison to $SnCl_4$ as discussed above. A higher conversion temperature and longer reaction time might be required for Al and Fe to deposit on the humins. Further characterization in terms of the surface area, metal species, functional groups, etc, would be necessary to develop the potential applications of the Sn-bound humins.

6.2.5 Economic feasibility of bread waste valorization

The financial viability of the valorization of bread waste was substantiated by our preliminary economic analysis (**Fig. 6.9**). Given that chemicals with industrial quality were considered, a net gain of USD 43 was estimated when 1000 g of bread waste was valorized, in which HMF was the key profit-making item that exceeded the cost. The benefit could further reach USD 236 per 1000 g bread waste if chemicals with a high purity could be produced (**Table D.1**), demonstrating the significance of the quality of products. It should be noted that the total cost was dominated by the solvent DMSO (~91%), followed by the catalyst $SnCl_4$ (~9%). Such results implied that the selection and engineering of recyclable/reusable solvents and catalysts will significantly reduce the total cost.

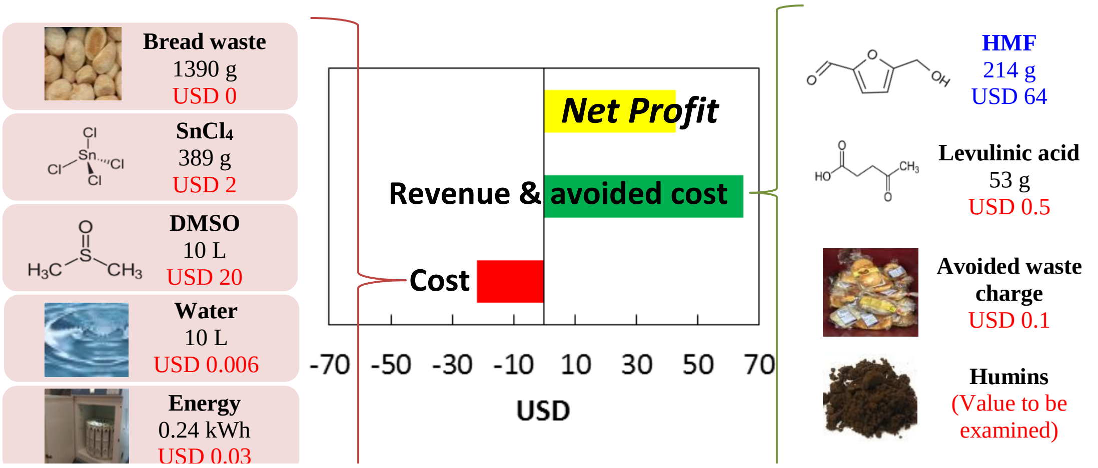

Figure 6.9. Preliminary estimation of mass balance, as well as costs and revenues from valorization of 1000 g bread waste (dry weight; equivalent to 1390 g as-received weight) into HMF in the Hong Kong context (conversion scenario: 5 wt/v% substrate and 55.5 mM $SnCl_4$ in DMSO/water (1:1 v/v) at 160°C for 20 min; remarks: chemicals with industrial quality were considered).

This simplified analysis took into account the production expenses, e.g., consumption of chemicals, water, and energy, the avoided waste disposal charge, as well as the revenue from produced chemicals. To maximize the business profitability and resource utilization, levulinic acid was considered as a secondary tradable product after HMF, while the potential value of humins was excluded. The scenario was based on the most promising conditions of our experiments in this study: $SnCl_4$-catalyzed conversion of bread waste at 160^oC for 20 min, which yielded around 30 mol% HMF. More information on the calculations and assumptions were given in **Table D.1**. A hybrid life cycle assessment and cost-benefit analysis are in progress to assess the economic viability together with the environmental performance and social acceptance. An expanded scope will be adopted for more realistic simulation, covering the upstream processes (e.g., collection and transportation of food waste) as well as the downstream treatments (e.g., material recycling and landfill disposal of the unavoidable waste). Scale factors will be taken into account to simulate the pilot-scale valorization of starch-rich food waste on the basis on our experimental results.

6.3 Summary

Valorization of bread waste to HMF mediated by $SnCl_4$ was the most productive (maximum 30 mol%). The catalyst selectivity governed the maximum HMF yield, in which the reaction kinetics and relative significance of desirable conversion pathways over off-path reactions played an important role. Temperature increase could not boost the HMF maximum because both desirable and undesirable pathways were accelerated to a similar degree, which may depend on the Brønsted and Lewis acidities.

The $SnCl_4$-derived humins showed distinctive properties, which may be transformed to biochar-based catalyst. The starch-rich food waste valorization business appears to be profitable and warrants future investigations.

Chapter 7 – Roles of Co-Catalyst in Controlling Selectivity and Kinetics

Abstract

This chapter examines the effect of addition of maleic acid (MA) as co-catalyst on the reaction kinetics and product selectivity in conversion of rice waste to HMF. The maximum yields of HMF by Sn(IV) and Cr(III) system were ~36 and ~26 mol%, respectively, in the medium of dimethyl sulfoxide (DMSO)/H_2O at 140 ^oC. The addition of MA to Sn(IV) did not noticeably alter the conversion kinetics, maintaining nearly constant rates of tandem reactions (i.e., hydrolysis of starch, isomerisation of glucose, and dehydration of fructose). In contrast, MA notably changed the kinetics in Cr(III)-based reaction, reducing the rate of glucose isomerisation while accelerating the starch hydrolysis. Hydration of MA under acidic environment resulted in malic acid (38.4%), which may increase the accessibility of starch by interrupting its hydrogen bond network in the Cr(III) system. The addition of MA enhanced the HMF selectivity for Cr(III), probably because MA and its derivatives may form complex with Cr(III) to moderate the Lewis acidity and suppress the side reactions that can consume sugars and HMF. Nevertheless, as a trade-off of enhanced selectivity, the overall conversion of rice waste to HMF was slower in Cr(III)/MA. This chapter elucidates the contrasting roles of co-catalyst in controlling the selectivity and kinetics of metal catalysts in biomass conversion.

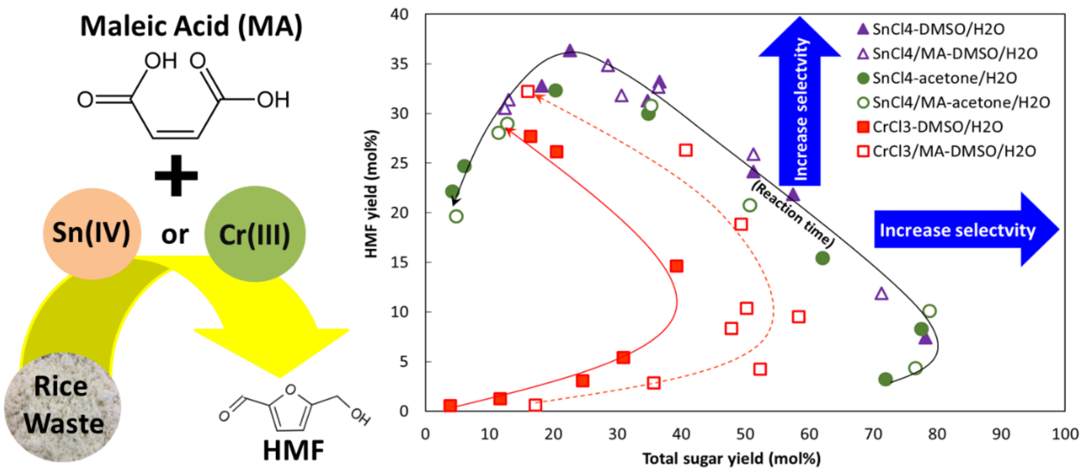

Figure 7.1. Graphical abstract of **Chapter 7**.

7.1 Research questions

Achieving high HMF selectivity is an elusive challenge due to the presence of irreversible side reactions that reduce HMF yield, such as rehydration of HMF and polymerisation among intermediates and HMF, which can also be promoted by Brønsted and Lewis acid (**Chapter 6**). The acid properties of catalysts (e.g., strength and quantity) play a critical role in determining the HMF selectivity (**Chapter 2.3.3**). The addition of organic acids as a co-catalyst can thus be considered to improve HMF selectivity as reported in the recent literature (Zhang et al., 2016; Delbecq et al., 2017; Lopes et al., 2017). Maleic acid-coordinated $AlCl_3$ was suggested to reduce energy barrier for glucose-to-fructose isomerisation (94.5 kJ mol^{-1}) compared with the HCl-$AlCl_3$ system (149 kJ mol^{-1}) (Zhang et al., 2016). Formic acid was seen to pair with $AlCl_3$ for catalytic isomerisation of xylose (a C5 analogue of glucose) to xylulose (Lopes et al., 2017), while betaine coupled with formic acid was reported to accelerate HMF formation possibly by offering an acidic ionic liquid-mimicking environment (Delbecq et al., 2017).

However, intriguing observations are reported. The reactions were slowed down in the maleic acid-$AlCl_3$ system (i.e., rate constant of glucose utilisation was 0.23 as compared with 0.68 in $AlCl_3$) (Zhang et al., 2015), while they were accelerated in case of formic acid-$AlCl_3$ (i.e., shortened reaction time for furfural production relative to $AlCl_3$ only) (Lopes et al., 2017). High-pressure CO_2 was applied to generate in-situ carbonic acid, which was suggested to interact with $CrCl_3$ to enhance the conversion kinetics of cellulose, although there was no apparent improvement in product selectivity (Jing et al., 2016). To reap the benefits offered by the co-catalysts in such an emerging area, it is necessary to elucidate the roles of the organic acids in controlling the product selectivity and reaction rates.

Interactions between a tetravalent metal and organic acid have not been investigated in catalytic biomass conversion to the best of our knowledge. It is contended that the complementary effects of the organic acid vary with the choice of metal catalyst, because there are different tendencies and forms of bindings between organic ligands and metals (Bala et al., 2007; Drábek et al., 2015). It is also contended that the previously reported synergy may take place to different extents depending on the reaction medium, which is yet poorly described because only one medium was considered in the previous studies (Zhang et al., 2016; Lopes et al., 2017). As for conversion of bread waste catalysed by $SnCl_4$ only, acetone- and acetonitrile-containing reaction media were reported to expedite the tandem reactions, compared with the other conventional solvents such as DMSO (**Chapter 8**).

This chapter aims to assess the interplay between catalyst (metal catalysts: i.e., $CrCl_3$ and $SnCl_4$)) and co-catalyst (maleic acid (MA)) in the production of HMF from rice waste, which is a significant type of waste worldwide (**Chapter 3.1**) The selected trivalent and tetravalent metals carry different acid properties related to their valences, i.e., stronger Brønsted acidity (developed via partial hydrolysis) and milder intrinsic Lewis acidity were observed for Sn^{4+} when compared with Cr^{3+} (**Chapter 5**). The effects of a co-catalyst in the production of HMF are scrutinised with respect to product selectivity and conversion rate, which will help elucidate the opportunities of engineered binary-catalyst systems in chemical production from biomass waste.

7.2 Results and discussion

7.2.1 Conversion rate affected by MA

The conversion of rice waste over Sn(IV) as the catalyst with respect to reaction time is shown in **Fig. 7.2a** (in DMSO/H_2O, at 140 °C). Approximately 90 mol% of total products were obtained after 10 min, among which 69 mol% was attributed to glucose as a result of hydrolysis of starch in rice waste. The glucose content decreased gradually, giving rise to fructose that was dehydrated to HMF subsequently. The HMF yield increased and reached the maximum of 36.3 mol% at 80 min, beyond which the HMF yield decreased and levulinic acid notably increased due to the rehydration of HMF as the reaction prolonged. In case of the Cr(III)-catalysed conversion of rice waste, the maximum total product yield of ~60 mol% was obtained after heating at 140 °C for 60 min in DMSO/H_2O (**Fig. 7.2b**), which implies less efficient hydrolysis of starch compared with the Sn(IV) system (~90% total product yield at 10 min; **Fig. 7.2a**). The Cr(III) system had an initial pH value higher than Sn(IV) (pH 2.2 vs 1.5). Brønsted acidity is developed as metal ions undergo partial hydrolysis in an aqueous medium (Choudhary et al., 2013; Yu et al., 2016). The lower hydrolysis constant of Cr(III) ($pK_1 = 4$ vs -1.6 for Sn(IV)) (Brown et al.,

1985) led to a smaller extent of proton release, as evidenced by the higher pH value measured. The intersection between the trends of sum of sugars (i.e., disaccharides, glucose and fructose) and HMF yield in **Fig. 7.2** represents the time (t) at which dehydration of sugars starts to emerge. The HMF formation was notably hindered in Cr(III) in view of $t_{Cr(III)}$ (~85 min) > $t_{Sn(III)}$ (~50 min). A lower HMF yield of 26.2 mol% was obtained in Cr(III) at 80 min (**Fig. 7.2b**), at which 36.3 mol% HMF appeared as the maximum in Sn(IV) (**Fig. 7.2a**). When MA was added as a co-catalyst in a way similar to previous studies (using glucose as substrate) (Zhang et al., 2015; 2016), the conversion kinetics in the Sn(IV) and Cr(III) systems showed distinctive responses (**Fig. 7.2c&d**). The rice waste conversion over Sn(IV)/MA resembled that catalysed by Sn(IV) only in terms of product profile and conversion rate (comparing **Fig. 7.2a & c**), suggesting a minor impact exerted by the MA addition on the kinetics.

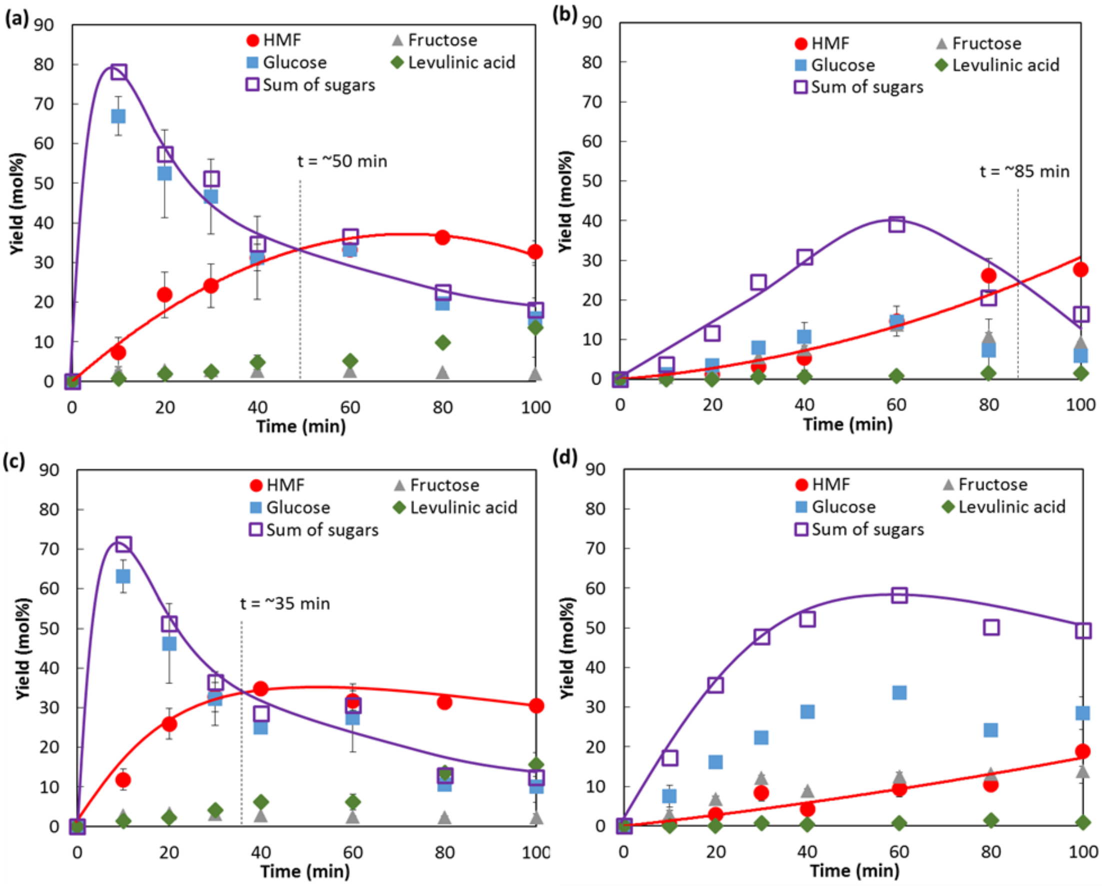

Figure 7.2. Product yields in relation to the catalytic conversion of rice waste in the (a) Sn(IV), (b) Cr(III), (c) Sn(IV)/MA, and (d) Cr(III)/MA systems in DMSO-water mixture (1:1 v/v) (conditions: 5 wt/v% substrate and 55.5 mM $SnCl_4$ or $CrCl_3$ and 13.9 mM MA at 140 ^oC; yield = $product_{Cmol}/substrate_{Cmol} \times 100\%$). Remark: the intersection between the trends of sum of sugars (i.e., disaccharides, glucose and fructose) and HMF yield represents the time (*t*) at which dehydration of sugars starts to emerge.

Using standard starch as the substrate, both Sn(IV) and Sn(IV)/MA resulted in approximately 80 mol% total products and 10 mol% HMF after heating at 140 ^oC for 10 min in DMSO/H_2O (**Fig. 7.3a&c**). Similarly, conversion of standard fructose over these catalysts gave a comparable HMF yield of 54-59 mol%. These results are consistent with the observed high resemblance between the Sn(IV)- and Sn(IV)/MA-catalysed conversion of rice waste (**Fig. 7.2a&c**). Given that starch hydrolysis and fructose dehydration are catalysed by a Brønsted acid, these results signify that the addition of MA had minimal effect on the Brønsted acidity in the Sn(IV) systems. It is probably because acid dissociation of MA was negligible in the Sn(IV)-containing mixture with an initial pH value of 1.2-1.5 (i.e., lower than pKa_1 of MA = 1.9; Skoog, 2000). In addition, control tests indicate that MA coupled with chloride ions (from NaCl) did not promote conversion of rice waste in the absence of Lewis acid metals (i.e., limited total product yields < 2 mol% at 140 ^{o}C, 10 min).

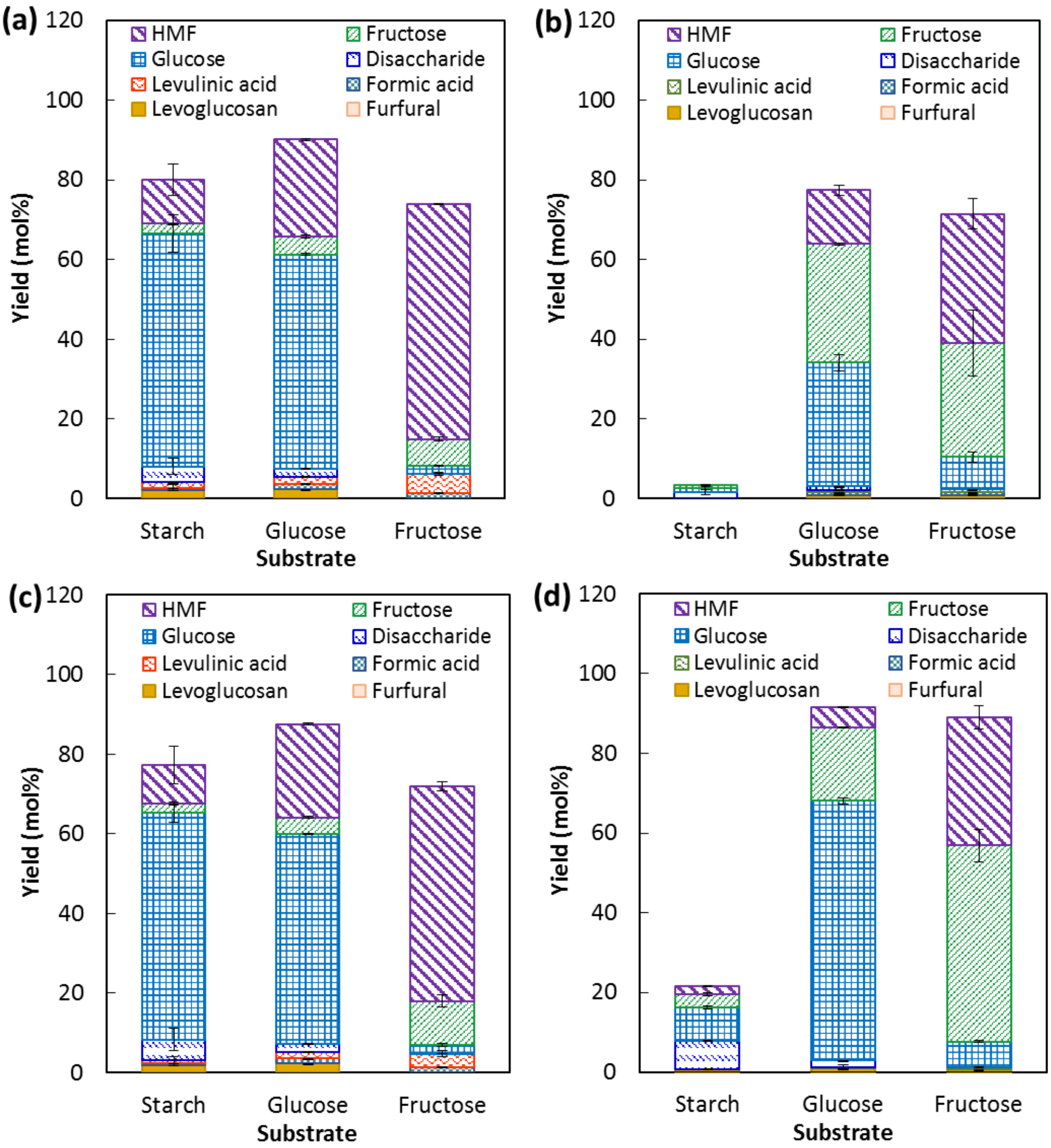

Figure 7.3. Product yields in relation to the catalytic conversion of standard compounds in the (a) Sn(IV), (b) Cr(III), (c) Sn(IV)/MA, and (d) Cr(III)/MA systems in DMSO-water mixture (1:1 v/v) (conditions: 5 wt/v% substrate and 55.5 mM $SnCl_4$ or $CrCl_3$ and 13.9 mM MA at 140 ^{o}C, 10 min; yield = $product_{Cmol}/substrate_{Cmol} \times 100\%$).

The Sn(IV) and Sn(IV)/MA systems also led to similar conversion of standard glucose, in terms of the unchanged isomerisation product yield of 31-32 mol% (including fructose and its derivatives, i.e., HMF, levulinic acid, and formic acid) (**Fig. 7.3a&c**). Therefore, provided that glucose-to-fructose isomerisation is a Lewis acid-catalysed reaction, the addition of MA also had marginal effect on the Lewis acidity of Sn(IV) systems. Previous studies illustrated that a lowered medium pH (i.e., higher Brønsted acidity) could impede catalytic isomerisation by hindering the formation of an active Lewis acid species (Choudhary et al., 2013) or effective Lewis acid-glucose coordination (Wrigstedt et al., 2015; Yu et al., 2016). In this study, the constant Brønsted acidity may partially account for the comparable Lewis acidity in Sn(IV) and Sn(IV)/MA systems, leading to the similar kinetics of rice waste conversion observed in **Fig. 7.2a&c**.

The Sn(IV)-catalysed conversion of rice waste was faster when using acetone/H_2O as the reaction medium. The maximum product yield of ~90 mol% was obtained only after 3 min at 140 ^{o}C (**Fig. E.1**), comparing with DMSO/H_2O that required 10 min to reach similar total product yields (**Fig. 7.2a**). This agrees with the findings that the acetone/H_2O medium can shorten the optimal reaction time of catalytic conversion of bread waste (**Chapter 8**). Yet, similar to the case in DMSO/H_2O, the Sn(IV)- and Sn(IV)/MA-catalysed conversions of rice waste were very much alike in acetone/H_2O (**Fig. E.1a&b**). This underlines the minimal effect of MA on Sn(IV)-catalysed reactions regardless of the studied solvents, which contradict to the positive effects reported for MA as a co-catalyst of Al(III) systems, e.g., an increase in rate constant of fructose dehydration from 0.25 to 1 upon the MA addition (Zhang et al., 2015).

In contrast, it is noteworthy that the addition of MA to the Cr(III) system accelerated hydrolysis of starch in the rice waste, as the total product yield increased from 4.4 to 18.2 mol% after 10-min heating (**Fig. 7.2b&d**). This is consistent with the results of standard starch conversion, in which more hydrolysis products were generated in the case of Cr(III)/MA compared with Cr(III) (140 ^oC, 10 min; **Fig. 7.3b&d**). However, the glucose utilisation over Cr(III)/MA was not improved. For example, the ratio of isomerisation product yields (i.e., fructose and its derivatives) to total product yields decreased from 0.84 in the Cr(III) system to 0.48 in Cr(III)/MA at 100 min, and the trends of sum of sugars and HMF yield in Cr(III)/MA did not intersect at all within 100 min (**Fig. 7.2b&d**). Reconcilable observation is noted when using standard glucose as the substrate, as the glucose conversion (34.8 mol%) and isomerisation product yields (24 mol%) of the Cr(III)/MA system were lower than that in Cr(III) (68.9 and 44.7 mol%, respectively) (**Fig. 7.3b&d**). These findings were distinctive from the case of the Sn(IV)-containing systems.

It is remarked that the standard starch and rice waste developed similar product profiles, e.g., 80-90 mol% total products and 7.4-11.8 mol% HMF in the Sn(IV)-containing systems (140 ^oC, 10 min; **Fig. 7.2a&c and 2a&c**). This suggests that the non-carbohydrate components in the rice waste, including proteins (8.4%) and fats (1%) (**Table 3.1**), did not cause observable interference on the tandem reactions to produce HMF in the catalytic systems. Nevertheless, the impacts of food waste composition should not be overlooked in future studies, in view of the recognised binding between some metal ions (e.g., Fe^{2+} and Cu^{2+}) and amino acids (Glusker, 1999), reduction of Sn(IV) to Sn(II) by cysteine (Tao and Nakahara, 2002), and complexation between organotin(IV) and histidine (Garza-Ortiz et al., 2013), which are components of rice protein (de Souza et al., 2016).

7.2.2 HMF selectivity in the presence of MA

Correlations between HMF yield and total sugar yield (including disaccharide, glucose, and fructose) of all the studied systems for rice waste conversion are shown in **Fig. 7.4** (140 ^{o}C, 0-150 min). Such data expression presents the characteristics of catalytic systems in terms of selectivity by excluding the consideration of kinetics. The arrows at the end of the curves indicate the direction of temporal development of patterns. There was a positive correlation between HMF yield and total sugar yield during the early stage of conversion at which hydrolysis of starch in rice waste was active to produce sugars, followed by facile dehydration of the sugars to HMF. A negative correlation observed subsequently may suggest that dehydration prevailed over hydrolysis at the later stage, resulting in a net consumption of sugars for HMF production.

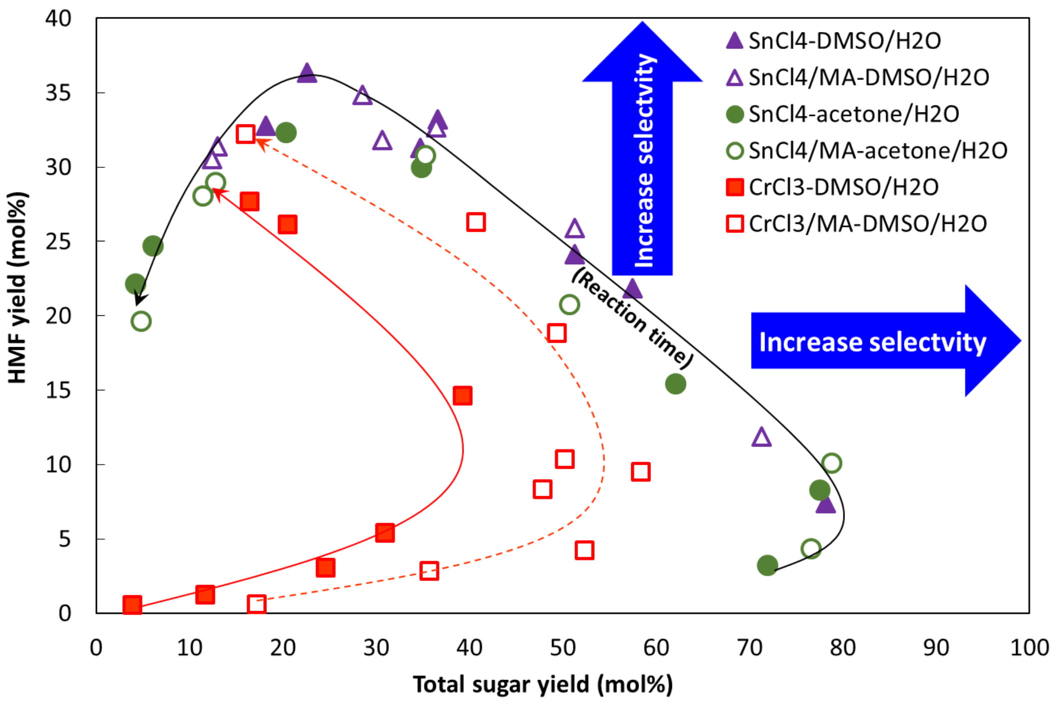

Figure 7.4. HMF yield as a function of total sugar yields (disaccharide, glucose, and fructose) during the catalytic conversion of rice waste (conditions: 5 wt/v% substrate and 55.5 mM metal chloride and 13.9 mM MA in an organic solvent-water mixture (1:1 v/v) at 140 °C; yield = product$_{\mathrm{Cmol}}$/substrate$_{\mathrm{Cmol}}$ × 100%). Remark: the arrows at the ends of the curved lines indicate the direction of temporal development of patterns; upward and rightward movement of the curves are desirable for increasing HMF selectivity (illustrated by the blue pointers).

The correlation patterns between different conversion systems make it possible to assess the selectivity toward HMF formation in a qualitative sense, although direct quantification of the selectivity is currently infeasible as rice waste remains and humins (formed via polymerisation) are inseparable in the solid residue. Patterns of all Sn(IV)-containing systems grow more upward and rightward than those of the Cr(III)-containing systems (**Fig. 7.4**). At approximately 15 mol% HMF formation as an example, there were 60-70 mol% sugars remaining in the Sn(IV)-containing systems, which were available for further generation of HMF. Comparatively, less available sugars, i.e., 40-50 mol%, were retained in the Cr(III)-containing systems.

Thus, the theoretical maximum HMF yield of the latter would be lower than the former. As such, one can assume a higher selectivity for HMF production in the Sn(III) systems based on the correlation patterns (**Fig. 7.4**).

The lower maximum HMF yield implies that HMF-consuming side reactions were relatively more competitive in the Cr(III)-containing systems. As shown in bread waste conversion, an enhanced HMF selectivity by Sn(IV) was ascribable to a stronger Brønsted acidity and weaker Lewis acidity, e.g., relative to Al(III) (Yu et al., 2017a). The current study remarks that the acidities of Sn(IV) may be also more favourable than that of Cr(III) for achieving a higher HMF selectivity (**Fig. 7.4**). The rate constant of glucose isomerisation catalysed by Cr(III) was reported to be greater than that of Sn(IV) in water as the reaction medium at 120 ^{o}C (i.e., 15.8 x 10^{-5} vs 2.5 x 10^{-5} s^{-1}) (Tang et al., 2015), demonstrating a stronger Lewis acidity of Cr(III). As medium to strong Lewis acid sites trigger significant side reactions (Li et al., 2017b), the Sn(IV)-containing systems with a milder Lewis acidity exhibited a higher HMF selectivity than their Cr(III) counterparts in this study.

It is noteworthy that the correlation curve of Cr(III) shifts to the right as MA was added in the system (**Fig. 7.4**), implying an increased selectivity towards HMF production in Cr(III)/MA. In contrast, the overlapping patterns between Sn(IV) and Sn(IV)/MA systems indicate a minor contribution of MA in terms of selectivity improvement in the Sn(IV)-containing systems. This was further illustrated by their similar maximum HMF yields, i.e., 34.9 mol% in Sn(IV)/MA and 36.3 mol% in Sn(IV). In addition, Sn(IV)-containing systems showed high similarity in both DMSO/H_2O and acetone/H_2O, suggesting that the selected media impose negligible impact on the maximum HMF yield.

7.2.3 Mechanisms involved in interplay between metal and MA

As discussed, while MA did not induce observable effects on the Sn(IV) system, its addition comparatively enhanced the HMF selectivity in the Cr(III) system. It is possible that MA coordinated with Cr(III) to inhibit the polymerisation of sugars and HMF, in a way similar to MA-Al(III) complexes revealed by electrospray ionization mass spectrometry (ESI MS/MS) in a recent study (Zhang et al., 2016). This study further ascribes such inhibition to a moderated Lewis acidity after the MA-metal coordination, which was inferred from the slower glucose isomerisation observed in Cr(III)/MA relative to Cr(III) (**Fig. 7.3b&d**). Medium to strong Lewis acid sites have been associated with significant side reactions and lower HMF production (Li et al., 2017b). The speculated moderation of Lewis acidity also rationalises the observed conversion of standard fructose, in which the Cr(III)/MA system shows a higher HMF selectivity (63.2 mol% vs 45.4 mol% in Cr(III); **Fig. 7.3b&d**) as a result of suppressed polymerisation reactions. Our preliminary modelling results indicate that although both MA-Cr(III) and MA-Sn(IV) coordination are thermodynamically feasible, the MA...Cr distance is slightly shorter than MA…Sn by 0.03 Å, which highlights the need for further investigations on the contrasting effects of MA between systems with tetravalent and trivalent metal catalyst.

In the control runs of Cr(III)/MA without substrates, 91% conversion of the added MA after 10-min heating at 140 ^{o}C was revealed by HPLC analysis, which was considerably higher than that in the Sn(IV)/MA control (13.6%; **Table 7.1**). The majority of the MA was transformed to malic acid by hydration (42.3% selectivity) with a trivial portion converted to fumaric acid by isomerisation (5.8% selectivity) under the acidic environment (Davies and Evans, 1956). Therefore, Cr(III) coordinated to MA derivatives instead of MA itself may contribute more significantly to the change in Lewis acidity. The complexation characteristics (e.g., bonding length and number of coordination) between Cr(III) and MA (and its derivatives) should be verified in future modelling and spectroscopic investigations. In addition to the selectivity for HMF formation, MA also altered the kinetics of Cr(III)-catalysed rice waste conversion, because Cr(III) complexation with MA and its derivatives also moderated the desirable glucose isomerisation and reduced the rate of glucose conversion (**Fig. 7.2b&d**).

Table 7.1. Conversion of MA in the Sn(IV)/MA and Cr(III)/MA controls (without substrate) after heating at 140 °C for 10 min.

Systems	MA conversion (%)	Malic acid		Fumaric acid	
		Yield (%)	Selectivity (%)	Yield (%)	Selectivity (%)
$SnCl_4$/MA	13.6	3	21.8	7.3	54.1
$CrCl_3$/MA	90.8	38.4	42.3	5.3	5.8

In contrast, the rate of hydrolysis of starch was enhanced in Cr(III)/MA relative to Cr(III) alone. In view of the notable MA conversion in Cr(III)/MA (**Table 7.1**), the enhanced hydrolysis may be correlated to the MA derivatives. The acid dissociation constants of the organic acids in a descending order are: MA ($pKa_1 = 1.9$) > fumaric acid ($pKa_1 = 3.1$) ~ malic acid ($pKa_1 = 3.5$) (Skoog, 2000). Hence, the produced fumaric acid and malic acid are expected to remain protonated in the Cr(III)/MA system, in which an initial pH 2.2 is lower than the pKa_1 values of these organic acids. Malic acid is capable of forming cross-linkages with starch for the synthesis of biocomposite films (Bodirlau et al., 2013) and prebiotics (Tian et al., 2016). Based on this knowledge, we infer that the malic acid derived from MA hydration can disrupt the hydrogen bond network of starch, rendering it more accessible to protons to accelerate hydrolysis in the current study. Trivial products (< 2 mol%) were generated from rice waste over MA or malic acid with NaCl in the controls. While the metal ions serve as the primary catalysts for the rice waste conversion, the presence of MA play a complimentary role in the catalysis. When using fructose as the substrate, there was no noticeable improvement on HMF yield by MA addition as both Cr(III) and Cr(III)/MA achieved 32 mol% HMF (**Fig. 7.3b&d**). It is possibly because Brønsted acidity appears to be the only important factor in the case of fructose dehydration, which was comparable in the two systems.

It should be noted that the reduction of glucose conversion rate was more significant than the acceleration of hydrolysis in Cr(III)/MA. The overall conversion kinetics was slowed down in the Cr(III)/MA system, which emerges as a trade-off of the enhanced selectivity. Therefore, future studies that aim to increase product selectivity should also pay attention to the associated effects on kinetics, which is an important consideration for scaling up applications.

7.3 Summary

The Sn(IV) and Cr(III) systems incorporated with MA as an organic acid are examined in the catalytic conversion of rice waste to HMF. The Sn(IV) systems achieved a faster conversion kinetics than the Cr(III) systems in general, with the maximum HMF yield of ~36 mol% obtained within 80 min in dimethyl sulfoxide (DMSO)/H_2O at 140 ^oC. The addition of MA to the Sn(IV) system imposed negligible effects on the tandem reactions (i.e., hydrolysis of starch, isomerisation of glucose, and dehydration of fructose). In contrast, the MA addition to Cr(III) slowed down the glucose isomerisation but accelerated the starch hydrolysis. In the Cr(III)/MA system, MA was significantly converted to malic acid, which may disrupt the hydrogen bond network of starch and increase the access of protons (Brønsted acid) to the glycosidic bonds. Furthermore, the selectivity for HMF formation increased in Cr(III)/MA compared with Cr(III) only. The former suppressed the side reactions (i.e., rehydration and polymerisation) accounting for the loss of HMF and sugars, probably due to the moderated Lewis acidity through Cr(III) coordination to MA and/or its derivatives. This study illustrates the contrasting roles of an organic acid in altering the kinetics and selectivity of catalytic conversion systems for biomass valorisation.

Chapter 8 – Polar Aprotic Solvent-Water Reaction Media

Abstract

Valorisation of bread waste for hydroxymethylfurfural (HMF) synthesis was examined in dimethyl sulfoxide (DMSO)-, tetrahydrofuran (THF)-, acetonitrile (ACN)-, and acetone-water (1:1 v/v), under heating at 140°C with $SnCl_4$ as the catalyst. The overall rate of the process was the fastest in ACN/H_2O and acetone/H_2O, followed by DMSO/H_2O and THF/H_2O due to the rate-limiting glucose isomerisation. However, the formation of levulinic acid (via rehydration) and humins (via polymerisation) was more significant in ACN/H_2O and acetone/H_2O. The constant HMF maxima (26-27 mol%) in ACN/H_2O, acetone/H_2O, and DMSO/H_2O indicated that the rates of desirable reactions (starch hydrolysis, glucose isomerisation, and fructose dehydration) relative to undesirable pathways (HMF rehydration and polymerisation) were comparable among these media. They also demonstrated higher selectivity towards HMF production over the side reactions than THF/H_2O. This chapter differentiates the effects of polar aprotic solvent-water media on simultaneous pathways during biomass conversion.

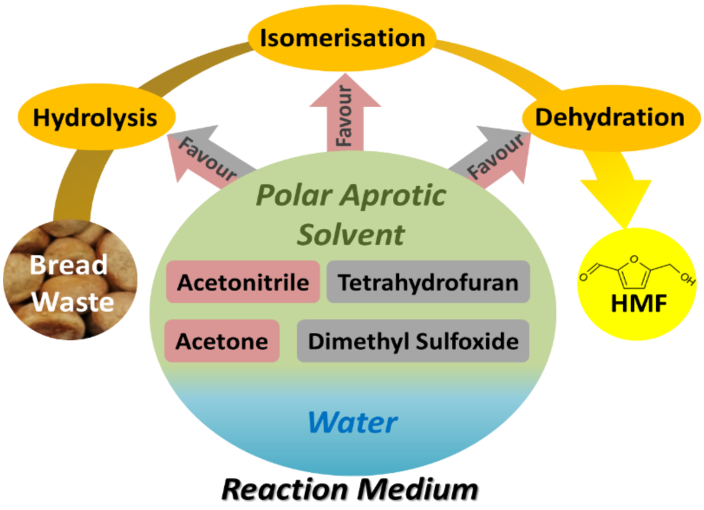

Figure 8.1. Graphical abtract of **Chapter 8**.

8.1 Research questions

The key to achieving high HMF production is to promote the desirable reactions (starch hydrolysis, glucose isomerisation, and fructose dehydration) and suppress the undesirable pathways (polymerization and rehydration of HMF) by manipulating the system components (**Chapter 2.3.3**). While tailoring the active sites in catalysts presents as a possible way (**Chapter 7**), engineering of the reaction medium shares equal importance for the selective promotion of the desirable reactions.

As an economically viable option, polar aprotic solvents, such as dimethyl sulfoxide (DMSO) and tetrahydrofuran (THF), enable the selective production of HMF with a promising yield (**Chapter 2.4.2**). Nevertheless, the potential environmental and health impact imposed by the use of these polar aprotic solvents may constrain their upscale application (**Chapter 2.7&2.8**). It is thereby important to seek or devise environmentally benign alternatives for food waste valorisation, with a better understanding of the favourable medium properties upfront. Although the solvation effect has been revealed for some particular solvents (Mushrif et al., 2012; Vasudevan and Mushrif, 2015), there is limited comparison of their performance in the literature. The critical properties of a selective reaction medium for HMF production remain uncertain.

Some knowledge on manipulating the medium properties by adjusting the type and proportion of the co-solvent has been in place. For instance, in the binary system of polar aprotic solvent and water, the extrema of the mixture properties (i.e., polarity, viscosity, and molar excess enthalpy that vary with the water-to-solvent ratio) showed a linear dependence on the electrostatic basicity of the organic solvent (Duereh et al., 2017). To apply such knowledge for developing a selective valorisation system, it is necessary to unravel the effects of solvents on the simultaneous reactions during the food waste-to-HMF process, enlightening the desirable physicochemical properties of the reaction medium. Different reaction environments may show selectivity towards different pathways.

Herein, bread waste was used as a model of starch-rich food waste in the catalytic production of HMF, in several binary mixtures of polar aprotic solvent and water. This chapter aims to differentiate the effects of selected media on the desirable reactions (i.e., hydrolysis, isomerisation, and dehydration) and undesirable pathways (rehydration and polymerisation). Four types of polar aprotic solvents, namely, DMSO, THF, acetone, and acetonitrile (ACN), were selected as the organic phase considering their satisfactory performance in HMF production based on the recent reviews (**Chapter 2.4**). $SnCl_4$ served as the catalyst as it showed the best performance in terms of HMF yield in **Chapter 4 and 5**.

8.2 Results and discussion

8.2.1 Facile HMF production in ACN- and acetone-water systems

Using ACN/H_2O and acetone/H_2O as the medium, the maximum HMF yield of approximately 26 mol% was obtained from bread waste within 10 min over $SnCl_4$ as the catalyst (**Fig. 8.2a&b**). It was promising with reference to the recent studies, which reported, for example, 23-58 mol% HMF from lignocellulosic biomass waste after heating at 160-175°C for 0.5-2 h (Wang et al., 2014; Zhang et al., 2017). Yet, it should be noted that direct comparison remains difficult due to the varying conditions (e.g., catalyst, medium, and total volume) in these studies.

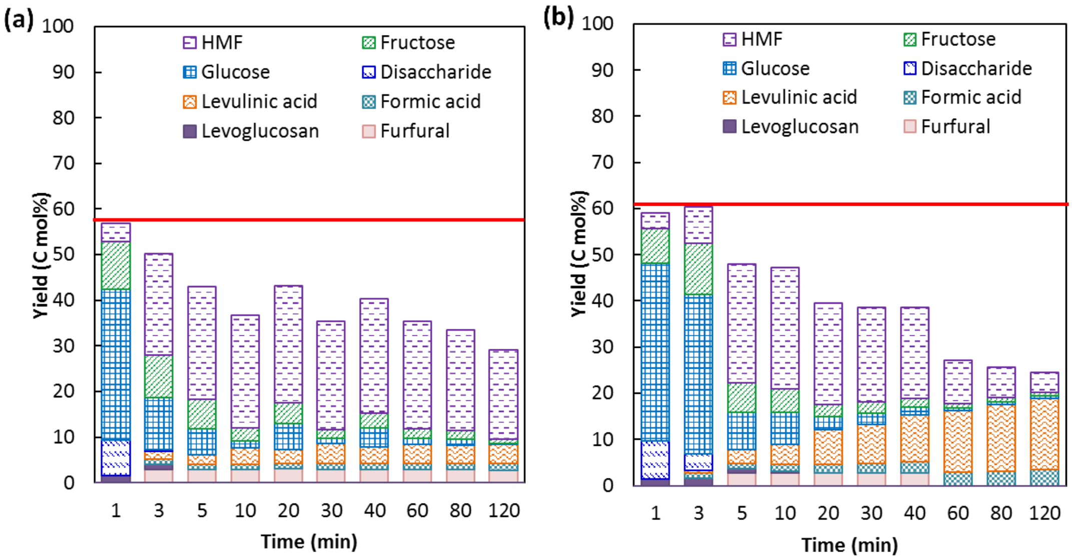

Figure 8.2. Product yields during the catalytic conversion of bread waste in (a) ACN/H_2O and (b) acetone/H_2O (conditions: 5 wt/v% substrate and 55.5 mM $SnCl_4$ in solvent mixture (1:1 v/v) at 140°C; yield = $\text{product}_{\text{Cmol}}/\text{substrate}_{\text{Cmol}} \times 100\%$; the red line represents the highest total product yield).

Our results also showed that the maximum yield of products was attained within 3 min in both media (**Fig. 8.2a&b**). The short optimal reaction time for the solubilisation of bread waste and formation of HMF implied that the desirable tandem reactions, i.e., starch hydrolysis, glucose isomerisation, and fructose dehydration, were fast in these systems. Starch hydrolysis and fructose dehydration were probably promoted by protons (Brønsted acid) released upon the partial hydrolysis of Sn^{4+} in water as observed in **Chapter 4-7**. The noticeable amount of fructose (6-9 mol%) at the early stage of conversion (≤ 3 min) evidenced isomerisation as the intermediate step, where the critical hydride shift within glucose was catalysed by Sn^{4+} as the Lewis acid (Binder et al., 2010; Li et al., 2014; Delidovich and Palkovits, 2016).

The moderate accumulation of fructose in the product profiles (≤ 3 min) suggested the faster glucose isomerisation compared to fructose dehydration in both ACN/H_2O and acetone/H_2O (**Fig. 8.2a&b**), given that the stoichiometric ratio of both glucose-to-fructose and fructose-to-HMF is 1:1. This led to the speculation that the presence of ACN and acetone facilitated the isomerisation step in particular, possibly by activating the substrate (glucose) or catalyst (Sn^{4+}). According to a previous study on molecular dynamics simulation, the former possibility may be low in view of the relatively minor interaction between ACN and glucose (Saielli and Bagno, 2010), because glucose was preferentially solvated by water in the ACN/H_2O mixture. The average number of ACN molecules bound to a hydroxyl group of glucose decreased significantly from 0.4 to 0.3 (i.e., by 25%) as the H_2O-to-ACN molar ratio increased from 1:1 to 2:1. In the current work, glucose was probably less solvated by ACN, where the H_2O-to-ACN molar ratio was close to 3:1. Therefore, the good performance of ACN in bread waste conversion to HMF may be associated with the activation of Sn catalyst instead of glucose. Yet, the literature contains little information on the solvation of glucose in the acetone-water mixture, which should be further addressed by future modelling studies.

8.2.2 Glucose conversion as the major hurdle in DMSO- and THF-water systems

In contrast with ACN/H_2O and acetone/H_2O, the HMF formation was much slower in DMSO/H_2O and THF/H_2O (comparing **Fig. 8.2** and **8.3**). The highest HMF yield of 27.4 mol% was achieved in DMSO/H_2O after 60-min reaction, while it was only 8 mol% at maximum in THF/H_2O after 120 min (the longest tested reaction time). It was noted that the THF/H_2O mixture in this work was less effective compared to those reported previously, e.g., up to 19 mol% HMF from biomass over $AlCl_3$ at 140°C (Yang et al., 2012c), in which THF at a high proportion served as an extractive layer in the presence of salt.

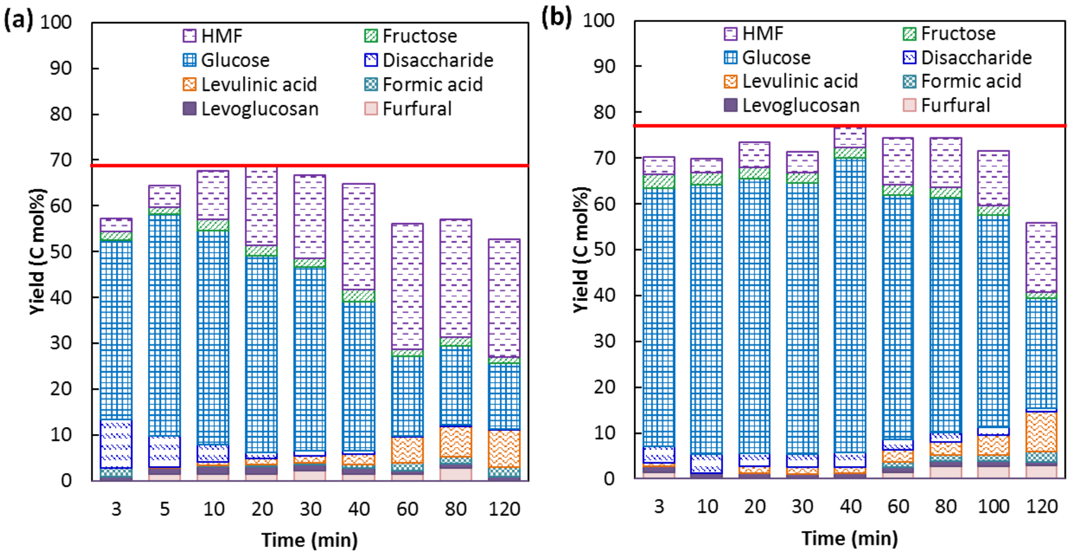

Figure 8.3. Product yields during the catalytic conversion of bread waste in (a) DMSO/H_2O and (b) THF/H_2O (conditions: 5 wt/v% substrate and 55.5 mM $SnCl_4$ in solvent mixture (1:1 v/v) at 140°C; yield = $\text{product}_{\text{Cmol}}/\text{substrate}_{\text{Cmol}} \times 100\%$; the red line represents the highest total product yield).

Our results indicated that glucose was the dominating substance in the product profile of both DMSO/H_2O and THF/H_2O, which was distinctive from the ACN/H_2O and acetone/H_2O. Such glucose accumulation was evident of the impeded isomerisation of glucose released from the starch hydrolysis, limiting the availability of fructose for HMF formation. This was substantiated by **Fig. 8.4**, in which less fructose was yielded from standard glucose in DMSO/H_2O and THF/H_2O (~4%) than in ACN/H_2O and acetone/H_2O (13-16%) after the 3-min heating.

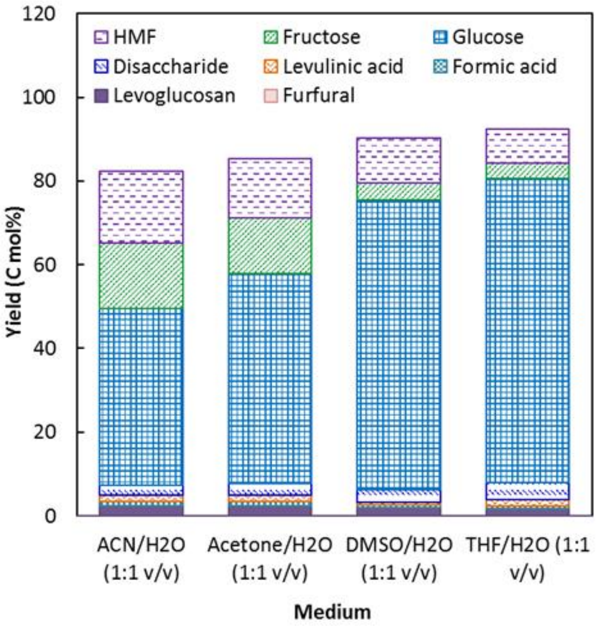

Figure 8.4. Product yields during the catalytic conversion of standard glucose in different solvent mixtures (1:1 v/v) (conditions: 5 wt/v% substrate and 55.5 mM $SnCl_4$ in solvent mixture (1:1 v/v) at 140°C for 3 min; yield = $product_{Cmol}/substrate_{Cmol}$ × 100%).

The isomerisation efficiency may be related to the activity of metal ion and the distribution of glucose tautomers. Recent studies suggested that solvents could promote the formation of reactive tautomer of fructose and xylose for enhancing the dehydration reaction (Lin et al., 2017; Wang et al., 2017). Solvent characters may also play an important role. Among the studied systems, the glucose conversion to HMF was the lowest in THF/H_2O, in which heat transfer could be hindered because of the particularly low dielectric constant and low dipole moment of THF that disfavoured microwave absorption (**Table 8.1**). Nevertheless, the relative significance should be evaluated via future spectroscopic analysis and modelling work, to expand our understanding on the local environment of substrate and catalyst in different solvent mixtures.

Table 8.1. Physicochemical properties[a] of different solvents and glucose.

	Density (g/ml)	DE[b]	DM[c]	Polarity
Acetone	0.78	20.7	2.91	5.1
ACN	0.78	37.5	3.44	5.8
DMSO	1.09	46.7	3.96	7.2
THF	0.88	7.6	1.63	4
Water	1	78.5	1.8	9
Glucose	1.54	-	8.6	-

[a] extracted from Gajula et al. (2017);
[b] dielectric constant (DE);
[c] dipole moment (DM) in D units.

In common with the ACN- and acetone-containing medium, the catalytic hydrolysis of bread starch was fast in both DMSO/H_2O and THF/H_2O because the total product yield reached the maximum within 10 min (~70 mol%) (**Fig. 8.3a&b**). The results showed a trace amount of fructose (< 3 mol%) throughout the conversion period, implying that fructose dehydration was highly efficient, or an alternative pathway (i.e., direct glucose dehydration to HMF bypassing fructose formation) was activated under the strong Brønsted acid derived from the hydrolysis of Sn (Yu et al., 2017a). The strong acidity may also pertain to the proton activity in association with its solvation status in these media (Mellmer et al., 2014). A recent simulation study proposed the complex of DMSO and proton as the active species, of which the catalytic performance was better than that of the discrete proton without coordination (Ren et al., 2017). Further computational investigations should be conducted to reveal the proton solvation in different mixtures of solvents.

8.2.3 Slow formation of side-products in the presence of DMSO and THF

In all the studied systems, the HMF production from bread waste became less appealing as the reaction time prolonged beyond the respective optimum, at which the highest HMF yield was achieved (**Fig. 8.2&8.3**). The HMF was partly lost via rehydration reaction, as evidenced by the significant generation of levulinic acid (e.g., 15.4 mol% in acetone/H_2O at 120 min). The decrease in the sum of detectable products was probably attributed to the formation of insoluble humins via polymerisation among HMF and intermediates. The occurrence of polymerisation was substantiated by TG and TDG analysis of the solid residues collected after the 120-min conversion in different media. The solid fractions exhibited high thermal stability as a feature of char-like substance (**Fig. 8.5a**), pointing to the formation of carbonaceous humins under long reaction time. None of them contained remaining starch, as the characteristic peak of starch at 240–340^{o}C was absent (**Fig. 8.5b**). Both rehydration and polymerisation were frequently reported as the major hindrance to effective HMF production in the literature (Moreno-Recio et al., 2016; Qing et al., 2017; Zhang et al., 2017).

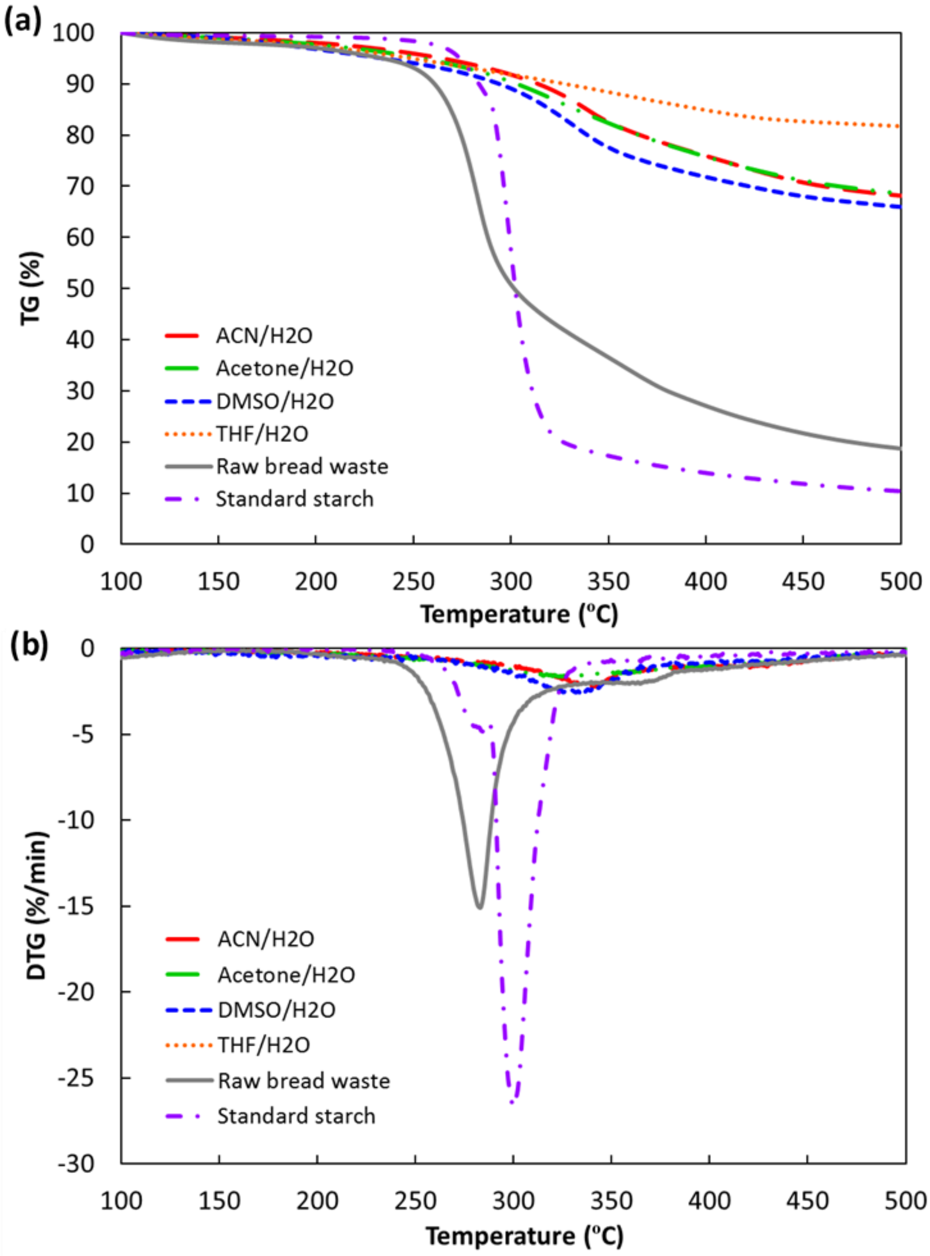

Figure 8.5. (a) TG and (b) DTG spectra of solid residues from catalytic conversions of bread waste in different solvent mixtures (1:1 v/v), raw bread waste, and standard starch (conditions: 5 wt/v% substrate and 55.5 mM $SnCl_4$ at 140°C for 120 min).

The degree of side reactions varied across the solvent mixtures. After the 120-min conversion, the HMF yield tended to increase further in THF/H_2O, whereas it dropped slightly by 6.1% in DMSO/H_2O (relative to the HMF maximum) (**Fig. 8.3a&b**). Comparatively, the reduction of HMF yield was more pronounced in acetone/H_2O (84%), followed by ACN/H_2O (25%) under the same conditions (**Fig. 8.2a&b**). Similarly, the decline in the total product yield at 120 min relative to the maximum was less significant in DMSO/H_2O (23%) and THF/H_2O (28%), compared to ACN/H_2O (42%) and acetone/H_2O (59%). These results demonstrated that the sugars, HMF, and other intermediates were more stable in the presence of DMSO and THF during the course of bread waste valorisation, which will be further addressed in **Section 8.2.4**.

The HMF yield was more stable in ACN/H_2O than acetone/H_2O (**Fig. 8.2**). It was observed that in ACN/H_2O, the final pH increased from the value of ~1 at 3 min to ~3.5 at 120 min, such that the decreasing acidity helped to suppress the acid-catalysed side reactions. The hydrolysis of ACN is found to develop alkalinity (Lei et al., 2016), because ammonium acetate forms as a buffer and counteracts the existing acidity in the medium. This was further supported by the detection of acetate/acetic acid in the current study, with the concentration ranging from 4 to 16 mg ml^{-1} depending on the reaction time. The solvent loss was insignificant, amounting to 3 mol% of the initial ACN loading only.

Interestingly, it was noted that the maximum HMF yield of 27.4 mol% in DMSO/H_2O was comparable to that in ACN/H_2O and acetone/H_2O (~26 mol%), despite the faster HMF production in the latter two systems (**Fig. 8.2&8.3**). The constant maximum HMF yield implied that the relative rates of HMF formation were comparable among the three mixtures. In other words, when changing the organic phase from DMSO to ACN or acetone, the desirable reactions (hydrolysis, isomerisation, and dehydration) were promoted to a similar extent as the undesirable pathways (rehydration and polymerisation), resulting in faster HMF formation but a negligible change in the maximum yield. These results highlighted the difference in considerations for achieving different goals – fast overall rate for rapid HMF production; and fast rate of the desirable reactions relative to the undesirable reactions for high yield and selectivity of HMF (Yu et al., 2017a; Yu and Tsang, 2017). The solvent effect on the system selectivity towards the desirable and undesirable pathways will be further discussed in the **Section 8.2.4**.

8.2.4 Qualitative selectivity towards desirable and undesirable reactions

The yield of HMF was correlated to its precursors (i.e., sugars) as well as its rehydration product (i.e., levulinic acid) in different media for comparison (**Fig. 8.6a&b**). This approach allowed direct experimental result-based examination on the selectivity towards particular reaction steps in a qualitative manner, without considering reaction time that masked the reaction preference.

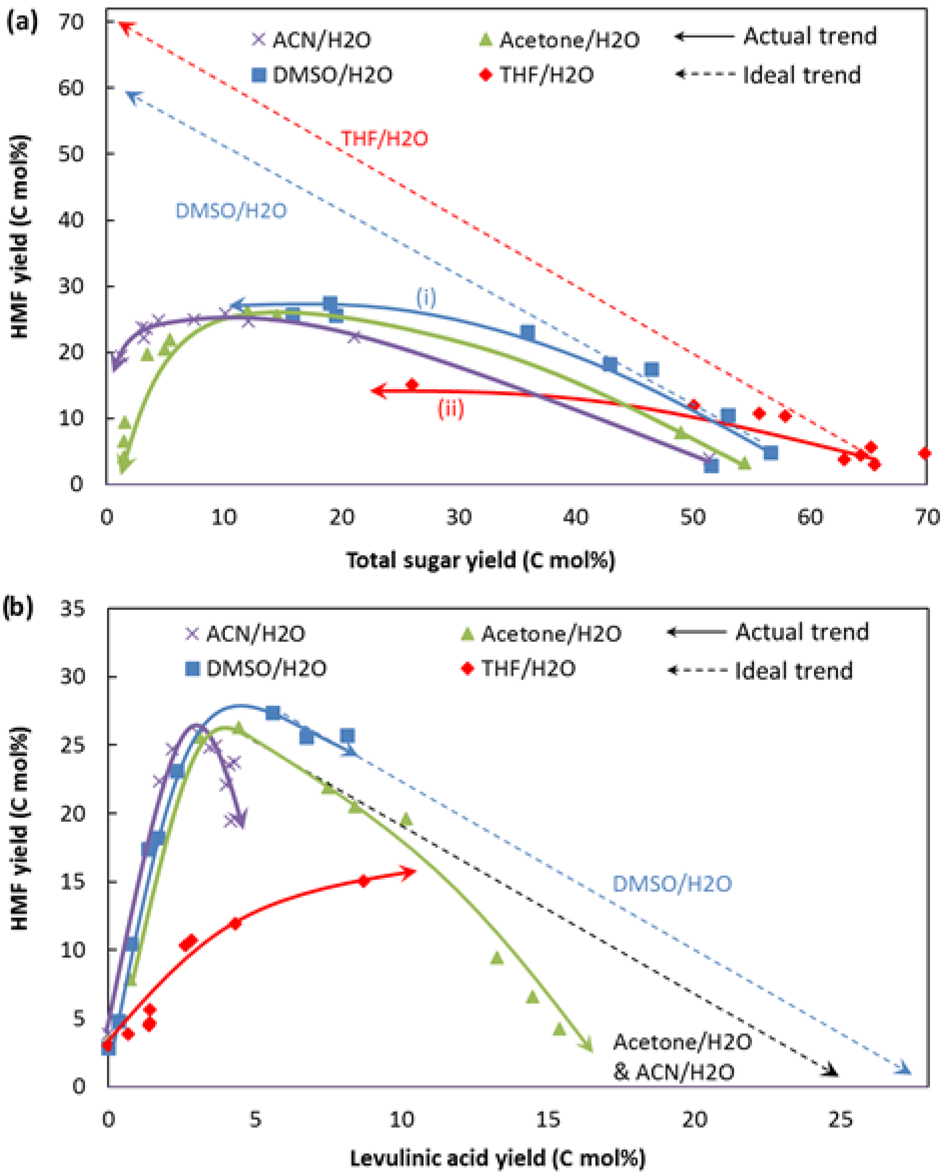

Figure 8.6. Yield of HMF as a function of (a) total sugar yield and (b) levulinic acid yield during the catalytic conversion of bread waste in different solvent mixtures (1:1 v/v) (conditions: 5 wt/v% substrate and 55.5 mM $SnCl_4$ at 140^{o}C; yield = product$_{Cmol}$/substrate$_{Cmol}$ × 100%) (remarks: the ideal trend was proposed assuming negligible HMF-consuming side reaction(s); projected maximum HMF [C mol%] = actual maximum total sugar [C mol%] + actual co-existing HMF [mol%] for (a); projected maximum levulinic acid [C mol%] = actual maximum HMF [C mol%] x 5/6 + actual co-existing levulinic acid [C mol%] for (b); arrows indicate the direction of temporal development of patterns; line (i) and (ii) represents the actual trend of HMF evolution in DMSO/H_2O and THF/H_2O in (a), respectively).

In the HMF vs total sugars correlation, solid line (i) and (ii), which depicted the increase of HMF at the expense of the total sugars (disaccharides, glucose, and fructose), represented that sugars released from starch hydrolysis were converted to HMF during the early stage of bread waste conversion (Yu et al., 2017a) (**Fig. 8.6a**). The slope (i) for DMSO/H_2O was steeper than slope (ii) for THF/H_2O. Moreover, the band gap between solid and dotted line was smaller for DMSO/H_2O. The dotted line was the ideal trend of HMF evolution projected from the maximum total sugar yield detected in each system, assuming complete transformation of released sugars to HMF without any side reactions. Therefore, the steeper slope and smaller band gap can be interpreted as a smaller loss of HMF and sugars to rehydration and polymerisation products, i.e., the higher selectivity of sugar conversion to HMF, in DMSO/H_2O than in THF/H_2O. It can be deduced that ACN/H_2O and acetone/H_2O showed a similar selectivity towards HMF formation as DMSO/H_2O (i.e., similar slopes in **Fig. 8.6a**), reinforcing the observation that these three media generated nearly the same maximum HMF yield despite different optimal reaction times (**Fig. 8.2&8.3**).

The HMF vs levulinic acid profile added that HMF was less susceptible to rehydration in ACN/H_2O, acetone/H_2O, and DMSO/H_2O as their rising solid lines were steeper than that of THF/H_2O (**Fig. 8.6b**). These rising solid lines illustrated the positive correlation between the yield of HMF and levulinic acid, which appeared during the most productive stage of HMF formation with concurrent HMF rehydration to levulinic acid.

The selectivity towards desirable reactions may be attributed to the favourable coordination between the solvent molecules and sugars and HMF. Previous computational studies on solvent-water mixtures reported the favourable arrangement of DMSO molecules near the hydroxyl group of glucose and fructose, protecting the side reaction-susceptible sites without blocking water access to where the desirable reactions were initiated (Mushrif et al., 2012; Vasudevan and Mushrif, 2015). It was also revealed that DMSO preferentially coordinated with the carbonyl group of HMF, where off-path rehydration and polymerisation were triggered (Mushrif et al., 2012). In the current work, it was hypothesized that such solvent-sugar and solvent-HMF interactions also existed in ACN/H_2O and acetone/H_2O, but were reduced in THF/H_2O, resulting in the lower selectivity towards HMF formation in the latter (**Fig. 8.6&b**). These interactions were possibly governed by the polarity, dipole moment, and dielectric constant of the organic solvent, because the values of these parameters are the lowest for THF (**Table 8.1**).

On the other hand, the HMF vs levulinic acid correlation provided insights into the dominating undesirable pathway that accounted for the majority of HMF loss. Similar to **Fig. 8.6a**, the solid line in **Fig. 8.6b** depicts the experimental evolution of levulinic acid, whereas the dotted line represents the projected evolution with the assumption of no HMF loss to polymerisation. It was observed that the solid line overlapped with the dotted line for the DMSO system, implying that HMF was lost to rehydration rather than polymerisation (**Fig. 8.6b**). Comparatively, polymerisation was suggested to be the major HMF consumption pathway in ACN/H_2O, where the solid line clearly diverted from the dotted line.

It was interesting to note that in acetone/H_2O, the levulinc acid production followed the projected dotted line but gradually became divergent at high levulinic acid yields, i.e., at long reaction times, denoting the changing selectivity towards rehydration and polymerisation (**Fig. 8.6b**). Such divergence possibly emerged in the case of DMSO/H_2O if the conversion duration extended beyond the studied range (120 min), which might complete the correlation profiles for DMSO/H_2O and THF/H_2O.

In summary, ACN/H_2O and acetone/H_2O allowed a higher rate of HMF production from bread waste than DMSO/H_2O and THF/H_2O, whereas the HMF selectivity, which depended on the relative rate of the desirable reactions, was similar among ACN/H_2O, acetone/H_2O, and DMSO/H_2O and was lower in THF/H_2O. Nevertheless, these solvents may incur moderate environmental or safety concerns according to the recent CHEM21 solvent selection guide (Prat et al., 2016). For instance, acetone, DMSO, and THF share the same environmental score of 5, whereas the safety and health score of ACN, acetone, and THF range from 3 to 7, compared to water that is rated at 1 in every aspect. Therefore, green alternatives, especially the bio-derived candidates such as Cyrene, γ-Valerolactone, and 2-methyltetrahydrofuran, should be examined as the reaction medium for HMF synthesis in future studies.

8.3 Summary

The overall rate of bread waste valorisation to HMF was the fastest in ACN/H_2O and acetone/H_2O, followed by DMSO/H_2O and THF/H_2O that were limited by glucose isomerisation. Yet, the nearly constant HMF maxima in ACN/H_2O, acetone/H_2O, and DMSO/H_2O suggested the similar selectivity towards HMF formation in these media. This was a result of the comparable rates of desirable reactions (hydrolysis, isomerisation, and dehydration) relative to undesirable pathways (rehydration and polymerisation). These media were more selective for HMF formation compared to THF/H_2O. This study expanded our understanding on the effects of solvent mixtures on individual desirable and undesirable reactions.

Chapter 9 – Efficiency and Selectvitiy of Green Solvent Systems

Abstract

Two green solvents, namely propylene carbonate (PC) and γ-valerolactone (GVL), were examined as co-solvents in the conversion of bread waste to hydroxymethylfurfural (HMF) over $SnCl_4$ as the catalyst under microwave heating at 120 °C, and their performances were compared with water and acetone as a common solvent. The results showed that a HMF yield of ~20 mol% was achieved at 7.5 and 20 min in the PC/H_2O and GVL/H_2O (1:1 v/v) systems, respectively, implying that the tandem reactions (starch hydrolysis, glucose isomerisation, and fructose dehydration) were efficient. The green systems played a critical role in maintaining effective Lewis acid sites, *i.e.*, Sn^{4+}, to a greater extent compared with acetone/H_2O and water, where loss of Sn^{4+} from the liquid phase to colloidal SnO_2 particles via hydrolysis was evidenced by X-ray diffraction analysis. In comparison, the utilisation of glucose (47−59 mol% from bread starch within 10 min) appeared as the rate-limiting step in the acetone/H_2O and water systems. When comparing PC/H_2O with GVL/H_2O, the kinetics of overall conversion in the former was more favourable, which was associated with the high in-vessel pressure developed via liberation of CO_2 from PC. In addition, dipole moment and dielectric constant of the solvents may also account for their respective performance. This chapter elucidates the multiple roles of the solvents and their interplay with the catalysts, and advocates the application of green solvents to facilitate catalytic conversion of biomass with a lower energy requirement.

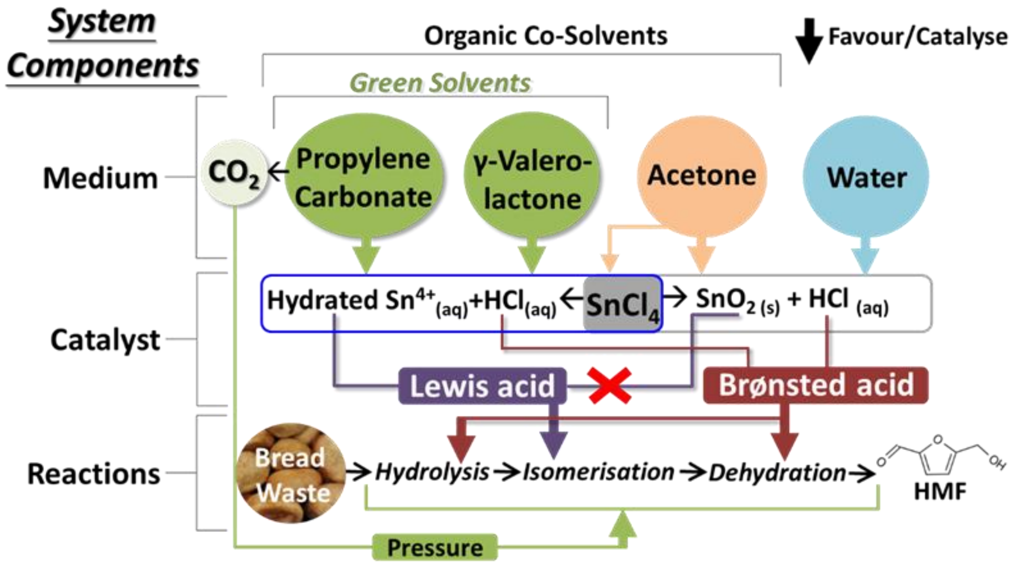

Figure 9.1. Graphical abstract of **Chapter 9**.

9.1 Research questions

While conventional solvents, *e.g.*, dimethyl sulfoxide (DMSO) and tetrahydrofuran, have been widely studied for biomass conversion, concerns have been raised over their potential cost and environmental implications (**Chapter 2.4&2.7**). Therefore, it is favourable to replace the common industrial solvents (**Chapter 8**) by green alternatives for more sustainable biomass conversion.

Propylene carbonate (PC) is recognised as a green solvent in view of its low toxicity, high biodegradability, economical manufacturing, and utilisation of CO_2 in its production (Parker et al., 2014). γ-valerolactone (GVL) is a biomass-derived solvent and a platform chemical itself (Yan et al., 2015), so using GVL as the reaction medium for fuel or chemical generation can simplify the downstream separation processes. Both solvents are polar aprotic in nature, and offer a great potential for replacing DMSO, THF, and DMA, etc., in organic synthesis. Notably, PC and GVL possess polarity comparable to DMSO ($\pi^* = 0.83$ for PC and GVL, $\pi^* = 0.94$ for

DMSO on the Kamlet-Taft solvatochromic π^* scale) (Jessop et al., 2012). The latter has been reported to be an effective solvent in HMF production from microcrystalline cellulose (Zhang et al., 2016) and food waste (**Chapter 4**). The use of PC in conversion of biomass to HMF has not been evaluated in the literature to the best of our knowledge, except a general remark on its potential based on its polar aprotic nature (Dumesic et al., 2016). The GVL was demonstrated to be effective for the catalytic conversion of corncob (Zhang et al., 2017) and cellulose (He et al., 2017), where the good solubility of the biomass substrate in GVL was considered accountable for the high product yields. However, the influences of solvent on the activity of a catalyst (*e.g.*, Brønsted acidity and Lewis acidity) remains uncertain.

Solvents can alter the activity and selectivity of catalysts via various mechanisms (ligand-metal complex formation, proton transfer, modulation of ion paring, etc.). However, this subject matter has seldom been discussed in the context of biorefineries (**Chapter 2**; Dyson and Jessop, 2016). Previous studies proposed that GVL can increase the reactivity of protons relative to that in water (Mellmer et al., 2014a, 2014b). Regarding Lewis acids, it has been recently revealed that the rate of $SnCl_4$-driven glucose conversion varied with the choice of the organic co-solvent in a binary solvent-water system (**Chapter 8**), pointing to a possible effect of the solvent on the metal activity.

This chapter aims to examine the use of GVL and PC as green co-solvents in a binary solvent-water medium for the conversion of biomass to HMF over $SnCl_4$ as the catalyst. The effects of the solvents on hydrolysis, isomerisation, and dehydration are differentiated in relation to their interactions with the catalyst. For comparison, water and an acetone-water mixture are also selected as the reaction media, respectively, because water is the simplest system serving as a baseline, while acetone-water showed a good performance in **Chapter 8**. Bread waste is used herein as a biomass waste, because of its high conversion feasibility that allows valid comparison among the selected solvent systems (**Chapter 4-6**). Owing to the immense volumes of bread waste generated globally, selecting this waste as a feedstock exhibits significant environmental relevance (**Chapter 3.1**). $SnCl_4$ served as the catalyst as it showed the best performance in **Chapter 4 and 5**.

9.2 Results and discussion

9.2.1 Efficient tandem reactions in green solvent systems

PC/H_2O is the best among the solvent systems studied herein for bread waste conversion (**Fig. 9.2**). Approximately 70 mol% of total products were generated from bread waste over 13.9 mM $SnCl_4$ at 120 ^{o}C in 10 min, of which 53 mol% was accounted by glucose produced from hydrolysis of bread starch (**Fig. 9.2a**). As the catalyst loading increased fourfold (*i.e.*, 55.5 mM), a HMF yield of 20 mol% could be obtained under the same heating conditions. While the application of PC was briefly mentioned before (Dumesic et al., 2016), the HMF production from biomass in the PC-containing medium is verified for the first time in this study. The presence of fructose (2-13 mol%) and glucose (9-62 mol%) in the product profiles (**Fig. 9.2a**) suggests that HMF was generated via the hydrolysis-isomerisation-dehydration pathway reported in the literature (**Chapter 2**).

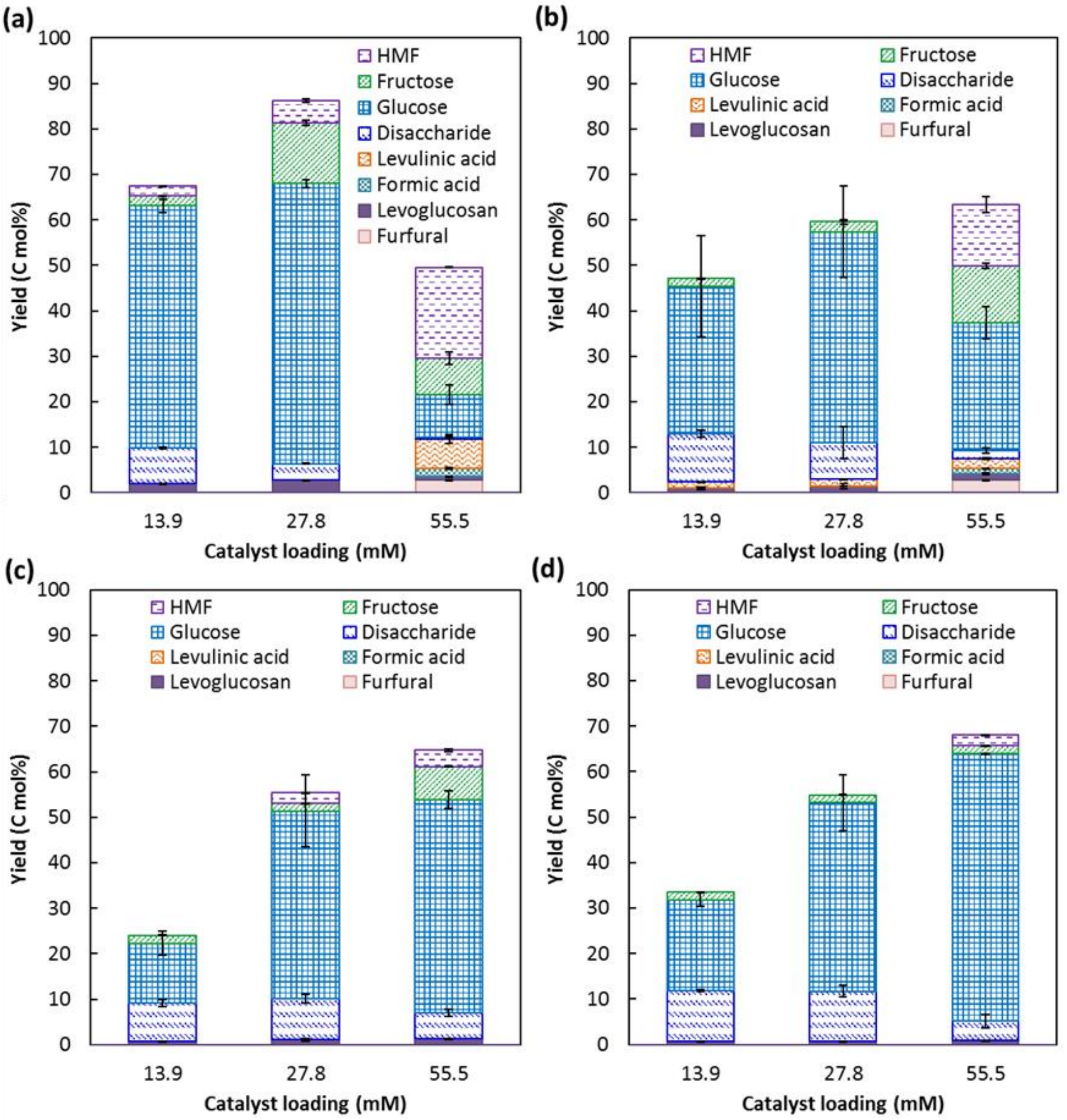

Figure 9.2. Product yields resulted from the catalytic conversion of bread waste in (a) PC/H_2O, (b) GVL/H_2O, (c) acetone/H_2O, and (d) water under different loadings of $SnCl_4$ (conditions: 5 wt/v% substrate in solvent mixture (1:1 v/v) or water at 120 ^oC for 10 min; yield = $product_{Cmol}/substrate_{Cmol} \times 100\%$).

To differentiate the feasibility of individual reactions, model compounds, including starch, maltose, glucose, and fructose, were used as the substrates. The results show that conversion of maltose and starch resulted in 73−76 mol% hydrolysis products (*i.e.*, sugars, HMF, levulinic acid, and formic acid) in PC/H_2O (120 ^oC, 10 min, 55.5 mM $SnCl_4$), whereas fructose conversion yielded 31.8 mol% HMF under the same condition (**Fig. 9.3a**). Given the fact that hydrolysis and dehydration are proton-catalysed, the substantial amount of hydrolysis products and HMF demonstrate the presence of Brønsted acidity in the system. The Brønsted acidity could be developed as protons were released via partial hydrolysis of Sn^{4+} in the water-containing environment (**Chapter 5**). In the case of glucose conversion, the total yield of fructose and its derivatives (*i.e.*, HMF, levulinic acid, and formic acid) was 49 mol%, indicating the occurrence of glucose-fructose isomerisation that was catalysed by Sn^{4+} as the Lewis acid.

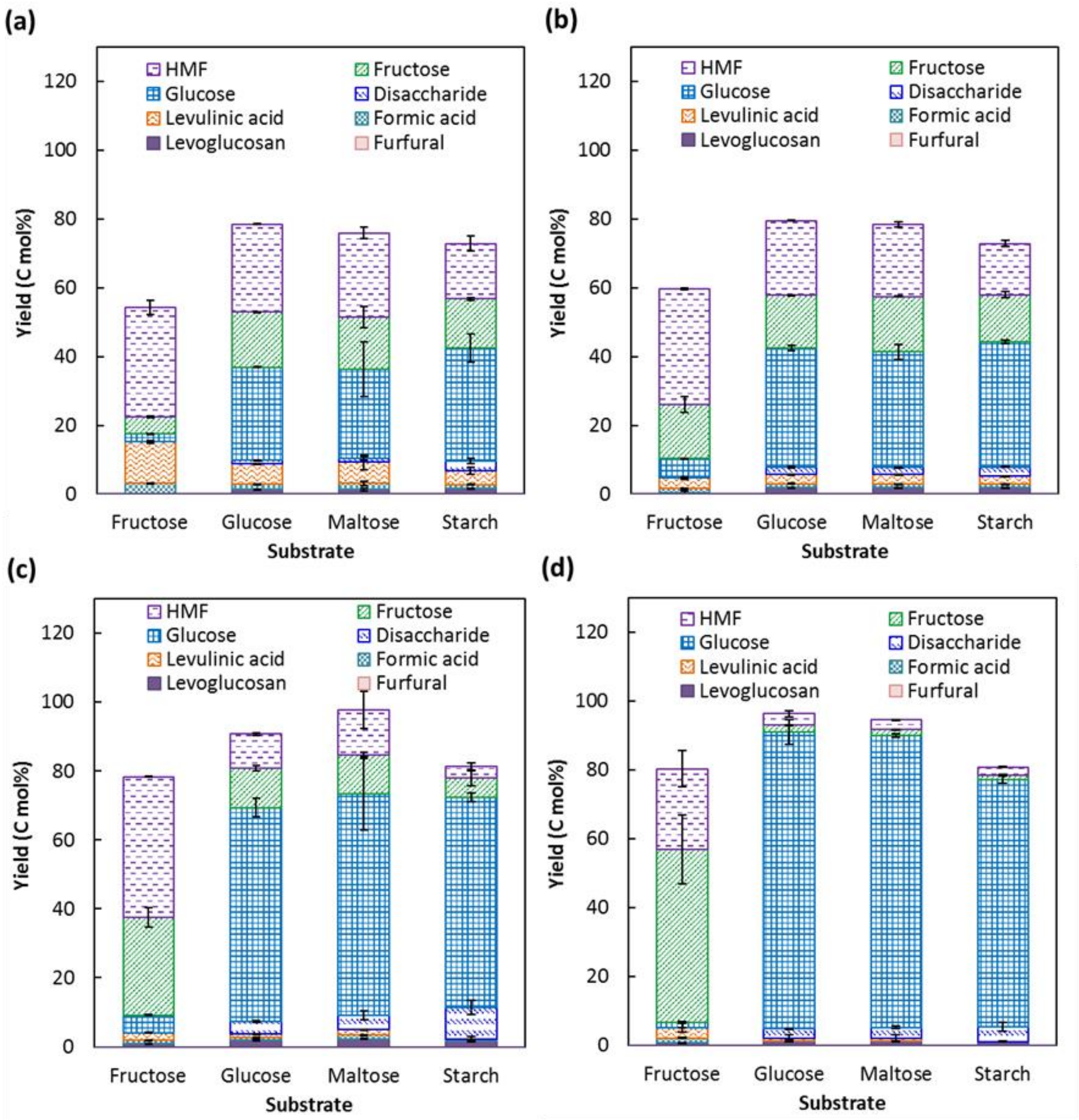

Figure 9.3. Product yields resulted from catalytic conversion of model compounds in (a) PC/H_2O, (b) GVL/H_2O, (c) acetone/H_2O, and (d) water (conditions: 5 wt/v% substrate and 55.5 mM $SnCl_4$ in solvent mixture (1:1 v/v) or water at 120 ^oC for 10 min; yield = $product_{Cmol}/substrate_{Cmol}$ × 100%).

In GVL/H_2O as the reaction medium, 13.5 mol% of HMF was produced from bread waste with 13 mol% fructose and 28 mol% glucose as the co-products at the $SnCl_4$ loading of 55.5 mM (**Fig. 9.2b**), suggesting a similar pathway of bread waste conversion as in PC/H_2O medium. The HMF yield was comparable to those reported in previous studies on GVL-assisted conversions. For example, cellulose yielded

11.9% HMF in GVL (with negligible water) after heating at 210 ^{o}C for 30 min in the presence of H_2SO_4 (He et al., 2017) and 19.5% HMF was obtained from corn stalk in GVL/H_2O (10:1 v/v) under catalysis by resin-based acid at 190 ^{o}C for 100 min (Xu et al., 2015). In comparison with these studies, the rapid synthesis of HMF in moderate heating condition (120 ^{o}C, 10 min) using PC or GVL in the current work is more desirable for potential scale-up processes. Conversion of standard maltose and starch gave 73−78 mol% hydrolysis products, glucose resulted in 41 mol% isomerisation products, and fructose yielded 33.6 mol% HMF (**Fig. 9.3b**). These results demonstrate the Brønsted and Lewis acidity in the GVL/H_2O system to catalyse the tandem reactions during bread waste conversion (*i.e.*, hydrolysis, isomerisation, and dehydration), similar to the case of PC/H_2O. It is noteworthy that the product profile of maltose conversion resembles that of glucose in PC/H_2O and GVL/H_2O, suggesting that hydrolysis of the α-(1,4) glycosidic bond in maltose is far more rapid than glucose transformation (**Fig. 9.3a & b**).

In comparison with PC/H_2O and GVL/H_2O, glucose (47−59 mol%) emerged as the dominant product in the acetone/H_2O and water systems at 55.5 mM $SnCl_4$, respectively (120 ^{o}C, 10 min; **Fig. 9.2c&d**). The catalytic hydrolysis of starch in bread waste took place readily, and further conversion of glucose to fructose and HMF occurred to a much lesser extent. Only small amounts of HMF (3.5 mol%) and fructose (7.3 mol%) were produced in acetone/H_2O, while the yields of HMF and fructose were the lowest in water among all the tested media (< 5 mol% in total). A higher reaction temperature is needed to improve the HMF yield in these conventional media. For instance, at 140 ^{o}C, a higher HMF yield of ~26 mol% can be obtained in acetone/H_2O after 10-min heating as reported previously (**Chapter 8**).

In conversion of standard compounds, a high yield of hydrolysis products from maltose and starch (81−98 mol%), and a moderate to high yield of HMF from fructose (23−41 mol%) were achieved in acetone/H_2O and water (**Fig. 9.3c&d**), indicating the presence of Brønsted acidity as in the PC/H_2O and GVL/H_2O systems. However, when using glucose as the substrate, a significant portion of it remained unreacted in acetone/H_2O (62 mol%) and water (86 mol%), reconfirming that the subsequent glucose transformation is a critical hurdle for bread waste conversion in these two media (**Fig. 9.2c&d**). These results signify that Brønsted acidity can be maintained in all of the studied media for catalytic starch hydrolysis and fructose dehydration, whereas Lewis acidity may vary despite the same initial catalyst loading, resulting in distinctive glucose reactivity in different media.

9.2.2 Maintenance of active Lewis acid in green solvent systems

In the control experiments without substrate addition, white colloidal particles appeared in the acetone/H_2O and water systems (120 ^{o}C, 10 min; **Fig. 9.4**). The solids were revealed as SnO_2, of which the XRD spectra shows characteristic peaks at 26.1, 33.8, and 51.5^{o} that correspond to the (110), (101), and (211) crystal facets, respectively (**Fig. 9.5**) (Chen et al., 2017b). The fructose conversion profile of the solution phase was comparable to that of the reaction catalysed by freshly prepared aqueous $SnCl_4$, whereas the derived SnO_2 exhibited negligible catalytic activity for fructose dehydration to HMF (**Fig. 9.6a**). These results suggest that in water, $SnCl_4$-mediated conversion would depend entirely on the Brønsted acidity retained in the liquid fraction. The added $SnCl_4$ was hydrolysed to form colloidal SnO_2 and HCl upon heating in water (Omari et al., 2012). Therefore, during bread waste conversion, only acid catalysis (*i.e.*, hydrolysis and dehydration) could take place in the HCl-containing liquid phase (**Fig. 9.2d&9.3d**). The formed SnO_2 may not carry sufficient Lewis acid sites for catalysing glucose-to-fructose isomerisation (**Fig. 9.2d&9.3d**), corroborating the previous findings about the insignificant conversion of glucose (Moliner et al., 2010) and chitosan (a polysaccharide) (Omari et al., 2012) over pre-synthesised SnO_2.

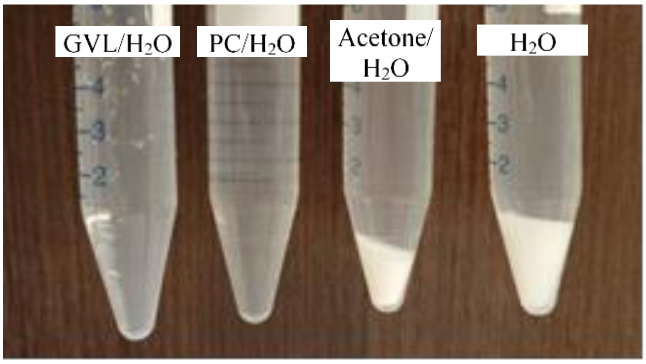

Figure 9.4. Controls experiments without substrate (conditions: 55.5 mM $SnCl_4$ in solvent mixture (1:1 v/v) or water at 120°C for 10 min).

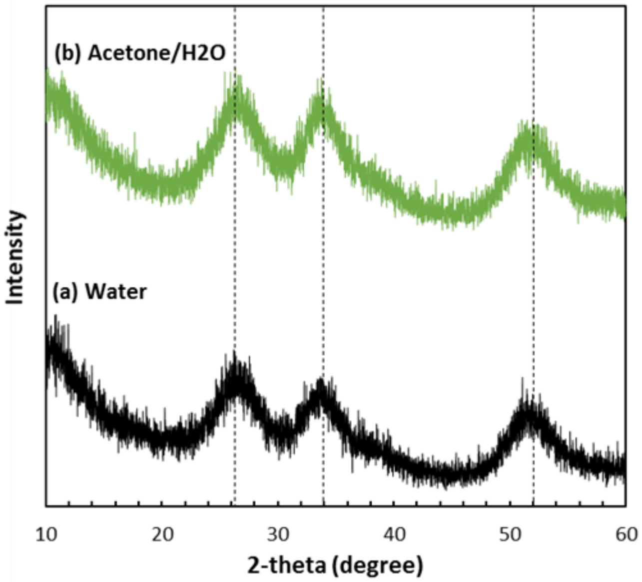

Figure 9.5. XRD spectrum of solids collected from controls without the addition of substrate (conditions: 55.5 mM $SnCl_4$ in solvent mixture (1:1 v/v) or water at 120 °C for 10 min).

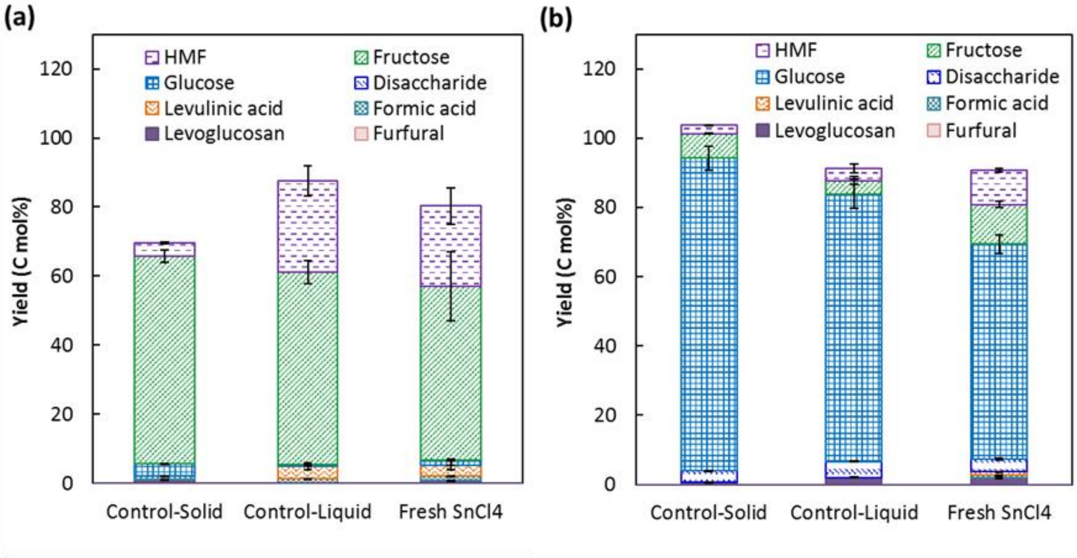

Figure 9.6. Product yields resulted from conversion of (a) standard fructose in water and (b) standard glucose in acetone/H_2O (1:1 v/v), using solid and liquid collected from controls (without the addition of substrate) as the catalysts, for comparison to the performance of freshly prepared $SnCl_4$ (conditions: 5 wt/v% substrate at 120 °C for 10 min; yield = $\text{product}_{\text{Cmol}}/\text{substrate}_{\text{Cmol}} \times 100\%$).

The acetone/H_2O system also generated SnO_2, as evidenced by the XRD spectra (**Fig. 9.5**), but in a smaller amount than that in water (**Fig. 9.4**). Heating of the separated liquid phase in an open vessel generated more white precipitates as the acetone evaporated, suggesting that more Sn remained in a soluble form in the acetone/H_2O system. The presence of acetone possibly slowed down the kinetics of $SnCl_4$ hydrolysis, thus maintaining stronger Lewis acidity for the faster conversion of bread waste to HMF compared with the water system (**Fig. 9.2c&d**). When reaction of standard glucose was performed in the liquid fraction isolated from the heated $SnCl_4$-acetone/H_2O mixture, the total yield of the isomerisation products (*i.e.*, fructose and its derivatives) was only 32% of that produced in the freshly prepared medium (**Fig. 9.6b**). It is inferred that isomerisation was the fastest at the beginning with the initially high Sn^{4+} loading, and became slow with increasing reaction time as $SnCl_4$ underwent hydrolysis to progressively form the inactive SnO_2.

Contrary to acetone/H_2O and water, the PC/H_2O and GVL/H_2O controls remained as clear solutions (**Fig. 9.4**). In other words, the addition of PC and GVL as the co-solvent successfully suppressed the formation of the inactive SnO_2 solids, maintaining Sn^{4+} as the effective Lewis acid, which cooperated with the Brønsted acid to facilitate the tandem reactions during bread waste conversion (**Fig. 9.2a&b**). These findings underscore the significance of the interplay between the catalysts and solvents in determining the characteristics of conversion system, *e.g.,* in terms of acid properties (Lewis or Brønsted acid). This is seldom addressed in the literature, of which most studies tend to consider and discuss the effects of catalysts and solvents as discrete factors.

Solvation of Sn^{4+} in PC/H_2O and GVL/H_2O is very likely to be favourable that the Sn^{4+}-water interactions can be reduced to prevent metal hydrolysis. Previous studies reported the preferential solvation of metal ions by organic solvents and weakened metal ion-water interactions in binary mixtures (Alia, 2001; Vaden and Lisy, 2005). In the current study, the molar ratio of organic solvent to water is 0.19 and 0.21 for GVL/H_2O and PC/H_2O, respectively, which are lower than the ratio of 0.24 for acetone/H_2O (**Fig. 9.7a**). Therefore, the quantity of co-solvent molecules in the studied range may not be the primary factor controlling favourable interactions among metal ions, water, and co-solvent in the matrix for the prevention of metal hydrolysis. Nevertheless, there is a positive correlation between the dipole moment of the organic co-solvent and the HMF yield from bread waste (**Fig. 9.7b**). This corroborates a recent study proposing dipole moment as one of the determinants of product yields in conversion of cellulose (He et al., 2017). We deduce that the greater the dipole moment is, the stronger the organic solvent molecule is as a ligand to coordinate with Sn^{4+}, thus suppressing the metal hydrolysis to the inactive SnO_2. Future thermodynamic modelling studies should be performed to reveal the solvated structure of Sn^{4+} in PC/H_2O and GVL/H_2O, disclosing information about preserving the active species for catalytic glucose isomerisation, as well as to explore the favourable properties of the solvents.

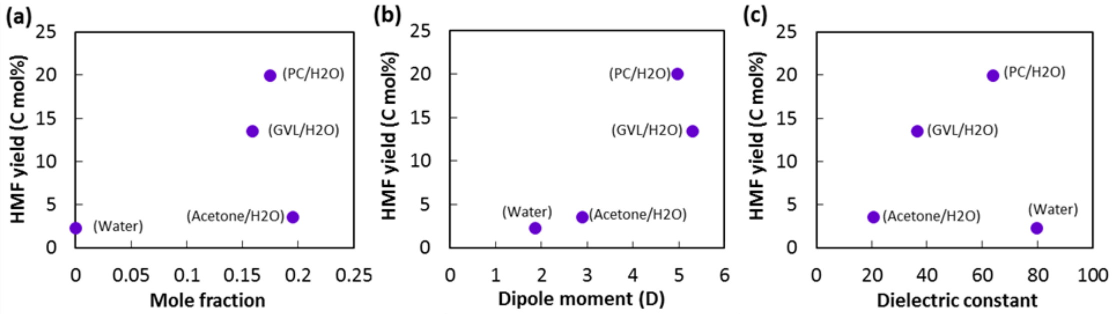

Figure 9.7. Correlation between HMF yields from bread waste conversions and (a) mole fraction of organic co-solvent in the binary mixtures, (b) dipole moment of the organic co-solvent, and (c) dielectric constant of the organic co-solvent, respectively (conditions: 5 wt/v% substrate in solvent mixture (1:1 v/v) or water at 120 ^oC for 10 min; yield = $product_{Cmol}/substrate_{Cmol} \times 100\%$). The values of dipole moment and dielectric constant are obtained from Gajula *et al.*[52], He *et al.*[28], and SMC[53].

SnO_2 and SnO_2-containing materials synthesised via alkaline precipitation have been shown to exhibit a certain degree of catalytic activity towards glucose isomerisation (Liu et al., 2015; Zhang et al., 2015b; Zhao et al., 2017). This is plausibly due to the presence of hydroxide that promotes the base-driven mechanism (Zhang et al., 2015b), which is consistent with the finding that extra framework SnO_2 acts as a base for catalytic glucose isomerisation on Sn-zeolites (Bermejo-Deval et al., 2012). Another possibility is that the modified SnO_2 species may carry coordinatively unsaturated cations as the Lewis acid sites (Liu et al., 2015; Zhao et al., 2017). Based on the literature, it can be deduced that the colloidal SnO_2 generated in the acetone/H_2O and water systems lacks effective Lewis acid sites, accounting for marginal glucose transformation in bread waste conversion in the current study (**Fig. 9.2&9.3**). More comprehensive characterisation should be conducted to reveal the structures and acid properties of the SnO_2 solids, by employing high-resolution transmission electron microscopy, temperature programmed desorption of ammonia and pyridine, etc. Notably, fructose conversion over the SnO_2 derived from metal hydrolysis in water generated ~30 mol% of unidentified compounds (**Fig. 9.6a**), suggesting the occurrence of side reactions such as polymerisation, for which the accountable characteristics of the SnO_2 should be evaluated in the future.

As for Brønsted acidity, previous research suggested that the reactivity of proton is enhanced in GVL, thus leading to higher rates of reactions compared with that in water where the solvated proton is stabilised to a greater degree (Mellmer et al., 2014a, 214b). Similarly, GVL and PC may preferentially solvate the protons in this study, accounting for the superior performance in HMF synthesis from model compounds compared with that in acetone/H_2O and water (**Fig. 9.3**).

9.2.3 Conversion kinetics favoured by in-situ pressure in PC/H_2O vs GVL/H_2O

The kinetics of Sn-catalysed bread waste conversions were investigated over 55.5 mM $SnCl_4$, which resulted in the highest product yield in all the studied media (**Fig. 9.2**). The product profiles of PC/H_2O and GVL/H_2O were found to be similar (**Fig. 9.8a&b**). During the early stage of conversion, the contents of glucose, fructose, and HMF increased as a result of simultaneous starch hydrolysis, glucose isomerisation, and fructose dehydration. The glucose peak indicates that sugar formation (via hydrolysis) became less significant than sugar consumption (via dehydration to HMF) in the system. The HMF concentration continued to increase in response to consumption of sugars and reached a maximum of 20.5 mol% at 7.5 min in PC/H_2O (**Fig. 9.8a**). The kinetics was slower in GVL/H_2O such that 20 min was required to achieve a comparable HMF yield (21.4 mol%), which gradually increased to 24.3 mol% at 40 min as the highest yield (**Fig. 9.8b**). The maximum HMF yields in the green solvent systems are comparable to those obtained in conventional solvent systems, *e.g.*, 25-30 mol% HMF maximum from bread waste in DMSO/H_2O and acetonitrile/H_2O (**Chapter 6&8**). Nevertheless, the latter systems required a higher temperature (140 ^oC) and/or a longer reaction time (40-60 min), *i.e.*, more energy consumption with lower throughput.

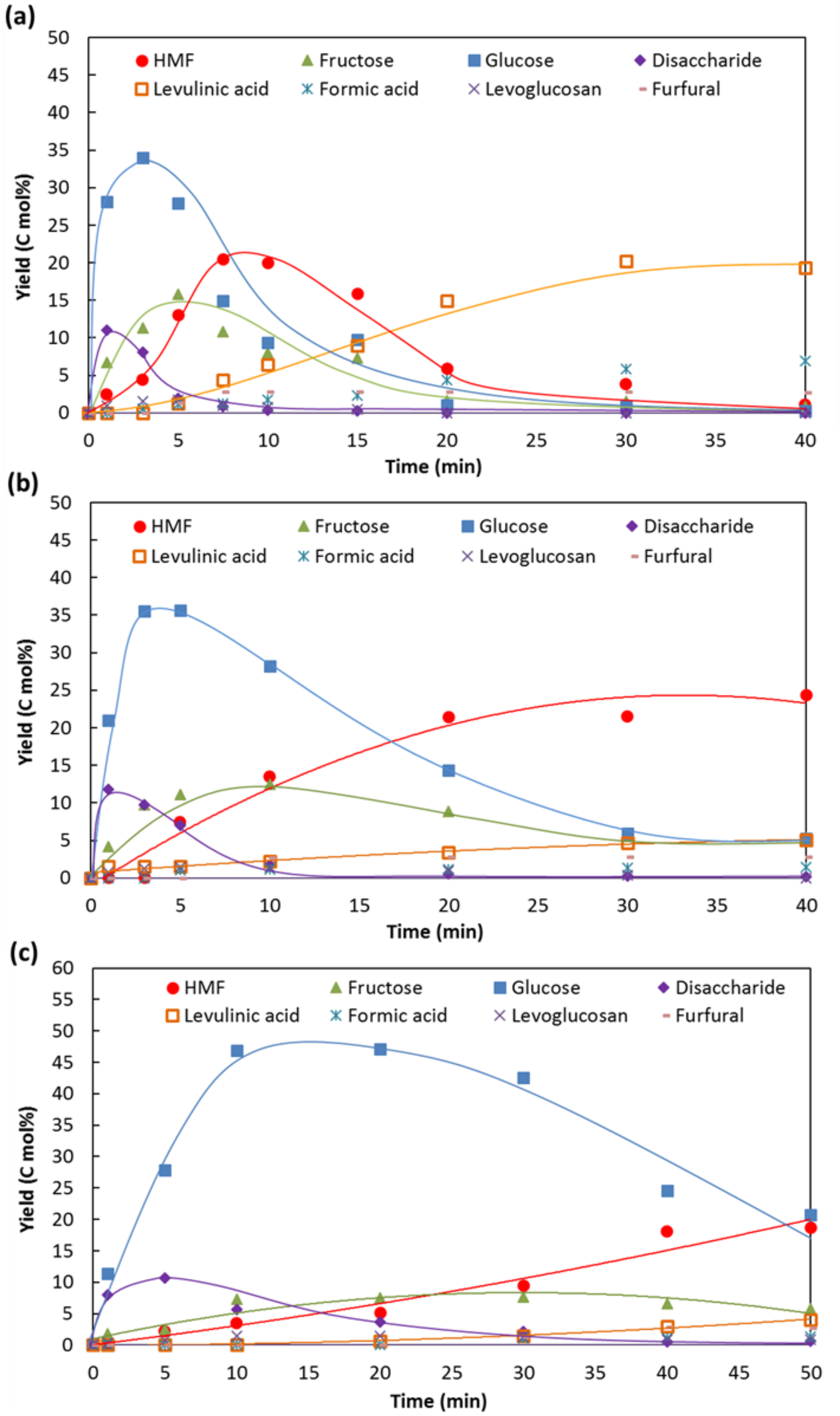

Figure 9.8. Product yields during the catalytic conversion of bread waste in (a) PC/H_2O, (b) GVL/H_2O, and (c) acetone/H_2O (conditions: 5 wt/v% substrate and 55.5 mM $SnCl_4$ in solvent mixture (1:1 v/v) at 120 °C; yield = $\text{product}_{\text{Cmol}}/\text{substrate}_{\text{Cmol}} \times 100\%$). Remark: curves are fitted manually for clearer presentation.

Among the studied solvent systems, only the PC/H_2O mixture had a biphasic nature (**Fig. 9.4**) as the solubility of PC in water is 21 wt% (at 25 ^oC) (LyondellBasell, 2017). Biphasic systems have been reported to be conducive to high HMF yield and selectivity, because HMF that partitions into the organic layer is protected against the side reactions (**Chapter 2.4.4**). Nevertheless, the biphasic nature of PC/H_2O exerted minor effects on the formation of HMF in this study, probably because of the even product distribution across the organic and aqueous layer of the reacted mixture (**Table F.1, Appendix F**).

Significant build-up of the in-vessel pressure was observed in PC/H_2O (**Fig. F.1a**). The autogenous pressure was ~10 bar at 7.5 min (*i.e.*, the optimal reaction time) and increased progressively to ~30 bar as the heating prolonged to 40 min. The pressure remained high at ~20 bar after cooling, suggesting an irreversible production of gas in PC/H_2O. It has been documented that PC decomposes to CO_2 and propylene glycol upon heating in water (LyondellBasell, 2017). In contrast, a low and steady pressure of ~4 bar was developed in GVL/H_2O (**Fig. F.1b**). This suggested that the pressure is an important factor in determining the rate of bread waste conversion. This hypothesis was substantiated by supplementary experiments (**Chapter 3.3.3**), in which 25% less HMF was produced from bread waste when a pressure release was performed midway, as compared with the control trial (**Fig. 9.9**). The autogenous pressure was ~4 bar at both mid- and end-point in the case of conversion with pressure release (**Fig. F.2**), while it was ~10 bar when the reactor remained closed throughout the process (**Fig. F.3**). Therefore, although both PC/H_2O and GVL/H_2O outcompeted acetone/H_2O and water by maintaining effective Lewis acid catalysts (**Chapter 9.2.2**), the former with the higher in-vessel pressure was even more favourable for fast conversion kinetics.

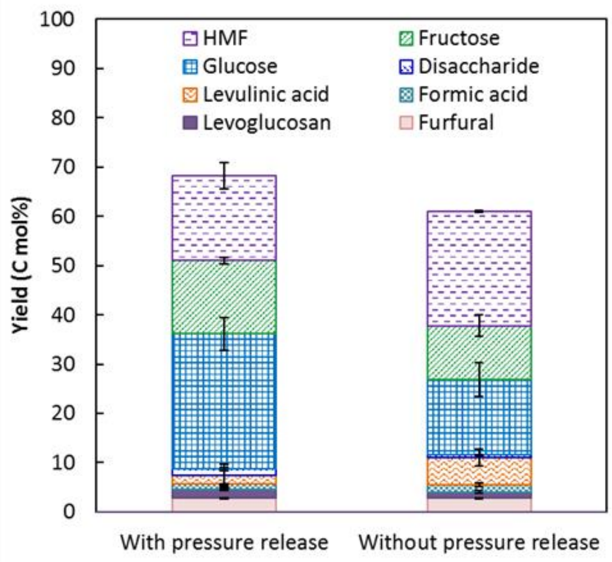

Figure 9.9. Product yields resulted from the catalytic conversion of bread waste in PC/H_2O with and without pressure release midway (conditions: 5 wt/v% substrate and 55.5 mM $SnCl_4$ in solvent mixture (1:1 v/v) at 120 ^oC for 2.5 min each for the first and second heating; yield = $product_{Cmol}/substrate_{Cmol} \times 100\%$).

In comparison with the green solvent systems (**Fig. 9.8a&b**), conversion of bread waste to HMF in acetone/H_2O at 120 ^oC was slower as only 18.7 mol% HMF was obtained after 50 min (**Fig. 9.8c**). Glucose (28-47 mol%) produced from hydrolysis of starch in bread waste dominated the product profile during the first 30 min, reinforcing that the utilisation of glucose was the rate-limiting step as discussed, despite an in-vessel pressure of ~8 bar in acetone/H_2O. In addition, **Fig. 9.7c** depicts a positive correlation between the dielectric constant of the organic co-solvent and HMF yield from bread waste. Solvents with a lower dielectric constant (*e.g.*, acetone (20.7) < GVL (36.4) < PC (64), **Fig. 9.7c**) exhibit poorer absorption of microwave. A lower heating efficiency is unfavourable to the catalytic conversion (**Chapter 2&8**).

In spite of the highest dielectric constant (78.5), the water system gave the worst performance reflecting the importance of catalyst availability in the solvent.

The content of levulinic acid and formic acid increased with the reaction time in the studied systems as a result of HMF rehydration (**Fig. 9.8a-c**). The decrease in the yield of total detectable products (**Fig. F.4**) indicates the formation of heterogeneous and carbonaceous humins via polymerisation among the sugars and HMF. These side reactions are commonly reported (Cao et al., 2017; **Chapter 6**). Both rehydration and polymerisation were more rapid in PC/H_2O than in GVL/H_2O, underscoring that the kinetics of the side reactions as well as the desired conversion steps were all enhanced in PC/H_2O with the higher autogenous in-vessel pressure.

9.2.4 Enhanced Lewis and Brønsted acid catalysis in PC/H_2O vs GVL/H_2O

To further understand the effects of pressure in PC/H_2O, correlation between the sum of derivatives of sugars (*i.e.*, HMF, levulinic acid, and formic acid) and total sugar yield (*i.e.*, disaccharide, glucose, and fructose) in PC/H_2O and GVL/H_2O is shown in **Fig. 9.10a**, in which Zone A represents the early stage of conversion with significant sugar production, and Zone B depicts the later stage that the produced sugars are notably dehydrated and rehydrated. The overlapping trends of PC/H_2O and GVL/H_2O illustrate a similar balance between production and consumption of sugars in the two systems. Nevertheless, the generation of isomerisation products (*i.e.*, fructose and HMF and its derivatives) and the generation of dehydration products (*i.e.*, HMF and its derivatives) were both faster in PC/H_2O than in GVL/H_2O (**Fig. 9.10b**). This is in good agreement with the observation that standard glucose and fructose transformed more rapidly in PC/H_2O (**Fig. 9.3a&b**). These results suggest that the relatively high autogenous pressure in PC/H_2O may favour the kinetics of Brønsted and Lewis acid catalysis to a comparable extent, promoting faster overall conversion of bread waste without altering the selectivity of the catalytic system. Such characteristics of the PC/H_2O system have not been revealed previously to the best of our knowledge.

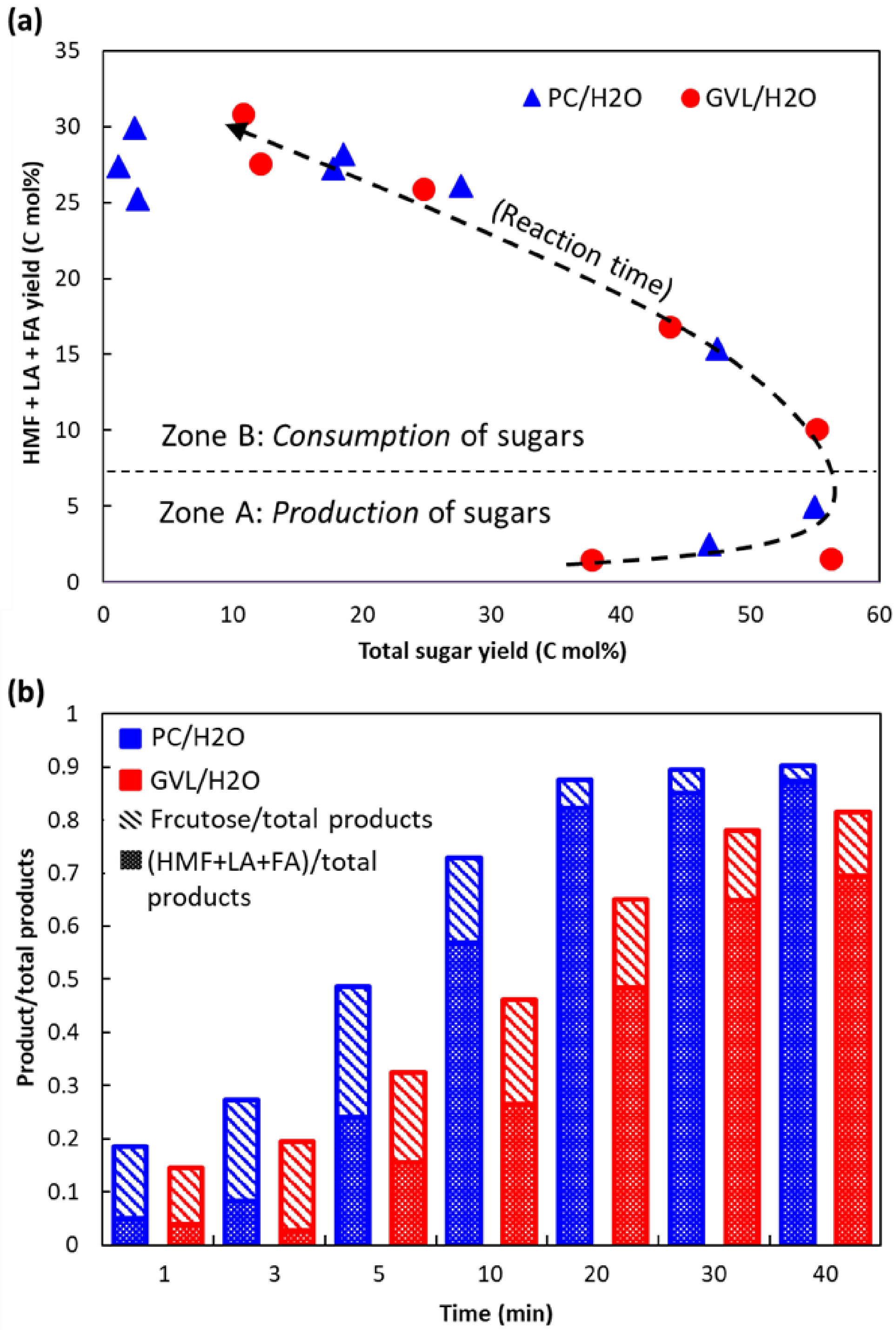

Figure 9.10. (a) Sum of sugar derivatives (HMF, levulinic acid (LA), and formic acid (FA)) as a function of total sugar yields (disaccharide, glucose, and fructose), and (b) yields of isomerisation products (fructose, HMF, LA, and FA) and dehydration products (HMF, LA, and FA) normalised by total product yields during the catalytic conversion of bread waste in PC/H_2O and GVL/H_2O (conditions: 5 wt/v% substrate and 55.5 mM $SnCl_4$ in solvent mixture (1:1 v/v) at 120 ^{o}C; yield = $\text{product}_{\text{Cmol}}/\text{substrate}_{\text{Cmol}} \times 100\%$). Remark: the arrow in (a) indicates the direction of temporal development of patterns.

The roles of pressure on HMF production remain inconclusive in the literature. A high system pressure in the range of 1−22 MPa (10−220 bar) has been suggested to alter the product distribution in previous studies on hydrothermal liquefaction of biomass (Jindal and Jha, 2016; Gollakota et al., 2018). Yet, it was reported that the rate of glucose decomposition did not vary notably with pressure in subcritical water ($\leq$ 220 bar, 374 °C) (Kabyemela et al., 1997). Under the application of high-pressure CO_2 (10-65 bar), Liu *et al.* (2012) suggested that the produced carbonic acid served as a Brønsted acid to catalyse dehydration of fructose to HMF but not glucose isomerisation, whereas Jing *et al.* (2016) proposed that carbonic acid may assist isomerisation in the presence of a Lewis acid (*e.g.,* $CrCl_3$) as the major catalyst. Further investigation is necessary to elucidate how the PC-induced pressure enhances the catalytic system. In the current study, only a trivial loss of PC was recorded at the optimal reaction time (*i.e.,* <5% v/v at 7.5 min), highlighting its potential for scale-up of the food waste conversion process.

The faster conversion kinetics of PC/H_2O and GVL/H_2O systems at a relatively low temperature signify the low energy requirement as an environmental merit in addition to their environmentally benign manufacturing. For further improvement of the HMF selectivity, an extractive layer of solvent and/or catalysts with an appropriate Lewis-to-Brønsted acid ratio can be employed to suppress the side reactions (**Chapter 2.3.3**). Downstream separation of HMF from the green solvent systems should be demonstrated in future studies, although it has been suggested that adsorption on carbon-based sorbent or solvent extraction is a possible means (**Chapter 2.7**; Liu et al., 2012).

9.3 Summary

The green solvent-containing binary systems explored herein, *i.e.*, PC/H_2O and GVL/H_2O, efficiently facilitated the tandem reactions during bread waste conversion, including starch hydrolysis, glucose isomerisation, and fructose dehydration. In the acetone/H_2O and water systems, glucose isomerisation was a critical barrier to the conversion of bread waste. Although Brønsted acidity was maintained in all of the media studied, the Lewis acidity remarkably varied with the type of the co-solvent. The PC/H_2O and GVL/H_2O systems effectively suppressed the hydrolysis of Sn^{4+} to the inactive SnO_2, which evidently occurred in acetone/H_2O and water as revealed by XRD analysis. In particular, PC/H_2O allowed more rapid bread waste conversion compared with GVL/H_2O, because of favourable in-vessel pressure developed via liberation of CO_2 from PC. This study provides insight into the roles of solvents beyond serving as a medium and highlights the potential of using green solvents for high-performance conversion of biomass waste.

Chapter 10 – Conclusions and Recommendations

10.1 Conclusions

This thesis investigates the use of different homogeneous catalysts and solvents to promote valorization of food waste for the synthesis of HMF as a value-added chemical. The maximum HMF yields achieved are 25-35% using the starch-rich waste (e.g., bread and rice waste) as substrate, using tetravalent metal catalyst (e.g., Sn(IV)) in organic solvent-water mixture as the reaction medium (e.g., acetone/H_2O, PC/H_2O, and GVL/H_2O) under heating at 120-140 ºC for 8-60 min. The key findings are summarized below.

- The conversion of starchy waste to HMF is highly efficient using metal chlorides (e.g., $SnCl_4$ and $AlCl_3$) as the catalyst, in comparison to cellulosic waste in which the crystalline cellulose is resistant against hydrolysis. (**Chapter 4**)
- Protons released from hydrolysis of metal ion serve as a Brønsted acid to facilitate hydrolysis of starch and dehydration of fructose. The Lewis acidity, which is governed by the electronegativity, electronic configuration, and charge density of metal ions, could catalyze glucose isomerization and potentially fructose dehydration. (**Chapter 5**)
- The catalyst selectivity depends on the Brønsted and Lewis acidities, which govern the relative kinetics of desirable conversion pathways over off-path reactions to determine the maximum HMF yield. Temperature increase could not boost the HMF maximum because both desirable and undesirable pathways are accelerated to a similar degree. (**Chapter 6**)

- In tivalent metal-based system (e.g., Cr(III)), addition of maleic acid increases HMF selectivity by moderating Lewis acidity to suppress side reactions, and assists starch hydrolysis via disrupting its hydrogen bond network. In contrast, maleic acid exerts limited effects, e.g., on Sn(IV)-based conversion system in terms of selectivity and kinetics. (**Chapter 7**).
- As for solvent selection, acetone/H_2O and ACN/H_2O serving as the media can accelerate the conversion of food waste to HMF, compared to DMSO/H_2O and THF/H_2O. Yet, the nearly constant HMF maxima in ACN/H_2O, acetone/H_2O, and DMSO/H_2O suggest the similar selectivity towards HMF formation in these media. (**Chapter 8**)
- The green solvent-containing binary systems, e.g., PC/H_2O and GVL/H_2O, facilitate food waste conversion to HMF more rapidly than the conventional acetone/H_2O and water systems. The PC/H_2O and GVL/H_2O systems effectively maintain active Lewis acid sites, e.g., via suppressing the transformation of Sn(IV) into the inactive SnO_2. In particular, the in-vessel pressure developed via the liberation of CO_2 from PC is beneficial to the conversion efficiency. (**Chapter 9**)

10.2 Recommendations and future work

These research efforts elucidate the roles of catalysts and solvents in governing the rate and selectivity of HMF production from food waste. Based on the current findings, starch-rich food waste (e.g., rice and bread waste) are recommended due to their high conversion feasibility, wordwide abundance, and manageable separation at source in commercial sectors. The application of $SnCl_4$ as the catalyst is suggested in view of the favourable balance of Brønsted and Lewis acidities to facilitate more rapid and selective conversion, compared to other metal chlorides such as $CrCl_3$ and $AlCl_3$. As for solvents, the use of green solvents such as PC and GVL is recommended as they facilitate faster HMF production with a lower energy requirement, presenting technical advantages in addition to their environmental merits, compared to the common industrial solvents, e.g., DMSO, THF, acetone, and acetonitrile. As for operating parameters, the control of reaction temperature and reaction time depends on the preference of practitioners in consideration of the trade-off between product yield and selectivity. Adopting the optimal temperature and time can achieve the highest HMF yield, yet, with a lower selectivity, which will require more intensive downstream separation process. If high HMF selectivity is desired more than high HMF yield, lower temperature and shorter time can be employed and circulation of the reacted mixture for further conversion is needed to maximize the substrate utilization.

In view of such trade-off between yield and selectivity as the limitation of the current technology, it is necessary to design high-performance catalytic system that selectively promotes the desirable reactions and suppresss side reactions. Such system selectivity depends on the ratio of Brønsted to Lewis acidity (B:L). Therefore, future studies will focus on manipulating the B:L ratio, by using an array of solid catalysts such as modified zeolite and graphene oxide. The application of solid catalysts allows quantification of acid properties to provide evidences on the significance of B:L ratio (e.g., via temperature-programmed desorption of pyridine and NH_3 to measure Lewis and Brønsted acid site amounts, respectively), which was a limitation in this thesis that adopted homogeneous catalysts. In addition, the development of high-performance solid catalysts serves a purpose of material recycling that is important to upscale application.

Based on the intriguing findings of using green solvents in the reaction medium, investigation will continue to reveal the solvation of substrates and catalytic sites in the media via spectroscopic analyses and computational simulation, in order to verify the speculated roles of organic co-solvents in this research. In addition, more potential and environmentally begnin candidates will be explored, such as N-butylpyrrolidinone that is polar aprotic in nature similar to PC and GVL. Solvent selection should be carried out in a prudent manner taking into account the environmental impacts associated with their production and application. To achieve good mass balance, the gas phase should also be collected for analysis.

As a long-term study, life-cycle assessment should be carried out to evaluate the environmental impacts of the conversion technologies, in which various catalysts and organic solvents are involved. In the current thesis, despite the good performance, $SnCl_4$ exerts a higher environmental impact compared to $AlCl_3$, in consideration of the metal abundance and mining impacts (Lam et al., 2018). Downstream processes such as separation and material recycling should be taken into account. While homogeneous catalysts that make recycling difficult were used in this thesis, future research on the development of heterogeneous catalysts is expected to offer more sustaible catalytic systems. Pilot-scale study should also be performed to validate the technological feasibility in larger scale. These issues are critical to realize valorization of food waste for synthesis of value-added chemicals, in order to achieve sustainable development in the future.

Appendix A

Table A.1. Major components in different food waste substrates on a dry mass basis.

Category	**Substrate**	**Component**	**Content (dry wt%)**	**Reference**
Starchy food waste	Rice	Starch	85.5^{a}	USDA, 2016 (report no. 20058)
		Total fibre^{b}	2.4^{a}	
		Protein	8.5^{a}	
		Total lipid	0.7^{a}	
		Ash	0.4^{a}	
	Penne/pasta	Starch	66.8^{a}	USDA, 2016 (report no. 20125)
		Total fibre^{b}	10.3^{a}	
		Protein	15.7^{a}	
		Total lipid	4.5^{a}	
		Ash	1.2^{a}	
Cellulosic food waste	Mixed vegetables (cabbage, spinach, and cauliflower)	Cellulose	41.3	Thulluri et al., 2013
		Hemicellulose	28	
		Lignin	11.6	
	Mixed vegetables (species unknown)	Protein	18.6^{a}	USDA, 2016 (report no. 11583)
		Total lipid	2.9^{a}	
		Ash	3.3^{a}	
Sugary food waste	Kiwifruit	Fructose	27^{a}	Wang and Buta, 2003
		Glucose	22^{a}	
		Citric acid	3.5^{a}	
		Malic acid	5.3^{a}	
		Cellulose	3.4-6.1^{a}	Carnachan et al., 2012
		Total fibre^{b}	17.6^{a}	USDA, 2016 (report no. 09148)
		Protein	6.7^{a}	
		Total lipid	3.1^{a}	
		Ash	3.6^{a}	
	Watermelon	Fructose	11.8-17.5	Liu et al., 2012
		Glucose	4.1-5.6	
		Citric acid	2.4-6.5	
		Malic acid	1.2-2.3	
		Total fibre^{b}	4.7^{a}	USDA, 2016 (report no. 09326)
		Protein	7.1^{a}	
		Total lipid	1.8^{a}	
		Ash	2.9^{a}	

[a] Content on a dry mass basis calculated using the water content obtained from USDA National Nutrient Database;

[b] Including cellulose, hemicellulose, lignin, and pectin.

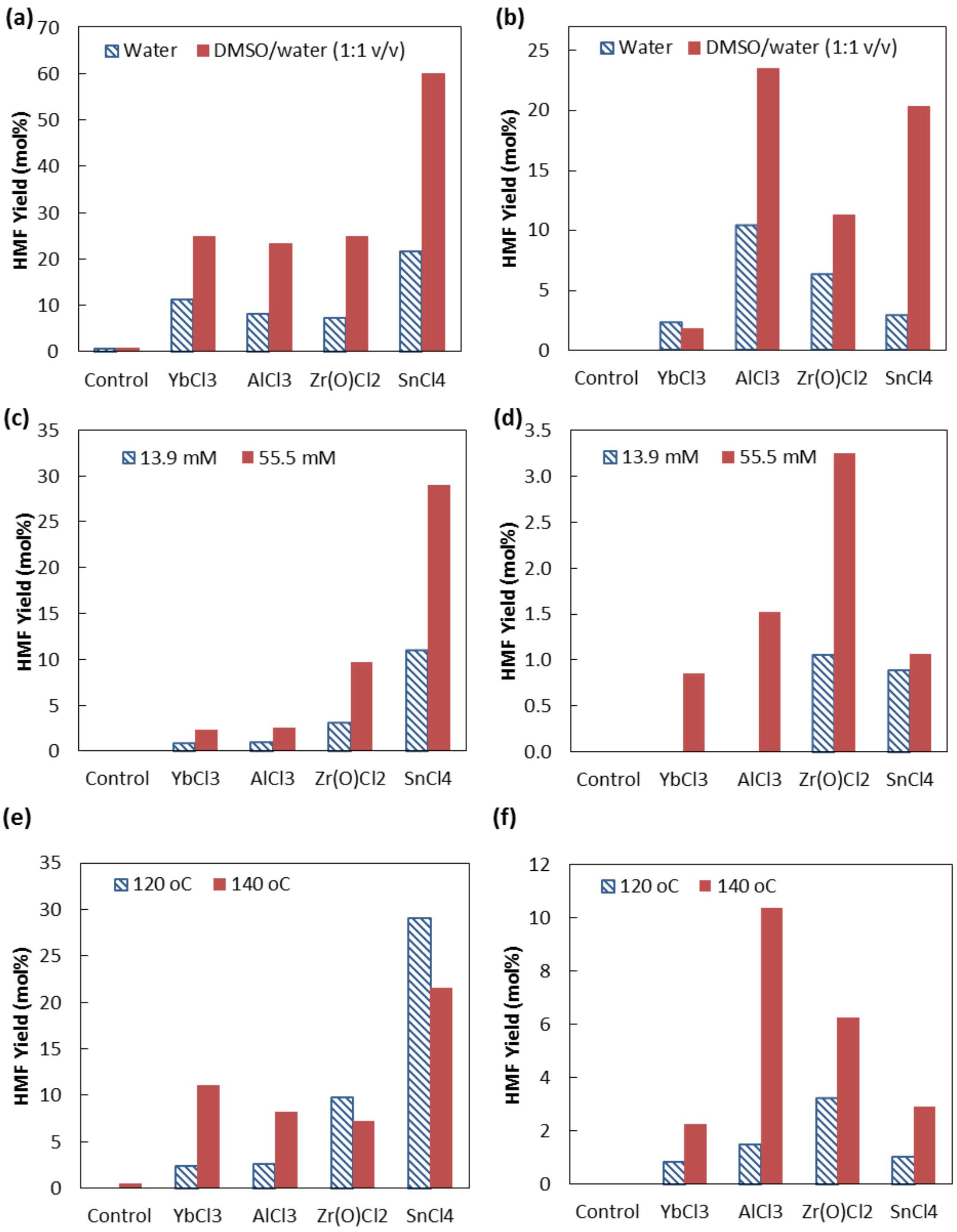

Figure A.1. HMF yield from (a) fructose and (b) glucose in the medium of water and DMSO/water (1:1 v/v) (conditions: substrate 5 wt/v%, catalyst 55.5 mM, 140°C, 20 min). HMF yield from (c) fructose and (d) glucose over Lewis acids of 13.9 mM and 55.5 mM (conditions: substrate 5 wt/v%, 120°C, 20 min, in water). HMF yield from (e) fructose and (f) glucose under the temperature of 120°C and 140°C (conditions: substrate 5 wt/v%, catalyst 55.5 mM, 20 min, in water). Yield = $\text{product}_{\text{mol}}/\text{substrate}_{\text{mol}}$ × 100%.

Appendix B

Table B.1. Speciation of metal catalysts in the presence of citrate and malate from kiwifruit [a].

Metal	**% of total concentration**	**Species**
Al^{3+} (pH = 2.82)	83.9	Al^{3+}
	0.13	$AlOH^{2+}$
	0.04	$Al_2(OH)_2^{4+}$
	6.18	Al-Citrate (aq)
	9.81	AlH-Citrate^{+}
Cr^{3+} (pH = 2.29)	96.7	Cr^{3+}
	1.11	$CrOH^{2+}$
	0.01	$Cr_3(OH)_4^{5+}$
	2.14	$Cr_2(OH)_2^{4+}$
Fe^{3+} (pH = 2.33)	0.89	Fe^{3+}
	41.5	$FeOH^{2+}$
	10.8	$Fe(OH)_2^{+}$
	0.11	$Fe_2(OH)_2^{4+}$
	12.7	Fe-Citrate (aq)
	1.48	FeH-Citrate^{+}
	32.4	Fe-Malate^{+}
Zr^{4+} (pH = 1.96)	4.41	Zr^{4+}
	0.93	$Zr(OH)_4$ (aq)
	94.7	$ZrOH^{3+}$
Sn^{4+} (pH = 1.58)	100.00	Sn^{4+}

[a] Calculated by using Visual MINTEQ Version 3.1 under the following conditions: 55.5 mM metals; 9 mM citrate, 20 mM malate based on their contents in kiwifruit (Wang and Buta, 2003) and pH measured after the each catalytic conversion of kiwifruit; 25°C).

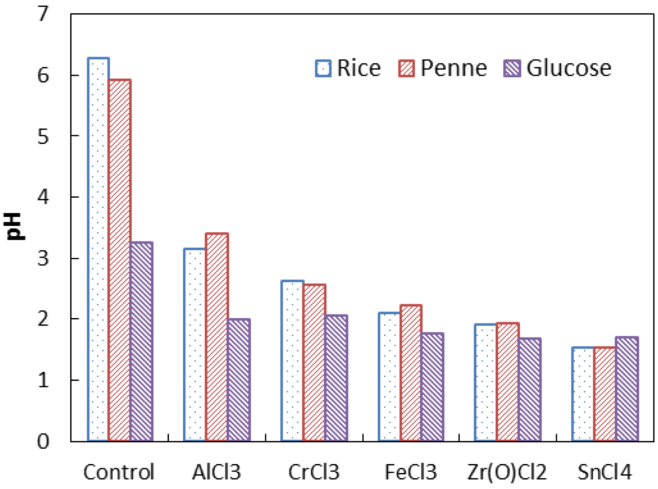

Figure B.1. Final pH in the conversion of cooked rice, cooked penne, and standard glucose in the presence of different metal chloride catalysts (conditions: 5 wt/v% substrate and 55.5 mM metal chloride in DMSO/water (1:1 v/v) at 140°C for 20 min).

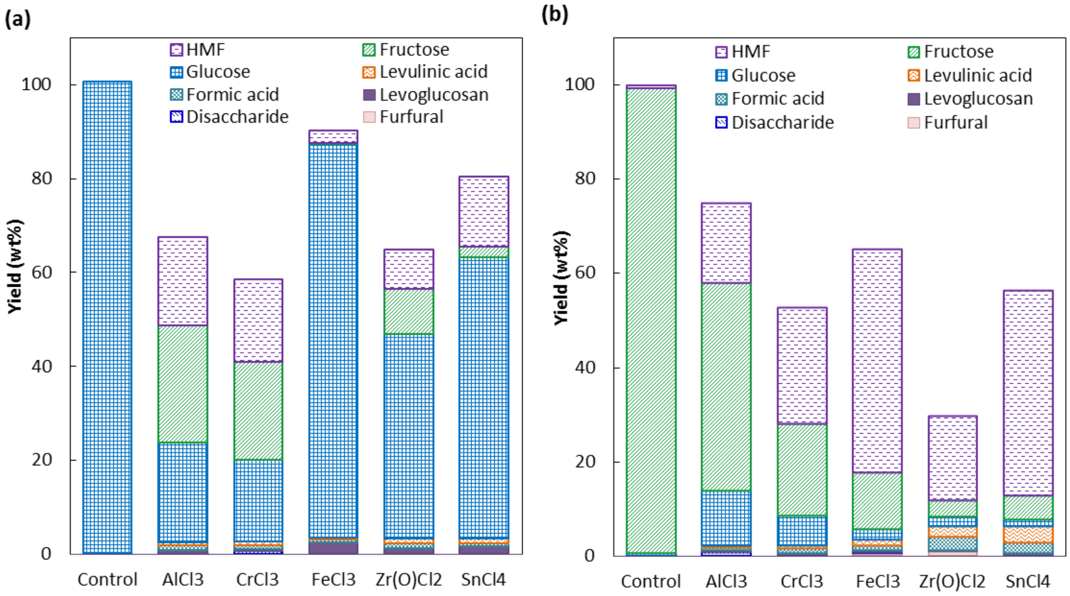

Figure B.2. Yield of different products in (a) standard glucose and (b) standard fructose conversion in the presence of different metal chloride catalysts (conditions: 5 wt/v% substrate and 55.5 mM metal chloride in DMSO/water (1:1 v/v) at 140°C for 20 min; yield = product$_{wt}$/substrate$_{wt}$ × 100%).

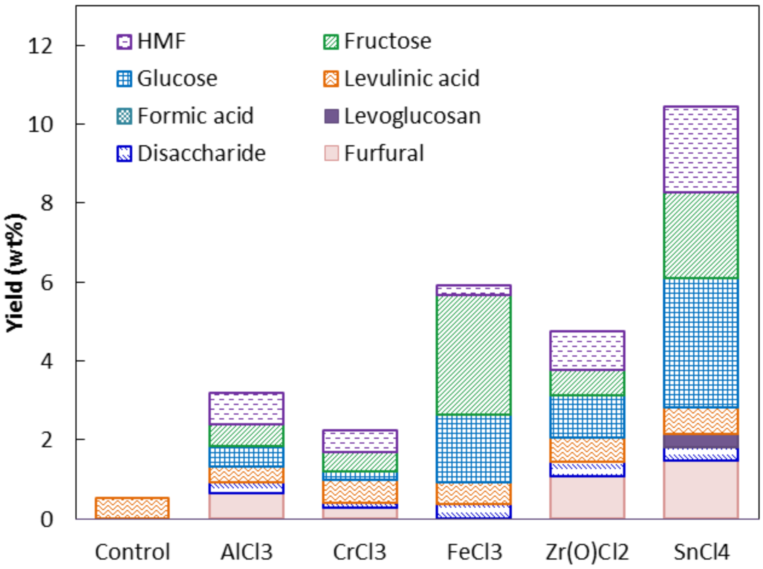

Figure B.3. Yield of different products in standard cellulose conversion in the presence of different metal chloride catalysts (conditions: 5 wt/v% substrate and 55.5 mM metal chloride in DMSO/water (1:1 v/v) at 140°C for 20 min; yield = $product_{wt}/substrate_{wt}$ × 100%).

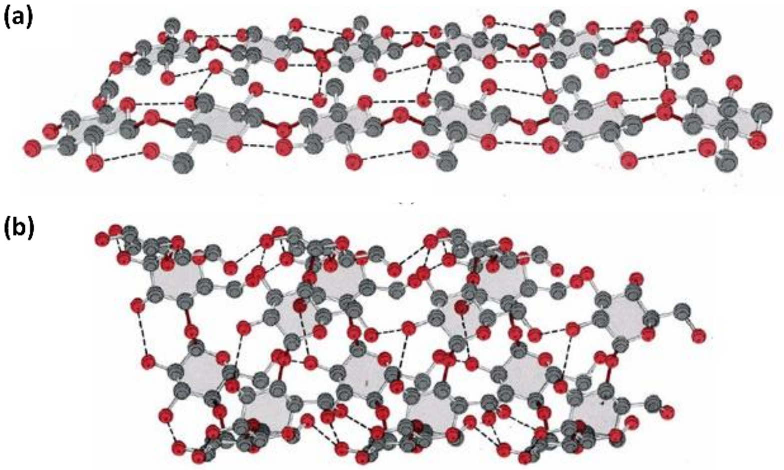

Figure B.4. Structures of (a) cellulose and (b) starch (Moore et al., 1978). Black spot = carbon atom; red spot = oxygen atom; hydrogen atoms omitted for simplification; dotted line = hydrogen bond.

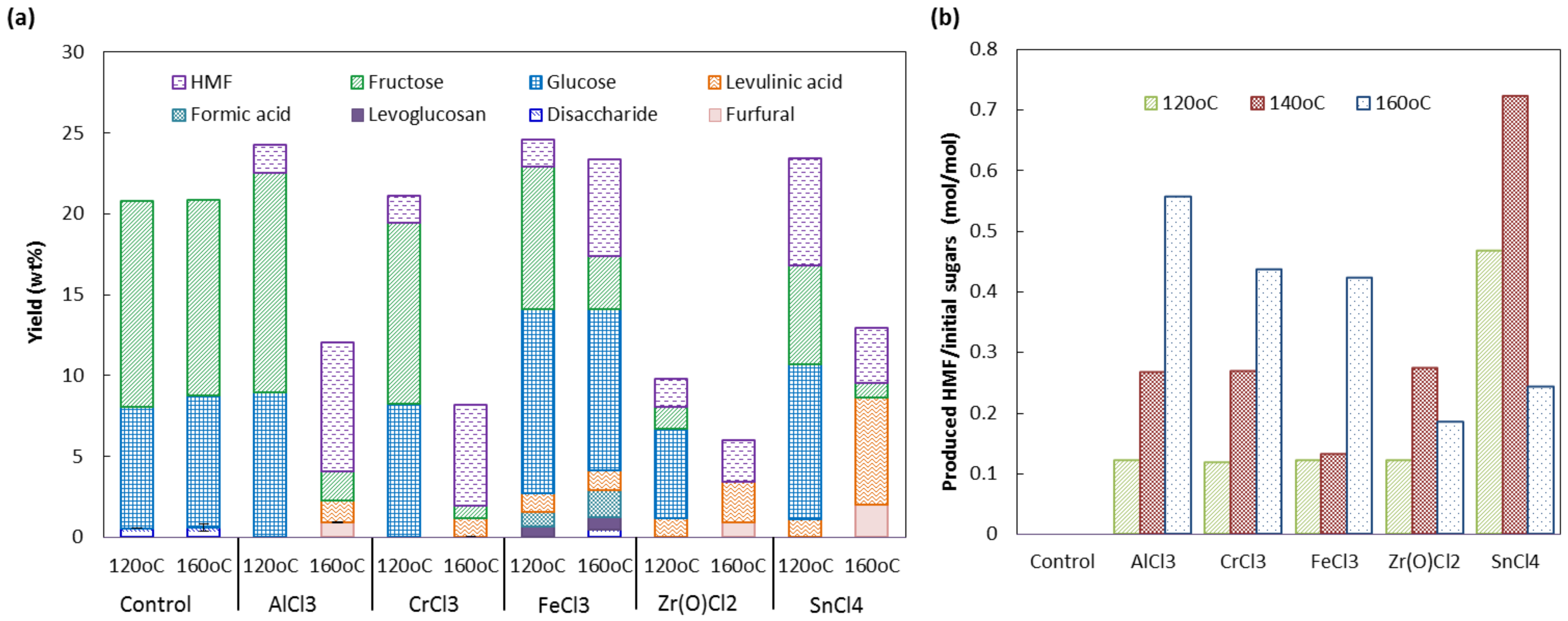

Figure B.5. (a) Yield of different products and (b) ratio of produced HMF to naturally present sugars (in the control experiments) in conversion of raw mixed vegetables at 120, 140, and 160°C in the presence of different metal chloride catalysts (conditions: 2.5 wt/v% substrate and 55.5 mM metal chloride in DMSO/water (1:1 v/v) for 20 min; yield = $product_{wt}/substrate_{wt}$ × 100%; remarks: the second batch of vegetables containing more naturally present sugars was used for the conversion at 120 and 160°C because the first batch was out of stock).

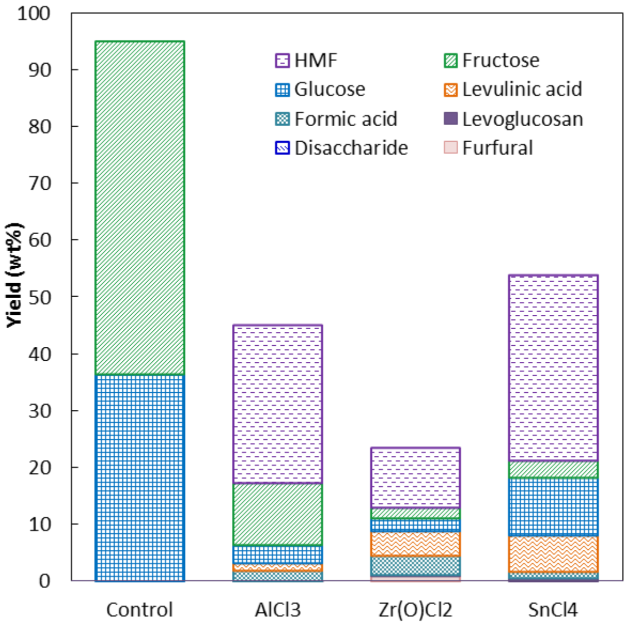

Figure B.6. Yield of different products in conversion of standard fructose of 1.5 wt/v% and glucose of 0.9 wt/v% (loadings based on the concentrations in the control of kiwifruit conversion) in the presence of different metal chloride catalysts (conditions: 55.5 mM metal chloride in DMSO/water (1:1 v/v) at 140°C for 20 min; yield = $\text{product}_{wt}/\text{substrate}_{wt} \times 100\%$).

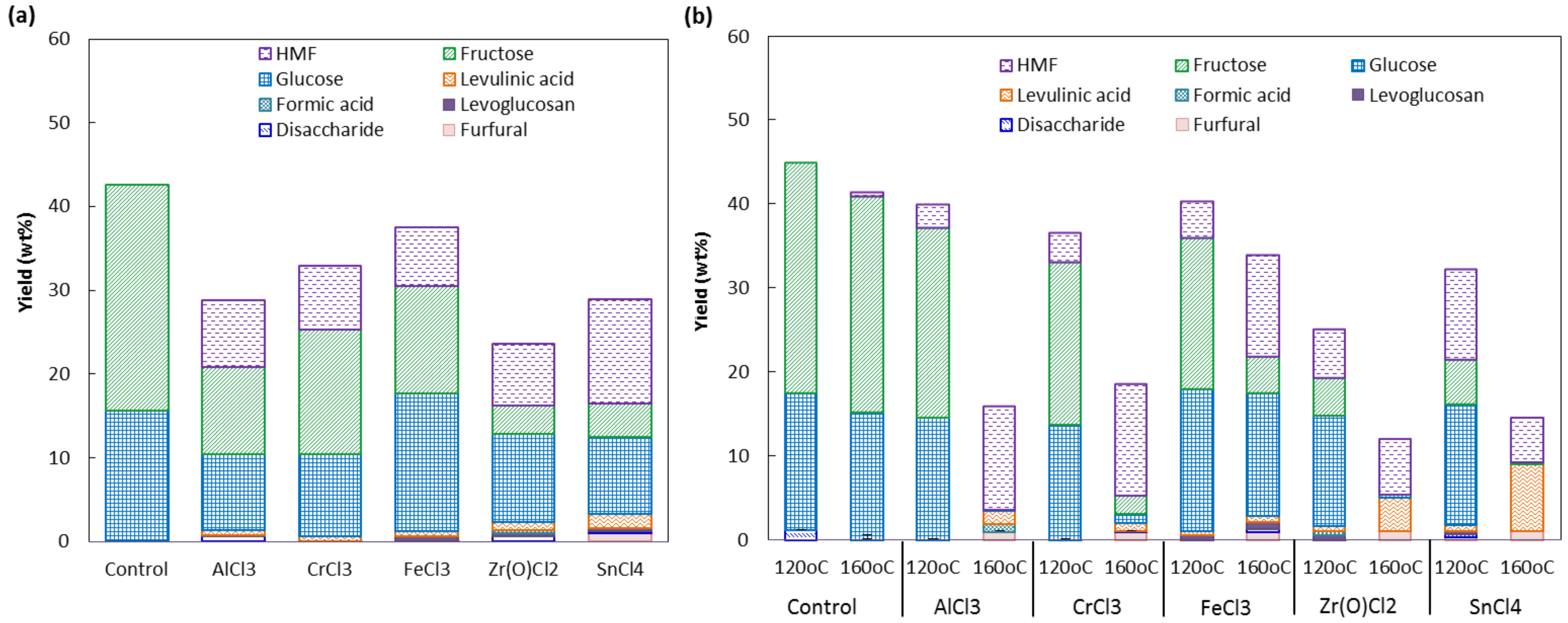

Figure B.7. Yield of different products in conversion of unskinned kiwifruit at: (a) 140°C for 40 min, and (b) 120 and 160°C for 20 min in the presence of different metal chloride catalysts (conditions: 5 wt/v% substrate and 55.5 mM metal chloride in DMSO/water (1:1 v/v); yield = $\text{product}_{wt}/\text{substrate}_{wt}$ × 100%).

References

1. Carnachan, S.M., Bootten, T.J., Mishra, S., Monro, J.A., Sims, I.M., 2012. Effects of simulated digestion in vitro on cell wall polysaccharides from kiwifruit (*Actinidia* spp.). Food Chem. 133, 132-139.
2. Liu, C., Zhang, H., Dai, Z., Liu, X., Liu, Y., Deng, X., Chen, F., Xu, J., 2012. Volatile chemical and carotenoid profiles in watermelons [Citrullus vulgaris (Thunb.) Schrad (Cucurbitaceae)] with different flesh colors. Food Sci. Biotechnol. 21, 531-541.
3. Lucas-Torres, C., Lorente, A., Cabañas, B., Moreno, A., 2016. Microwave heating for the catalytic conversion of melon rind waste into biofuel precursors. J. Clean. Prod. 138, 59-69.
4. Moore, J.W., Davis, W.G., Collins, R.W., 1978. Chemistry. McGraw-Hill, New York.
5. Parshetti, G.K., Suryadharma, M.S., Pham, T.P.T., Mahmood, R., Balasubramanian, R., 2015. Heterogeneous catalyst-assisted thermochemical conversion of food waste biomass into 5-hydroxymethylfurfural. Bioresour. Technol. 178, 19-27.
6. Peleteiro, S., Garrote, G., Santos, V., Parajó, J.C., 2014. Furan manufacture from softwood hemicelluloses by aqueous fractionation and further reaction in a catalyzed ionic liquid: a biorefinery approach. J. Clean. Prod. 76, 200-203.
7. Thulluri, C., Goluguri, B.R., Konakalla, R., Shetty, P.R., Addepally, U. 2013. The effect of assorted pretreatments on cellulose of selected vegetable waste and enzymatic hydrolysis. Biomass Bioenergy, 49, 205-213.
8. USDA 2016. National Nutrient Database, United States Department of Agriculture, https://ndb.nal.usda.gov/
9. Wang, C.Y., Buta, J.G., 2003. Maintaining quality of fresh-cut kiwifruit with volatile compounds. Postharvest Biol. Technol. 28, 181-186.
10. Wang, J., Liu, X., Hu, B., Lu, G., Wang, Y., 2014. Efficient catalytic conversion of lignocellulosic biomass into renewable liquid biofuels via furan derivatives. RSC Adv. 4, 31101–31107.
11. Yemiş, O., Mazza, G., 2012. Optimization of furfural and 5-hydroxymethylfurfural production from wheat straw by a microwave-assisted process. Bioresour. Technol. 109, 215-223.
12. Yi, Y.B., Ha, M.G., Lee, J.W., Chung, C.H., 2013. Effect of different halide types on HMF synthesis from kudzu extract in ionic liquid. J. Clean. Prod. 41, 244-250.

Appendix C

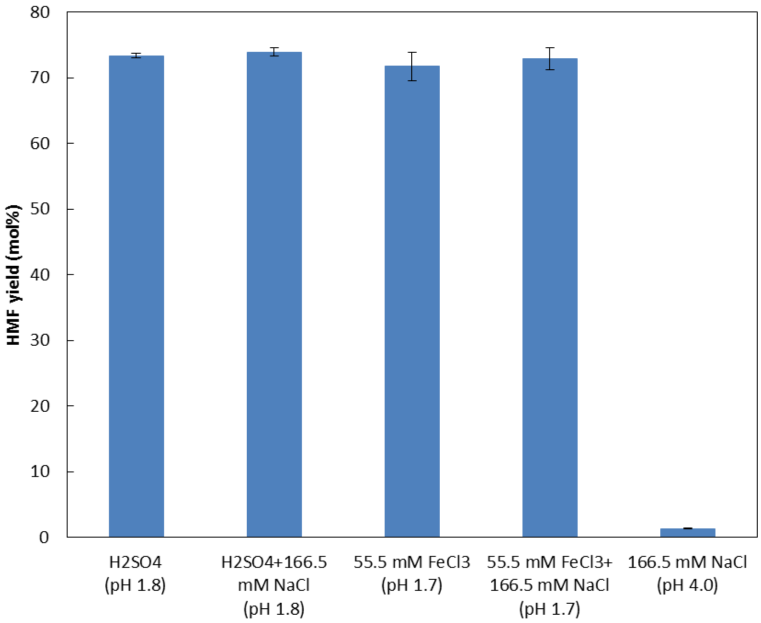

Figure C.1. HMF yield from fructose under the effect of chloride addition (conditions: fructose 5 wt/v%, $FeCl_3$ 55.5 mM and NaCl 166.5 mM, H_2SO_4 added to reach pH 1.7-1.8, 140°C, 20 min, in DMSO/water (1:1 v/v); yield = $\text{product}_{\text{mol}}/\text{substrate}_{\text{mol}} \times 100\%$).

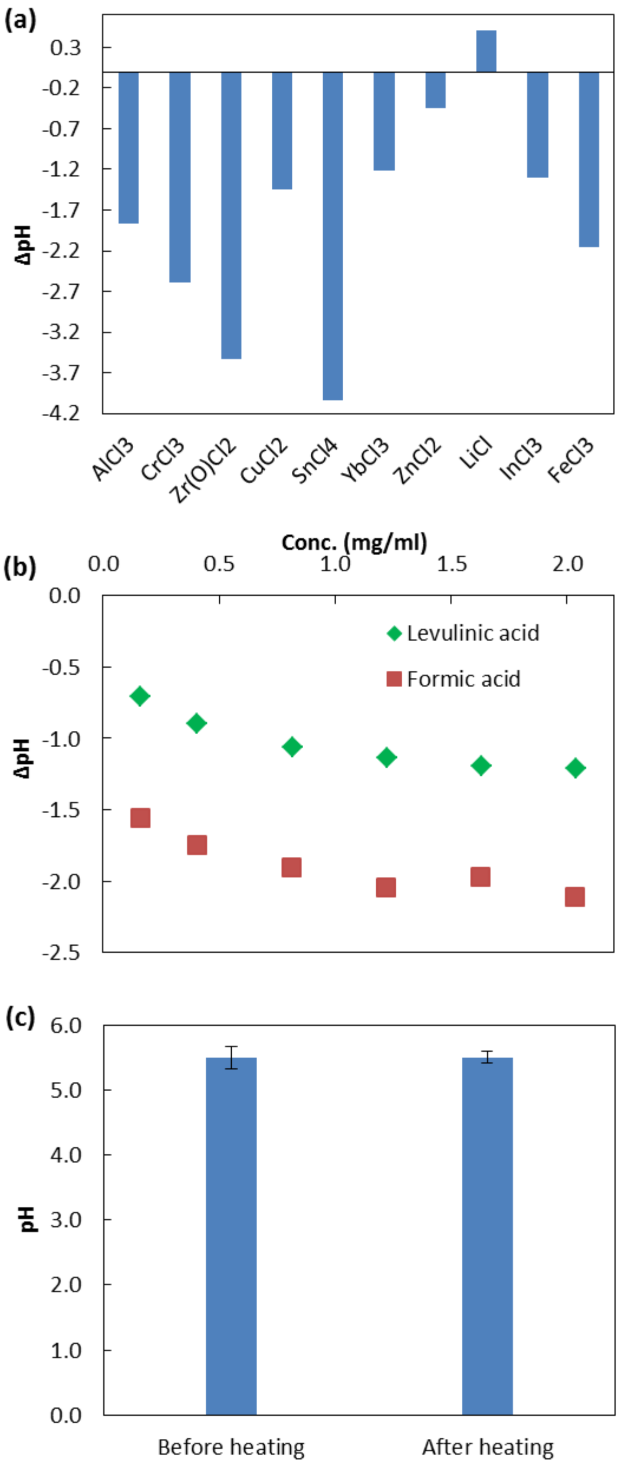

Figure C.2. Change in pH upon addition of (a) various metal chlorides (55.5 mM) and (b) levulinic acid and formic acid in DMSO/water (1:1 v/v) relative to solvent without catalyst at pH 5.5, and (c) pH of DMSO/water (1:1 v/v) before and after heating at 140°C for 20 min.

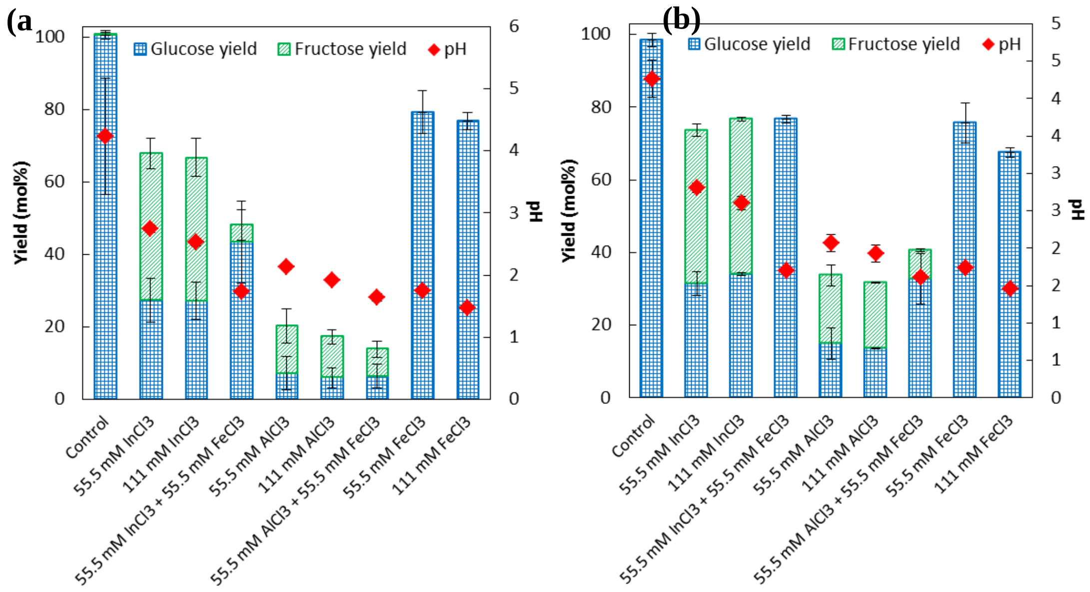

Figure C.3. The glucose remained and fructose generated from glucose as well as medium pH in the presence of single and binary catalyst in (a) sequential addition at 0 and 20 min; and (b) simultaneous addition at 0 min (conditions: glucose 5 wt/v%, catalyst 55.5 mM for single and 111 mM for binary catalyst, 140^{o}C, 40 min, in DMSO/water (1:1 v/v); yield = product$_{mol}$/substrate$_{mol}$ × 100%).

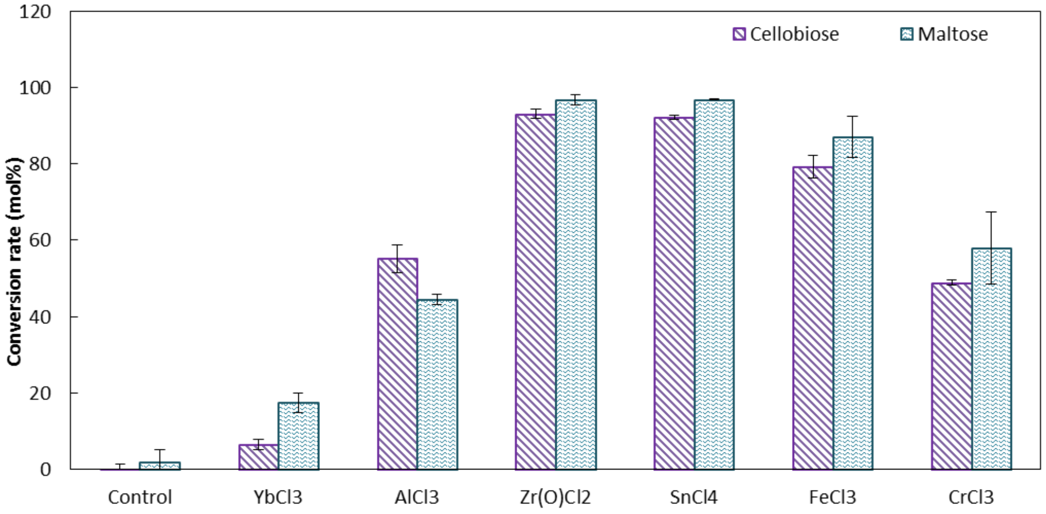

Figure C.4. The conversion rate of cellobiose and maltose under different Lewis acid catalysts (conditions: 5 wt/v% glucose and 55.5 mM Lewis acid catalyst in DMSO/water (1:1 v/v) at 140^{o}C for 20 min; conversion rate = [substrate$_{intial,mol}$ – substrate$_{final,mol}$]/substrate$_{initial\ mol}$ × 100%).

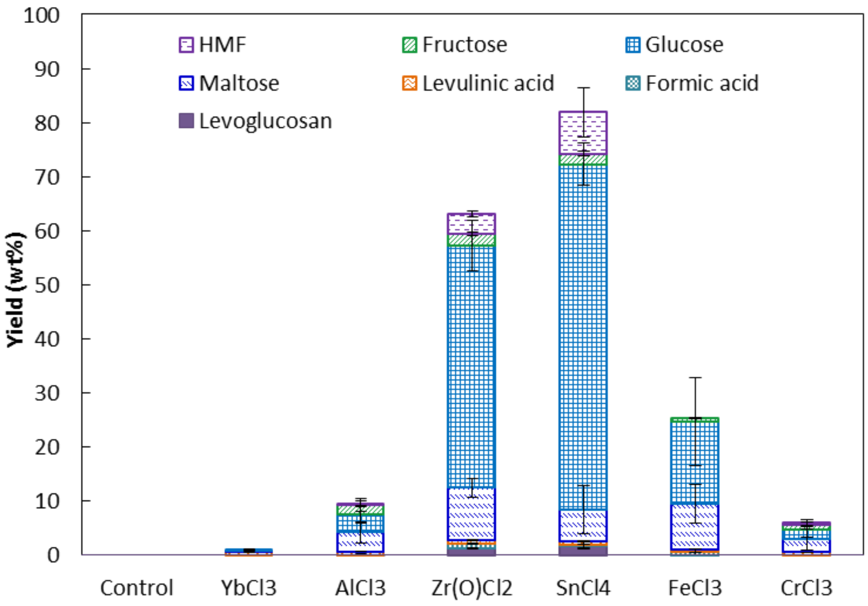

Figure C.5. The yield of hydrolysis derivatives from standard starch conversion under different catalysts (conditions: starch 5 wt/v%, catalyst 55.5 mM, 140°C, 20 min, in DMSO/water (1:1 v/v); yield = product$_{wt}$/substrate$_{wt}$ × 100%).

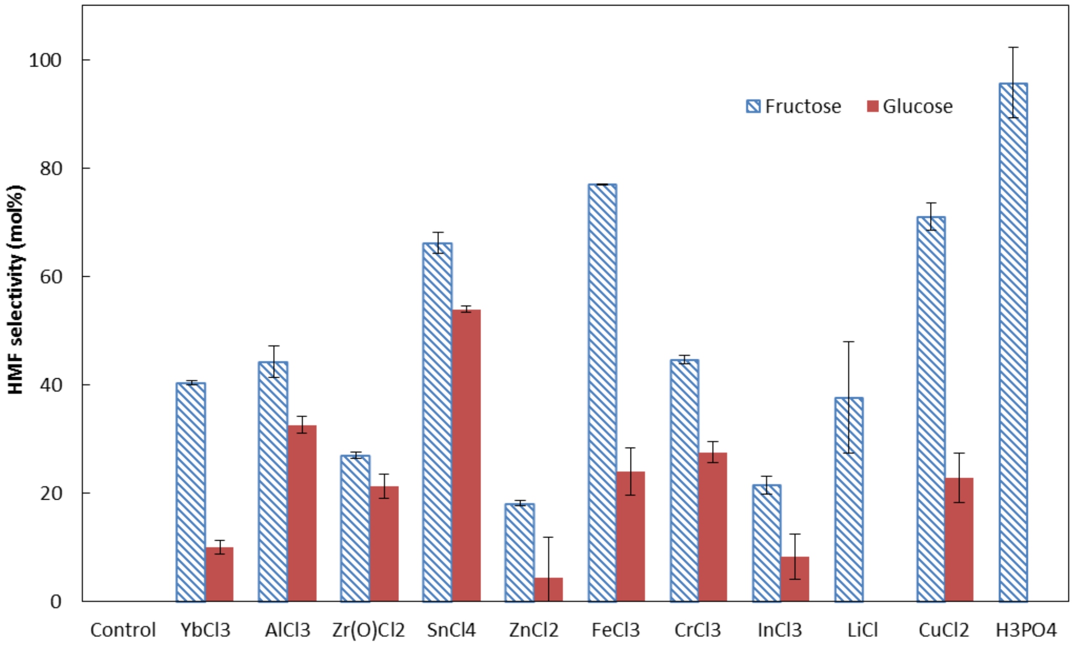

Figure C.6. The HMF selectivity in fructose and glucose conversion under different Lewis acid catalysts (conditions: 5 wt/v% substrate and 55.5 mM Lewis acid catalyst in DMSO/water (1:1 v/v) at 140°C for 20 min; selectivity = $\text{product}_{\text{mol}}/[\text{substrate}_{\text{intial,mol}} - \text{substrate}_{\text{final,mol}}] \times 100\%$).

Appendix D

Table D.1. Preliminary economic analysis of valorization of 1000 g bread waste (dry weight) into HMF in the Hong Kong context (conversion scenario: 5 wt/v% substrate and 55.5 mM $SnCl_4$ in DMSO/water (1:1 v/v) at 160°C for 20 min).

	Item	**Quantity**	**Unit**	**Unit price (USD)**	**Unit price reference**	**Total (USD)**
Cost	Bread waste	1390[a]	g	0[b]	-	0
	$SnCl_4$	389	g	0.005	Alibaba, 2016	2
				0.23	Sigma Aldrich, 2016	91
	DMSO	10	L	2	Alibaba, 2016	20
				94.2	Sigma Aldrich, 2016	942
	Water	10	L	0.0006	HK WSD, 2016	0.006
	Energy	0.24[c]	kWh	0.13	HK CLP, 2016	0.03
Avoided cost	Waste charging	1390	g	0.00006	HK ENB, 2014[d]	0.1
Revenue	HMF	214	g	0.3	Alibaba, 2016	64
				5.9	Sigma Aldrich, 2016	1265
	Levulinic acid	53	g	0.01	Alibaba, 2016	0.5
				0.07	Sigma Aldrich, 2016	3.5
					Balance = (Revenue + Avoided cost) - Cost	**43–236[e]**

[a] As-received weight of bread waste was used, which was calculated based on its measured water content, i.e., 28.1±0.4 wt%.

[b] The cost of bread waste as substrate was assumed to be zero since it was an unwanted material to be sent to landfills.

[c] The energy consumption was estimated using the data on power usage indicated by the microwave reactor.

[d] The quantity-based waste charging scheme is under legislation stage in Hong Kong. The charge anticipated by the industry and government was adopted here.

[e] Chemicals with both industrial and analytical quality were considered. The upper and lower bound of the net gain was calculated using the chemical prices provided by Sigma Aldrich (analytical quality) and Alibaba (industry quality), respectively.

References:

1. Alibaba 2016, http://www.alibaba.com/
2. HK CLP 2016, https://www.clp.com.hk/en/customer-service/tariff/business-and-other-customers/non-residential-tariff
3. HK ENB 2014, A Food Waste & Yard Waste Plan for Hong Kong 2014-2022.
4. HK WSD 2016, http://www.wsd.gov.hk/en/customer_services_and_water_bills/water_and_sewage_tariff/water_and_sewage_tariff/
5. Sigma Aldrich 2016, http://www.sigmaaldrich.com/

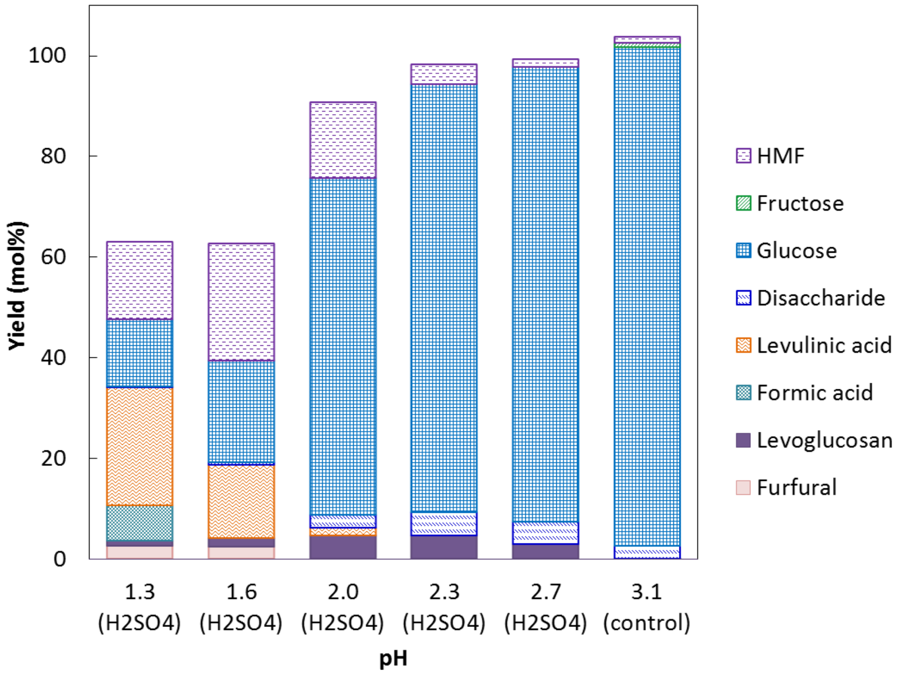

Figure D.1. Yields of different products from conversion of standard glucose under a range of pH adjusted by concentrated H_2SO_4 (conditions: 5 wt/v% substrate in DMSO/water (1:1 v/v) at 160°C for 30 min; yield = $product_{Cmol}/substrate_{Cmol}$ × 100%).

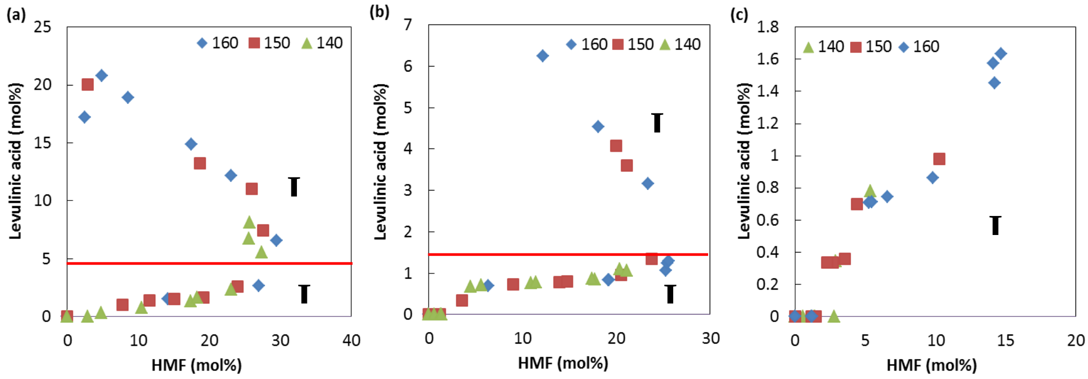

Figure D.2. Concentration of levulinic acid as a function of HMF during the conversion of bread waste over (a) $SnCl_4$, (b) $AlCl_3$, and (c) $FeCl_3$ at different temperatures (conditions: 5 wt/v% substrate and 55.5 mM metal chloride in DMSO/water (1:1 v/v); yield = $product_{Cmol}/substrate_{Cmol}$ × 100%; remarks: the product profiles were divided into Zone I and II, which represented the beginning and final stage of the conversion, respectively).

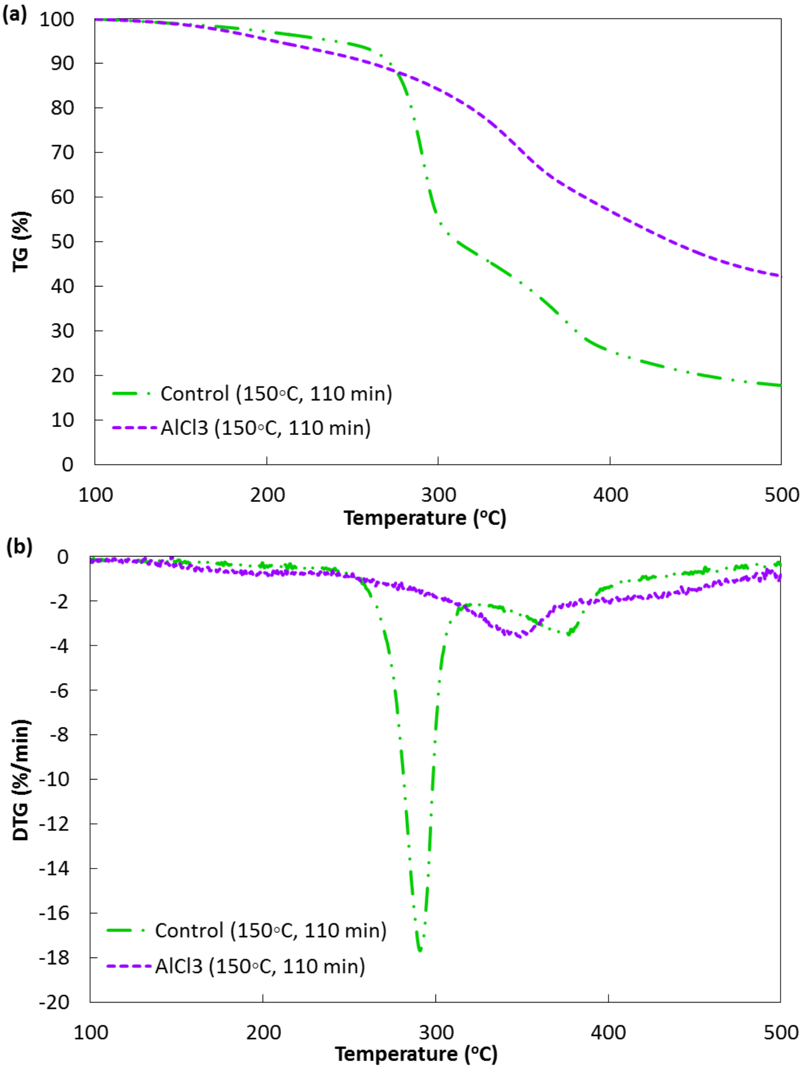

Figure D.3. (a) Thermogravimetry (TG) and (b) derivative thermogravimetry (DTG) spectra of solid residues from $AlCl_3$-catalyzed conversion of bread waste and control (i.e., without metal chloride catalyst).

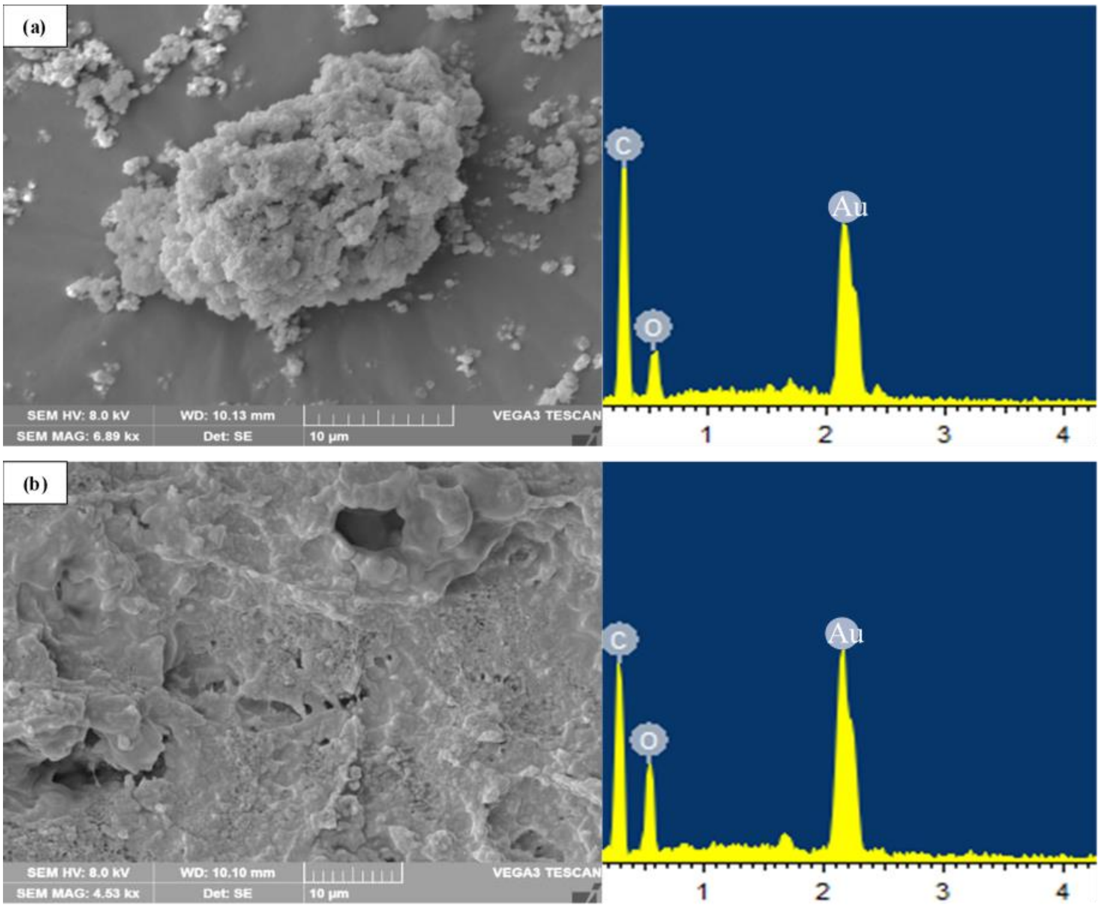

Figure D.4. Scanning electron microscope (SEM) image and energy dispersive X-ray (EDX) spectra of solid residues from (a) $AlCl_3$-catalyzed conversion of bread waste and (b) control (i.e., without metal chloride catalyst) (conditions: 5 wt/v% substrate and 55.5 mM metal chloride (except control) in DMSO/water (1:1 v/v) at 150°C for 110 min; remarks: samples were coated by gold to enhance conductivity for analysis).

Appendix E

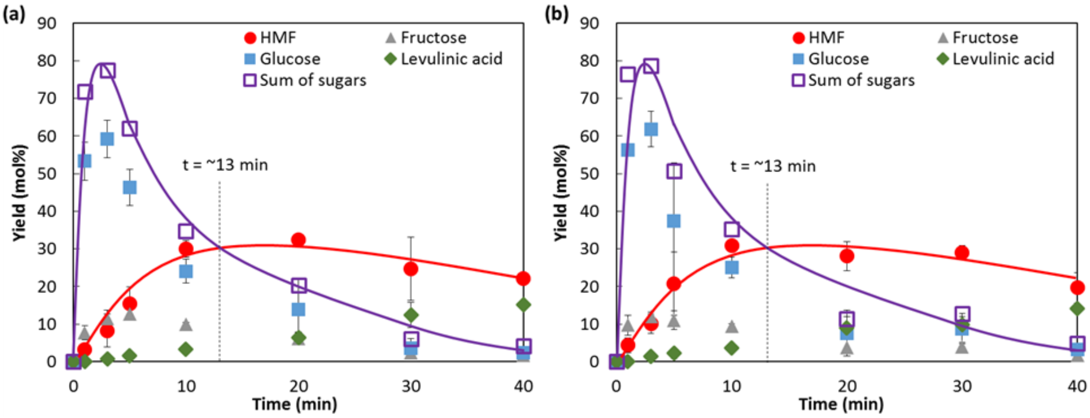

Figure E.1. Product yields in relation to the catalytic conversion of rice waste between two Sn(IV) systems: (a) Sn(IV) and (b) Sn(IV)/MA in acetone-water mixture (1:1 v/v) (conditions: 5 wt/v% substrate and 55.5 mM $SnCl_4$ and 13.9 mM MA at 140 ^oC; yield = $product_{Cmol}/substrate_{Cmol}$ × 100%). Remark: the intersection between the trends of sum of sugars (i.e., disaccharides, glucose and fructose) and HMF yield represents the time (t) at which dehydration of sugars starts to emerge.

Appendix F

Table F.1. Distribution of products after $SnCl_4$-catalysed conversion of bread waste in PC/H_2O at 120°C for 10 min.

Fraction	Product concentration (mg/ml)							
	Disaccharide	Glucose	Fructose	Levoglucosan	Formic acid	Levulinic acid	HMF	Furfural
Shaken mixture	0.28	8.18	5.26	0.42	1.32	2.64	6.84	0.94
Upper layer	0.30	9.06	5.80	0.44	1.36	2.66	6.45	0.91
Lower layer	0.28	7.50	4.84	0.42	1.36	2.70	7.23	0.97

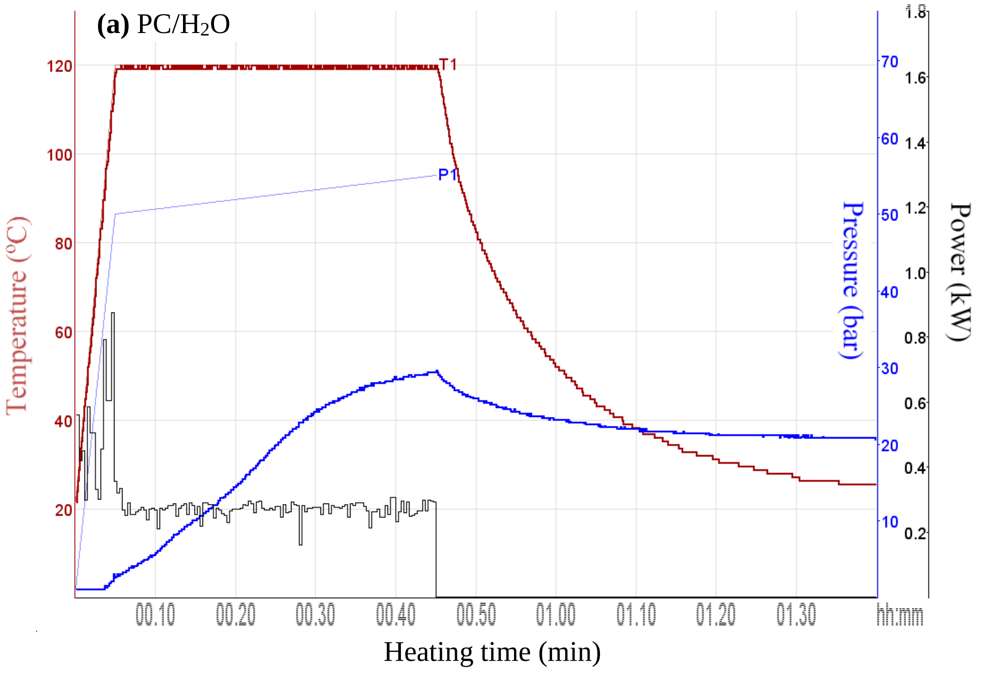

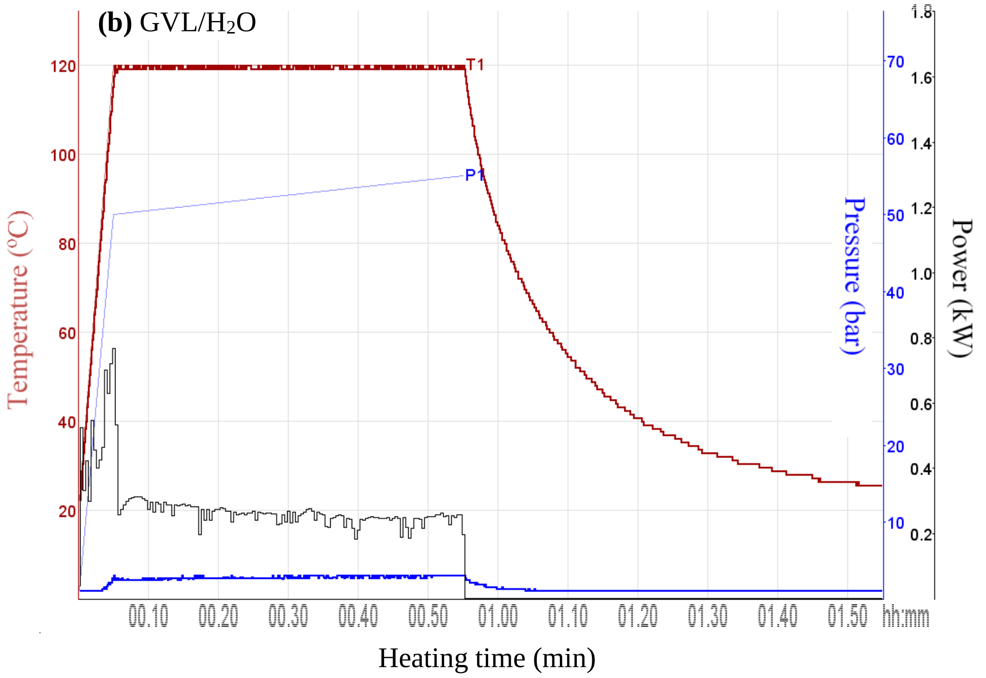

Figure F.1. Records of in-vessel pressure and temperature during reaction in (a) PC/H_2O and (b) GVL/H_2O.

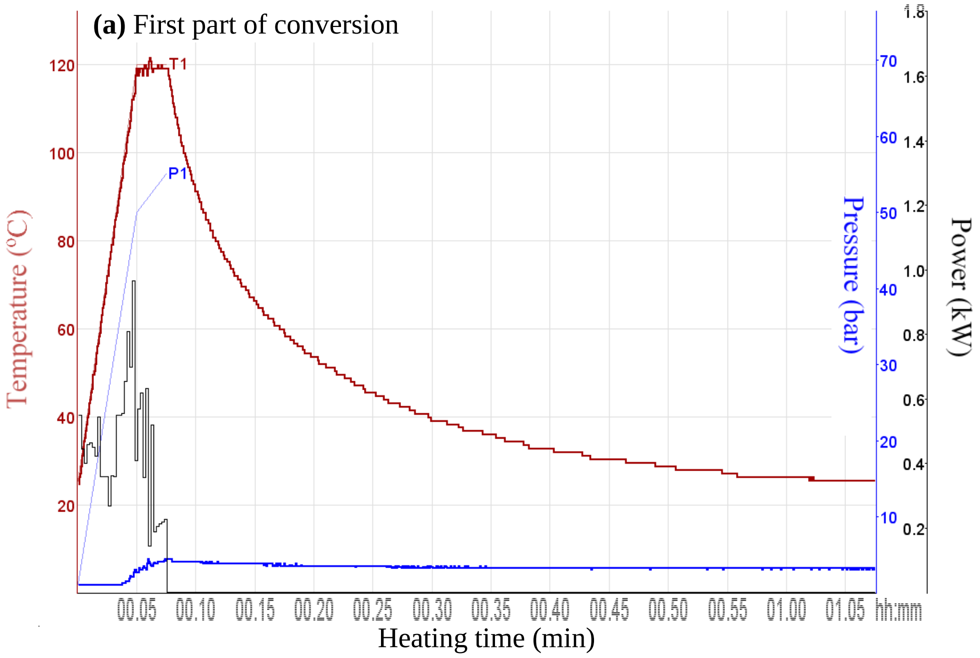

(a) First part of conversion

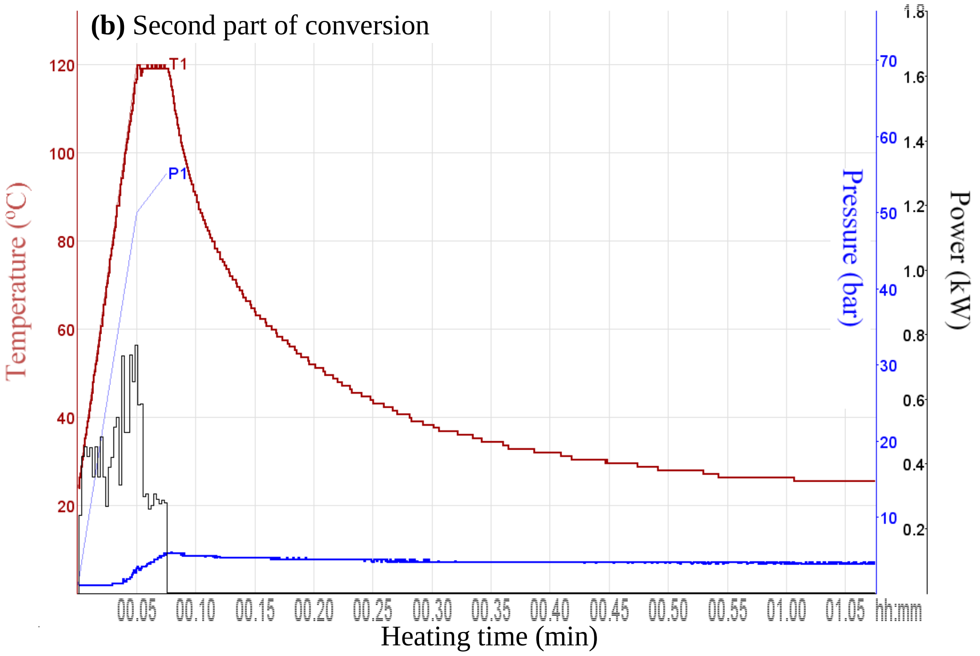

(b) Second part of conversion

Figure F.2. Records of in-vessel pressure and temperature during reaction in PC/H_2O (1:1 v/v) *with* pressure release midway: (a) heating 5 wt/v% substrate with 55.5 mM $SnCl_4$ at 120°C for 2.5 min; after cooling and opening the vessel for pressure release, (b) the mixture was heated again at 120°C for 2.5 min. Ramping was completed in 5 min.

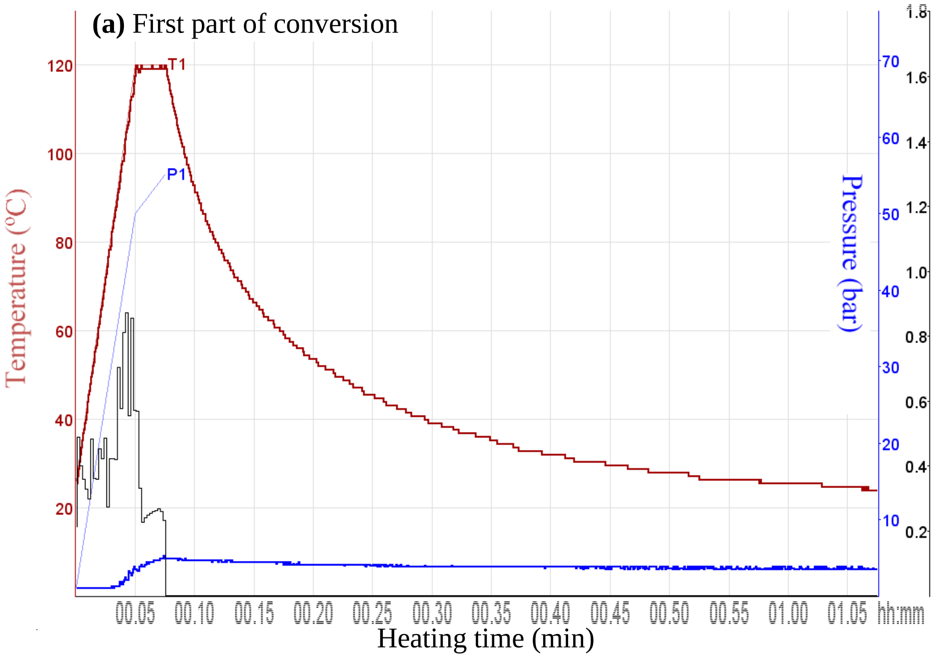

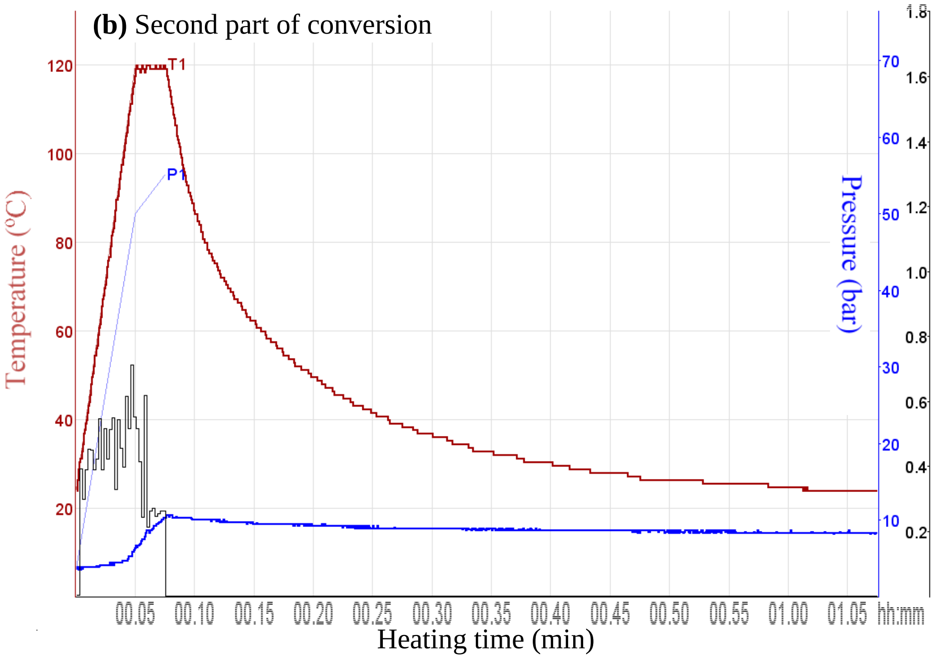

Figure F.3. Records of in-vessel pressure and temperature during reaction in PC/H_2O (1:1 v/v) *without* pressure release midway: (a) heating 5 wt/v% substrate with 55.5 mM $SnCl_4$ at 120°C for 2.5 min; after cooling, (b) the mixture was heated again at 120°C for 2.5 min. Ramping was completed in 5 min.

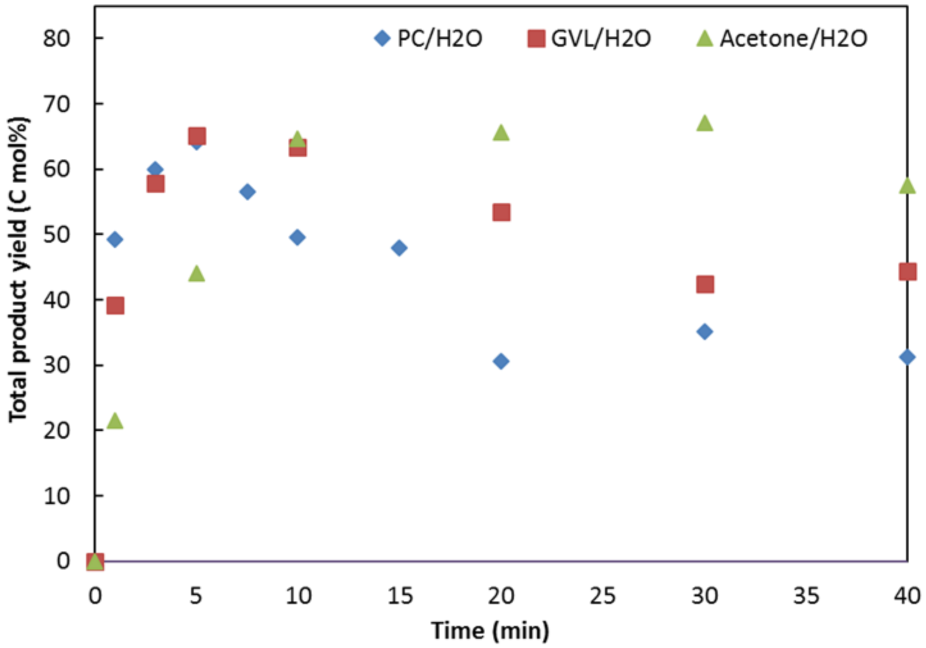

Figure F.4. Total product yields resulted from the catalytic conversion of bread waste in different solvent mixtures (1:1 v/v) (conditions: 5 wt/v% substrate and 55.5 mM $SnCl_4$ at 120 °C; yield = $product_{Cmol}/substrate_{Cmol} \times 100\%$).

References

Alam, M.I., Saha, B., 2015. Catalysis for the production of sustainable chemicals and fuels from biomass, in: Saha, B., Fan, M., Wang, J. (Eds.), Sustainable Catalytic Processes. Elsevier, Amsterdam, Oxford, Waltham, pp. 99–124.

Albonetti, S., Lolli, A., Morandi, V., Migliori, A., Lucarelli, C., Cavani, F., 2015. Conversion of 5-hydroxymethylfurfural to 2, 5-furandicarboxylic acid over Au-based catalysts: Optimization of active phase and metal–support interaction. Appl. Catal. B 163, 520-530.

Alia, J.M., 2001. Raman spectroscopic studies of ion-ion interactions in aqueous and nonaqueous electrolyte solutions, in: Lewis, I.R., Edwards, H. (Ed), Handbook of Raman Spectroscopy: From the Research Laboratory to the Process Line. Marcel Dekker, New York.

Alibaba, 2017. Available in: www.alibaba.com/ (Accessed June 2017)

Alves Costa Pacheco, A., Sherwood, J., Zhenova, A., McElroy, C.R., Hunt, A.J., Parker, H.L., Farmer, T.J., Constantinou, A., De bruyn, M., Whitwood, A.C., Raverty, W., Clark, J. H., 2016. Intelligent approach to solvent substitution: the identification of a new class of levoglucosenone derivatives. ChemSusChem 9, 3503-3512.

Amarasekara, A S., Williams, L.D., Ebede, C.C. 2008., Mechanism of the dehydration of d-fructose to 5-hydroxymethylfurfural in dimethyl sulfoxide at 150oC: an NMR study. Carbohydr. Res. 343, 3021-3024.

Amarasekara, A.S., Razzaq, A., 2014. Mechanism of 1-(1-propylsulfonic)-3-methylimidazolium chloride catalyzed transformation of D-glucose to 5-hydroxymethylfurfural in DMSO: an NMR study. Carbohydr. Res. 386, 86-91.

Amiri, H., Karimi, K., Roodpeyma, S., 2010. Production of furans from rice straw by single-phase and biphasic systems. Carbohydr. Res. 345, 2133-2138.

Antal, M.J., Mok, W.S.L., Richards, G.N. 1990. Mechanism of formation of 5-(hydroxymethyl)-2-furaldehyde from D-fructose and sucrose. Carbohydr. Res. 199, 91-109.

Aristizábal M., V., Gómez P., Á., Cardona A., C.A., 2015. Biorefineries based on coffee cut-stems and sugarcane bagasse: Furan-based compounds and alkanes as interesting products. Bioresour. Technol. 196, 480-489.

Arsova, L., 2010. Anaerobic digestion of food waste: Current status, problems and an alternative product. Columbia University, New York.

Asghari, F.S., Yoshida, H., 2007. Kinetics of the decomposition of fructose catalyzed by hydrochloric acid in subcritical water: formation of 5-hydroxymethylfurfural, levulinic, and formic acids. Ind. Eng. Chem. Res. 46, 7703-7710.

Asghari, F.S., Yoshida, H., 2010. Conversion of Japanese red pine wood (Pinus densiflora) into valuable chemicals under subcritical water conditions. Carbohydr. Res. 345, 124-131.

Bala, T., Prasad, B.L.V., Sastry, M., Kahaly, M.U., and Waghmare, U.V., 2007. Interaction of different metal ions with carboxylic acid group: a quantitative study. J. Phys. Chem. A 111, 6183-6190.

Bermejo-Deval, R., Gounder, R., Davis, M.E., 2012. Framework and extraframework tin sites in zeolite beta react glucose differently. ACS Catal. 2, 2705-2713.

Bevilaqua, D.B., Rambo, M.K., Rizzetti, T.M., Cardoso, A.L., Martins, A.F., 2013. Cleaner production: levulinic acid from rice husks. J. Clean. Prod. 47, 96-101.

Binder, J.B., Cefali, A.V., Blank, J.J., Raines, R.T., 2010. Mechanistic insights on the conversion of sugars into 5-hydroxymethylfurfural. Energy Environ. Sci. 3, 765-771.

Binder, J.B., Raines, R.T., 2009. Simple chemical transformation of lignocellulosic biomass into furans for fuels and chemicals. J. Am. Chem. Soc. 131, 1979-1985.

Bodirlau, R., Teaca, C.A., Spiridon, I., 2013. Influence of natural fillers on the properties of starch-based biocomposite films. Compos. Pt. B Eng. 44, 575-583.

Bozell, J.J., Petersen, G.R., 2010. Technology development for the production of biobased products from biorefinery carbohydrates—the US Department of Energy's "Top 10" revisited. Green Chem. 12, 539-554.

Brown, P.L., Sylva, R.N., Ellis, J., 1985. An equation for predicting the formation constants of hydroxo-metal complexes. J. Chem. Soc. Dalton Trans. 4, 723-730.

Byrne, F.P., Jin, S., Paggiola, G., Petchey, T.H., Clark, J.H., Farmer, T.J., Hunt, A.J., McElroy, C.R., Sherwood, J., 2016. Tools and techniques for solvent selection: green solvent selection guides. Sustain. Chem. Process. 4, 1-24.

Byrne, F.P., Jin, S., Paggiola, G., Petchey, T.H.M., Clark, J.H., Farmer, T.J., Hunt, A.J., Robert McElroy, C., Sherwood, J., 2016. Tools and techniques for solvent selection: green solvent selection guides. Sustain. Chem. Process. 4, 1-24.

Cai, C.M., Nagane, N., Kumar, R., Wyman, C.E., 2014. Coupling metal halides with a co-solvent to produce furfural and 5-HMF at high yields directly from lignocellulosic biomass as an integrated biofuels strategy. Green Chem. 16, 3819-3829.

Cai, C.M., Zhang, T., Kumar, R., Wyman, C.E., 2013. THF co-solvent enhances hydrocarbon fuel precursor yields from lignocellulosic biomass. Green Chem. 15, 3140-3145.

Cao, L., Yu, I. K.M., Chen, S.S., Tsang, D.C.W., Wang, L., Xiong, X., Zhang, S., Ok, Y.S., Kwon, E.E., Song, H., Poon, C.S., 2018. Production of 5-hydroxymethylfurfural from starch-rich food waste catalyzed by sulfonated biochar. Bioresour. Technol. 252, 76-82.

Caratzoulas, S., Davis, M.E., Gorte, R.J., Gounder, R., Lobo, R.F., Nikolakis, V., Sandler, S.I., Snyder, M.A., Tsapatsis, M., Vlachos, D.G., 2014. Challenges of and insights into acid-catalyzed transformations of sugars. J. Phys. Chem. C 118, 22815-22833.

Carraher, J.M., Fleitman, C.N., Tessonnier, J.P., 2015. Kinetic and mechanistic study of glucose isomerization using homogeneous organic Brønsted base catalysts in water. ACS Catal. 5, 3162-3173.

Chen, S.S., Maneerung, T., Tsang, D.C.W., Ok, Y.S., Wang, C.H. Valorization of biomass to hydroxymethylfurfural, levulinic acid, and fatty acid methyl ester by heterogeneous catalysts. Chem. Eng. J., 2017a, 328, 246-273.

Chen, S.S., Maneerung, T., Tsang, D.C.W., Ok, Y.S., Wang, C.H., 2017a. Valorization of biomass to hydroxymethylfurfural, levulinic acid, and fatty acid methyl ester by heterogeneous catalysts. Chem. Eng. J. 328, 246-273

Chen, S.S., Yu, I.K.M., Tsang, D.C.W., Yip, A.C.K., Khan, E., Wang, L., Ok, Y.S., Poon, C.S., 2017. Valorisation of cellulosic food waste into levulinic acid catalyzed by heterogeneous Brønsted acids: Temperature and solvent effects. Chem. Eng. J. 327, 328-335.

Chen, Y., Sun, F., Huang, Z., Chen, H., Zhuang, Z., Pan, Z., Long, J., Gu, F., 2017b. Photochemical fabrication of SnO2 dense layers on reduced graphene oxide sheets for application in photocatalytic degradation of p-Nitrophenol. Appl. Catal. B 215, 8-17.

Choudhary, V., Burnett, R.I., Vlachos, D.G., Sandler, S.I., 2012. Dehydration of glucose to 5-(hydroxymethyl)furfural and anhydroglucose: thermodynamic insights. J. Phys. Chem. C 116, 5116-5120.

Choudhary, V., Mushrif, S.H., Ho, C., Anderko, A., Nikolakis, V., Marinkovic, N.S., Frenkel, A.I., Sandler, S.I., Vlachos, D.G., 2013. Insights into the interplay of Lewis and Brønsted acid catalysts in glucose and fructose conversion to 5-(hydroxymethyl)furfural and levulinic acid in aqueous media. J. Am. Chem. Soc. 135, 3997-4006.

Ciesielski, W., Lii, C.Y., Yen, M.T., Tomasik, P., 2003. Interactions of starch with salts of metals from the transition groups. Carbohydr. Polym. 51, 47-56.

Clark, J.H., Farmer, T.J., Herrero-Davila, L., Sherwood, J., 2016. Circular economy design considerations for research and process development in the chemical sciences. Green Chem. 18, 3914-3934.

Dashtban, M., Gilbert, A., Fatehi, P., 2014. Recent advancements in the production of hydroxymethylfurfural. RSC Adv. 4, 2037-2050.

Davies, M., Evans, F.P., 1956. The isomerization of maleic acid in aqueous solutions. Trans. Faraday Soc., 52, 74-80.

de Souza, D., Sbardelotto, A.F., Ziegler, D.R., Marczak, L.D.F., Tessaro, I.C., 2016. Characterization of rice starch and protein obtained by a fast alkaline extraction method. Food Chem, 191, 36-44.

de Souza, R.L., Yu, H., Rataboul, F., Essayem, N., 2012. 5-Hydroxymethylfurfural (5-HMF) production from hexoses: limits of heterogeneous catalysis in hydrothermal conditions and potential of concentrated aqueous organic acids as reactive solvent system. Challenges 3, 212-232.

De, S., Dutta, S., Saha, B., 2016. Critical design of heterogeneous catalysts for biomass valorization: current thrust and emerging prospects. Catal. Sci. Technol. 6, 7364-7385.

Deguchi, S., Tsujii, K., Horikoshi, K., 2006. Cooking cellulose in hot and compressed water. Chem. Commun. 3293-3295.

Delbecq, F., Wang, Y., Len, C., 2017. Various carbohydrate precursors dehydration to 5-HMF in an acidic biphasic system under microwave heating using betaine as a co-catalyst. Mol. Catal. 434, 80-85.

Delidovich, I., Palkovits, R., 2016. Catalytic isomerisation of biomass-derived aldoses: a review. ChemSusChem 9, 547 –561.

Ding, D., Wang, J., Xi, J., Liu, X., Lu, G., Wang, Y., 2014. High-yield production of levulinic acid from cellulose and its upgrading to γ-valerolactone. Green Chem. 16, 3846-3853.

Drábek, O., Kiplagat, I.K., Komarek, M., Tejnecký, V., Borůvka, L., 2015. Study of interactions between relevant organic acids and aluminium in model solutions using HPLC and IC. Soil Water Res. 10, 172–180.

Duereh, A., Sato, Y., Smith, R.L., Inomata, H., Pichierri, F., 2017. Does synergism in microscopic polarity correlate with extrema in macroscopic properties for aqueous mixtures of dipolar aprotic solvents? J. Phys. Chem. B 2017, 121, 6033–6041

Dumesic, J.A., Huber, G.W., Weingarten, R., Wisconsin Alumni Research Foundation, 2016. Method for selectively preparing 5-hydroxymethylfurfual (HMF) from biomass in polar aprotic solvents. U.S. Patent 9, 242, 952.

Dutta, A., Gupta, D., Patra, A.K., Saha, B., Bhaumik, A., 2014. Synthesis of 5-hydroxymethylfurural from carbohydrates using large-pore mesoporous tin phosphate. ChemSusChem, 7, 925-933.

Dutta, S., De, S., Alam, M.I., Abu-Omar, M.M., Saha, B., 2012. Direct conversion of cellulose and lignocellulosic biomass into chemicals and biofuel with metal chloride catalysts. J. Catal. 288, 8-15.

Dyson, P.J., Jessop, P.G., 2016. Solvent effects in catalysis: rational improvements of catalysts via manipulation of solvent interactions. Catal. Sci. Technol. 6, 3302-3316.

Enslow, K.R., Bell, A.T., 2015. SnCl4-catalyzed isomerization/dehydration of xylose and glucose to furanics in water. Catal. Sci. Technol. 5, 2839-2847.

Fan, J., De Bruyn, M., Budarin, V.L., Gronnow, M.J., Shuttleworth, P.S., Breeden, S., Macquarrie, D.J., Clark, J.H., 2013. Direct microwave-assisted hydrothermal depolymerization of cellulose. J. Am. Chem. Soc. 135, 11728-11731.

FAO, 2013. Food Wastage Footprint: Impacts on Natural Resources—Summary Report. Food and Agriculture Organization of the United Nations.

Fu, X., Dai, J., Guo, X., Tang, J., Zhu, L., Hu, C., 2017. Suppression of oligomer formation in glucose dehydration by CO2 and tetrahydrofuran. Green Chem. 19, 3334-3343.

Gao, Z., Li, C., Fan, G., Yang, L., Li, F., 2018. Nitrogen-doped carbon-decorated copper catalyst for highly efficient transfer hydrogenolysis of 5-hydroxymethylfurfural to convertibly produce 2,5-dimethylfuran or 2,5-dimethyltetrahydrofuran. Appl. Catal. B 226, 523–533.

Garza-Ortiz, A., Camacho-Camacho, C., Sainz-Espuñes, T., Rojas-Oviedo, I., Gutiérrez-Lucas, L.R., Gutierrez Carrillo, A., Vera Ramirez, M.A., 2013. Novel organotin (IV) schiff base complexes with histidine derivatives: Synthesis, characterization, and biological activity. Bioinorg. Chem. Appl. 2013.

Ge, X., Xu, F., Li, Y., 2016. Solid-state anaerobic digestion of lignocellulosic biomass: recent progress and perspectives. Bioresour. Technol. 205, 239-249.

Glusker, J.P., 1999, The binding of ions to proteins, in: Allen, G. (Ed), Protein, Volume 2. Elsevier, Amsterdam.

Gollakota, A.R.K., Kishore, N., Gu, S., 2018. A review on hydrothermal liquefaction of biomass. Renew. Sustain. Energy. Rev. 81, 1378–1392.

Gou, C., Yang, Z., Huang, J., Wang, H., Xu, H., Wang, L., 2014. Effects of temperature and organic loading rate on the performance and microbial community of anaerobic co-digestion of waste activated sludge and food waste. Chemosphere 105, 146-151.

Guan, J., Cao, Q., Guo, X., Mu, X., 2011. The mechanism of glucose conversion to 5-hydroxymethylfurfural catalyzed by metal chlorides in ionic liquid: a theoretical study. Comput. Theor. Chem. 963, 453-462.

Gustavsson, J., Cederberg, C., Sonesson, U., van Otterdijk, R., Meybeck, A., 2011. Global Food Losses and Food Waste. Food and Agriculture Organization of the United Nations, Rome.

Hammond, B., Kough, J., Herouet-Guicheney, C., Jez, J.M., 2013. Toxicological evaluation of proteins introduced into food crops. Crit. Rev. Toxicol. 43, 25-42.

Hansen, T.S., Woodley, J.M., Riisager, A., 2009. Efficient microwave-assisted synthesis of 5-hydroxymethylfurfural from concentrated aqueous fructose. Carbohydr. Res. 344, 2568-2572.

He, J., Liu, M., Huang, K., Walker, T.W., Maravelias, C.T., Dumesic, J.A., Huber, G.W., 2017. Production of levoglucosenone and 5-hydroxymethylfurfural from cellulose in polar aprotic solvent–water mixtures. Green Chem. 19, 3642-3653.

HK EPD, Dec 2016. Monitoring of Solid Waste in Hong Kong - Waste Statistics for 2015. Hong Kong Environmental Protection Department, Hong Kong.

HK EPD, Oct 2015. Monitoring of Solid Waste in Hong Kong - Waste Statistics for 2014. Hong Kong Environmental Protection Department, Hong Kong.

HK FEHD, Jun 2008. Method Guidance Notes on Nutrition Labelling and Nutrition Claims. Centre for Food Safety, Food and Environmental Hygiene Department, Hong Kong.

Hu, L., Zhao, G., Tang, X., Wu, Z., Xu, J., Lin, L., Liu, S., 2013. Catalytic conversion of carbohydrates into 5-hydroxymethylfurfural over cellulose-derived carbonaceous catalyst in ionic liquid. Bioresour. Technol. 148, 501-507.

Hu, X., Kadarwati, S., Wang, S., Song, Y., Hasan, M.D.M., Li, C.Z., 2015. Biomass-derived sugars and furans: Which polymerize more during their hydrolysis? Fuel Process. Technol. 137, 212-219.

Iryani, D.A., Kumagai, S., Nonaka, M., Sasaki, K., Hirajima, T., 2013. Production of 5-hydroxymethyl furfural from sugarcane bagasse under hot compressed water. Procedia Earth Planet. Sci. 6, 441-447.

Jessop, P.G., Jessop, D.A., Fu, D., Phan, L., 2012. Solvatochromic parameters for solvents of interest in green chemistry. Green Chem. 14, 1245-1259.

Jia, S., Xu, Z., Zhang, Z.C., 2014. Catalytic conversion of glucose in dimethylsulfoxide/water binary mix with chromium trichloride: Role of water on the product distribution. Chem. Eng. J. 254, 333-339.

Jin, F., Zhou, Z., Moriya, T., Kishida, H., Higashijima, H., Enomoto, H., 2005. Controlling hydrothermal reaction pathways to improve acetic acid production from carbohydrate biomass. Environ. Sci. Technol. 39, 1893-1902.

Jindal, M.K., Jha, M.K., 2016. Effect of process parameters on hydrothermal liquefaction of waste furniture sawdust for bio-oil production. RSC Adv. 6, 41772-41780.

Jing, S., Cao, X., Zhong, L., Peng, X., Zhang, X., Wang, S., Sun, R., 2016. In situ carbonic acid from CO2: A green acid for highly effective conversion of cellulose in the presence of Lewis acid. ACS Sustainable Chem. Eng. 4, 4146-4155.

Kabyemela, B.M., Adschiri, T., Malaluan, R. M., Arai, K., 1997. Kinetics of glucose epimerization and decomposition in subcritical and supercritical water. Ind. Eng. Chem. Res. 36, 1552–1558.

Karimi, B., Mirzaei, H.M., 2013. The influence of hydrophobic/hydrophilic balance of the mesoporous solid acid catalysts in the selective dehydration of fructose into HMF. RSC Adv. 3, 20655-20661.

Karunanithi, R., Szogi, A.A., Bolan, N., Naidu, R., Loganathan, P., Hunt, P.G., Vanotti, M.B., Saint, C.P., Ok, Y.S., Krishnamoorthy, S., 2015. Chapter three – Phosphorus recovery and reuse from waste streams. Adv. Agron. 131, 173-250.

Kazi, F.K., Patel, A.D., Serrano-Ruiz, J.C., Dumesic, J.A. and Anex, R.P., 2011. Techno-economic analysis of dimethylfuran (DMF) and hydroxymethylfurfural (HMF) production from pure fructose in catalytic processes. Chem. Eng. J. 169, 329-338.

Kimura, H., Yoshida, K., Uosaki, Y., Nakahara, M., 2013. Effect of water content on conversion of D-cellobiose into 5-hydroxymethyl-2-furaldehyde in a dimethyl sulfoxide-water mixture. J. Phys. Chem. A 117, 10987–10996.

Kläusli, T., 2014. AVA Biochem: Commercialising renewable platform chemical 5-HMF. Green Process Synth. 3, 235-236.

Koutinas, A.A., Du, C., Lin, C.S.K., Webb, C., 2014a. Developments in cereal-based biorefineries, in: Waldron, K.W. (Ed), Advances in Biorefineries: Biomass and Waste Supply Chain Exploitation. Woodhead Publishing, Cambridge, Waltham, Kidlington, pp. 303-334.

Koutinas, A.A., Vlysidis, A., Pleissner, D., Kopsahelis, N., Garcia, I.L., Kookos, I.K., Papanikolaou, S., Kwan, T.H., Lin, C.S.K., 2014b. Valorisation of industrial waste and by-product streams via fermentation for the production of chemicals and biopolymers. Chem. Soc. Rev. 43, 2587-2627.

Kreissl, H.T., Nakagawa, K., Peng, Y.K., Koito, Y., Zheng, J., Tsang, S.C.E., 2016. Niobium oxides: Correlation of acidity with structure and catalytic performance in sucrose conversion to 5-hydroxymethylfurfural. J. Catal. 338, 329-339.

Lam, C.M., Yu, I.K.M., Hsu, S.C., Tsang, D.C.W., 2018. Life-cycle assessment on food waste valorisation to value-added products. J. Clean. Prod. 199, 840-848.

Lei, X.R., Gong, C., Zhang, Y.L., Xu, X., 2016. Influence of the acetamide from acetonitrile hydrolysis in acid-contained mobile phase on the ultraviolet detection in high performance liquid chromatography. Chromatographia 79, 1257-1262.

Levis, J.W., Barlaz, M.A., 2011. What is the most environmentally beneficial way to treat commercial food waste? Environ. Sci. Technol. 45, 7438-7444.

Lew, C.M., Rajabbeigi, N., Tsapatsis, M., 2012. Tin-containing zeolite for the isomerization of cellulosic sugars. Microporous Mesoporous Mater. 153, 55-58.

Li, G., Pidko, E.A., Hensen, E.J., 2014. Synergy between Lewis acid sites and hydroxyl groups for the isomerisation of glucose to fructose over Sn-containing zeolites: a theoretical perspective. Catal. Sci. Technol. 4, 2241-2250.

Li, G., Pidko, E.A., Hensen, E.J., 2016a. A periodic DFT study of glucose to fructose isomerization on tungstite (WO3· H2O): influence of group IV–VI dopants and cooperativity with hydroxyl groups. ACS Catal. 6, 4162-4169.

Li, K., Xue, D., 2006. Estimation of electronegativity values of elements in different valence states. J. Phys. Chem. A 110, 11332-11337.

Li, M., Li, W., Lu, Y., Jameel, H., Chang, H.M., Ma, L., 2017a. High conversion of glucose to 5-hydroxymethylfurfural using hydrochloric acid as a catalyst and sodium chloride as a promoter in a water/γ-valerolactone system. RSC Adv. 7, 14330-14336.

Li, W., Wang, J., Hu, X., Shen, K., Wang, W., Chu, Y., Lin, L., Liu, X., Feng, X., 2010. Catalytic Asymmetric Roskamp reaction of α-alkyl-α-diazoesters with aromatic aldehydes: Highly enantioselective synthesis of α-alkyl-β-keto asters. J. Am. Chem. Soc. 132, 8532-8533.

Li, X., Peng, K., Liu, X., Xia, Q., Wang, Y., 2017b. Comprehensive understanding the role of Brønsted and Lewis acid sites in glucose conversion to 5-hydromethylfurfural. ChemCatChem. 9, 2739–2746.

Li, Z., Lu, H., Ren, L., He, L., 2013. Experimental and modeling approaches for food waste composting: A review. Chemosphere 93, 1247-1257.

Lin, C.S.K., Pfaltzgraff, L.A., Herrero-Davila, L., Mubofu, E.B., Abderrahim, S., Clark, J.H., Koutinas, A.A., Kopsahelis, N., Stamatelatou, K., Dickson, F., Thankappan, S., Mohamed Z., Brocklesby, R., Luque, R., 2013. Food waste as a valuable resource for the production of chemicals, materials and fuels. Current situation and global perspective. Energy Environ. Sci. 6, 426-464.

Lin, H., Xiong, Q., Zhao, Y., Chen, J., Wang, S., 2017. Conversion of carbohydrates into 5-hydroxymethylfurfural in a green reaction system of CO2-water-isopropanol. AIChE J. 63, 257-265.

Liu, B., Zhang, Z., Zhao, Z. K., 2013. Microwave-assisted catalytic conversion of cellulose into 5-hydroxymethylfurfural in ionic liquids. Chem. Eng. J. 215, 517-521.

Liu, F., Barrault, J., De Oliveira Vigier, K., Jérôme, F., 2012. Dehydration of highly concentrated solutions of fructose to 5-hydroxymethylfurfural in a cheap and sustainable choline chloride/carbon dioxide system. ChemSusChem, 5, 1223-1226.

Liu, Q.Y., Yang, F., Liu, Z.H. and Li, G., 2015. Preparation of SnO2–Co3O4/C biochar catalyst as a Lewis acid for corncob hydrolysis into furfural in water medium. Journal of Industrial and Engineering Chemistry, 26, 46-54.

Liu, W.J., Jiang, H., Yu, H.Q., 2015. Development of biochar-based functional materials: Toward a sustainable platform carbon material. Chem. Rev. 115, 12251-12285.

Lopes, M., Dussan, K., Leahy, J.J., 2017. Enhancing the conversion of D-xylose into furfural at low temperatures using chloride salts as co-catalysts: Catalytic combination of AlCl3 and formic acid. Chem. Eng. J. 323, 278-286.

Lucas-Torres, C., Lorente, A., Cabañas, B., Moreno, A., 2016. Microwave heating for the catalytic conversion of melon rind waste into biofuel precursors. J. Clean. Prod. 138, 59-69.

Luterbacher, J.S., Rand, J.M., Alonso, D.M., Han, J., Youngquist, J.T., Maravelias, C.T., Pfleger, B.F., Dumesic, J.A., 2014. Nonenzymatic sugar production from biomass using biomass-derived γ-valerolactone. Science 343, 277-280.

LyondellBasell, 2017, Technical Data - Propylene Carbonate, Available in: www.lyondellbasell.com/ (Accessed Dec 2017)

Ma, H., Wang, F., Yu, Y., Wang, L., Li, X., 2015. Autocatalytic production of 5-hydroxymethylfurfural from fructose-based carbohydrates in a biphasic system and its purification. Ind. Eng. Chem. Res. 54, 2657-2666.

Manila Times, JUNE 17, 2017, http://www.manilatimes.net/unlimited-rice/333208/

Marcus, Y., 1987. The thermodynamics of solvation of ions. Part 2.—The enthalpy of hydration at 298.15 K. J. Chem. Soc., Faraday Trans. 1 83, 339-349.

Market Research Hub, 2018, https://www.marketresearchhub.com/report/global-5-hydroxymethylfurfural-5-hmf-cas-67-47-0-sales-market-report-2018-report.html

Martell, A.E., Hancock, R.D., 1996. Metal Complexes in Aqueous Solutions. Plenum Press, New York.

Martell, A.E., Smith, R.M., 1977. Critical Stability Constants, Vol. 3, Other Organic Ligands. Plenum Press, New York.

Matsumiya, H., Hara, T., 2015. Conversion of glucose into 5-hydroxymethylfurfural with boric acid in molten mixtures of choline salts and carboxylic acids. Biomass Bioenergy, 72, 227-232.

Mellmer, M.A., Alonso, D.M., Luterbacher, J.S., Gallo, J.M.R., Dumesic, J.A., 2014a. Effects of γ-valerolactone in hydrolysis of lignocellulosic biomass to monosaccharides. Green Chem. 16, 4659-4662.

Mellmer, M.A., Sener, C., Gallo, J.M.R., Luterbacher, J.S., Alonso, D.M. and Dumesic, J.A., 2014b. Solvent effects in acid-catalyzed biomass conversion reactions. Angew. Chem. Int. Ed. 53, 11872-11875.

Minich, D.M., Bland, J.S., 2007. Acid-alkaline balance: role in chronic disease and detoxification. Altern. Ther. Health Med. 13, 62-65.

Mirzaei, H.M., Karimi, B., 2016. Sulphanilic acid as a recyclable bifunctional organocatalyst in the selective conversion of lignocellulosic biomass to 5-HMF. Green Chem. 18, 2282-2286.

Mohan, S.V., Nikhil, G.N., Chiranjeevi, P., Reddy, C.N., Rohit, M.V., Kumar, A.N., Sarkar, O., 2016. Waste biorefinery models towards sustainable circular bioeconomy: critical review and future perspectives. Bioresour. Technol. 215, 2-12.

Moliner, M., Román-Leshkov, Y., Davis, M.E., 2010. Tin-containing zeolites are highly active catalysts for the isomerization of glucose in water. PNAS 107, 6164-6168.

Moliner, M., Román-Leshkov, Y., Davis, M.E., 2010. Tin-containing zeolites are highly active catalysts for the isomerization of glucose in water. Proc. Natl. Acad. Sci. USA 107, 164-6168.

Möller, M., Harnisch, F., Schröder, U., 2012. Microwave-assisted hydrothermal degradation of fructose and glucose in subcritical water. Biomass Bioenergy 39, 389-398.

Möller, M., Harnisch, F., Schröder, U., 2013. Hydrothermal liquefaction of cellulose in subcritical water—the role of crystallinity on the cellulose reactivity. RSC Adv. 3, 11035-11044.

Morales, G., Melero, J.A., Paniagua, M., Iglesias, J., Hernández, B., Sanz, M., 2014. Sulfonic acid heterogeneous catalysts for dehydration of C6-monosaccharides to 5-hydroxymethylfurfural in dimethyl sulfoxide. Chin. J. Catal. 35, 644-655.

Moreno-Recio, M., Santamaría-González, J., Maireles-Torres, P., 2016. Brönsted and Lewis acid ZSM-5 zeolites for the catalytic dehydration of glucose into 5-hydroxymethylfurfural. Chem. Eng. J. 303, 22-30.

Mukherjee, A., Dumont, M.J., Raghavan, V., 2015. Review: Sustainable production of hydroxymethylfurfural and levulinic acid: Challenges and opportunities. Biomass Bioenergy 72, 143-183.

Mushrif, S.H., Caratzoulas, S., Vlachos, D.G., 2012. Understanding solvent effects in the selective conversion of fructose to 5-hydroxymethyl-furfural: a molecular dynamics investigation. Phys. Chem. Chem. Phys. 14, 2637-2644.

Mushrif, S.H., Varghese, J.J., Vlachos, D.G., 2014. Insights into the Cr(III) catalyzed isomerization mechanism of glucose to fructose in the presence of water using ab initio molecular dynamics. Phys. Chem. Chem. Phys. 16, 19564-19572.

Nguyen, H., Nikolakis, V., Vlachos, D.G., 2016. Mechanistic insights into Lewis acid metal salt-catalyzed glucose chemistry in aqueous solution. ACS Catal. 6, 1497-1504.

Nikbin, N., Caratzoulas, S., Vlachos, D.G., 2012. A first principles-based microkinetic model for the conversion of fructose to 5-hydroxymethylfurfural. ChemCatChem 4, 504-511.

OECD-FAO, 2014. OECD-FAO Agricultural Outlook 2014-2023. The Organisation for Economic Co-operation and Development, Food and Agriculture Organization of the United Nations.

Ohara, M., Takagaki, A., Nishimura, S., Ebitani, K., 2010. Syntheses of 5-hydroxymethylfurfural and levoglucosan by selective dehydration of glucose using solid acid and base catalysts. Appl. Catal., A 383, 149-155.

Omari, K.W., Besaw, J.E., Kerton, F.M., 2012. Hydrolysis of chitosan to yield levulinic acid and 5-hydroxymethylfurfural in water under microwave irradiation. Green Chem. 14, 1480-1487.

Ordomsky, V.V., Sushkevich, V.L., Schouten, J.C., Van der Schaaf, J., Nijhuis, T.A., 2013. Glucose dehydration to 5-hydroxymethylfurfural over phosphate catalysts. J. Catal. 300, 37-46.

Pagán-Torres, Y.J., Wang, T., Gallo, J.M.R., Shanks, B.H., Dumesic, J.A., 2012. Production of 5-hydroxymethylfurfural from glucose using a combination of Lewis and Brønsted acid catalysts in water in a biphasic reactor with an alkylphenol solvent. ACS Catal. 2, 930-934.

Parker, H.L., Sherwood, J., Hunt, A.J., Clark, J.H., 2014. Cyclic carbonates as green alternative solvents for the Heck reaction. ACS Sustainable Chem. Eng. 2, 1739-1742.

Parshetti, G.K., Suryadharma, M.S., Pham, T.P.T., Mahmood, R., Balasubramanian, R., 2015. Heterogeneous catalyst-assisted thermochemical conversion of food waste biomass into 5-hydroxymethylfurfural. Bioresour. Technol. 178, 19-27.

Parthasarathi, R., Bellesia, G., Chundawat, S.P.S., Dale, B.E., Langan, P., Gnanakaran, S. 2011. Insights into hydrogen bonding and stacking interactions in cellulose. J. Phys. Chem. A 115, 14191-14202.

Patil, S.K.R., Heltzel, J., Lund, C.R.F., 2012. Comparison of structural features of humins formed catalytically from glucose, fructose, and 5-hydroxymethylfurfuraldehyde. Energy Fuels 26, 5281-5293.

Pearson, R.G., 1968. Hard and soft acids and bases (HSAB), Part I. Fundamental principles. J. Chem. Educ. 45, 581-587.

Peleteiro, S., Garrote, G., Santos, V., Parajó, J.C., 2014. Furan manufacture from softwood hemicelluloses by aqueous fractionation and further reaction in a catalyzed ionic liquid: a biorefinery approach. J. Clean. Prod. 76, 200-203.

Pham, T.P.T., Kaushik, R., Parshetti, G.K., Mahmood, R., Balasubramanian, R., 2015. Food waste-to-energy conversion technologies: Current status and future directions. Waste Manage. 38, 399-408.

Piccinno, F., Hischier, R., Seeger, S., Som, C., 2015. Life cycle assessment of a new technology to extract, functionalize and orient cellulose nanofibers from food waste. ACS Sustainable Chem. Eng. 3, 1047-1055.

Pidko, E.A., Degirmenci, V., van Santen, R.A., Hensen, E.J.M., 2010. Coordination properties of ionic liquid-mediated chromium (II) and copper (II) chlorides and their complexes with glucose. Inorg. Chem. 49, 10081-10091.

Pleissner, D., Kwan, T.H., Lin, C.S.K., 2014. Fungal hydrolysis in submerged fermentation for food waste treatment and fermentation feedstock preparation. Bioresour. Technol. 158, 48-54.

Pleissner, D., Lam, W.C., Sun, Z., Lin, C.S.K., 2013. Food waste as nutrient source in heterotrophic microalgae cultivation. Bioresour. Technol. 137, 139-146.

Pleissner, D., Qi, Q., Gao, C., Rivero, C.P., Webb, C., Lin, C.S.K., Venus, J., 2016. Valorisation of organic residues for the production of added value chemicals: a contribution to the bio-based economy. Biochem. Eng. J. 116. 3-16.

Poerschmann, J., Weiner, B., Koehler, R., Kopinke, F.D., 2015. Organic breakdown products resulting from hydrothermal carbonization of brewer’s spent grain. Chemosphere 131, 71-77.

Prat, D., Wells, A., Hayler, J., Sneddon, H., McElroy, C.R., Abou-Shehada, S., Dunn, P.J., 2016. CHEM21 selection guide of classical- and less classical-solvents. Green Chem. 18, 288-296.

Qian, K., Kumar, A., Zhang, H., Bellmer, D., Huhnke, R., 2015. Recent advances in utilization of biochar. Renew. Sust. Energ. Rev. 42, 1055-1064.

Qian, X., 2012. Mechanisms and energetics for Brønsted acid-catalyzed glucose condensation, dehydration and isomerization reactions. Top. Catal. 55, 218-226.

Qing, Q., Guo, Q., Zhou, L., Wan, Y., Xu, Y., Ji, H., Gao, X., Zhang, Y., 2017. Catalytic conversion of corncob and corncob pretreatment hydrolysate to furfural in a biphasic system with addition of sodium chloride. Bioresour. Technol. 226, 247-254.

Qu, Y., Wei, Q., Li, H., Oleskowicz-Popiel, P., Huang, C., Xu, J. 2014. Microwave-assisted conversion of microcrystalline cellulose to 5-hydroxymethylfurfural catalyzed by ionic liquids. Bioresour. Technol. 162, 358-364.

Rajabbeigi, N., Ranjan, R., Tsapatsis, M., 2012. Selective adsorption of HMF on porous carbons from fructose/DMSO mixtures. Microporous Mesoporous Mater. 158, 253-256.

Rajapaksha, A.U., Chen, S.S., Tsang, D.C.W., Zhang, M., Vithanage, M., Mandal, S., Gao, B., Bolan, N.S., Ok, Y.S., 2016. Engineered/designer biochar for contaminant removal/immobilization from soil and water: Potential and implication of biochar modification. Chemosphere 148, 276-291.

Ramli, N.A.S., Amin, N.A.S., 2018. Thermo-kinetic assessment of glucose decomposition to 5-hydroxymethyl furfural and levulinic acid over acidic functionalized ionic liquid. Chem. Eng. J. 335, 221-230.

Rasrendra, C.B., Soetedjo, J.N.M., Makertihartha, I.G.B.N., Adisasmito, S., Heeres, H.J., 2012. The catalytic conversion of d-glucose to 5-hydroxymethylfurfural in DMSO using metal salts. Top. Catal. 55, 543-549.

Ren, L., Zhu, L., Qi, T., Tang, J., Yang, H., Hu, C., 2017. Performance of dimethyl sulfoxide and Brønsted acid catalysts in fructose conversion to 5-hydroxymethylfurfural. ACS Catal. 7, 2199-2212.

Román-Leshkov, Y., Chheda, J.N., Dumesic, J.A., 2006. Phase modifiers promote efficient production of hydroxymethylfurfural from fructose. Science 312, 1933-1937.

Román-Leshkov, Y., Davis, M.E., 2011. Activation of carbonyl-containing molecules with solid Lewis acids in aqueous media. ACS Catal. 1, 1566-1580.

Román-Leshkov, Y., Dumesic, J.A., 2009. Solvent effects on fructose dehydration to 5-hydroxymethylfurfural in biphasic systems saturated with inorganic salts. Top. Catal. 52, 297-303.

Román-Leshkov, Y., Moliner, M., Labinger, J.A., Davis, M.E., 2010. Mechanism of glucose isomerization using a solid Lewis acid catalyst in water. Angew. Chem., Int. Ed. 49, 8954-8957.

Rosatella, A.A., Simeonov, S.P., Frade, R.F.M., Afonso, C.A.M., 2011. 5-Hydroxymethylfurfural (HMF) as a building block platform: Biological properties, synthesis and synthetic applications. Green Chem. 13, 754-793.

Rout, P.K., Nannaware, A.D., Prakash, O., Kalra, A., Rajasekharan, R., 2016. Synthesis of hydroxymethylfurfural from cellulose using green processes: a promising biochemical and biofuel feedstock. Chem. Eng. Sci.142, 318-346.

S. Gajula, K. Inthumathi, S.R. Arumugam, K. Srinivasan, ACS Sustainable Chem. Eng. 2017, 5, 5373-5381.

Saha, B., Abu-Omar, M.M., 2014. Advances in 5-hydroxymethylfurfural production from biomass in biphasic solvents. Green Chem. 16, 24-38.

Saha, B., De, S., Fan, M., 2013. Zr(O)Cl2 catalyst for selective conversion of biorenewable carbohydrates and biopolymers to biofuel precursor 5-hydroxymethylfurfural in aqueous medium. Fuel 111, 598-605.

Saielli, G., Bagno, A., 2010. Preferential solvation of glucose and talose in water–acetonitrile mixtures: a molecular dynamics simulation study. Phys. Chem. Chem. Phys. 12, 2981-2988.

Salam, M.A., Abdullah, B., Ramli, A., Mujtaba, I.M., 2016. Structural feature based computational approach of toxicity prediction of ionic liquids: Cationic and anionic effects on ionic liquids toxicity. J. Mol. Liq. 224, 393-400.

Salemdeeb, R., zu Ermgassen, E.K., Kim, M.H., Balmford, A., Al-Tabbaa, A., 2017. Environmental and health impacts of using food waste as animal feed: a comparative analysis of food waste management options. J. Clean. Prod. 140, 871-880.

Sarwono, A., Man, Z., Muhammad, N., Khan, A.S., Hamzah, W.S.W., Rahim, A.H.A., Ullah, Z., Wilfred, C.D., 2017. A new approach of probe sonication assisted ionic liquid conversion of glucose, cellulose and biomass into 5-hydroxymethylfurfural. Ultrason. Sonochem. doi: 10.1016/j.ultsonch.2017.01.028.

Scaglia, B., Baglieri, A., Tambone, F., Gennari, M., Adani, F., 2016. Chlorpyrifos-methyl solubilisation by humic acids used as bio-surfactants extracted from lignocelluloses and kitchen wastes. Chemosphere 159, 208-213.

Seemala, B., Haritos, V., Tanksale, A., 2016. Levulinic acid as a catalyst for the production of 5-Hydroxymethylfurfural and furfural from lignocellulose biomass. ChemCatChem 8, 640–647.

Shannon, R.D., 1976. Revised effective ionic radii and systematic studies of interatomic distances in halides and chalcogenides. Acta Crystallogr. A 32, 751-767.

Shi, N., Liu, Q., Zhang, Q., Wang, T., Ma, L., 2013. High yield production of 5-hydroxymethylfurfural from cellulose by high concentration of sulfates in biphasic system. Green Chem. 15, 1967-1974.

Siankevich, S., Fei, Z., Scopelliti, R., Jessop, P.G., Zhang, J., Yan, N., Dyson, P.J., 2016. Direct conversion of mono-and polysaccharides into 5-hydroxymethylfurfural using ionic-liquid mixtures. ChemSusChem 9, 2089-2096.

Sigma Aldrich, 2017. Available in: http://www.sigmaaldrich.com. (Accessed June 2017)

Skoog, D., 2000. Analytical Chemistry: An Introduction (7th ed.). Fort Worth: Harcourt College Pub.

SMC, Propylene Carbonate. http://www.propylenecarbonate.net/, 2011 (accessed Mar 2018)

Souza, R.O.L., Fabiano, D.P., Feche, C., Rataboul, F., Cardoso, D., Essayem, N., 2012. Glucose–fructose isomerisation promoted by basic hybrid catalysts. Catal. Today 195, 114-119.

Sposito, G., 1994. Chemical Equilibria and Kinetics in Soils. Oxford University Press, New York.

Su, Y., Brown, H.M., Li, G., Zhou, X.D., Amonette, J.E., Fulton, J.L., Camaioni, D.M., Zhang, Z.C., 2011. Accelerated cellulose depolymerization catalyzed by paired metal chlorides in ionic liquid solvent. Appl. Catal., A 391, 436-442.

Swift, T.D., Nguyen, H., Anderko, A., Nikolakis, V., Vlachos, D.G., 2015. Tandem Lewis/Brønsted homogeneous acid catalysis: Conversion of glucose to 5-hydoxymethylfurfural in an aqueous chromium (III) chloride and hydrochloric acid solution. Green Chem. 17, 4725-4735.

Swift, T.D., Nguyen, H., Erdman, Z., Kruger, J.S., Nikolakis, V., Vlachos, D.G., 2016. Tandem Lewis acid/Brønsted acid-catalyzed conversion of carbohydrates to 5-hydroxymethylfurfural using zeolite beta. J. Catal. 333, 149-161.

Szymońska, J., Molenda, M., Wieczorek, J., 2015. Study of quantitative interactions of potato and corn starch granules with ions in diluted solutions of heavy metal salts. Carbohydr. Polym. 134, 102-109.

Tang, J., Guo, X., Zhu, L., Hu, C., 2015. Mechanistic study of glucose-to-fructose isomerization in water catalyzed by [Al(OH)2(aq)]+. ACS Catal. 5, 5097-5103.

Tang, J., Zhu, L., Fu, X., Dai, J., Guo, X., Hu, C., 2016. Insights into the kinetics and reaction network of aluminum chloride-catalyzed conversion of glucose in NaCl–H2O/THF biphasic system. ACS Catal. 7, 256-266.

Tao, F., Song, H., Chou, L., 2011. Catalytic conversion of cellulose to chemicals in ionic liquid. Carbohydr. Res. 346, 58-63.

Tao, H., Nakahara, T., 2002, Hydride generation techniques in atomic spectroscopy, in: Sneddon, J. (Ed), Advances in Atomic Spectroscopy, Volume 7. Elsevier, Amsterdam.

Taylor, A.L., 2012. Why is bread Britain's most wasted food? BBC. Assessed Jan 2018.

Teong, S. P., Yi, G., Zhang, Y., 2014. Hydroxymethylfurfural production from bioresources: past, present and future. Green Chem. 16, 2015-2026.

Thyberg, K.L., Tonjes, D.J., Gurevitch, J., 2015. Quantification of food waste disposal in the United States: A meta-analysis. Environ. Sci. Technol. 49, 13946-13953.

Tian, S.Q., Wang, Z.L., Wang, X.W., Zhao, R.Y., 2016. Development and digestion of resistant malate starch produced by L-malic acid treatment. RSC Adv. 6, 96182-96189.

Tsilomelekis, G., Josephson, T.R., Nikolakis, V., Caratzoulas, S., 2014. Origin of 5-hydroxymethylfurfural stability in water/dimethyl sulfoxide mixtures. ChemSusChem 7, 117-126.

Tsilomelekis, G., Orella, M.J., Lin, Z., Cheng, Z., Zheng, W., Nikolakis, V., Vlachos, D.G., 2016. Molecular structure, morphology and growth mechanisms and rates of 5-hydroxymethyl furfural (HMF) derived humins. Green Chem. 18, 1983-1993.

Tuck, C.O., Pérez, E., Horváth, I.T., Sheldon, R.A., Poliakoff, M., 2012. Valorisation of biomass: deriving more value from waste. Science 337, 695-699.

USDA, MAY 2016, USDA National Nutrient Database for Standard Reference, https://ndb.nal.usda.gov/ndb/

Vaden, T.D., Lisy, J.M., 2005. Investigation of competing interactions in alkali metal ion–acetone–water clusters. Chem. Phys. Lett. 408, 54-58.

van Zandvoort, I., Wang, Y., Rasrendra, C.B., van Eck, E.R.H., Bruijnincx, P.C.A., Heeres, H.J., Weckhuysen, B.M., 2013. Formation, molecular structure, and morphology of humins in biomass conversion: Influence of feedstock and processing conditions. ChemSusChem 6, 1745-1758.

Vasudevan, V. and Mushrif, S.H., 2015. Insights into the solvation of glucose in water, dimethyl sulfoxide (DMSO), tetrahydrofuran (THF) and N, N-dimethylformamide (DMF) and its possible implications on the conversion of glucose to platform chemicals. RSC Adv. 5, 20756-20763.

Voronova, M.I., Lebedeva, T.N., Radugin, M.V., Surov, O.V., Prusov, A.N., Zakharov, A.G., 2006. Interactions of water–DMSO mixtures with cellulose. J. Mol. Liq. 126, 124-129.

Wang, J., Liu, X., Hu, B., Lu, G., Wang, Y., 2014. Efficient catalytic conversion of lignocellulosic biomass into renewable liquid biofuels via furan derivatives. RSC Adv. 4, 31101–31107.

Wang, J., Xu, W., Ren, J., Liu, X., Lu, G., Wang, Y., 2011. Efficient catalytic conversion of fructose into hydroxymethylfurfural by a novel carbon-based solid acid. Green Chem 13, 2678-2681.

Wang, S., Zhao, Y., Lin, H., Chen, J., Zhu, L., Luo, Z., 2017. Conversion of C5 carbohydrates into furfural catalyzed by a Lewis acidic ionic liquid in renewable γ-valerolactone. Green Chem. 19, 3869-3879.

Wang, T., Glasper, J.A., Shanks, B.H., 2015. Kinetics of glucose dehydration catalyzed by homogeneous Lewis acidic metal salts in water. Appl. Catal., A 498, 214-221.

Wei, Q., Zhang, W., Guo, J., Wu, S., Tan, T., Wang, F., Dong, R., 2014. Performance and kinetic evaluation of a semi-continuously fed anaerobic digester treating food waste: effect of trace elements on the digester recovery and stability. Chemosphere 117, 477-485.

Wölkart, G., Schrammel, A., Koyani, C.N., Scherübel, S., Zorn-Pauly, K., Malle, E., Pelzmann, B., Andrä, M., Ortner, A., Mayer, B., 2017. Cardioprotective effects of 5-hydroxymethylfurfural mediated by inhibition of L-type Ca2+ current. Br. J. Pharmacol. 174, 3640–3653

WRAP, November 2013a, Household Food and Drink Waste in the United Kingdom 2012, http://www.wrap.org.uk/sites/files/wrap/hhfdw-2012-main.pdf.pdf

WRAP, November 2013b, Overview of Waste in the UK Hospitality and Food Sector, http://www.wrap.org.uk/sites/files/wrap/Overview%20of%20Waste%20in%20the%20UK%20Hospitality%20and%20Food%20Service%20Sector%20FINAL.pdf

Wrigstedt, P., Keskiväli, J., Leskelä, M., Repo, T., 2015. The role of salts and Brønsted acids in Lewis acid-catalyzed aqueous-phase glucose dehydration to 5-hydroxymethylfurfural. ChemCatChem 7, 501-507.

Wrigstedt, P., Keskiväli, J., Repo, T., 2016. Microwave-enhanced aqueous biphasic dehydration of carbohydrates to 5-hydroxymethylfurfural. RSC Adv. 6, 18973-18979.

Wulfsberg, G., 1987. Principles of Descriptive Chemistry. Brooks Cole.

Xiao, S., Liu, B., Wang, Y., Fang, Z., Zhang, Z., 2014. Efficient conversion of cellulose into biofuel precursor 5-hydroxymethylfurfural in dimethyl sulfoxide–ionic liquid mixtures. Bioresour. Technol. 151, 361-366.

Xiong, X., Yu, I.K.M., Cao, L., Tsang, D.C.W., Zhang, S., Ok, Y.S., 2017. A review of biochar-based catalysts for chemical synthesis, biofuel production, and pollution control. Bioresour. Technol. 246, 254-270.

Xu, Z., Li, W., Du, Z., Wu, H., Jameel, H., Chang, H.M., Ma, L., 2015. Conversion of corn stalk into furfural using a novel heterogeneous strong acid catalyst in γ-valerolactone. Bioresour. Technol. 198, 764-771.

Yan, K., Yang, Y., Chai, J., Lu, Y., 2015. Catalytic reactions of gamma-valerolactone: a platform to fuels and value-added chemicals. Appl. Catal. B 179, 292-304.

Yang, L., Tsilomelekis, G., Caratzoulas, S., Vlachos, D.G., 2015. Mechanism of Brønsted acid-catalyzed glucose dehydration. ChemSusChem 8, 1334-1341.

Yang, Y., Hu, C., Abu-Omar, M.M., 2012a. Conversion of glucose into furans in the presence of AlCl3 in an ethanol–water solvent system. Bioresour. Technol. 116, 190-194.

Yang, Y., Hu, C., Abu-Omar, M.M., 2012b. Conversion of carbohydrates and lignocellulosic biomass into 5-hydroxymethylfurfural using AlCl3· 6H2O catalyst in a biphasic solvent system. Green Chem. 14, 509-513.

Yang, Y., Hu, C.W., Abu-Omar, M.M., 2012c. Synthesis of furfural from xylose, xylan, and biomass using AlCl3· 6 H2O in biphasic media via xylose isomerization to xylulose. ChemSusChem 5, 405-410.

Yang, Y., Liu, W., Wang, N., Wang, H., Song, Z., Li, W., 2015b. Effect of organic solvent and Brønsted acid on 5-hydroxymethylfurfural preparation from glucose over CrCl3. RSC Adv. 5, 27805-27813.

Yemiş, O., Mazza, G., 2012. Optimization of furfural and 5-hydroxymethylfurfural production from wheat straw by a microwave-assisted process. Bioresour. Technol. 109, 215-223.

Yi, Y.B., Ha, M.G., Lee, J.W., Chung, C.H., 2013. Effect of different halide types on HMF synthesis from kudzu extract in ionic liquid. J. Clean. Prod. 41, 244-250.

Yi, Y.B., Lee, J.W., Chung, C.H., 2015. Conversion of plant materials into hydroxymethylfurfural using ionic liquids. Environ. Chem. Lett. 13, 173-190.

Yin, S., Pan, Y., Tan, Z., 2011. Hydrothermal conversion of cellulose to 5-hydroxymethyl furfural. Int. J. Green Energy 8, 234-247.

Yu, F., Sun, L., Zhou, Y., Gao, B., Gao, W., Bao, C., Feng, C., Li, Y., 2016a. Biosorbents based on agricultural wastes for ionic liquid removal: An approach to agricultural wastes management. Chemosphere 165, 94-99.

Yu, I.K.M., Tsang, D.C.W, Chen, S.S., Wang, L., Hunt, A.J., Sherwood, J., Vigier, K.D.O., Jérôme, F., Ok, Y.S., Poon, C.S., 2017a. Polar aprotic solvent-water mixture as the medium for catalytic production of hydroxymethylfurfural (HMF) from bread waste. Bioresour. Technol. 245, 456-462.

Yu, I.K.M., Tsang, D.C.W., 2016a. Valorization of pre-consumer food waste into hydroxymethylfurfural, in: Proceeding of the 1st International Conference on

Bioresource Technology for Bioenergy, Bioproducts & Environmental Sustainability. Sitges, Spain.

Yu, I.K.M., Tsang, D.C.W., 2017. Conversion of biomass and carbohydrates to hydroxymethylfurfural: a review of catalytic systems and underlying mechanisms. Bioresour. Technol. 238, 716–732.

Yu, I.K.M., Tsang, D.C.W., Yip, A.C.K., Chen, S.S., Ok, Y.S., Poon, C.S., 2016b. Valorization of food waste into hydroxymethylfurfural: Dual role of metal ions in successive conversion steps. Bioresour. Technol. 219, 338-347.

Yu, I.K.M., Tsang, D.C.W., Yip, A.C.K., Chen, S.S., Ok, Y.S., Poon, C.S., 2017b. Valorisation of starchy, cellulosic, and sugary food waste into hydroxymethylfurfural by one-pot catalysis. Chemosphere 184, 1099-1107.

Yu, I.K.M., Tsang, D.C.W., Yip, A.C.K., Chen, S.S., Wang, L., Ok, Y.S., Poon, C.S., 2017a. Catalytic valorisation of starch-rich food waste into hydroxymethylfurfural (HMF): controlling relative kinetics for high productivity. Bioresour. Technol. 237, 222–230.

Zhang, J., Das, A., Assary, R.S., Curtiss, L.A., Weitz, E.A., 2016b. A combined experimental and computational study of the mechanism of fructose dehydration to 5-hydroxymethylfurfural in dimethylsulfoxide using Amberlyst 70, PO43−/niobic acid, or sulfuric acid catalysts. Appl. Catal. B 181, 874-887.

Zhang, L., Xi, G., Zhang, J., Yu, H., Wang, X., 2017. Efficient catalytic system for the direct transformation of lignocellulosic biomass to furfural and 5–hydroxymethylfurfural. Bioresour. Technol. 224, 656-661.

Zhang, M., Su, K., Song, H., Li, Z., Cheng, B., 2015b. The excellent performance of amorphous Cr2O3, SnO2, SrO and graphene oxide–ferric oxide in glucose conversion into 5-HMF. Catal. Commun. 69, 76-80.

Zhang, T., Kumar, R., Wyman, C.E., 2013. Enhanced yields of furfural and other products by simultaneous solvent extraction during thermochemical treatment of cellulosic biomass. RSC Adv. 3, 9809-9819.

Zhang, X., Hewetson, B.B., Mosier, N.S., 2015a. Kinetics of maleic acid and aluminum chloride catalyzed dehydration and degradation of glucose. Energy Fuels 29, 2387−2393.

Zhang, X., Murria, P., Jiang, Y., Xiao, W., Kenttämaa, H.I., Abu-Omar, M.M., Mosier, N.S., 2016a. Maleic acid and aluminum chloride catalyzed conversion of glucose to 5-(hydroxymethyl)furfural and levulinic acid in aqueous media. Green Chem. 18, 5219-5229.

Zhang, X., Zhang, D., Sun, Z., Xue, L., Wang, X., Jiang, Z., 2016. Highly efficient preparation of HMF from cellulose using temperature-responsive heteropolyacid catalysts in cascade reaction. Appl. Catal. B 196, 50-56.

Zhang, Y., Pan, J., Shen, Y., Shi, W., Liu, C., Yu, L., 2015a. Brønsted acidic polymer nanotubes with tunable wettability toward efficient conversion of one-pot cellulose to 5-hydroxymethylfurfural. ACS Sustainable Chem. Eng. 3, 871-879.

Zhang, Y., Wang, J., Li, X., Liu, X., Xia, Y., Hu, B., Lu, G., Wang, Y., 2015c. Direct conversion of biomass-derived carbohydrates to 5-hydroxymethylfurural over water-tolerant niobium-based catalysts. Fuel 139, 301-307.

Zhang, Y., Wang, X.C., Cheng, Z., Li, Y., Tang, J., 2016. Effect of fermentation liquid from food waste as a carbon source for enhancing denitrification in wastewater treatment. Chemosphere 144, 689-696.

Zhao, H., Holladay, J.E., Brown, H., Zhang, Z.C., 2007. Metal chlorides in ionic liquid solvents convert sugars to 5-hydroxymethylfurfural. Science 316, 1597-1600.

Zhao, X., Wen, T., Zhang, J., Ye, J., Ma, Z., Yuan, H., Ye, X., Wang, Y., 2017. Fe-Doped SnO2 catalysts with both BA and LA sites: facile preparation and biomass carbohydrates conversion to methyl lactate MLA. RSC Adv. 7, 21678-21685.

Zhou, L., Liang, R., Ma, Z., Wu, T., Wu, Y., 2013. Conversion of cellulose to HMF in ionic liquid catalyzed by bifunctional ionic liquids. Bioresour. Technol. 129, 450-455.

Zhou, P., Zhang, Z., 2016. One-pot catalytic conversion of carbohydrates into furfural and 5-hydroxymethylfurfural. Catal. Sci. Technol. 6, 3694-3712.